Developing and characterising imaging biomarkers for pain and analgesia

Sophie Elizabeth Charlotte Clarke

Nuffield Department of Clinical Neurosciences & Trinity College
University of Oxford

Thesis submitted in partial fulfilment of the requirements for the degree of Doctor of Philosophy in Clinical Neurosciences

Trinity Term 2023

Developing and characterising imaging biomarkers for pain and analgesia

Sophie Elizabeth Charlotte Clarke

Nuffield Department of Clinical Neurosciences & Trinity College, University of Oxford

Thesis submitted in partial fulfilment of the requirements for the degree of Doctor of Philosophy

ABSTRACT

There is a need to improve translation of novel pain treatments from pre-clinical to clinical research, and the development of objective standardised biomarkers to verify target engagement is a vital step towards this goal. Features of chronic pain conditions, such as central sensitisation, can be experimentally induced in healthy humans. Functional magnetic resonance imaging (fMRI) is a highly valuable method to explore the neural basis for pain and also analgesic activity. This thesis combines these two research tools to develop and characterise neuroimaging biomarkers for pain and analgesia.

The first chapter consists of a systematic literature review, evidencing that this combination of techniques has provided a wealth of information about brain activity during pain states and analgesia. Co-ordinate based meta-analysis conducted to summarise results for a simple comparison between the neural responses during experimental hyperalgesia compared to control showed activation clusters in the insula cortex and thalamus.

Next, exploratory analysis of early 7 Tesla MRI data was conducted to investigate the neural changes that occur during the onset of central sensitisation. Conclusions were limited due to a low sample size, but there were interesting results showing increased blood oxygen-level dependent (BOLD) response in the insula and in the nucleus cuneiformis, a brainstem region shown to be specific to maintenance of central sensitisation.

The remaining three chapters comprise primary results and exploratory analysis from the IMI-PainCare BioPain RCT4 trial. The trial utilises the high frequency stimulation (HFS) model to induce central sensitisation, the neural basis for which had not previously been studied using fMRI. Comparison between pre-HFS and post-HFS data showed that the neural basis for HFS-induced central sensitisation was aligned to that seen with the well-characterised capsaicin model in imaging studies.

Subsequently, analysis of the main trial endpoints was conducted, to investigate the effects of lacosamide, pregabalin and tapentadol on biomarkers of pain processing observed by fMRI. Pregabalin reduced the punctate-evoked BOLD response in the posterior insula cortex. Lacosamide modulated resting state functional connectivity between the thalamus and secondary somatosensory cortex. In whole-brain analyses, tapentadol modulated responses in areas relevant to pain processing such as the anterior insula cortex.

Finally, exploratory analysis was conducted to characterise the placebo effect in the trial, showing that during placebo analgesia changes in brain activity were observed in regions associated with pain perception, including the insula and anterior cingulate cortices, and regions involved in affective and cognitive aspects of pain processing, such as the amygdala and dorsolateral prefrontal cortex.

Overall, this work comprises a valuable contribution to increase the utility and standardisation of applying experimental models in conjunction with fMRI in the assessment of novel analgesics prior to large scale clinical trials. As evidenced in the systematic review, individual fMRI studies are highly informative, but lack of standardisation makes comparison between studies difficult. The BioPain work addresses this challenge, providing a standardised assessment of multiple drugs across many pain biomarkers, demonstrating how these biomarkers can be valuably employed in drug development.

ACKNOWLEDGEMENTS

I would like to thank many colleagues and friends who have supported me in the completion of my DPhil. Firstly, thank you to Irene for giving me the opportunity to do the DPhil in your lab, and for all of your help right from the initial application. I am very grateful for your direction and for your encouragement, which gave me the confidence to push myself outside my comfort zone. Thank you to Vishvarani for all of your guidance, it has been a pleasure working closely with you on the BioPain trial and learning from your expertise on all aspects of MRI research. I am also thankful for your help in developing this thesis, as it has benefitted immensely from our discussions and your reviews of the content. Thank you to Richard for all your support throughout my DPhil, particularly for completing so many of the BioPain study visits with me and always brightening my day at the 8am start. It was not easy given the complexities of the trial, the high number of visits and the very short timelines due to COVID, and without Richard and Vishvarani's support and positive attitudes this wouldn't have been possible. Similarly, thank you to the team at WIN for helping us to run the study, particularly to Jon, Mike, David and Jemma for their flexibility to complete the scanning visits, and to Stuart and Nancy for helping us to set-up the study. I would also like to thank all those who collaborated on the IMI-PainCare project, especially those who worked directly on the BioPain RCT4 project, including Nanna, Francesca, Gisele, Nicolas and Vincent. I very much enjoyed working with you all. I'd also like to thank all the friends I have made during my time at Oxford, especially Hanna for all your help with my research and for the moral support, and to all the Pain Group members for sharing their amazing research and the great discussions. Thank you to my friends from Trinity College for making the Oxford experience so fun. Finally, I'd like to thank my parents and Neil for their never-ending support and encouragement.

Source of Financial Support: The BioPain Trial sections of this thesis received funding from the Innovative Medicines Initiative 2 Joint undertaking under grant agreement No 777500. This Joint Undertaking receives support from the European Union's Horizon 2020 research and innovation program and EFPIA.

PUBLICATIONS AND CONFERENCE PRESENTATIONS

Topical workshop session (invited speaker presentation and panel discussion):

Clarke, S., Wanigasekera, V., Rogers, R., Tracey, I. (2022). Neuroimaging-based biomarkers for experimental pain. Topical workshop session: "Functional biomarkers of nociceptive signal processing – back-translation of human studies to preclinical models". European Pain Federation (EFIC) Congress, April 2022, Dublin, Ireland.

Poster presentations:

Clarke, S., Wanigasekera, V., Rogers, R., Fardo, F., Pia, H., Nochi, Z., Macian, N., Leray, V., Finnerup, N., Pickering, G., Mouraux, A., Truini, A., Treede, R-D., Tracey, I. (2022). Characterisation of the neural correlates of central sensitisation induced by the high frequency stimulation (HFS) model in healthy humans using functional magnetic resonance imaging (fMRI). Federation of European Neuroscience Societies (FENS) Forum, July 2022, Paris, France.

Clarke, S., Wanigasekera, V., Rogers, R., Fardo, F., Pia, H., Nochi, Z., Macian, N., Leray, V., Finnerup, N., Pickering, G., Mouraux, A., Truini, A., Treede, R-D., Tracey, I. (2022). Characterisation of the neural correlates of central sensitisation induced by the high frequency stimulation (HFS) model in healthy humans using functional magnetic resonance imaging (fMRI). International Association for the Study of Pain (IASP) World Congress, September 2022, Toronto, Canada.

Publications:

Clarke, S., Wanigasekera, V., Rogers, R., Fardo, F., Pia, H., Nochi, Z., Macian, N., Leray, V., Finnerup, N., Pickering, G., Mouraux, A., Truini, A., Treede, R-D., Garcia-Larrea, L., Tracey, I. (2023 – *In Preparation*). Systematic review and co-ordinate based meta-analysis to summarise the utilisation of functional brain imaging in conjunction with human models of peripheral and central sensitisation. For submission to the European Journal of Pain.

TABLE OF CONTENTS

INTRODUCTION

In the UK, a review of population studies indicates the prevalence of chronic pain is as high as 35-51%, and the prevalence of moderate to severely disabling chronic pain is 10-14% (Fayaz et al. 2016). Chronic pain causes distress and suffering, and has a huge impact on individuals (Goldberg and McGee 2011). It affects ability to carry out daily activities (Dueñas et al. 2016), is commonly associated with psychological co-morbidities (de Heer et al. 2018), and has been shown to be associated with loneliness and social exclusion (Allen et al. 2020). In addition, it represents a major challenge for healthcare systems, associated with a significant social and economic impact (Phillips 2009).

Challenges associated with the high prevalence and burden of chronic pain are heightened by the fact that there remains a significant unmet need for effective pain relief interventions. Current chronic pain treatment guidelines focus on a patient-centred approach with the main goal to improve quality of life. Treatment strategies include non-pharmacological and non-invasive options such as exercise programs, psychological therapies and acupuncture, as well as pharmacological therapies, surgical treatments and non-surgical interventional treatments (Cohen, Vase, and Hooten 2021; Carville et al. 2021). However, currently available therapies provide only modest improvements in pain and minimal improvements in physical and emotional functioning. Despite the availability of these treatment strategies, treatment of people with chronic pain rarely leads to complete resolution of pain symptoms and many people with chronic pain will continue to live with some level of pain (Turk, Wilson, and Cahana 2011; Breivik, Eisenberg, and O'Brien 2013). In addition, many pharmacological treatments can be associated with side effects and complications (Dydyk and Conermann 2023), as well as the major issue of addiction with opioids (Cohen, Vase, and Hooten 2021). Hence, chronic pain mechanisms and improved treatment strategies are key priorities in medical research.

While the unmet need for improved pain treatments is well recognised, there are many challenges associated with analgesic drug development, meaning clinical trials for these treatments are expensive, take a long time to implement and have low success rates. These factors result in limited investment in this area by pharmaceutical companies due to the financial risks associated with trial failures. The most impactful challenges include the subjective nature of pain perception, a lack of reliable pain biomarkers and high placebo responses, all of which reduce the likelihood of a clinical trial for a novel analgesic drug or therapy having a positive outcome (Davis et al. 2020; Maher et al. 2022). Similar challenges also impact the development of emerging interventions that target psychological and cognitive aspects of chronic pain, such as cognitive behavioural therapy, with a need

to develop and optimise trial designs for detecting treatment benefit (Eccleston and Crombez 2017). A recent study showed that the probability of successful development of a pain drug from phase I to approval is only 10.4%, with attrition most commonly occurring between phase III and approval (Maher et al. 2022). Poor translation from promising preclinical data to success in human clinical trials is a particular issue. This highlights the need for reliable pain biomarkers that are able to address a number of important aspects contributing to this attrition, including proof of target engagement and patient stratification to predict therapeutic response (Tracey, Woolf, and Andrews 2019). Given the heterogeneous nature of pain pathophysiology, the ability to conduct trials in the patient population most likely to respond to a treatment, and thus reducing the variability of response, could be highly valuable in reducing the scale of clinical trials needed to demonstrate efficacy (Davis et al. 2020).

Biomarkers for pain and analgesia

A simple definition of a biomarker is a characteristic that is objectively measured as an indicator of biological processes in health or disease, or of response to an intervention. The "Biomarkers, Endpoints and other Tools – BEST" working group from the U.S. Food and Drug Administration (FDA) and National Institutes of Health (NIH) have produced categories of biomarkers relevant across medical research. The most relevant types of biomarkers in analgesic drug development include pharmacodynamic response biomarkers; defined as measures to show a biological response occurs following exposure to a medical product, and predictive biomarkers; defined as measures to identify individuals more likely to experience an effect following exposure to a medical product than those without the biomarker (FDA and NIH 2016; Tracey, Woolf, and Andrews 2019). Diagnostic, monitoring and prognostic biomarkers are also relevant for chronic pain research, detecting the presence of a chronic pain condition, assessing the status of the condition and identifying likelihood of recurrence or progression, respectively (FDA and NIH 2016).

There are multiple potential biomarkers of pain mechanisms that originate from across the pain system. These include measures of peripheral pain signalling such as immunohistochemistry, skin biopsy, microneurography and quantitative sensory testing (QST), to measures of pain signalling in the spinal cord such as spinal reflexes, and measures of brain activity such as electroencephalography (EEG) and functional magnetic resonance imaging (fMRI) (Tracey, Woolf, and Andrews 2019; Smith et al. 2017). Within these types of measurements, specific pain biomarkers can be utilised depending on which aspect of nociception, chronic pain or analgesic activity is being investigated.

The nociceptive pain circuit has been well-characterised. In summary, high threshold nociceptors are activated by intense mechanical, thermal or chemical stimuli and feed this information to nociceptive neurons in the spinal cord, which project via the thalamus to cortical areas generating the sensory and emotional qualities of pain (Tracey 2010).

In the skin, nociception starts when noxious thermal, mechanical or chemical stimuli are detected by specialised sensory neurons (nociceptors). Fast initial onset pain is mediated by Aδ-fibre nociceptors, which are myelinated, whereas sustained pain is mediated by C-fibres which have small diameter unmyelinated axons. The peripheral terminals of these fibres express different combinations of ion channels that transduce heat, cold or mechanical stimuli, such as the transient receptor potential V1 (TRPV1) channel that transduces heat, conferring different levels of selectivity of each individual nociceptor to different stimulus modalities (though most are multi-modal) (Dubin and Patapoutian 2010). Action potentials initiated by these receptors encoding the intensity of a noxious stimulus are propagated along the nociceptor axon which terminate predominantly in laminae I, II, and V of the dorsal horn of the spinal cord (Dubin and Patapoutian 2010). Here they synapse with relay neurones that transmit the nociceptive information to higher centres of the central nervous system or various interneurons responsible for signal modification (Dubin and Patapoutian 2010; Millan 1999). Similar, but not identical, mechanisms are involved in the detection and processing of nociceptive information from non-cutaneous tissues such as joints, muscles and viscera (Millan 1999).

Once signals have been integrated in the dorsal horn, projection neurones conduct the signals to the brain via ascending pathways. There are many ascending pathways that have been characterised, one example being the spinothalamic tract which is a monosynaptic tract which projects to the thalamus, a crucial relay centre for processing nociceptive information on the way to cortical regions (Millan 1999). Human neuroimaging studies investigating how nociceptive inputs are encoded to produce pain experiences have identified many cortical regions that are activated, which is consistent with the fact that pain is a complex multidimensional experience that encompasses altered attention, anxiety, threat, emotional response and many other non-specific features reflected in these activations (Ploghaus et al. 1999; Ploghaus et al. 2001; Berna et al. 2010). These early studies were designed specifically to dissect pain into neural components that subserve these different features using a combination of psychological and pharmacological approaches (Wiech, Ploner, and Tracey 2008; Wiech and Tracey 2009; Tracey 2010). Nociceptive signals are subject to processing at all levels of the pain perception pathway. Descending control mechanisms play a role in modulating the pain signal

before it reaches higher centres, allowing preferential inhibition or facilitation (Heinricher et al. 2009). An overview of ascending and descending pain pathways is shown in Figure 1.

In chronic pain, defined as persistent or recurrent pain lasting three months or more (Treede et al. 2015), pain processing is altered in some way. The nervous system itself may be injured or damaged, and/or changes can occur within the descending pain modulatory network, leading to persistent changes in sensitivity (Treede et al. 2019; Cohen and Mao 2014). As a result, pain can occur spontaneously, the pain threshold may fall dramatically, and the duration and magnitude of response to noxious stimuli is amplified (von Hehn, Baron, and Woolf 2012; Tracey 2008). Chronic pain is heterogeneous and can be idiopathic, as is the case with chronic primary pain conditions where the pain cannot be attributed to another condition, such as fibromyalgia, chronic widespread pain or irritable bowel syndrome. It can also be related to inflammatory or neuropathic causes (Treede et al. 2015).

Patient studies indicate an important role for central sensitisation to the phenotype of chronic pain in multiple pain conditions. Central sensitisation describes an overall enhancement in the function of nociceptive processing, caused by increased membrane excitability and synaptic efficacy, and reduced inhibition, leading to amplification of pain signalling (Latremoliere and Woolf 2009). It is characterised by allodynia (a pain response to non-noxious stimuli) and hyperalgesia (both primary hyperalgesia; an increased pain response at the site of injury, and secondary hyperalgesia; an increased pain response to in the area surrounding the injured tissue itself) (Woolf 1983; Woolf 2011).This hypersensitivity can be temporarily elicited in healthy humans using multiple methodologies – for example with topical capsaicin or high frequency electrical stimulation (HFS) as used in this thesis. These techniques produce peripheral and central sensitisation resulting in changes in the brain response which can be studied using imaging techniques such as fMRI (Woolf 2011). Peripheral sensitisation describes threshold reduction and response amplification of peripheral nociceptors (C- and Aδ-fibres), and is therefore restricted to the injury site. This is in contrast to central sensitisation, which alters pain sensitivity in non-injured tissues as a result of changes in the properties of central neurones, and recruits new inputs to nociceptive pathways from Aβ-fibres (which are low threshold mechanoreceptors that do not normally respond to painful stimuli) (Latremoliere and Woolf 2009). Hypersensitivity to different stimulus modalities are predominantly mediated by different mechanisms; peripheral sensitisation plays a more important role in altered heat sensitivity while altered sensitivity to mechanical stimuli is a key feature of central sensitisation (Latremoliere and Woolf 2009).

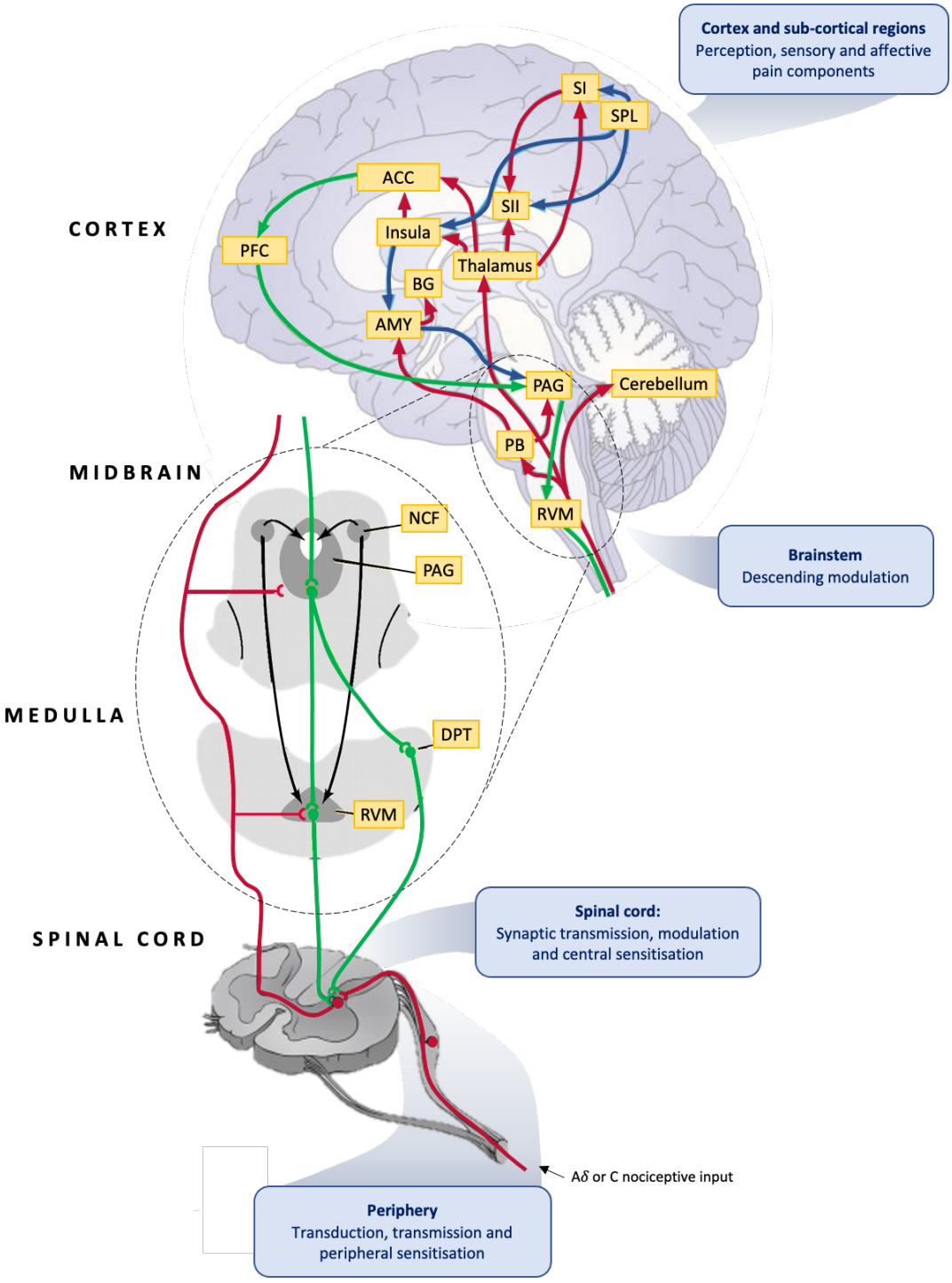

Figure 1: Ascending afferent and descending modulatory pain pathways.

Diagram showing areas of the nervous system involved in the transduction, transmission, modulation, and perception of pain. PFC, prefrontal cortex; ACC, anterior cingulate cortex; BG, basal ganglia; AMY, amygdala; SI, primary somatosensory cortex; SII, secondary somatosensory cortex; SPL, superior parietal lobe; PAG, periaqueductal grey; PB, parabrachial nucleus; RVM, rostral ventromedial medulla; NCF, nucleus cuneiformis; DPT, dorsolateral pontine tegmentum. Diagram adapted from: (Tracey and Mantyh 2007; Ringkamp, Dougherty, and Raja 2018; Bingel and Tracey 2008; Bushnell, Ceko, and Low 2013).

Despite significant advances in our understanding of pain perception using acute evoked painful stimuli, fMRI studies investigating the neural response to acute stimuli are not fully representative of an ongoing chronic pain state. There is a need to develop paradigms that can replicate an ongoing tonic pain state, to understand more about the neural signature in chronic pain. Recent developments focus on imaging tools that provide signals reflecting slowly varying and more tonic neural states (Howard et al. 2011; Loggia et al. 2013; Tracey and Johns 2010).

Analgesic drugs act to relieve pain. Different types of analgesics work by modulating different aspects of pain processing. This modulation can occur at any level from the peripheral nociceptors in the skin to the spinal cord and the brain, and many analgesics act on multiple targets across the pain system. One example of this is opioids, a mainstay treatment used primarily in acute pain management. These drugs act at opioid receptors that are located throughout central and peripheral compartments of the nervous system (Stein 2016). There are many analgesics that are used in different chronic pain conditions depending on the 'type' of pain present (though most chronic pain conditions have mixed mechanisms). For pain conditions with primarily neuropathic mechanisms, treatments include antidepressants (tricyclic antidepressants and serotonin-noradrenaline reuptake inhibitors) and antiepileptics (pregabalin and gabapentin), as well as topical treatments such as topical lidocaine or capsaicin (Finnerup et al. 2015). For pain conditions with primarily non-neuropathic mechanisms, such as osteoarthritis and inflammatory conditions, non-steroidal anti-inflammatories (NSAIDs) are primarily used, though antidepressants and pregabalin/gabapentin are effective in fibromyalgia and lower back pain too (Cohen, Vase, and Hooten 2021). Interventional treatments are also used for some chronic pain conditions, for example steroid injections for joints or joint replacement surgeries for osteoarthritis, and spinal cord stimulation for chronic neuropathic pain (Cohen, Vase, and Hooten 2021).

Pain biomarkers are important tools to understand whether an analgesic is effective and give information about the mechanism by which they exert their analgesic effects. This is especially important in the process of developing of new analgesics, during which it is vital to demonstrate that the new drug is engaging with relevant pain targets and modulating pain-related mechanisms (Tracey, Woolf, and Andrews 2019). The use of biomarkers to prove this pharmacodynamic efficacy can be highly valuable to enable investment to be directed towards drugs with the highest likelihood of showing good efficacy in chronic pain patients, and hopefully improve success rates of clinical trials.

Magnetic resonance imaging (MRI) biomarkers

The generation of brain images using magnetic resonance imaging (MRI) relies on the manipulation of hydrogen nuclei ("spins") within water molecules, using a strong magnetic field (B_0) to align the spins in one direction. The hydrogen nuclei in the B_0 field rotate at a frequency proportional to the strength of the magnetic field, creating oscillating B_1 magnetic fields that can be measured and also manipulated via the radio frequency coil (the head coil within the MRI scanner). This rotation (resonance) is the key basis allowing the MRI signals to be obtained. Gradient fields (magnetic fields that vary in strength across three planes – x, y and z) are applied during signal acquisition to enable the resonance frequency to vary depending on location, thereby measuring signal that can be aligned to specific locations in the brain and allowing formation of an image (Jenkinson and Chappell 2018).

There are many different modalities of MRI used depending on the specific research being conducted, including structural MRI to view the anatomy of the brain, diffusion MRI to investigate the anatomical connectivity between different brain structures, and functional MRI to investigate neuronal activity (either during a task or during rest). Functional MRI (fMRI) has been used most extensively in pain research studies, for example to examine how neuronal activity changes during a painful stimulus. The most common fMRI method, and that used in this thesis, is blood oxygen-level dependent (BOLD) imaging. BOLD imaging measures signal changes that occur due to haemodynamic changes in the blood (and is therefore an indirect, rather than direct, measure of neuronal activity). This is possible due to the fact that oxygenated and deoxygenated haemoglobin molecules interact with the magnetic fields in different ways, resulting in contrast in the images that can be detected (Jenkinson and Chappell 2018). The main alternative to BOLD imaging is arterial spin labelling (ASL), a technique which quantifies cerebral blood perfusion. ASL has also been applied in pain research and offers advantages in its ability to detect signal changes during ongoing or longer-lasting pain stimulation, which may be more reflective of the pain experienced by chronic pain patients than the short, acute pain stimuli that can be studied using BOLD imaging (Loggia et al. 2019). Both modalities can also be used to detect signal changes during rest, enabling researchers to make comparisons between resting brain activity in different experimental conditions. Proton Magnetic Resonance Spectroscopy (^{1}H-MRS) is a further technique that enables the composition of molecules to be profiled to explore brain metabolism and biochemistry (Tognarelli et al. 2015).

The pain research that has been conducted using various MRI/MRS modalities has produced a number of neuroimaging-based biomarkers of different aspects of pain perception, pain pathology and pain

modulation by analgesics (Tracey, Woolf, and Andrews 2019). Biomarkers for pain pathology can include structural or anatomical changes and functional changes (either in resting state connectivity or in response to painful stimuli). For example, a study using ASL quantitative perfusion imaging alongside a tonic pain paradigm identified a fundamental role for the dorsal posterior insula in pain (Segerdahl et al. 2015), and the change in the cerebral blood flow in this brain region has subsequently been validated and used as a biomarker of transcranial direct current stimulation (tDCS) analgesic efficacy (Lin et al. 2017). Another example of a biomarker for pain modulation by analgesics is suppression of the neural response in an area of the brainstem involved in the descending pain modulatory system. During an experimentally-induced sensitised pain state, this biomarker has been shown to be modulated by an effective analgesic (gabapentin) but not to an ineffective analgesic (ibuprofen) (Wanigasekera et al. 2016). Crucially this study also demonstrated that the biomarker distinguished the drug conditions from the placebo condition, which is key for demonstrating efficacy of novel analgesics during drug development and clinical research. Potential of MRI biomarkers for distinguishing between drug and placebo activity has been further demonstrated in a patient study, in which MRI data demonstrated pharmacodynamic effects with pregabalin in post-traumatic neuropathic pain patients, and also showed modulation of resting state connectivity in the placebo arm of the trial (Wanigasekera et al. 2018).

Machine learning and multi-variate pattern analysis approaches have also been used to develop pain biomarkers that consist of response patterns during pain and analgesia in healthy humans, either with or without an experimentally-induced pain state, and in pain patient cohorts (Wager et al. 2013; Duff et al. 2015). This approach offers potential utility as a pharmacodynamic biomarker for assessment of novel analgesics, both indicating whether the drug is modulating brain activity and whether the modulation is aligned to that of the signatures produced by drugs of known efficacy in the database, thus aiding decision making for proceeding with development of the novel drug (Duff et al. 2015; Tracey, Woolf, and Andrews 2019).

^{1}H-MRS has been used to explore neurochemical changes in patients with fibromyalgia compared to healthy controls, and has shown that the level of the inhibitory neurotransmitter GABA is decreased and the level of the excitatory neurotransmitter glutamate is increased in the posterior insula (Foerster et al. 2012). Further, it was shown that this pathological brain chemistry in the posterior insula cortex is rectified by pregabalin in fibromyalgia patients, providing evidence that ^{1}H-MRS is able to detect analgesic activity in this setting (Harris et al. 2013). Overall, these examples demonstrate the value of utilising MRI/MRS biomarkers in the development and assessment of analgesics.

Conclusions

In conclusion, there is a significant medical unmet need for effective analgesics, and in order to facilitate the development of new treatments it is imperative that the neural mechanisms underlying pain sensation in chronic pain patients are fully understood. Development of improved analgesics is hindered by the lack of reliable and objective biomarkers to support the subjective and behavioural measures currently used in animal studies and clinical trials. Advances in functional imaging offer ongoing improvements in the identification of the neural basis for chronic pain, and crucially for analgesic efficacy, and can provide objective biomarkers for use in analgesic development. This thesis includes research into imaging biomarkers of pain and analgesia, with the overall objective to further our understanding of the neural signature underlying the pain response and explore how this neural signature is modified by analgesics. Ultimately, it aims to provide evidence supporting the use of imaging biomarkers for evaluation of candidate analgesics in clinical trials.

Summary of experimental chapters and research objectives

Chapter 1: This chapter consists of a systematic literature review on the use of human hyperalgesia models in conjunction with functional neuroimaging, with a co-ordinate based meta-analysis on the reported activation co-ordinates for the brain response during the hyperalgesia state.

Research objective: *To summarise the results of published research studies that utilised experimental models of peripheral and central sensitisation in conjunction with MRI to elucidate the neural basis for the pain response in the sensitised state or to investigate the efficacy of analgesics.*

Chapter 2: This chapter presents the results of exploratory analysis conducted on an early-stage 7 Tesla MRI experiment to investigate the onset of central sensitisation induced by topical capsaicin in healthy humans. Data was collected by a former DPhil student in the pain group, and the results presented consist of data analysis work I have completed using this dataset.

Research objective: *To explore and understand the neural response to pain stimuli during the onset of a centrally sensitised state (induced by topical capsaicin) in healthy participants, using ultra-high-field 7 Tesla MRI.*

Chapter 3: This chapter outlines a characterisation of the neural correlates underlying the secondary hyperalgesia induced by the high frequency stimulation (HFS) model using fMRI, an experimental model that has not previously been characterised using imaging. This data was collected as part of the screening visit for the BioPain Trial, which is outlined in the fourth chapter in detail.

Research objective: *To profile the neural correlates of electrically-induced central sensitisation through comparison of baseline imaging data and post-HFS imaging data (in the absence of drug intervention).*

Chapter 4: In this chapter the results of the IMI-PainCare BioPain RCT4 Trial are presented. The trial is a randomized, double-blind, placebo-controlled, cross-over trial in healthy subjects to investigate the effects of lacosamide, pregabalin and tapentadol on biomarkers of pain processing observed by fMRI of the brain. This trial forms the main part of my DPhil and I was a lead researcher involved in all aspects of trial set-up, recruitment, data collection and data analysis.

Research objective: *To profile biomarkers of analgesia derived from fMRI measures of brain activity, after the experimental induction of hyperalgesia using HFS, including objectives to explore: a) punctate evoked blood oxygen level dependent (BOLD) response in the posterior insula, and b) resting state connectivity between the thalamus and the secondary somatosensory cortex, with three analgesic drugs compared to placebo.*

Chapter 5: This final chapter includes characterisation of the placebo effect in the BioPain trial, with a detailed investigation of the placebo effect seen in this study, and comparison of subject responses and fMRI outcomes in the placebo visit to data collected in the screening visit (with no drug/placebo administered).

Research objective: *To explore the neural basis for the placebo analgesia observed in the BioPain trial through conducting a comparison between fMRI data collected at the placebo visit and data collected during the screening visit (after sensitisation has been induced using HFS, but in the absence of any drug or placebo intervention).*

Work undertaken to conduct IMI-PainCare BioPain RCT4 trial

Chapters 3-5 of this thesis consist of analyses conducted on data collected in the IMI-PainCare BioPain RCT4 trial. The IMI-PainCare Consortium is composed of many organisations across Europe and aims to improve care of patients suffering from acute or chronic pain through three main projects. These focussed on patient reported outcome measures (PROMPT), pharmacological validation of functional pain biomarkers (BIOPAIN) and improving translation in chronic pelvic pain (TRiPP). The BioPain part of the project consisted of four clinical trials, one of which was the RCT4 trial focussing on neuroimaging.

The BioPain RCT4 study protocol was designed before I joined Oxford, but, since starting my DPhil in 2019, I have led or been significantly involved in all subsequent stages. This includes the preparation and submission of documents for the ethics review and subsequent amendments, study set-up activities with the university departments and Oxford University Hospitals NHS Trust, and all trial monitoring at the Oxford site which involved preparation of documentation for review by an external trial monitor. I was significantly involved in development of the MRI scan protocols and harmonisation of these across the three trial sites, as well as all participant recruitment and data collection at the Oxford site. I developed the detailed data analysis pipeline for the MRI data and completed data analysis for all RCT4 data. I have also participated in the Consortium meetings throughout the project, to feedback progress and discuss next steps, and I have really enjoyed collaborating with other researchers and organisations involved in the project.

EXPERIMENTAL CHAPTER 1

Systematic review and co-ordinate based meta-analysis to summarise the utilisation of functional brain imaging in conjunction with human models of peripheral and central sensitisation

1.1 Abstract

Background and objective: Functional magnetic resonance imaging (fMRI), in conjunction with models of peripheral and/or central sensitisation, has been used to assess analgesic efficacy in healthy humans. This systematic review aims to summarise the use of these techniques in previous studies, to both characterise the neural mechanisms of hyperalgesia and allodynia, and to evaluate the efficacy of different analgesics.

Databases and data treatment: The primary searches were conducted using four electronic databases: PubMed-Medline, Cochrane, Web of Science and Clinicaltrials.gov. The search terms "[hyperalgesia AND human AND pain AND brain AND imaging AND fMRI]" were used to identify and review studies. A co-ordinate based meta-analysis (CBMA) was conducted to quantify neural activity in the hyperalgesic condition using GingerALE software.

Results: Searches identified 217 publications. There were 31 studies that met the inclusion criteria and were included for further analysis. Included studies applied fMRI in conjunction with 9 different models of hyperalgesia and/or allodynia. Studies focussed on characterisation of the neural correlates of peripheral or central sensitisation showed consistent activity changes in brain regions including the somatosensory cortex, prefrontal cortices, insula cortex, anterior cingulate cortex, thalamus and brainstem regions. Studies focussing on the effect of analgesics demonstrate the contribution of fMRI techniques to elucidate the mechanisms by which each analgesic modulates the response to stimuli. The co-ordinate based meta-analysis conducted on extracted co-ordinates from a sub-set of 12 studies produced 6 activation clusters that were statistically significant at the FDR of 0.05. These clusters were located in brain regions are consistent with activations observed during secondary hyperalgesia.

Conclusions: Experimental pain models that provide a surrogate for features of pathological pain conditions in healthy humans and functional imaging techniques are both highly valuable research tools. This review shows that use of these experimental models in conjunction with fMRI techniques to explore the neural correlates of peripheral and/or central sensitisation and to evaluate analgesic target engagement and efficacy provides a wealth of information about brain activity during pain states and analgesia. These tools are promising candidates to help bridge the gap between animal and human studies, to improve translatability and provide opportunities for identification of new targets for back-translation to animal studies.

1.2 Introduction

There is an unmet need for effective treatments for chronic pain, and numerous challenges in drug development (Davis et al. 2020). Poor translation of promising candidate analgesics from animal studies to human studies indicates a need to improve the use of animal data for decision making and to develop animal models that utilise more clinically-relevant endpoints (Denayer, Stöhr, and Van Roy 2014). Also, the endpoints studied in pain clinical trials are primarily self-reported ratings, which are shown to have low sensitivity even with training (Smith et al. 2016), especially when baseline pain is variable (Harris et al. 2005; Farrar et al. 2014). Pain ratings are non-specific; while ratings can be modulated by the analgesic, they can also be modulated by other factors such as expectation, attention, anxiety and emotional responses (Ploghaus et al. 2001; Ploghaus et al. 1999; Berna et al. 2010; Bingel et al. 2011; Wiech, Ploner, and Tracey 2008; Wiech and Tracey 2009). In a clinical trial setting it cannot be determined if a decrease in pain ratings is attributable to the drug alone. While behavioural data is highly valuable, there is a need for objective measures for assessing target engagement in humans and accurately evaluating efficacy, to help improve go/no-go decision making in bringing new analgesics to large-scale clinical trials (Tracey, Woolf, and Andrews 2019). Brain imaging could prove to be one of the tools that enables this (Borsook, Becerra, and Hargreaves 2011a, 2011b).

Hyperalgesia, defined as increased pain in response to a painful stimulus, and allodynia, defined as a sensation of pain in response to a usually non-painful stimulus, arise as a result of tissue injury (IASP 2011). These characteristics occur at the site of injury (primary hyperalgesia) primarily due to peripheral sensitisation, and surrounding the injured tissue itself (secondary hyperalgesia) primarily due to central sensitisation (Latremoliere and Woolf 2009; Woolf 1983). Peripheral sensitivity at the primary injury site (primary hyperalgesia) mediates an increased sensitivity to heat and mechanical stimuli whereas central sensitisation in the area outside the injury site (secondary hyperalgesia) primarily results in sensitivity to mechanical stimuli only (Latremoliere and Woolf 2009; Treede et al. 1992). Patient studies indicate an important role for central sensitisation to the phenotype of chronic pain in multiple pain conditions, resulting in distressing symptoms for patients (Jensen and Finnerup 2014; Latremoliere and Woolf 2009). Peripheral and central sensitisation symptoms of pain hypersensitivity can be temporarily induced in healthy humans using multiple experimental methodologies (Quesada et al. 2021). These techniques produce changes in the brain response which can be studied using imaging techniques such as fMRI (Woolf 2011). Crucially, they have also been

shown to be responsive to effective analgesics targeting central sensitisation mechanisms (Quesada et al. 2021; Wanigasekera et al. 2016).

Functional neuroimaging has been instrumental in gaining understanding of pain processing (Lee and Tracey 2013). Across multiple imaging modalities, fMRI offers a range of temporal resolutions, good spatial resolution and the ability to evaluate whole-brain activity and cognitive processing (Morton, Sandhu, and Jones 2016). More recent co-ordinate based meta-analysis (CBMA) techniques have enabled statistical inference to identify brain regions that are consistently activated in multiple related fMRI studies, mitigating potential limitations of individual studies such as small sample sizes (Tanasescu et al. 2016; Samartsidis et al. 2017; Eickhoff et al. 2009; Wager et al. 2009). Using fMRI techniques in conjunction with experimental models of central sensitisation in early-phase clinical trials could support improved translatability of new medicines, through demonstrating target engagement in humans at an early stage prior to progressing to larger clinical trials (Olesen et al. 2012; Cho, Deol, and Martin 2021).

The aims of this review were to summarise the use of fMRI in conjunction with models of peripheral and/or central sensitisation in previous studies, to both characterise the neural mechanisms of hyperalgesia and allodynia and to explore how these techniques have been applied to study the efficacy of various analgesics.

1.3 Methods

The review has been conducted in accordance with the Preferred Reporting Items for Systematic reviews and Meta-Analyses (PRISMA) 2020 statement and guidance (Page et al. 2021). The CBMA section of this review has been conducted following guidelines specific for neuroimaging meta-analyses (Müller et al. 2018).

1.3.1 Systematic search methodology

The primary search was conducted using four electronic databases: PubMed-Medline, Cochrane, Web of Science and Clinicaltrials.gov. We used the search terms "[hyperalgesia AND human AND pain AND brain AND imaging AND fMRI]". Duplicates were removed. The results (n=226) were then sorted based on set inclusion and exclusion criteria:

Inclusion criteria: Studies primarily focussed on fMRI studies using a human experimental model of peripheral and/or central sensitisation were included.

Exclusion criteria: Studies primarily focussed on animal models, patient cohort or case studies, human studies exploring other features of pain (e.g., placebo/nocebo effects) and review articles were excluded from further analysis.

After this primary search was conducted, a number of secondary searches were conducted using PubMed to ensure publications on certain specific topics were not missed. One secondary search focussed on spinal cord imaging, using the terms: "[hyperalgesia AND human AND pain AND model AND spinal cord AND imaging]" to identify additional spinal cord studies. This search identified one additional study that fit the inclusion criteria and was therefore included in the results for further analysis. Further individual searches for less common human experimental models were conducted, using the following format: "[*model* AND neuroimaging]". The models run in this series of searches included menthol, mustard oil, cinnamaldehyde, nerve growth factor (NGF) injection, hypertonic saline injection, and incisional models. One additional study was identified in the results from the menthol search that fit the inclusion criteria, so it was included in the results for further analysis. None of the other model-specific searches identified publications that fit the inclusion criteria. A manual search was conducted for studies listed in literature references but not detected automatically in the electronic searches. This manual search did not identify any further studies that met the inclusion criteria. Searches were limited to English language only, since database inception to 10 October 2022.

1.3.2 Data extraction and analysis

For all studies included in the final list the following parameters were extracted: date of publication, sample size, experimental model used, site of model application, stimulation area relative to model application site (determining whether stimuli were applied in the primary or secondary hyperalgesia area), type of stimuli applied, whether the study included a drug/analgesia component and whether or not the paper reports activation coordinates for the contrast of interest (hyperalgesia state and control or non-hyperalgesia state) to be included in the CBMA.

It was verified that all included studies reported behavioural data demonstrating that hyperalgesia had developed and that the time at which the imaging results were obtained occurred within a model-specific suitable time frame after application of the model. This was to ensure that the experimental models were successfully inducing hyperalgesia, and that results were obtained neither too early (before hyperalgesia has developed) or too late (once hyperalgesia has worn off).

For all identified studies, risk of bias was assessed using the Cochrane tool for assessing risk of bias in randomised trials (Higgins et al. 2011). Some of the five main tool domains were adapted to adequately assess the identified studies, as many were observational research studies rather than randomised trials. The information on the study design needed for risk of bias assessment was widely and variably distributed in manuscripts, so searches were conducted in the PDF text for key word stems (including random-, control-, blind-, hypothe- and aim-).

1.3.3 Co-ordinate based meta-analysis (CBMA)

1.3.3.1 Research question, co-ordinate extraction and pre-processing

The CBMA included in this review was conducted to answer the following research question; 'what areas of the brain are activated during pain perception when hyperalgesia is present, compared to control (hyperalgesia not present), in studies using experimental models of peripheral and/or central sensitisation in healthy human participants?'.

The reports included in this systematic review were screened to identify those suitable for inclusion in the CBMA. The inclusion criteria required there to be activation co-ordinates reported for a hyperalgesic state vs. a control state (without hyperalgesia present). Co-ordinates were required to be reported as 3D co-ordinates in the format x, y, and z, within either Montreal Neurological Institute (MNI) or Talairach space. If present, activation co-ordinates were extracted manually for the hyperalgesia state vs. control/non-hyperalgesia state contrast. Differences in the standard space used (Talaraich vs. MNI) were accounted for by converting all co-ordinates to MNI space using the BrainMap icbm2tal transform (https://www.brainmap.org/icbm2tal/). For studies that reported co-ordinates, only activations were included since deactivations were rarely reported.

1.3.3.2 CBMA methodology

The GingerALE BrainMap application version 3.0.2 (available at: https://www.brainmap.org/ale/) was used to carry out the CBMA. The GingerALE algorithm applies an activation likelihood estimate (ALE) technique. Reported coordinates are represented by 3D Gaussian distributions, defined by a specified full-width half-maximum (FWHM), to provide an estimate of the likelihood of activation of a particular location across all studies (Eickhoff et al. 2009; Eickhoff et al. 2012; Turkeltaub et al. 2012).

The CBMA was performed using the false discovery rate (FDR) method with p-value threshold based on independence or positive dependence (pID) to assess statistical significance, with an FDR of 0.05 (Laird et al. 2005).

1.4 Results

The primary search conducted using electronic databases provided 282 results. These results were processed by removing duplicates (n=56) and then by assessing each publication to determine whether they met the pre-determined inclusion and exclusion criteria. After this assessment, there were 29 publications identified.

This list was then finalised with the addition of publications identified in secondary searches (n=2). There were no additional publications identified during manual review of the reference lists in literature and other sources. The final list of studies that met the inclusion criteria (n=31) were taken forwards for data extraction and analysis. The search results are outlined in Figure 1.

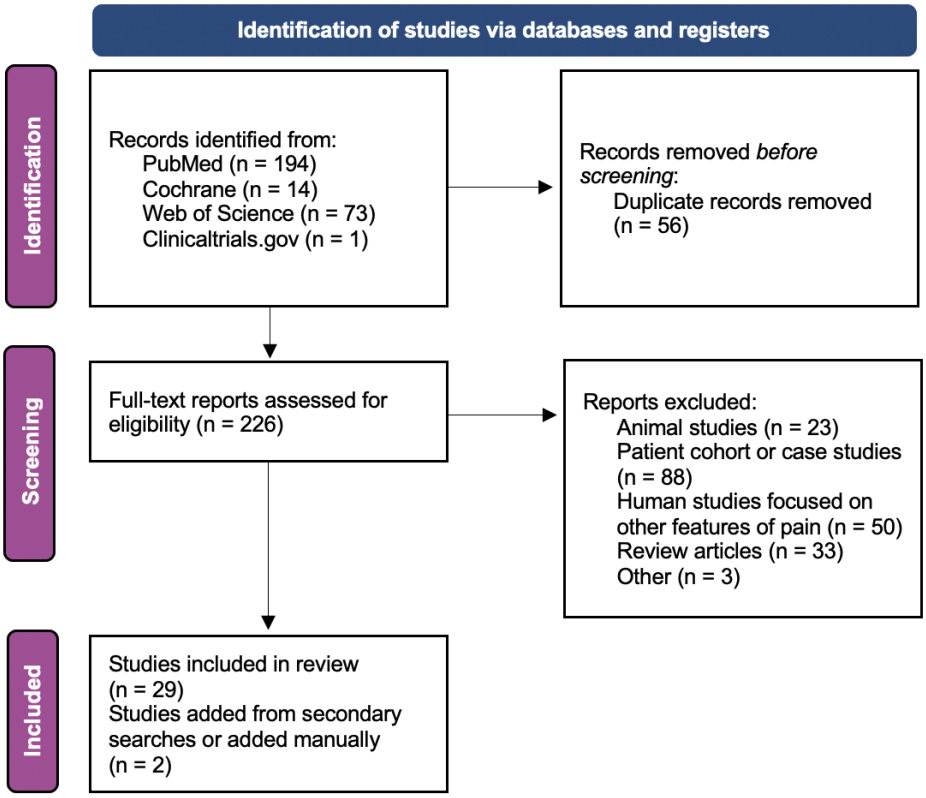

Figure 1. Systematic search results.

The primary electronic search was conducted using PubMed-Medline, Cochrane, Web of Science and Clinicaltrials.gov databases. Duplicates were removed and full-text reports were evaluated against pre-determined inclusion and exclusion criteria, with reports meeting the inclusion criteria (n=29) taken forwards for data extraction and analysis. Further secondary searches were conducted to identify studies using spinal cord imaging and those using less common human models of central sensitisation, identifying a further 2 studies. Template flow diagram adapted from PRISMA 2020 statement (Page et al. 2021).

For all included studies, risk of bias assessment was completed using the Cochrane tool for assessing risk of bias in randomised trials (Higgins et al. 2011). Additional phrasing was added to the five domains to allow the parallel analysis of observational studies with the interventional studies. The five assessed domains were selection bias (randomisation and allocation concealment, or the inclusion of a control condition in observational studies), performance bias (whether participants and researchers were blinded to the test condition, such as capsaicin vs. sham, or to the intervention, such as drug vs. placebo), detection bias (whether outcome assessment was blinded), attrition bias (whether studies reported outcome data completeness), and reporting bias (whether studies reported a specific testable hypothesis or research question that the experiment was addressing, or whether the study was pre-registered). Summarised results are shown in Figure 2.

Regarding selection bias, the assessment of the presence of a control condition is likely to be an over-simplification, as control conditions must be carefully designed, and the use of an inappropriate control may introduce bias. Blinding status of the outcome assessment was often not reported; in these cases, if researchers were unblinded during data collection it was assumed that outcome assessment was also unblinded and therefore categorised as high risk. Studies that were blinded during data collection that did not mention blinding of the outcome assessment were categorised as unclear risk. Regarding attrition, many studies simply reported the total number of subjects included but did not state if this was the total number that were originally screened or included in data collection; in these cases, the risk of bias was categorised as unclear. This is particularly important given not all participants respond to some models of hyperalgesia; it is essential to know the proportion of 'non-responders', and whether these were excluded from analysis. Pre-registration has become increasingly common and is very useful in assessing reporting bias and determining if analysis was pre-specified. In the absence of pre-registration, reporting bias was assessed to be low risk if there was a clearly-defined disprovable hypotheses, as it suggests that results could be interpreted in a logical framework. Overall, the small sample sizes typically used in this type of fMRI study (due to cost and technicality of data collection) may introduce reporting bias in the number of foci that are false positives. More lenient analysis methods can be used to increase the number of foci, or region of interest analysis methods can be designed post-hoc to identify significant results that were not present in the whole-brain analysis (David et al. 2013).

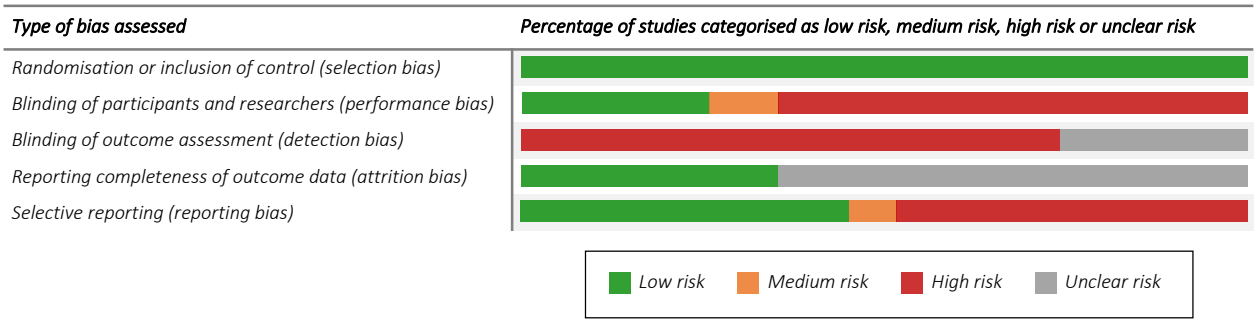

Figure 2. Risk of bias assessment for all included studies.

For each study, the risk of bias was assessed based on five standardised domains; selection bias, performance bias, detection bias, attrition bias and reporting bias. Assessment criteria for each domain were adapted for the types of study included in this review. The percentage of studies categorised as low risk (green), medium risk (orange), high risk (red) or unclear risk (grey) for each domain are shown with the coloured bars.

1.4.1 Models of central and/or peripheral sensitisation

In this review, studies that utilised nine different human experimental models of central and/or peripheral sensitisation were identified. There were 19 studies using a capsaicin model (2 using intradermal injection and 16 using topical application, either with or without heat application with a thermode). There were 2 studies that utilised a UV-B model, 3 studies that utilised an electrical stimulation paradigm, 1 study that used opioid withdrawal to induce hyperalgesia, 1 study that used intradermal endothelin-1 (ET-1) and 3 studies that utilised thermal stimulation. There were 2 studies that utilised a menthol model and 1 study utilised a CTX model, both to induce cold allodynia. The range of experimental models identified in the studies, and the frequency at which they were used, is shown in Figure 3.

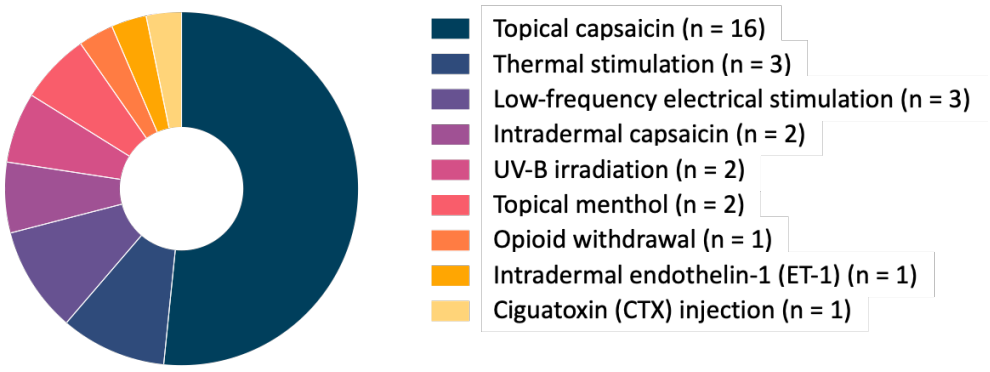

Figure 3. Experimental models utilised by the studies identified in this systematic literature review

The review identified 31 studies in total, across which there were 9 different human experimental models used. The most common model by far was the use of topical capsaicin (with or without additional heat application with a thermode), which was used in 19 of the studies identified. All other central sensitisation models identified were used in 1-3 studies each.

The majority of studies primarily focussed on characterising the brain activation involved in processing primary or secondary hyperalgesia. Two studies compared stimuli responses in the primary and secondary hyperalgesia conditions, and two studies investigated whether the area of secondary hyperalgesia that develops is correlated with anatomical volumes of pain related brain regions.

In total, 8 studies identified in this review included assessment of some form of analgesia, including pharmacological treatments (5 studies), application of cold stimulus (1 study), application of repetitive transcranial magnetic stimulation (rTMS) 1Hz over the posterior parietal cortex (1 study), or application of anodal motor cortex (M1) transcranial direct current stimulation (tDCS) (1 study). Pharmacological treatments assessed include gabapentin, ibuprofen, cyclooxygenase inhibitors (parecoxib and acetylsalicylic acid (ASA)), lidocaine and delta-9-tetrahydrocannabinol (THC).

As per the inclusion criteria for the review, all studies included fMRI data acquisition. The strength of the MRI scanner used varied; 13 out of the 31 studies used a 1.5 Tesla scanner, while the remaining 18 studies used a 3 Tesla scanner.

All studies included in the systematic literature review analysis are summarised in Table 1, which includes the number of participants, the model of central sensitisation used, the stimulus modality, the site of stimulus application relative to the model application site, and whether or not the study includes an analgesic component.

Table 1. Studies included in the systematic literature review analysis.

There were 31 studies identified in total from the literature searches. Data extracted from each study is shown, including the number of participants (N), experimental model used, site of application, stimulus modality used, stimulation area relative to model application site, and whether the study included the assessment of analgesics.

First author, YEAR	*N*	*Experimental model*	*Site of application*	*Stimulus modality*	*Stimulation area relative to model application site*	*Analgesic component*
Baron, 1999	9	Intradermal capsaicin	Dominant forearm	Mechanical	Secondary	-
Maihöfner, 2004	11	Topical capsaicin + heat	Left forearm	Mechanical	Secondary	-
Ianetti, 2005	12	Topical capsaicin + heat	Leg	Mechanical	Secondary	Gabapentin and placebo
Maihöfner, 2005	12	Topical capsaicin	Left forearm	Thermal and mechanical	Primary and secondary	-
Zambreanu, 2005	12	Topical capsaicin + heat	Right lower leg	Mechanical	Secondary	-
Maihöfner, 2007	14	UV-B	Left forearm	Mechanical	Primary	Parecoxib and acetylsalicylic acid (ASA) and placebo
Mainero, 2007	12	Topical capsaicin + heat	Right ophthalmic division (V1) of trigeminal nerve	Mechanical	Primary and secondary	-
Moulton, 2007	12	Topical capsaicin	Left maxillary division (V2) of trigeminal nerve	Thermal and mechanical	Primary	-
Seifert, 2007	12	Menthol	Forearm	Thermal (cold)	Primary	-
Lee, 2008	15	Intradermal capsaicin	Right leg	Mechanical	Secondary	-
Mohr, 2008	17	Topical capsaicin	Right leg	Thermal	Primary	-
Mohr, 2008	15	Topical capsaicin	Right hand	Thermal	Primary	Cold stimulus
Seifert, 2008	14	UV-B	Right forearm	Thermal and mechanical	Primary	-
Stammler, 2008	12	Electrical stimulation	Right forearm	Mechanical	Secondary	-
Seifert, 2009	12	Electrical stimulation	Right foot	Mechanical	Secondary	Lidocaine and placebo
Seifert, 2010	10	Electrical stimulation	Right forearm	Mechanical	Secondary	Repetitive transcranial magnetic stimulation (rTMS) or sham stimulation

Shenoy, 2011	12	Topical capsaicin	Left forearm	Thermal	Primary	-
Wanigasekera, 2011	33	Opioid withdrawal	Right forearm	Thermal and mechanical	N/A (injury-free model)	-
Hans, 2013	9	Intradermal endothelin-1	Forearm	Mechanical	Secondary	-
Lee, 2013	15	Topical capsaicin	Right leg	Mechanical	Secondary	Delta-9-tetrahydrocannabinol (THC) and placebo
Liljencrantz, 2013	18	Topical capsaicin + heat	Left leg	Tactile	Secondary	-
Rempe, 2014	16	Topical capsaicin + heat	Right forearm	Mechanical	Secondary	-
Asghar, 2015	40	Heat (contact thermode)	Non-dominant leg	Mechanical	Primary and secondary	-
Rempe, 2015	16	Topical capsaicin + heat	Right forearm	Thermal	Primary	-
Wanigasekera, 2016	24	Topical capsaicin	Right leg	Tactile and mechanical	Secondary	Gabapentin, ibuprofen and placebo
Eisenblätter, 2017	12	Ciguatoxin (CTX) injection	Foot	Thermal	Primary	-
Löken, 2017	19	Topical capsaicin	Forearm	Tactile	Primary	-
Hansen, 2018	118	Heat (contact thermode)	Right leg	-	-	-
Forstenpointner, 2019	8	Menthol or nerve block	Right forearm	Thermal (cold)	Primary	-
Hansen, 2019	115	Heat (contact thermode)	Right leg	-	-	-
Meeker, 2019	27	Topical capsaicin + heat	Left leg	Mechanical	Secondary	Anodal motor cortex (M1) transcranial direct current stimulation (tDCS)

1.4.1.1 Capsaicin-induced hyperalgesia models

Capsaicin (8-methyl-N-vanillyl-6-nonenamide) is a transient receptor potential vanilloid-1 (TRPV1) agonist (Nelson 1919; Caterina et al. 1997). It is commonly used in pain studies; it causes a burning sensation when applied topically or intradermally, and produces an area of secondary mechanical hyperalgesia outside the primary application site which is an analogue of the mechanical hyperalgesia often seen in patients with neuropathic pain. Three types of capsaicin model have been used in functional imaging studies identified in this review: intradermal capsaicin injection (Baron et al. 1999; Lee et al. 2008), topical capsaicin application (Maihöfner and Handwerker 2005; Moulton et al. 2007; Mohr, Leyendecker, and Helmchen 2008; Mohr et al. 2008; Shenoy et al. 2011; Lee et al. 2013;

Wanigasekera et al. 2016; Löken, Duff, and Tracey 2017), and topical capsaicin application with heat applied by a thermode (most commonly 45°C, either before or after capsaicin application to the skin) (Maihöfner et al. 2004; Iannetti et al. 2005; Zambreanu et al. 2005; Mainero et al. 2007; Liljencrantz et al. 2013; Rempe et al. 2014, 2015; Meeker et al. 2019).

Capsaicin studies to characterise neuronal response during hyperalgesia:

The two studies using the intradermal capsaicin injection model both aimed to characterise the neural response to secondary hyperalgesia. The first compared an identical mechanical stimulus on both forearms, one without capsaicin (perceived as non-painful) and one following injection of 20 µL of 0.5% capsaicin solution to evoke secondary hyperalgesia (perceived as painful). fMRI data were acquired using a 1.5 Tesla scanner. The study identified that, during hyperalgesia, the left middle frontal gyrus and the left inferior frontal gyrus showed significantly higher activation compared to during mechanical non-painful stimulation. However, the authors discuss that the number of active voxels was highly variable between individuals meaning subtle changes may have been missed, and that changes in the brainstem and thalamus that could be involved in mechanical hyperalgesia were not addressed (Baron et al. 1999). The low samples size of 9 participants and a 1.5T resolution may have also contributed to the variability in the findings and the lack of activation in other well-known pain processing brain regions shown in later studies.

The second study builds on this, using a crossover design to investigate the neural activation to central sensitisation elicited following intradermal injection of capsaicin (50µg of dissolved in 0.1 ml of Tween 80). fMRI data was acquired using a 3 Tesla scanner. Punctate stimulation matched for perception of pain intensity in the hyperalgesia state and the no hyperalgesia state revealed significantly higher activity in the brainstem (specifically the mesencephalic pontine reticular formation) and the thalamus during hyperalgesia compared to no hyperalgesia. The study primarily concludes a role for the brainstem in maintaining a centrally sensitised state, while activity in the somatosensory cortex is associated with the perception of increased pain intensity that is present during central sensitisation (Lee et al. 2008). This finding is aligned to an earlier finding in a topical capsaicin study described below, which also identified a role for brainstem regions (NCF and the rostral PAG and superior colliculi) in facilitation central sensitisation. A key feature of the intradermal capsaicin model used in these two studies is that it does not result in an ongoing pain sensation, therefore the findings are specific for the neural response to hyperalgesia and not contaminated with any ongoing pain component.

The topical capsaicin model, both with or without heat applied using a thermode, has been the most extensively used hyperalgesia model used in imaging studies. Studies using topical capsaicin (without heat) most commonly used 1% capsaicin (range 0.075% to 2.5%), either in cream format or in 70% ethanol solution. The capsaicin was left on the skin for at least 15 minutes in all studies before fMRI data acquisition, with some studies removing the capsaicin prior to scanning and some leaving it on for the duration of the scan. Studies using topical capsaicin with heat primarily used a heat/capsaicin sensitisation model previously described (Petersen and Rowbotham 1999). Skin is heated to 45°C for 5 minutes, before capsaicin is applied topically. Capsaicin concentration ranged from 0.075% to 10%, and was also either in cream format or ethanol solution.

In many of the studies using topical capsaicin (with or without heat) the primary aim of the study was to characterise different aspects of the neural signature of peripheral or central sensitisation, by applying thermal or mechanical stimuli to the areas of primary or secondary hyperalgesia. Topical capsaicin models also result in ongoing unprovoked pain in addition to any pain stimuli applied.
One study looked specifically at a role for the brainstem in central sensitisation, based on data from animal studies that have shown evidence for supraspinal contributions to the development and maintenance of central sensitisation and secondary hyperalgesia (Zambreanu et al. 2005). fMRI data were acquired using a 3 Tesla scanner to record brain responses to punctate stimulation with capsaicin-induced secondary hyperalgesia compared to control. Two distinct activation regions showing significantly increased activity during secondary hyperalgesia compared to control were observed in the brainstem, identified as the NCF and the rostral PAG and superior colliculi. The results support a role for these brainstem regions in facilitating central sensitisation.

One study investigated whether brain activations for primary and secondary hyperalgesia may differ (Maihöfner and Handwerker 2005). The study looked at differential coding of thermal hyperalgesia (primary hyperalgesia) and mechanical hyperalgesia (secondary hyperalgesia), using a block design consisting of randomised 21 second blocks. Stimuli consisted of mechanical stimuli (pin-prick stimuli with frequency 1Hz) and thermal stimuli (thermode heated to 2°C below the individual's heat pain threshold). While there was no significant difference in pain intensity ratings, the study results show a significant difference in pain unpleasantness ratings between the two types of hyperalgesia. Individual differences in unpleasantness ratings were shown to correlate with individual differences in the contralateral anterior insula cortex, cingulate cortex and middle frontal cortex. Overall, the study concludes there are different brain activations produced by thermal and mechanical hyperalgesia, due to different psychophysical properties.

Three studies looked at features of allodynia specifically; the neural activation during dynamic-mechanical allodynia (DMA) (Maihöfner et al. 2004), the contribution of C-tactile afferents in dynamic-tactile allodynia (Liljencrantz et al. 2013) and the modulation of the unpleasantness of capsaicin-induced DMA by Aβ afferent firing rate (Löken, Duff, and Tracey 2017). Stimuli to test allodynia were applied by stroking a soft brush or cotton wool swab on the skin; in the first two studies the stimuli were applied to the secondary area (i.e., not the same site as capsaicin was applied), whereas in the third study the stimuli were applied to the primary area of capsaicin application. The first study demonstrated significant increases in the BOLD response in the contralateral primary somatosensory cortex, parietal association cortex, and inferior frontal cortex, and bilateral secondary somatosensory cortices (SII) and insula cortex during painful brush stroking in allodynia compared to non-painful brush stroking (Maihöfner et al. 2004). Allodynia is due to central sensitisation enabling low threshold mechanoreceptors (LTMs) to signal to sensitised nociceptive neurons in the spinal dorsal horn, and the LTMs responsible for allodynia are considered to be Aβ afferents. However, the second study indicates an additional role for C-tactile afferents. C-tactile afferents signal pleasantness of gentle stroking in normal conditions. Imaging results showed multivoxel pattern differences in the posterior insula cortex – the primary receiving area for thin fibre signalling – to stroking during allodynia compared to control. There was also a decrease in activation of the medial prefrontal cortices which are involved in processing pleasure from C-tactile fibre input. Overall, this suggests there is a decrease in C-tactile afferent processing during dynamic tactile allodynia. However, the study also included two patients lacking Aβ afferents who did not develop allodynia, indicating the development of allodynia is reliant on Aβ signalling (Liljencrantz et al. 2013). The final allodynia study demonstrates an unexpected relationship during DMA between frequency of Aβ firing rates and the unpleasantness of the sensation elicited, with low frequency firing (low brush stroke velocity) associated with higher unpleasantness compared to high frequency firing. Imaging data showed increased cortical activity in the somatosensory cortex and insula cortex in response to low Aβ firing rates. These regions were previously associated with pain processing during brushing of sensitized skin but not normal skin. Overall, the study concludes a dual role for Aβ afferents during the injured state, with both pleasant and unpleasant sensations evoked depending on stroking stimulus frequency (Löken, Duff, and Tracey 2017).

Two studies applied capsaicin to areas of the face to investigate sensitisation in the trigeminal nociceptive pathway, with one investigating thermal hyperalgesia (using two painful heat stimuli of different intensities) and allodynia (using brush stimuli) (Moulton et al. 2007). All stimuli (brush and thermal) were applied to the site of capsaicin application (primary hyperalgesia). The three types of

stimuli were applied in three fMRI sessions, with data collected on a 3-Tesla scanner. During each session, the stimuli were alternated between capsaicin and control sites, with intensity of the thermal stimuli adjusted to be perception matched at each site. The study identified differences between capsaicin and control sites across the trigeminal nociceptive pathway in all stimulus conditions, with higher activation in the trigeminal ganglion and nucleus, thalamus and somatosensory cortex for capsaicin compared to control, as well as significant changes in the bilateral dorsolateral prefrontal cortex and amygdala. The other study focussed on DMA, aiming to compare primary vs. secondary DMA using soft brush to apply stimuli to either normal skin, or the primary and secondary areas of DMA (Mainero et al. 2007). Brush stimuli were applied in four 30 second blocks each followed by 30 seconds rest, during two fMRI sessions (capsaicin session and control session) in which data were acquired using a 3-Tesla scanner. The results showed significantly increased activity in the ipsilateral spinal trigeminal nucleus in primary and secondary DMA compared to control. Some activity in supraspinal areas was shown to be increased in primary DMA compared to secondary DMA, including in the rostroventromedial medulla, pons reticular formation and dorsolateral PAG, whereas the medial reticular formation of the caudal medulla was more active during secondary DMA compared to primary DMA.

Two studies looked specifically at spinal cord activations in response to mechanical hyperalgesia (Rempe et al. 2014) and to thermal hyperalgesia (Rempe et al. 2015). The studies employed similar experimental protocols involving fMRI data acquisition using a 3T scanner in two sessions, with heat or mechanical stimuli applied before sensitisation, and then applied after sensitisation with capsaicin. For mechanical hyperalgesia stimuli were applied to an area outside the area of capsaicin application (secondary hyperalgesia), whereas for thermal hyperalgesia stimuli were applied to the primary area of capsaicin application (primary hyperalgesia). In both studies, it was shown there are changes in the spinal and supraspinal activity in the sensitised condition compared to control. There was increased activity in the ipsilateral dorsal grey matter of the spinal cord during secondary mechanical hyperalgesia compared to mechanical stimulation before sensitisation, which was shown to be correlated with a decrease in activity in some supraspinal centres including the dorsolateral pontine tegmentum (DLPT), RVM, and subnucleus reticularis dorsalis (SRD). The study concludes this suggests that during hyperalgesia nociception is facilitated by decreased descending endogenous inhibition (Rempe et al. 2014). In contrast, during thermal hyperalgesia, there was increased activation in similar areas (including bilateral ruber nuclei, contralateral DLPT, RVM and SRD), that were now positively correlated with activations in the ipsilateral dorsal horn of the spinal cord (Rempe et al. 2015).

One study focussed on how cognitive factors may result in differences in the neural response to self- vs. externally administered thermal hyperalgesia (Mohr, Leyendecker, and Helmchen 2008). During data acquisition with a 1.5 Tesla scanner, thermal stimuli of four different intensities (30, 37, 40, 43°C) were applied to capsaicin-treated skin on the participant's leg using a rope and lever system, with one rope controlled by the investigator and the other rope controlled by the participant. The 30°C stimulus served as a high-level baseline for each condition, used to eliminate components such as the motor response to move the rope. fMRI data showed graded activity in the anterior insula and ACC during thermal hyperalgesia depending on stimulus intensity (once the high-level baseline was subtracted), in addition to stronger activity in the posterior insula during self-administration and stronger activity in the prefrontal cortex during investigator-administration.

One study used fMRI to characterise the response to the Contact Heat Evoked Potential Stimulator (CHEPS) applied to an area of capsaicin-induced hyperalgesia, with the aim to develop topical capsaicin in conjunction with CHEPS and fMRI as a useful model of neuropathic pain. (Shenoy et al. 2011). The study design consisted of two scanning sessions, one baseline (pre-capsaicin) and one following application of capsaicin. During each session a 51°C CHEPS stimuli for duration 800 milliseconds was applied 32 times, during data acquisition using a 1.5 Tesla scanner. Subject mean pain ratings were significantly increased in the post-capsaicin session compared to the pre-capsaicin session, and this was accompanied by increased BOLD response in the contralateral posterior cingulate gyrus, precentral and postcentral gyrus, the superior frontal gyrus, left anterior cingulate gyrus, middle frontal gyrus, and cuneus with bilateral activation in the caudate nucleus. Region of interest analysis showed significant increase in BOLD signal in the contralateral insular during the post-capsaicin session compared to pre-capsaicin.

Capsaicin studies to characterise neural response to analgesia:

In other capsaicin studies, the primary aim was to characterise the neural response to various analgesics. The first explored pharmacological modulation by ***gabapentin*** during a normal state and a centrally sensitised state (Iannetti et al. 2005). The study design consisted of a four-way crossover design, with 4 sessions consisting of gabapentin (180mg) or placebo and centrally-sensitised state or normal state, with the order of the drug or placebo conditions randomised. In each session involving central sensitisation, thermal stimulation and capsaicin were applied to induce central sensitisation two hours after gabapentin/placebo were administered. Three hours after drug/placebo administration, during fMRI data acquisition using a 3 Tesla scanner, 20 mechanical stimuli were applied to each leg using a 60g von-Frey hair.During fMRI data acquisition using a 3 Tesla scanner, 20

mechanical stimuli were applied to each leg using a 60g von-Frey hair. The three main findings were that gabapentin reduced activations in the bilateral operculoinsular cortex independent of whether central sensitisation was present, that gabapentin reduced activation in the brainstem during central sensitisation only and that gabapentin reduced stimulus-induced deactivations during central sensitisation only, an effect that was more robust than the effect on brain activation. The study concludes that gabapentin has a major effect during the centrally-sensitised state and a reduced but measurable effect during the normal state.

One study investigated the use of cold stimuli to relieve capsaicin-induced pain (Mohr et al. 2008). Four thermal stimuli (0, 20, 30 and 43°C) were applied to the skin 20 times each in a random order, using a contact thermode applied for 4 seconds. This was repeated in two fMRI sessions, one pre-capsaicin and one post-capsaicin, with data acquired using a 1.5 Tesla scanner. Visual analogue scale (VAS) ratings showed that participants perceived the 0°C stimuli as painful in the pre-capsaicin session, but as pleasant in the post-capsaicin session. BOLD responses in the pre-frontal cortex and PAG were increased in the post-capsaicin session compared to the pre-capsaicin session, and were positively correlated with VAS ratings for perceived pleasantness. Connectivity analysis also showed contributions from the prefrontal cortex activity and PAG that were cold-dependent during the post-capsaicin session, leading the authors to propose that the pain relief perceived during the cold stimuli results in part from activation of endogenous descending inhibition.

One study investigated the pharmacological effects of a ***cannabinoid*** - delta-9-tetrahydrocannabinol (THC) – on the pain response in hyperalgesia (Lee et al. 2013). Participants completed four study sessions under different conditions; participants were administered either 15mg THC or placebo (orally), repeated in either normal state or capsaicin-induced hyperalgesia. Capsaicin or placebo cream was applied to the skin two hours post-dose, and fMRI was then performed three hours post-dose. During each session, fMRI data was acquired using a 3-Tesla scanner. Scans consisted of 5 minutes of resting state (no task), 15 minutes punctate mechanical stimuli (21 stimuli applied to the area of secondary hyperalgesia with a handheld probe) and 5 minutes of a visual control task (black and white checkerboard). Intensity and unpleasantness of ongoing and provoked pain was rated using a visual analogue scale (VAS). Behavioural data showed that during secondary hyperalgesia, THC significantly reduced the perceived unpleasantness of ongoing and provoked pain compared to placebo, but had no effect on the perceived intensity of ongoing or provoked pain. BOLD data showed that there was increased activity in the ACC and thalamus during capsaicin-induced hyperalgesia, and that there was a significant reduction in this ACC activity during the THC session compared to placebo, but no

significant change in the thalamus activity. Region of interest analysis also showed that THC significantly increased BOLD response in the right amygdala compared to placebo, and that the effect of THC on reducing pain unpleasantness was positively correlated with this effect of THC on the capsaicin-induced activity in the right amygdala compared to placebo. THC also significantly decreased the functional connectivity between the right amygdala and primary sensorimotor region during capsaicin-induced ongoing pain, and this reduction was positively correlated with the difference in drug effects on unpleasantness and intensity of the ongoing pain.

One study focussed on the ability of fMRI in conjunction with central sensitisation induced by capsaicin to differentiate between effective analgesia (***gabapentin***) and ineffective analgesia (***ibuprofen***), both compared to placebo, with a view to validate the use of fMRI to guide decision making in drug development (Wanigasekera et al. 2016). The study design comprised of three study visits at which participants received either gabapentin (1200mg), ibuprofen (600mg) or placebo orally, followed by application of capsaicin 90 minutes after dosing, and fMRI data acquisition using a 3-Tesla scanner 150 minutes after dosing. During each scan, 15 stimuli were applied using a soft brush (for allodynia) and 18 stimuli were applied using a punctate probe (for mechanical hyperalgesia). Stimuli were applied in the secondary hyperalgesia area adjacent to the site of capsaicin application. Participants were asked to rate pain intensity and unpleasantness using a visual analogue scale (VAS). Gabapentin, but not ibuprofen, significantly reduced pain intensity and unpleasantness ratings compared to placebo. Gabapentin, but not ibuprofen, also significantly reduced the BOLD response associated with hyperalgesia in the right NCF, left insula and left secondary somatosensory cortex (SII) compared to placebo. Resting state functional connectivity between the left thalamus and left SII was also reduced by gabapentin compared to placebo, but not by ibuprofen. This study demonstrates the ability of resting-state and task MRI techniques to differentiate between effective and ineffective analgesics.

The final study aimed to elucidate the neural mechanism underlying the analgesic effects of motor cortex stimulation using tDCS (Meeker et al. 2019). Following determination of pain thresholds at a screening visit, participants attended three sessions which included anodal, cathodal and sham tDCS in a randomised cross-over design. Following capsaicin application, anodal tDCS was shown to moderately reduce secondary hyperalgesia (measured using pain intensity in response to pin-prick mechanical stimuli) compared to cathodal or sham tDCS. fMRI data acquired using a 3 Tesla scanner showed that the BOLD response following anodal tDCS was normalised to the baseline level in the medial prefrontal cortex, ACC and PAG; key areas in the descending pain modulatory network.

1.4.1.2 UV-B models

Two studies used ultraviolet (UV)-B radiation to induce hyperalgesia on the forearm (Maihofner et al. 2007; Seifert et al. 2008). Both established the minimal erythema dose (MED) for UV-B irradiation in advance, using the same methodology. Both then irradiated an area of skin with UV-B at a dosage of 3 times the MED 24 hours prior to the experimental session itself. UV-B models are not associated with ongoing unprovoked pain. For both UV-B studies stimuli were applied to the site of irradiation, so investigated primary hyperalgesia.

The first study investigated UV-B induced mechanical hyperalgesia at three separate study visits, at which subjects received 5-min intravenous infusions of ***cyclooxygenase inhibitors*** (either 40 mg parecoxib or 1000 mg ASA) or placebo (0.9% saline) (Maihofner et al. 2007). fMRI data were acquired during each visit using a 1.5 Tesla scanner. The experiment consisted of a block design with 3 conditions; mechanical impact hyperalgesia (stimuli applied to UV-B site), acute mechanical pain and tactile stimuli (both applied approximately 5cm away from the UV-B site). Testing was conducted before and 30 mins after drug/placebo infusion. fMRI data showed that in the mechanical impact hyperalgesia and acute mechanical pain conditions there were activations of many brain regions involved in pain perception, including the primary (SI) and secondary (SII) somatosensory cortices, parietal association cortex (PA), inferior parietal lobule, orbitofrontal cortex, superior, middle and inferior frontal cortices, ACC, insula and supplementary motor cortex. With both parecoxib and ASA, there were smaller activations in certain regions, notably in SI, PA, SII, insula, ACC and prefrontal cortices. When comparing the hyperalgesic condition to the acute pain, there was more drug-induced modulation of the PA and inferior frontal cortex during mechanical hyperalgesia, and more drug-induced modulation of the bilateral SII during acute mechanical pain.

The second study investigated brain activations during UVB-induced thermal hyperalgesia and mechanical hyperalgesia (Seifert et al. 2008). The study design was a 2 x 2 factorial block design, in which the factors were sensitisation (hyperalgesia or no hyperalgesia) and stimulus modality (heat pain or mechanical pain). Thermal stimuli were applied with a thermode and mechanical stimuli were applied using a mechanical impact stimulator, and all stimulations for fMRI measurements were perception matched to a numeric rating scale (NRS) rating for pain intensity of 40. fMRI data were acquired using a 1.5 Tesla scanner. fMRI data demonstrated that there are differences in the neural activity associated with mechanical hyperalgesia vs. heat hyperalgesia in response to stimuli of perception matched intensities, suggesting different pathways may be involved in the different types

of hyperalgesia. For heat hyperalgesia activation increased in the prefrontal cortex and PA, whereas for mechanical hyperalgesia activation increased in the SII and posterior insula cortex.

1.4.1.3 Electrical stimulation models

Three studies utilised electrical stimulation models to induce secondary hyperalgesia. The first study applied two different electrical stimulation paradigms to the forearm, each over 35 min; the first paradigm consisted of continuous noxious low-frequency (0.5Hz) stimulation to induce hyperalgesia, and the second paradigm consisted of continuous noxious high-frequency (20Hz) stimulation to induce hypoalgesia/hypoesthesia (Stammler et al. 2008). fMRI data were acquired on a 1.5 Tesla scanner. The scan paradigm used a block design in which pin-prick (both sessions) and von Frey (hypoesthesia session only) mechanical stimuli were applied at a frequency of 1Hz for 21 seconds per block. In the pin-prick hyperalgesia session (which is most relevant for this review), activated brain regions included the somatosensory cortices, parietal cortices, insula, dorsolateral and ventrolateral prefrontal cortices, cuneus, anterior and posterior parts of the ACC, basal ganglia and the thalamus. These activations were greater in the hyperalgesic state compared to baseline (pre-stimulation).

The other two studies used the same transcutaneous low-frequency electrical stimulation model to induce secondary mechanical hyperalgesia, consisting of two electrodes mounted on the skin to deliver electrical pulses of 0.5ms duration at a frequency of 1Hz, with the current initially adjusted to a pre-defined pain rating target then kept constant for the rest of the session. This model applies a repeated painful stimulus for the duration of the session, therefore ongoing acute pain is present in addition to the secondary hyperalgesia (Koppert et al. 2001). Both studies included evaluation of an analgesia intervention. The first investigated the effects of pharmacological modulation by ***lidocaine***, a sodium channel blocker, compared to placebo, using pin-prick stimuli applied during fMRI acquisition with a 1.5 tesla scanner (Seifert et al. 2009). The second investigated the effects of 1Hz rTMS over the posterior parietal cortex (PPC), compared to a sham procedure, also using pin-prick stimuli, this time applied during fMRI acquisition with a 3 Tesla scanner. (Seifert et al. 2010).

To investigate pharmacological modulation by lidocaine, a 2 x 2 factorial analysis – in which factor 1 was pain sensitisation (pin-prick hyperalgesia vs. normal pin-prick) and factor 2 was pharmacological modulation (lidocaine vs. placebo) was performed. The lidocaine (or placebo) infusion was started 20 minutes after the start of the electrical stimulation. Initially, 12 mg/kg was infused intravenously for 10 min, followed by 2 mg/kg/h for 15 min, and the fMRI data was then collected 15 minutes after the start of the infusion. Psychophysics results indicated that lidocaine was anti-hyperalgesic, with

significantly reduced pain intensity ratings to the electrical stimulation and to the pin-prick stimuli applied in the hyperalgesia area, as well as a significantly smaller area of hyperalgesia, with lidocaine compared to placebo. The main fMRI finding of the study was that activity in the medial prefrontal cortex (mPFC) was reduced by lidocaine. The mPFC activity during hyperalgesia was shown to inversely correlate with the extent of hyperalgesia in each individual, and to be predictive for the responsiveness to lidocaine analgesia in each individual (Seifert et al. 2009).

To investigate the role of the PPC in pain perception, the effect of rTMS over the region was compared for three conditions; normal pin-prick, pin-prick hyperalgesia and dynamic-mechanical allodynia. Participants attended five visits, the first involving fMRI and the subsequent four visits involving rTMS (right and left hemispheric, sham-controlled). The rTMS or sham stimulation was applied 16 minutes after induction of hyperalgesia, for 10 minutes duration. It was demonstrated that, compared to sham stimulation, there was a significant decrease in the area of hyperalgesia when rTMS was applied to the contralateral PPC, while there was no significant difference in wither the pain stimulus intensity or the area of allodynia (Seifert et al. 2010).

1.4.1.4 Opioid withdrawal-induced hyperalgesia (OIH)

One study used an injury-free model of central sensitisation by inducing hyperalgesia with opioid withdrawal (Wanigasekera et al. 2011). The opioid used was remifentanil. Out of 23 participants included in the study, 12 participants demonstrated hyperalgesia to thermal stimuli ('responders') and only 3 participants developed hyperalgesia to punctate stimuli. Due to this small number, punctate data was not further analysed. Participants who developed hyperalgesia were identified using within-subject data. A significant increase in intensity scores in at least one of the post-infusion stimulation blocks of the opioid visit when compared with the corresponding stimulation blocks in the saline visit ($p < 0.05$; two-tailed paired t test) was assumed to be evidence of OIH to thermal or punctate stimuli. fMRI data was collected with a 3-Tesla scanner.

The fMRI data from responders showed a significant increase in neuronal response (BOLD activity) in a cluster of voxels in the mesencephalic-pontine reticular formation (MPRF) during the opioid withdrawal period compared to baseline. This area had been demonstrated in a previous fMRI study in humans to be involved in maintaining capsaicin-induced central sensitisation (Lee et al. 2008). A correlation analysis demonstrated a significant negative correlation between ($r=0.61$, $p=0.03$) between the opioid withdrawal-induced increase in pain perception and increase in BOLD activity in

the MPRF region. The authors conclude that this relationship indicates a net descending inhibitory response of the MPRF during OIH.

1.4.1.5 Intradermal Endothelin-1 (ET-1) model

One study used an intradermal endothelin-1 (ET-1) sensitization model to induce secondary mechanical hyperalgesia (Hans et al. 2013). ET-1 is a potent vasoconstrictor that has been shown to induce pain in humans. Prior to scanning, 40µL of a 10^{-6} M ET-1 solution was intradermally injected into the volar surface of the forearm. To assess development of mechanical hyperalgesia, punctate stimuli were applied using a von Frey monofilament at 10 min and 30 min post-injection, on both the injected and non-injected arms, and the hyperalgesic area was defined as a region in which participants reported a distinct change in the quality of the sensation. All participants reported a hyperalgesia state at both 10 min and 30 min time points, with a significant ($p < 0.05$) increase in responsiveness in the injected arm compared to the non-injected arm. There was also a low intensity of ongoing (spontaneous) pain.

After the 30 min time point, fMRI data was acquired using a 1.5 Tesla scanner in a block design, with two conditions (punctate stimulus and baseline), and stimulus blocks alternating between the injected and non-injected arms. The authors report that the fMRI results show that, during hyperalgesic stimulation, the most active cortical regions include the primary and secondary somatosensory cortices, the insula, the inferior parietal lobe, the superior and inferior frontal cortices and the ACC. They report an increase in fMRI signal in activated regions, and an increase in the number of regions activated, during the hyperalgesic condition (injected arm) compared to non-painful tactile stimulation (non-injected arm).

1.4.1.6 Thermal stimulation models

In three studies, a brief thermal sensitisation (BTS) model was used to induce first-degree burn injury (Asghar et al. 2015; Hansen et al. 2018; Hansen et al. 2019). The first study aimed to assess whether there are differences in the neuronal activation in participants who were categorised based on the size of the area of secondary hyperalgesia they develop (as either high- or low- sensitisation responders) (Asghar et al. 2015). The size of the area is based on their phenotypic expression of secondary hyperalgesia. Following screening, at which secondary hyperalgesia was induced and participants categorised based on the size of the hyperalgesia area, an MRI-compatible contact thermode (47°C, 7 min, 9cm^2) was used to induce a first-degree burn injury on the lower leg. During the scans, BOLD responses were measured for pre-burn injury painful pin-prick stimulation, post-burn

injury in the secondary hyperalgesia area and post-burn injury in the primary hyperalgesia area, with a 3-Tesla scanner. In total 40 participants were included (20 in each group). There were no statistical differences between the groups with regard to with regard to age, sex, height or weight ($p > 0.05$). the pin-prick stimulus applied was matched to the participants' mechanical pain threshold, and there were no statistical differences in the mechanical pain thresholds between the 2 groups. There was also no difference in the pain scores between groups in any experimental condition (pre-burn injury, post-burn secondary hyperalgesia or post-burn primary hyperalgesia). BOLD data did show significantly higher activation of the right post-central gyrus, left precuneus, left posterior cingulate cortex, right parahippocampal gyrus, right caudate nucleus and lower activation of right precuneus in high-sensitisation responders compared to low-sensitization responders, in response to pin-prick stimulation of the secondary hyperalgesia area, indicating the two groups are processing pain differently.

The subsequent studies built on this one, aiming to explore whether there is an association between the area of secondary hyperalgesia developed and the anatomical volumes of pain relevant brain regions, such as the caudate nuclei (Hansen et al. 2018), and to explore whether there is an association between the area of secondary hyperalgesia and brain connectivity in known resting-state networks (Hansen et al. 2019). A similar BTS model was used (contact thermode applied to the leg, area 2.5 x 5 cm heated to 45˚C for 3-5 minutes) to induce secondary hyperalgesia, and the area of hyperalgesia was measured using a von Frey filament.

In the first publication, 3-Tesla anatomical MRI data was used to quantify the volume of pain relevant brain structures. There were no significant associations between the area of secondary hyperalgesia and the volume of the right and left caudate nucleus (primary analysis) or the volume of other cortical and sub-cortical structures (secondary analysis), including primary somatosensory cortex, ACC and mid cingulate cortex, putamen, nucleus accumbens, globus pallidus, insula or the cerebellum's white matter and cortex (Hansen et al. 2018).

In the second, 3-Tesla resting state data identified that area of secondary hyperalgesia is associated with increasing and decreasing connectivity in multiple networks (sensorimotor network, fronto-parietal network, and default mode network), suggesting that differences in the phenotypic secondary hyperalgesia areas may be expressed as differences in the resting-state central neuronal activity (Hansen et al. 2019).

1.4.1.7 Models to induce cold allodynia

There were three studies that used models to induce cold allodynia. In all three studies stimuli were applied to the primary site at which the experimental model was applied. The first study used 200µl of 40% menthol solution applied to the forearm to induce cold allodynia (Seifert and Maihofher 2007). The study design consisted of a block design fMRI paradigm. Prior to fMRI data acquisition, the cold pain threshold was identified for each participant, then the experiment included 3 blocks; innocuous cold (5°C above cold pain threshold – not painful), noxious cold (5°C below cold pain threshold – painful), and then, following the application of menthol for 15 minutes, cold allodynia (5°C above cold pain threshold – now painful due to menthol-treatment).

fMRI data were acquired using a 1.5 Tesla scanner. The results of contrast analyses comparing cerebral activations in each of the 3 conditions showed stronger activation in the anterior insula, bilateral dorsolateral prefrontal cortices, the ACC and bilateral inferior frontal cortex in the cold allodynia condition compared to perception-matched noxious cold, whereas there was no difference in the posterior contralateral insula – which is expected as this region has been shown to code temperature intensity (Craig et al. 2000).

The second study, aiming to extend the previous study, induced reversible cold allodynia using shallow intracutaneous injection of 1.5nM CTX into the dorsal surface of the right foot (Eisenblätter et al. 2017). fMRI data was acquired on a 3-Tesla scanner. The experimental paradigm consisted of a block design with 4 sections; section 1 was warm stimulation (42-44°C) on the CTX site, section 2 was cold stimulation (18°C) on the CTX site, section 3 was warm stimulation (42-44°C) on the control site, and section 4 was cold stimulation (18°C) on the control site. For each stimulation there was a 4 second dynamic period, when increasing or decreasing to target temperature, followed by a 15 second constant temperature period. There was a 20 second rest between each stimulation.

fMRI data showed bilateral brain responses in the medial insula, medial cingulate cortex, secondary somatosensory cortex, frontal areas, and cerebellum during cold allodynia. When compared to innocuous cold, the cold allodynia predominantly activated mid-anterior parts of the insula cortex. There were more robust changes in the BOLD response, and more brain areas activated, during the dynamic period when the cold stimulus was applied to the CTX site compared to the constant temperature period. This was not seen in the control site data.

The final cold allodynia study used two experimental models, each repeated in every participant over two sessions. In one session, menthol was topically applied to the skin (causing peripheral nociceptor sensitisation, resulting in increased C fibre input) whereas in the other session, the superficial radial nerve at the right forearm was mechanically blocked (causing inhibition of A-delta fibre input, reducing inhibition of central pain processing) (Forstenpointner et al. 2019). fMRI data was acquired using a 1.5 Tesla scanner. A block design was used, with alternating blocks of neutral thermal stimulation (32°C) or cold thermal stimulation (adjusted to the participants cold pain threshold with 4 temperatures; +6°C, +3°C, −3°C, and −6°C above or below threshold). Spontaneous pain was not reported during the fMRI sessions by any subjects.

fMRI data demonstrated that the two different types of cold allodynia represented with the two experimental models induce activity in different brain areas representative of the different underlying mechanism of each type. Contrast analysis showed that menthol produced significantly stronger activation of the left lateral thalamus and primary and secondary somatosensory cortices, whereas nerve block produced significant BOLD signal increases in the left medial thalamus, ACC, and bilateral medial and superior frontal cortex.

1.4.2 Neural response during hyperalgesia compared to control: CBMA results

During further screening of the reports for eligibility to be included in the CBMA, there were 12 studies identified that met these inclusion criteria and reported activation coordinates of interest, with a total of 14 contrasts for the hyperalgesia state vs. control/non-hyperalgesia state. Co-ordinates for each contrast were manually extracted. The peripheral and/or central sensitisation models used in the eligible studies covered a range of the total spectrum of models included in this review; 7 studies used the topical capsaicin model, 1 study used the intradermal capsaicin model, 1 used menthol, one used UV-B, 1 used electrical stimulation and 1 used ciguatoxin (CTX) injection. Studies included in the CBMA are shown below in Table 2.

Table 2. Studies included in the co-ordinate based meta-analysis (CBMA)

There were 12 studies identified that included activation co-ordinates meeting the inclusion criteria. Data extracted from each study is shown, including the number of participants (N), model of central sensitisation used, stimulus modality used, contrast for which activation co-ordinates are reported, and the number of peak co-ordinates reported.

First author, YEAR	*N*	*Model of central sensitisation*	*Stimulus modality*	*Contrast*	*Number of peak co-ordinates*
Maihöfner, 2004	11	Topical capsaicin with heat	Mechanical	Allodynia minus brush-related activations	7
Maihöfner, 2005	12	Topical capsaicin	Thermal and mechanical	[A] Pin-prick hyperalgesia minus pin-prick stimulation [B] Thermal hyperalgesia minus thermal stimulation	7 15
Zambreanu, 2005	12	Topical capsaicin with heat	Mechanical	Secondary hyperalgesia compared with control	15
Mainero, 2007	12	Topical capsaicin with heat	Mechanical	Brush to the secondary area vs. brush to the untreated skin	11
Seifert, 2007	12	Menthol	Thermal (cold)	Cold allodynia vs. noxious cold	3
Lee, 2008	15	Intradermal capsaicin	Mechanical	Punctate stimulation hyperalgesic state vs. normal state	17
Mohr, 2008	15	Topical capsaicin	Thermal	Thermal stimulation on capsaicin-treated skin vs. untreated skin	11
Seifert, 2008	14	UV-B	Thermal and mechanical	[A] Thermal hyperalgesia vs. normal thermal pain [B] Mechanical hyperalgesia vs. normal mechanical pain	12 21
Seifert, 2009	12	Electrical stimulation	Mechanical	Areas more activated during hyperalgesia	21
Liljencrantz, 2013	18	Topical capsaicin with heat	Tactile	Allodynia > Control	17
Eisenblätter, 2017	12	Ciguatoxin (CTX) injection	Thermal	Cold allodynia vs innocuous cold	7
Löken, 2017	19	Topical capsaicin	Tactile	sensitised > normal skin	4

From the 12 studies included in the CBMA, a total of 168 activation foci were reported. Across studies, the foci commonly appeared in the key regions associated with hyperalgesia that are discussed above, including the primary and secondary somatosensory cortices, insula cortex, cingulate cortex, parietal cortex, thalamus, NCF and PAG. All reported co-ordinates for peak activations were transformed to a 2.5mm spherical mask and plotted onto the MNI512 1mm standard brain image, shown in Figure 4.

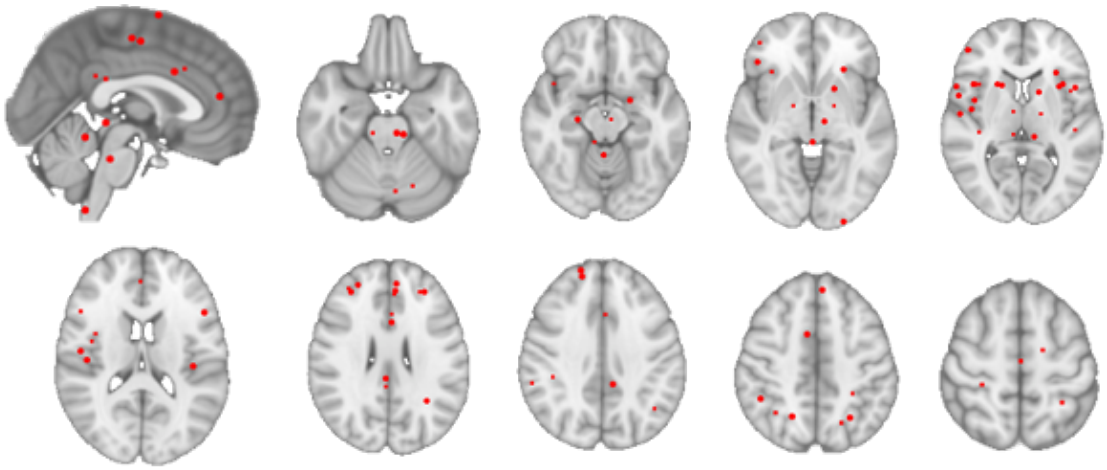

Figure 4. Extracted peak co-ordinates included in the CBMA

Co-ordinates for peak activation voxels were manually extracted from each study. Each was made into a peak voxel mask then transformed into a 2.5mm spherical mask. The spherical masks for all peaks are shown here on the MNI512 1mm brain. Slices shown are (L-R, top row first): sagittal section, axial sections taken at z = 48, 58, 68, 78, 88, 98, 108, 118, 128.

CBMA performed on the co-ordinates extracted for the contrast hyperalgesia state vs. control/no hyperalgesia state (n = 14) produced 6 clusters that were statistically significant at the FDR of 0.05. The cluster locations, in order of size from largest to smallest, were the right anterior insular cortex, left anterior insular cortex, left cingulate gyrus, right thalamus, right mid-insular cortex and right inferior parietal lobe. These regions summarise the most commonly reported regions showing increased pain response to secondary hyperalgesia across the 12 independent studies included. The activation clusters are shown in Figure 5.

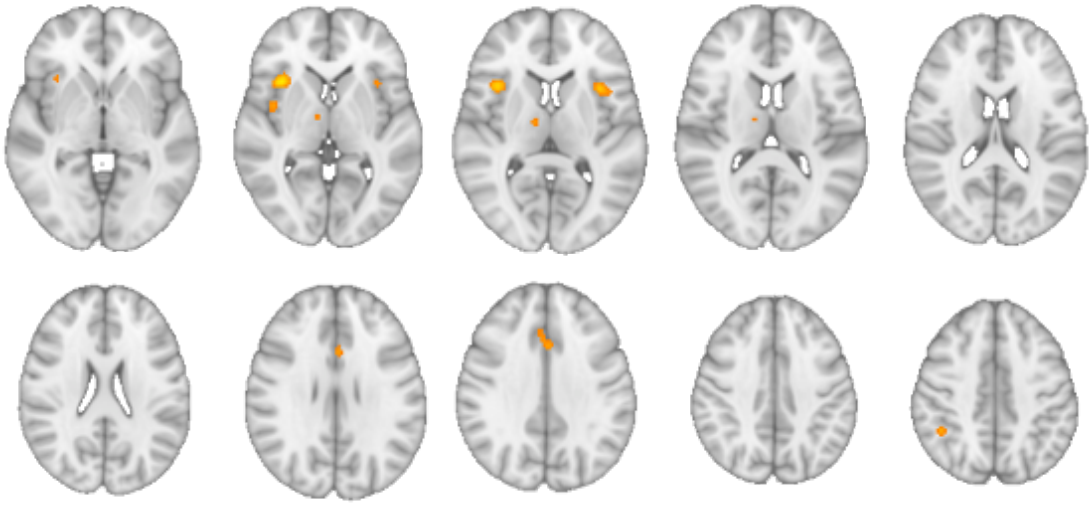

Figure 5. Activation clusters for CBMA of hyperalgesia state vs control/no hyperalgesia state

ALE cluster map showing the 6 clusters identified in the CBMA. Cluster locations, in descending size order, are right anterior insular cortex, left anterior insular cortex, left cingulate gyrus, right thalamus, right mid-insular cortex and right inferior parietal lobe. ALE clusters are shown here on the MNI512 1mm brain. Slices shown are (L-R, top row first): axial sections taken at z = 70, 75, 80, 85, 90, 95, 100, 105, 110, 115.

1.5 Discussion

1.5.1 Comparison of different peripheral and/or central sensitisation models

This review identified functional imaging studies using 9 different peripheral and/or central sensitisation models in humans, which represent a subset of all models as in a recent review there were more than 15 different central sensitisation models described (Quesada et al. 2021). The 9 models include the most commonly used human experimental models (such as capsaicin models, UV-B models and thermal stimulation models), with one notable exception being the use of cutaneous high-frequency electrical stimulation (HFS). This model typically involves stimulation via a small circular array of surface electrodes delivering high-frequency (100Hz) 1s duration trains repeated five times at 10s interval. Although there is limited data on the use of this model with pharmacological modulation, it does have relevant desirable features for imaging studies, including fast and straightforward induction of secondary hyperalgesia and maintenance of secondary hyperalgesia for several hours (Quesada et al. 2021; Klein et al. 2004; Pfau et al. 2011). These features make it a promising model to be utilised in future fMRI studies.

By far the most common model used in the studies was the use of topical capsaicin, which was used in 16 studies. Half (8 studies) used the topical capsaicin with application of heat using a thermode, whereas the other half used topical capsaicin alone. Both methodologies work well, with the major advantage of the heat and capsaicin model being a longer duration of sensitivity, with stable areas of secondary hyperalgesia lasting up to 4 hours with heat rekindling (Petersen and Rowbotham 1999). This is advantageous in fMRI studies as it is important that the hyperalgesia induced by the model remains stable for the duration of the data acquisition, which can be 1-2 hours depending on the study design. One challenge with using capsaicin models is that the response to capsaicin can be variable, with some developing very low hyperalgesia or allodynia response (Liu et al. 1998). It would be important to account for this in the experiment design to either conduct pre-screening to exclude non-responders or ensure a large enough sample size to achieve adequate power with the non-responders included in analysis, which is challenging in imaging studies due to the expensive and time-consuming nature of MRI data acquisition.

The further types of experimental models used (UV-B irradiation, electrical stimulation, opioid withdrawal, intradermal ET-1 injection, thermal stimulation, menthol and CTX injection) were used in only 1-3 studies per model. It is therefore challenging to make conclusions about the advantages and disadvantages of their use in imaging experiments. They have been shown to be feasible for use in imaging studies with spatial and temporal properties conducive to allow fMRI data acquisition. Similar to capsaicin as discussed above, the use of opioid withdrawal was shown to induce hyperalgesia in only a sub-set of participants, which is consistent with previous evidence (Wanigasekera et al. 2011; Jensen et al. 2009), and would need to be accounted for in the experiment design.

1.5.2 fMRI as an objective measure of pain perception and analgesic efficacy

The many types of sensitisation models in studies identified in this review, as well as the variation of experiment design, stimulus modalities and stimulus application sites make direct comparison of the studies challenging. However, a key strength noted is that despite this variability the fMRI data results describe consistent patterns of neural activation in the sensitised state across studies. This is further validated by the CBMA conducted in this review, demonstrating that even across multiple experimental conditions fMRI has provided consistent information about underlying neural activations in the hyperalgesia state. Although these regions are consistently activated in response to experimental pain models there remains uncertainty about whether it can be considered a neural 'signature' for pain perception, with a need for experiment control arms to be carefully designed to match unpleasantness, salience and relevance of the pain stimuli (Mouraux and Iannetti 2018). For

example, it has been demonstrated that the insula, a region repeatedly shown to be activated in response to pain stimuli is also responsive to other types of salient stimuli (Liberati et al. 2016). However, this does not reduce the potential utility of fMRI for evaluation of pain perception in experimental settings. FMRI is a technique that provides a wealth of information about the whole-brain response to pain stimuli and enables objective measurement of neural target engagement for analgesics. It also has valuable potential as a biomarker to predict treatment response and stratify patients (Mouraux and Iannetti 2018), and to provide objective pain-related indicators with the required specificity and sensitivity to diagnose pain conditions, to evaluate risk of developing chronic pain conditions and to demonstrate analgesic efficacy (Tracey, Woolf, and Andrews 2019).

The human experimental models of peripheral and/or central sensitisation in conjunction with fMRI are useful for assessing analgesic efficacy in placebo-controlled studies, as demonstrated by the studies included in this review that include assessment of gabapentin, parecoxib and acetylsalicylic acid (ASA), lidocaine, delta-9-tetrahydrocannabinol (THC), and ibuprofen. Importantly for clinical trials, fMRI has been shown to be effective in distinguishing between an effective analgesic (gabapentin) and an ineffective analgesic (ibuprofen) (Wanigasekera et al. 2016). There are limitations relating to the comparability of these studies with clinical applications; for example, all studies provide only a single dose of analgesic. In addition, experimental central sensitisation models are not fully representative of the ongoing pain characteristic of chronic pain conditions, although they do provide a useful surrogate (Quesada et al. 2021).

Although fMRI can provide information about analgesic efficacy, this alone does not necessarily meet the need to improve translation of novel therapeutics from animal models to clinical trials. A challenge remains that due to differences in experiment designs and data analysis techniques used it is not easy to compare across studies and identify consistent brain activity that indicates analgesic efficacy. More recently, multivariate pattern analysis techniques have enabled progress in developing pain signatures using neuroimaging data from multiple studies (Wager et al. 2013), and analgesic signatures characterising drug effect on pain perception, either following sensitisation with experimental models or in patients (Duff et al. 2015). The latter has potential to detect pharmacodynamic effects of novel analgesics if fMRI data with the new analgesic is demonstrated to match the analgesia signature (Tracey, Woolf, and Andrews 2019).

The utility of fMRI to detect analgesic activity has also been demonstrated in patient studies. A recent fMRI study including patients with post-traumatic neuropathic pain showed changes in relevant pain

processing brain regions even when changes in behavioural data were lacking (Wanigasekera et al. 2018). This provides further evidence that fMRI can provide valuable indication of pharmacodynamic efficacy and target engagement in early-stage human studies, prior to large scale clinical trials.

1.5.3 Strengths and limitations of this review and future directions

One potential limitation with this systematic literature review is the diversity of studies included, which makes it challenging to draw comparisons. The studies focus on different specific research questions and therefore use different experimental designs, with a large range of stimuli applied (including mechanical, tactile and thermal modalities) and stimuli locations (focussing mainly on the arms or legs but also including face and hands). Further, the imaging protocols are not well aligned, with differences in hardware and sequences used, and also will have developed significantly over the 20-year period included studies were from (1999 to 2019) (Bandettini 2012), so this does impact the comparability of the studies and consistency of the results. Finally, the results of the identified studies are also dependent on the analysis techniques applied to the data, which can also lead to variability (Carp 2012). However, these factors could be considered a strength, as the fact that activation is reported in a largely consistent set of brain regions despite this diversity of experimental designs, protocols and analysis techniques is reassuring, since it is important that findings are generalisable across different stimuli and experimental methods (Nichols et al. 2017).

The limitations described above emphasise the need for more standardisation of experiment designs, imaging protocols and analysis pipelines to produce consistent results in the future. To develop standardised protocols for assessment of novel analgesics there is a need to validate them, for example by using larger sample sizes, consistent protocols and a wider range of drugs with different mechanisms of action. This further validation will aid the continued development of robust biomarkers for clinical efficacy, against which novel analgesics can be assessed.

Meta-analysis techniques provide an opportunity to evaluate consistency of results across a group of studies and therefore can address the challenges outlined above (Wager et al. 2009). However, there were also limitations associated with the CBMA section of this review. While one of the key advantages of the CBMA approach is that the analysis only requires x, y, z co-ordinates, in this particular sample of 31 neuroimaging studies identified in the literature review, only 12 studies reported activation co-ordinates that met the criteria for this CBMA. Some further studies did report x, y, z co-ordinates for other contrasts (such as reporting co-ordinates for the control condition and hyperalgesic condition separately). The fact that not all studies reported co-ordinates that met the

inclusion criteria, resulting in a relatively small sample size, means that the results of the CBMA conducted here may not be generalisable (Müller et al. 2018). In future, this CBMA would need to be repeated to include more studies.

1.6 Conclusion

In summary, the use of human models of peripheral and/or central sensitisation in conjunction with functional neuroimaging have provided valuable insight into the neural mechanisms that underlie some key features of chronic pain conditions. The techniques have also been instrumental in expanding our understanding of the mechanisms for analgesic efficacy in hyperalgesia states. Experimental evidence amassed over the past 20 years of neuroimaging research and the ongoing development of new and improved imaging techniques positions functional imaging as a viable option to meet the need for objective biomarkers of analgesic efficacy in humans. As with any experimental model, the central sensitisation models are not able to fully replicate the clinical features of chronic pain conditions, but they do provide a useful surrogate for key symptoms that have been shown to be modulated by drugs that have a known action in relevant pathways.

EXPERIMENTAL CHAPTER 2

Use of 7 Tesla magnetic resonance imaging (MRI) to investigate the onset of central sensitisation induced by topical capsaicin in healthy human subjects

2.1 Abstract

Background and introduction: Central sensitisation is an important feature of chronic pain for many patients, resulting in hyperalgesia and allodynia. This early-stage exploratory 7 Tesla (7T) functional magnetic resonance imaging (fMRI) study aimed to explore the amplification of neural processing produced by experimental induction of central sensitisation with topical capsaicin, and identify which brain regions play a role in its development.

Methods: Central sensitisation was induced in the right lower leg using topical capsaicin cream in 16 healthy subjects, with 14 included for analysis. Pain ratings were collected using visual analogue scale (VAS) and neural response was measured indirectly with blood oxygen-level dependent (BOLD) using ultra-high field 7T fMRI. The study was double-blind placebo controlled; subjects attended two sessions and received capsaicin or placebo cream in a randomised order. Mechanical stimulation with weighted punctate probes (128mN, 256mN and 512mN) was carried out in a baseline scan. This was followed by cream application and then a second, post-treatment scan to capture central sensitisation onset. During the post-treatment scan, 37 mechanical stimuli (512mN) were applied over a total duration of ~25 mins. For analysis, the post-treatment scan data was split into a beginning phase, middle phase and end phase, to allow comparison to be made at different time points during hyperalgesia development.

Results: There was a significant increase in subject pain ratings for the mechanical stimuli in the capsaicin group compared to the placebo group from the 28^{th} stimulus onwards. There were no significant differences between capsaicin and placebo in the imaging data, for beginning, middle or end time phases or for individual stimuli. It was noted that only a sub-set of subjects developed hyperalgesia, therefore further exploratory analysis was conducted to characterise differences in the neural responses that may make some individuals more vulnerable to developing central sensitisation than others. Within-subject data was used to define subjects who developed hyperalgesia, which developed in 6 subjects. In the hyperalgesia group, there was a 3.5-fold increase in average pain ratings with capsaicin compared to placebo during the end phase of the treatment scan. This was associated with a 1.9-fold increase in the BOLD signal in the dorsal-posterior insula (dpIns) cortex. It was found that subjects who did not develop hyperalgesia had higher BOLD signal in pain modulation-associated brainstem regions during the placebo condition (no central sensitisation) compared to those who did, across all time phases.

Conclusions: The hyperalgesia shown in pain ratings during the onset of central sensitisation produces amplification of the neural signal in key pain processing areas, notably the dpIns, which has been shown previously to play a role in tracking pain intensity. Following capsaicin application only a sub-set of subjects (approximately 50%) developed central sensitisation, which is aligned to previous studies. The higher BOLD responses to a noxious stimulus in brainstem regions observed during the placebo condition in subjects who did not develop hyperalgesia could show a protective role of activity in the descending inhibitory system, resulting in lower vulnerability to develop central sensitisation in the capsaicin condition.

2.2 Introduction

Many chronic pain conditions are associated with symptoms of central sensitisation including hyperalgesia (increase in pain to painful stimuli) and allodynia (pain response to non-painful stimuli) (Woolf 2011; Arendt-Nielsen et al. 2018). Neuropathic pain is particularly strongly associated with these features (Jensen and Finnerup 2014), but they are also present for inflammatory conditions such as osteoarthritis (Fingleton et al. 2015) and more idiopathic conditions such as fibromyalgia (Julien et al. 2005). Experimental models can be used to temporarily induce features of central sensitisation, such as secondary mechanical hyperalgesia, in healthy humans to enable research into the underlying mechanisms of this sensitised state (Quesada et al. 2021). One example is the use of capsaicin, a substance from chilli peppers that causes a burning sensation via agonist action at transient receptor potential vanilloid-1 (TRPV-1) receptors (Nelson 1919; Caterina et al. 1997; Schmelz et al. 2000). It was first used in experiments in the 1960s, and can be applied topically on the skin or via intradermal injection (Jancso 1960; Simone, Baumann, and LaMotte 1989; LaMotte et al. 1991). Topical capsaicin can also be applied with heat to provide more stable secondary hyperalgesia (Petersen and Rowbotham 1999).

As discussed in chapter 1 of this thesis, 19 research studies have used capsaicin models in conjunction with fMRI to characterise the neural response during hyperalgesia and how this can be modulated by analgesics, with insightful results proving that this combination is highly valuable in pain research. In this study, the aim was to specifically explore and understand the neural response to pain stimuli **during the onset** of a centrally sensitised state (induced by topical capsaicin) in healthy human participants, using ultra-high-field 7T MRI.

The primary research question asks how the neural signal (indirectly measured via BOLD) changes during evolution of central sensitisation from initial onset. It is hypothesised that following capsaicin application there will be an increase in the BOLD response over time in brain regions known to be involved in pain processing and central sensitisation, particularly the dorsal-posterior insular cortex (dpIns) and brainstem regions. This increase will only be seen in the capsaicin condition (where pain intensity for each stimulus increases as secondary mechanical hyperalgesia develops, and will not be seen in the placebo condition, in which pain intensity is expected to remain constant throughout the experiment. This hypothesis will be tested by elucidating the scale of amplification of the neural signature in key pain processing brain areas, and using analysis to identify the brain regions that play a role in the development of this amplification. Conducting this study using the 7T MRI scanner allows

higher spatial specificity (Kraff et al. 2015), particularly within the areas of interest for this study such as brainstem regions (Napadow, Sclocco, and Henderson 2019), and sub-regions of key areas such as the insula cortex.

It has been shown in a previous imaging study that the dpIns has a key role in the perception of pain intensity during a tonic pain stimulus (more reflective of a chronic pain state compared to acute stimuli often applied in experimental settings) (Segerdahl et al. 2015). For this reason, it was selected as a region to investigate in this study to identify whether there will be an increase in the BOLD response in this region over time as secondary mechanical hyperalgesia develops (resulting in increased pain intensity).

Three brainstem regions were also selected to investigate; the ventrolateral periaqueductal grey (vlPAG), the rostral ventromedial medulla (RVM) and the nucleus cuneiformis (NCF). These regions are all key for the descending modulation of pain, a pathway fundamentally involved in the facilitation of pain responses during central sensitisation, which manifests as an enhancement of the neural response across all nociceptive pathways in addition to reduced inhibition (Latremoliere and Woolf 2009). There is extensive literature supporting the role of brainstem regions; in a study utilising a similar design using fMRI to study the neural response following application of topical capsaicin, the PAG and NCF regions were both shown to have increased BOLD response during secondary mechanical hyperalgesia (Zambreanu et al. 2005). In addition, a study applying a design with intensity-matched mechanical stimuli in the sensitised and non-sensitised states identified a specific role for the brainstem in the maintenance of central sensitisation. The brainstem activity identified was localised to the mesencephalic pontine reticular formation (MPRF), in which the NCF is located (Lee et al. 2008). For the vlPAG specifically, a recent mouse study has shown a critical role for the vlPAG in development of hypersensitivity after nerve injury (Huang et al. 2019). For the RVM, descending facilitation arising in this region has been shown in a study in rats to have an essential role in the maintenance of central sensitisation following nerve injury (Vera-Portocarrero et al. 2006). The modulatory neurones termed 'ON' and 'OFF' cells located within the RVM make this region a highly important centre for the regulation of pain signalling, receiving inputs both from higher cognitive centres and from peripheral sensory inputs (Chen and Heinricher 2022; Carlson et al. 2007).

2.3 Methods

2.3.1 Study participants and ethical approval

This study was approved by the National Research Ethics Committee (NRES); reference 11/SC/0249. All participants gave written informed consent prior to taking part. The study included 16 healthy human subjects in total. Data was excluded from 2 subjects due to excessive motion in the scanner, therefore 14 subjects were included for data analysis (6 females, 8 males).

2.3.2 Study design

The study design was a randomised, double-blinded, cross-over placebo-controlled design, with participants attending for two scanning sessions (one for capsaicin and one for placebo). During the capsaicin scan, topical capsaicin cream was applied to induce hyperalgesia, and during the placebo scan a sham cream was used. Capsaicin or placebo cream was applied to the right leg, as shown in Figure 1.

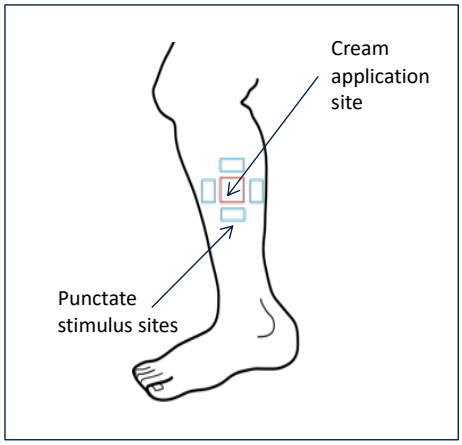

Figure 1: Cream application site and punctate stimuli sites

Capsaicin or placebo cream was applied to the anteromedial surface of the right leg in a 3 x 3cm area. Punctate stimuli were applied in 3 x 1cm areas surrounding the outside of the application site, with a 1cm gap separating the stimulation areas and the cream application site.

Each scanning session was split into 3 main sections; structural T1 scan, baseline scan and treatment phase scan (following application of capsaicin or placebo cream). During the baseline scan, 15 mechanical stimuli were applied, consisting of five 128mN stimuli, five 256mN stimuli and five 512mN stimuli. During the treatment scans, 37 mechanical stimuli (512mN) were applied at 45s intervals (jittered). The study design is shown in Figure 2.

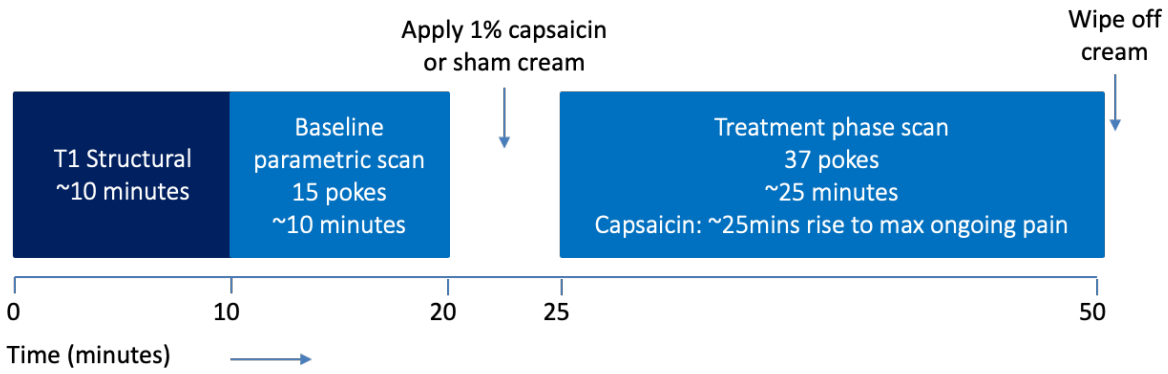

Figure 2: Scanning session experiment design

Each scanning session consisted of a T1 structural scan, followed by a baseline scan which included 15 punctate stimuli (pokes) applied with a 45s interval (jittered). Then, after a 5-minute gap during which the capsaicin or placebo cream was applied, a treatment phase scan took place where 37 pokes were applied, with a 45s interval (jittered).

All mechanical stimuli were applied using MRI-compatible weighted punctate probes (MRC Systems GmbH, Germany). During the scans, participants were asked to rate the pain intensity of each punctate stimulus using a visual analogue scale (VAS) from 0 to 100, where 0 is "no pain" and 100 is "pain as bad as can be imagined".

During the baseline scan, there were 5 stimuli applied with the 128nM probe, 5 applied with the 256nM probe and 5 applied with the 512nM probe, in ascending order. The rationale for using three different stimulus intensities was to characterise the neural response to increasingly painful stimuli in the absence of central sensitisation. During analysis, it was noted that the timing files for stimulus application for the baseline data provided are not aligned to the imaging data. In the design file generated by FEAT, only 14 of the 15 stimuli times included in the input text file occur during imaging data acquisition, with the 15th stimulus occurring later than the end of the imaging file. This error was not able to be resolved, as it was not possible to identify why this had occurred or to correct the timing file data available, so baseline data has not been further included in this analysis.

2.3.3 Imaging data acquisition

Imaging data was acquired at the Oxford Functional Magnetic Resonance Imaging of the Brain (FMRIB) Centre using a 7T Siemens MRI scanner. For functional scans, a limited field of view (FOV) echo-planar-imaging (EPI) sequence with a voxel size of 2 x 2 x 2mm was used. The repetition time (TR) was 2000ms and the echo time (TE) was 25ms. A T1-weighted structural image, with 0.7mm^3 voxels, was acquired

for the registration of the functional images. An expanded whole-brain functional image was also acquired to enable the partial-brain functional images to first be registered to this whole-brain image before registration to the main high resolution T1 image. A field map was acquired to after the functional scans to enable correction of field inhomogeneity during analysis, with voxel size 2mm x 2mm x 2mm and field of view 192 mm x 192mm.

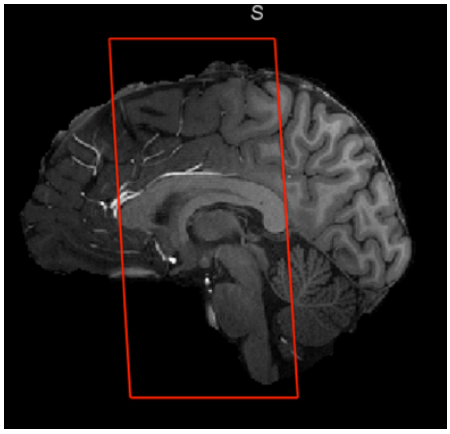

Figure 3: Field of view (FOV) used for functional scans

The field of view used for the functional MRI scans was limited to a central section of the brain as outlined in red in the figure. This area included the entire brainstem and key cortical areas involved in pain processing, including the insula cortices, anterior cingulate cortices, and primary and secondary somatosensory cortices.

2.3.4 Data analysis

For behavioural data, analysis was carried out using GraphPad PRISM version 9.4.1 (GraphPad Software, LLC). Statistical significance is reported with the following symbols; ns for $P > 0.05$; * for $P \leq 0.05$, ** for $P \leq 0.01$, *** for $P \leq 0.001$, and **** for $P \leq 0.0001$.

Within-subject pain rating data was used to identify the participants who developed hyperalgesia. Ratings from the five 512nM stimuli from the baseline scan and the last five 512nM stimuli administered at the end of the treatment scan were used. Response was defined as those who had a positive and statistically significant score based on the formula: (Xtreatment_capsaicin - Xbaseline_capsaicin) > (Xtreatment_placebo - Xbaseline_placebo), where (X) is the pain score ($p \geq 0.05$; two-tailed paired t test).

For fMRI data, analysis was carried out using tools in the FMRIB Software Library v6.0 (FSL) (Woolrich et al. 2009; Jenkinson et al. 2012; Smith et al. 2004). The same pipeline was used for baseline (pre-treatment) and treatment (post-capsaicin or post-placebo) scans. First, structural, magnitude and whole-brain functional images were brain extracted (Smith 2002), and a calibrated filed map image was prepared. Next, FEAT was used to perform B0 unwarping and registration to the whole brain functional image and the high-resolution structural image (Woolrich et al. 2001). Motion correction, spatial smoothing (5mm) and high-pass temporal filtering were applied. Individual statistical maps for

the response to the pin-prick stimuli were generated using the general linear model (GLM) approach implemented with FEAT (Woolrich et al. 2001). For individual maps from the treatment scans, the pin-prick stimuli were split into three time sections (beginning – first 13 pokes, middle – middle 14 pokes and end – last 10 pokes) to allow comparison to be made at different time points during hyperalgesia development. Then, a group-level whole brain, mixed effects analysis with a cluster-based correction for multiple comparisons ($Z > 2.3$, $p < 0.05$) was performed using FEAT to carry out a paired t-test to identify for differences in the pin-prick evoked neural activity in the capsaicin scan compared to the placebo scan, across the three time sections (Woolrich et al. 2004).

Two different data-cleaning methodologies were considered to remove noise from the data. These were physiological noise modelling (PNM) to regress out the effects of physiological noise in the data and independent component analysis (ICA) for removal of noise components. Ultimately these methodologies were not used for this data. The PNM was not possible due to issues with the quality of the physiological data recordings that were collected during the MRI scans, as use of the low-quality data would not have accurately removed the specific effects of the physiological noise. The ICA-based method was not used as the 7T-data generated a very large number of components, making hand-classification of these components into 'signal' or 'noise' very time consuming. Since it is only an early-stage study and due to the fact that it was a task-based design, meaning the ICA-based noise removal would only have offered a marginal improvement in the data quality, it was decided that this option would not be appropriate for this dataset.

The Featquery tool in FSL was used to extract mean percentage change in BOLD parameter estimates for the left dorsal-posterior insula, the periaqueductal grey (whole and constrained to the ventrolateral portion), rostral ventromedial medulla (RVM), midbrain reticular formation (MRF) and nucleus cuneformis (NCF) regions. The origins of the masks used for extraction of parameters from each area are outlined below and shown in Figure 4:

Dorsal-posterior insula cortex (dpIns): Functionally defined region from Segerdahl et al. 2015 paper which identifies a positive correlation between cerebral blood flow and ongoing pain intensity ratings in this region of the left dpIns. In addition to the main area of the dpIns it is noted that the mask does include some parts of the secondary somatosensory cortex as well (Segerdahl et al. 2015).

Ventro-lateral periaqueductal grey (vlPAG): Defined in a study by Ezra et al. using a connectivity-based segmentation approach. Diffusion MRI optimised for the brainstem was used with probabilistic

tractography to elucidate connectivity profiles of the voxels within the PAG, enabling it to be segmented into four clusters, one of which being the vlPAG (Ezra et al. 2015; Faull and Pattinson 2017).

Rostral ventromedial medulla (RVM): Anatomically defined region of the medulla including the nucleus gigantocellularis and nucleus raphe magnus that was manually created using Duvernoy's brainstem atlas as a reference ('Duvernoy's Atlas of the Human Brain Stem and Cerebellum' 2009), since a detailed brainstem atlas is not available in the FSL library.

Nucleus cuneformis (NCF): Functionally defined region from Zambreanu et al., a study which identifies a brainstem cluster showing significantly increased activation during secondary hyperalgesia (induced with topical capsaicin) compared to control stimulation, that is consistent with the location of the left NCF as described from human anatomical studies and animal studies (Zambreanu et al. 2005). Mask created using the peak activation voxel from this cluster to create a 5mm spherical mask, which was constrained to the brainstem region only.

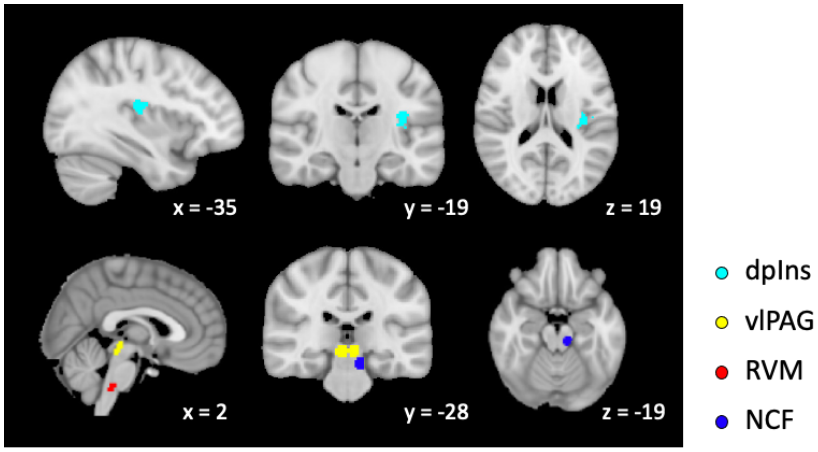

Figure 4: Masks used for Featquery analysis

Masks used in this study for extraction of BOLD parameter estimates are shown. The left dorsal-posterior insular cortex (dpIns) mask is a functional mask from a study using topical capsaicin to investigate cerebral blood flow responses during tonic pain (Segerdahl et al. 2015). The ventrolateral periaqueductal grey (vlPAG) was defined using a connectivity-based segmentation approach (Ezra et al. 2015). The rostral ventromedial medulla (RVM) mask was manually created using the Duvernoy's brainstem atlas ('Duvernoy's Atlas of the Human Brain Stem and Cerebellum' 2009). The left nucleus cuneiformis (NCF) mask is a 5mm spherical mask created using the peak activation voxel from Zambreanu et al., which identifies this region of the brainstem showing significantly increased activation during secondary hyperalgesia (Zambreanu et al. 2005).

2.4 Results

2.4.1 Behavioural results

In the capsaicin condition, the group mean pain intensity ratings for each stimulus increased over time (i.e., the longer the capsaicin was left on the skin the higher the pain ratings to the mechanical stimuli became). A two-way ANOVA was performed to test for the effect of the condition (capsaicin or placebo) and the stimulus number (1 to 37) on the pain intensity ratings. Simple main effects analysis showed that condition and stimulus number each had a statistically significant effect ($p = 0.0273$ and $p < 0.0001$, respectively). There was a statistically significant interaction between the effects of condition and stimulus number ($F (36, 468) = 2.195$, $p = 0.0001$). Bonferroni's multiple comparison test was performed comparing the capsaicin and placebo conditions at each stimulus, and showed there was a consistent significant difference between the capsaicin and placebo conditions from stimulus 28 onwards, as shown in Figure 5A.

Based on this, the treatment phase scan was split into 3 time periods; beginning, middle and end, in order to compare the magnitude of amplification of response during each phase. The time sections were: beginning = poke 1-13 (n=13 pokes), middle = poke 14-27 (n=14 pokes) and end = poke 28-37 (n=10 pokes). A two-way ANOVA again showed statistically significant interaction between condition and time section ($F (2, 26) = 7.771$, $p = 0.0023$) with main effects analysis showing condition and time section each had a significant effect ($p = 0.0218$ and $p = 0.0025$, respectively). Bonferroni's multiple comparison test comparing capsaicin and placebo conditions at each time section showed there was a significant difference between the conditions at the beginning, middle and end time sections ($p = 0.0235$, $p = 0.0002$ and $p < 000.1$, respectively), as shown in Figure 5B.

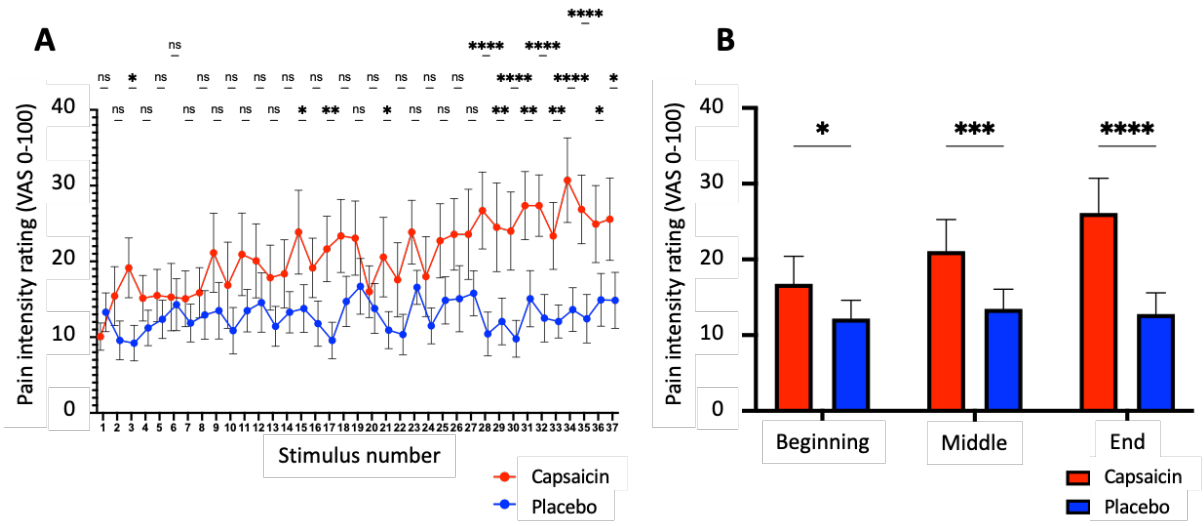

Figure 5: Group mean pain ratings for mechanical stimuli during the treatment scan

A: Group mean pain ratings for individual stimuli 1 to 37 during the treatment phase. Capsaicin vs. placebo difference in visual analogue scale (VAS) pain rating at $p < 0.05$, following two-way repeated measures ANOVA and Bonferroni's correction for multiple comparisons. Significant difference at poke 3, 15, 17, 21 and from poke 28-37.

B: Group mean pain ratings for time-section grouped stimuli. Capsaicin vs. placebo difference in pain ratings at $p < 0.05$, following two-way repeated measures ANOVA and Bonferroni's correction for multiple comparisons.

2.4.2 Whole-brain imaging results

At the group level, there is no significant difference between the capsaicin and placebo conditions at any of the time points (beginning, middle or end), or in all pokes together (mixed effects analysis, $Z > 2.3$, $p < 0.05$). The average BOLD response in each condition individually (capsaicin or placebo) shows significant increase in activation in response to the pin-prick stimuli in areas involved in pain perception such as the insula cortex anterior cingulate cortex and secondary somatosensory cortex (SII) (mixed effects analysis, $Z > 2.3$, $p < 0.05$). This was shown for stimuli in the beginning, middle and end time sections, and for all stimuli together. Whole-brain imaging results are shown in Figure 6.

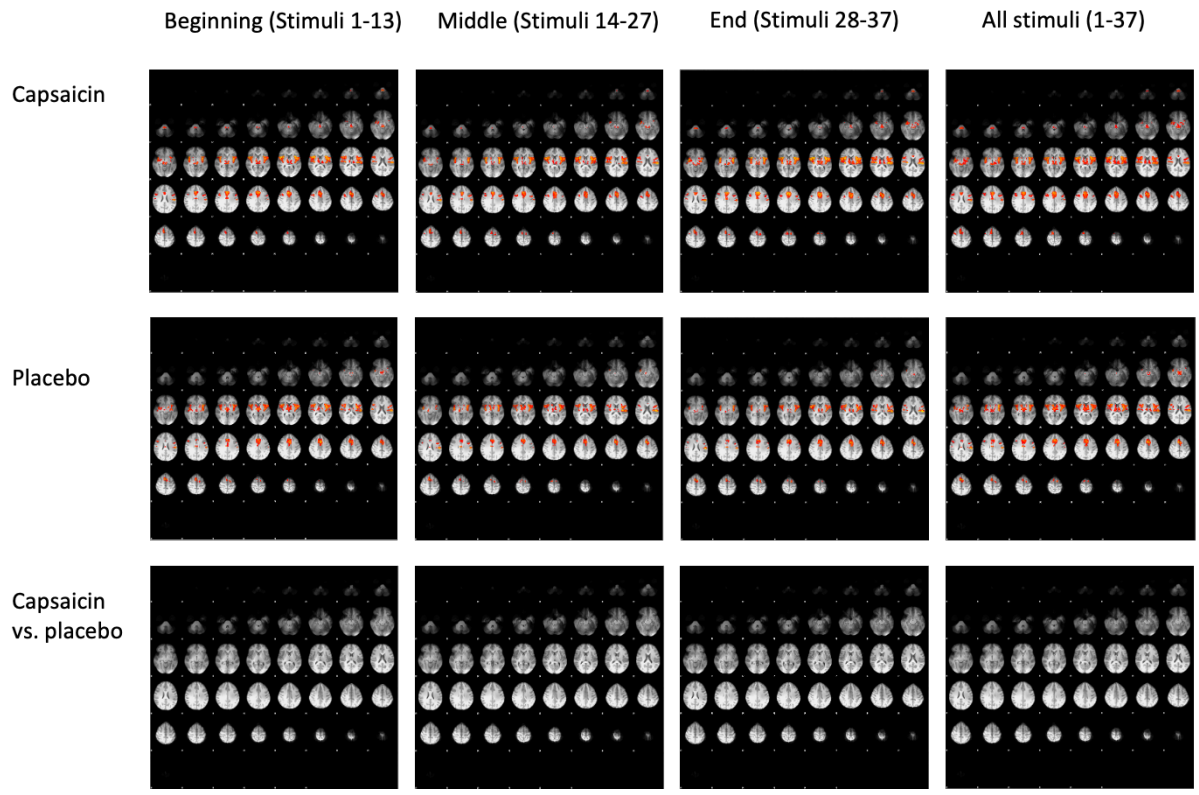

Figure 6: Group mean whole-brain BOLD responses

The mean BOLD responses in each condition (capsaicin and placebo) at each time period (beginning, middle and end), and for all pokes together, are shown in the top two rows. The final row shows the capsaicin vs. placebo difference in BOLD response, which shows there is no statistically significant difference between the two conditions in any time section, or for all stimuli together (mixed effects analysis, $Z > 2.3$, $p < 0.05$).

2.4.3 Change in BOLD response to individual stimuli in selected brain regions

In addition to comparing the BOLD response for capsaicin vs. placebo in the beginning, middle and end time sections, the imaging data was also analysed to obtain the BOLD response to the 37 individual stimuli (similar to the behavioural data analysis of the mean pain ratings to individual stimulus). For each individual stimulus, the mean percentage change in BOLD parameter estimates was extracted from selected brain areas (dpIns, vlPAG, RVM and NCF), using the Featquery tool in FSL. Example results are shown in Figure 7 for the dpIns (in Figure 7A) and the NCF (Figure 7B). A two-way ANOVA was performed for each region to test whether there was a significant effect of the factors condition (capsaicin or placebo) or stimulus number (1-37) on the BOLD response to the stimulus. These tests showed that there was not a significant effect of either factor for any of the brain regions included (dpIns, vlPAG, RVM and NCF).

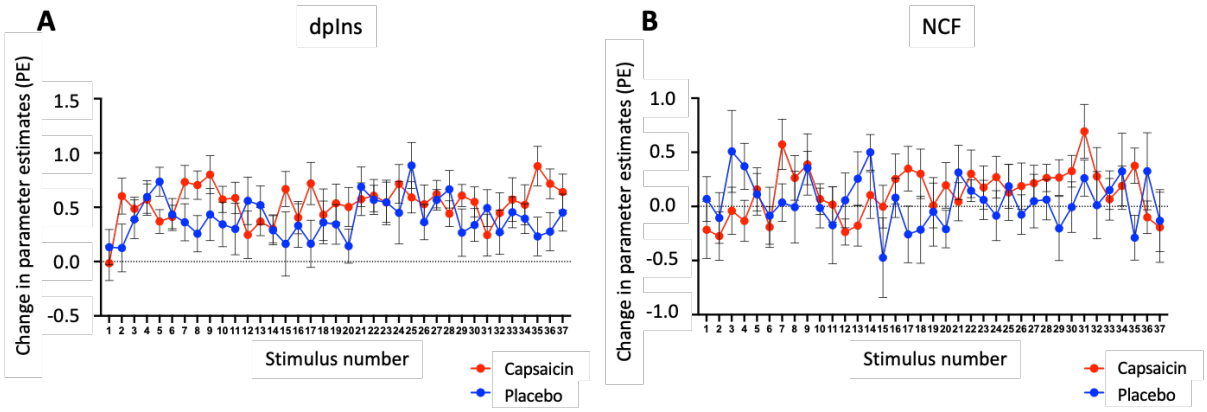

Figure 7: BOLD response to individual stimuli in selected brain regions

The BOLD parameter estimates for the left dorsal posterior insula (dpIns – A) and for the nucleus cuneiformis (NCF – B) for the 37 individual stimuli are plotted for the capsaicin condition (red) and placebo condition (blue). A two-way ANOVA was performed for each region to test whether there was a significant effect of the factors condition (capsaicin or placebo) or stimulus number (1-37) on the BOLD response to the stimulus. These tests showed that there was not a significant effect of either factor for either the dpIns or the NCF.

2.4.4 Results depending on whether subjects developed hyperalgesia or not

It was clear from the behavioural results for individual subjects that only a sub-set of subjects had developed hyperalgesia within the tested duration of 25min. In order to formalise which subjects had developed hyperalgesia and which had not, a within-subject comparison was conducted. Subjects who developed hyperalgesia were defined as those who had a significant increase in the pain intensity scores in the capsaicin condition vs. placebo condition, only subjects who had a positive and statistically significant score based on the formula: *(Xtreatment_capsaicin - Xbaseline_capsaicin) > (Xtreatment_placebo - Xbaseline_placebo)*, where (X) is the pain score, were considered to have developed hyperalgesia ($p \geq 0.05$; two-tailed paired t test). Subject pain ratings from the five 512nM stimuli from the baseline scan and the last five 512nM stimuli administered at the end of the treatment scan were used.

Using this methodology, it was identified that there were 6 subjects who developed hyperalgesia and 8 subjects that did not. Pain intensity ratings for each group separately showed that there was a much larger increase in the group who did develop hyperalgesia compared to the group who did not develop hyperalgesia, as shown in Figure 8.

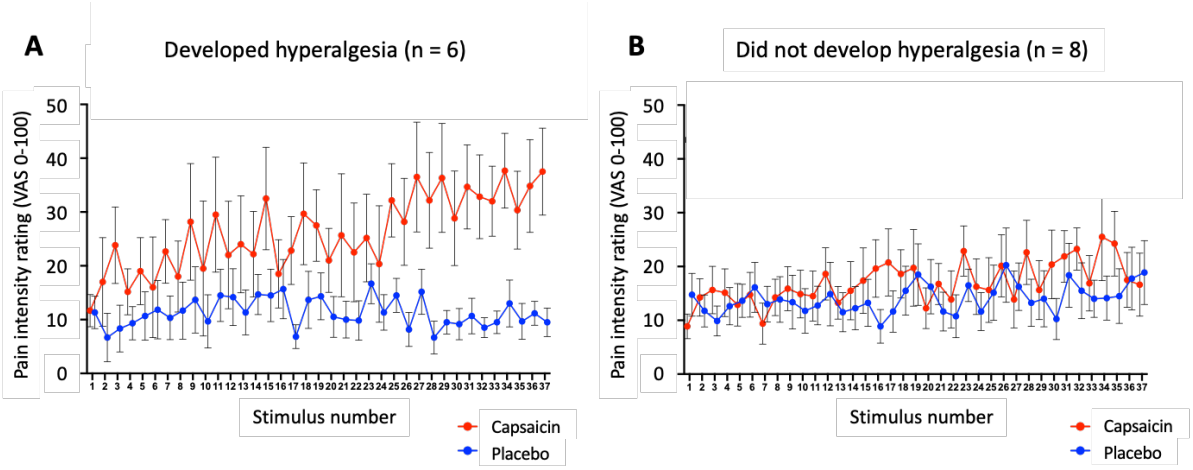

Figure 8: Group mean pain ratings for subjects who developed hyperalgesia (n = 6) and those who did not develop hyperalgesia (n = 8)

Group mean pain ratings for individual stimuli 1 to 37 during the treatment phase are plotted for subjects who developed hyperalgesia (A) and for subjects who did not develop hyperalgesia (B), showing a larger increase in ratings in the group who did develop hyperalgesia, particularly from stimulus 25 onwards.

Whole-brain analysis of the punctate-evoked BOLD response was completed for each group separately (developed hyperalgesia; n = 6, and did not develop hyperalgesia; n = 8), for all time sections. For the hyperalgesia group, there was no statistically significant activation in the whole-brain analysis for the beginning or middle time sections, but for the end time section there was a significant increase in the BOLD response to pin-prick stimulation in the anterior insula cortex for the capsaicin condition compared to placebo (mixed effects analysis, $Z > 2.3$, $p < 0.05$), shown in Figure 9.

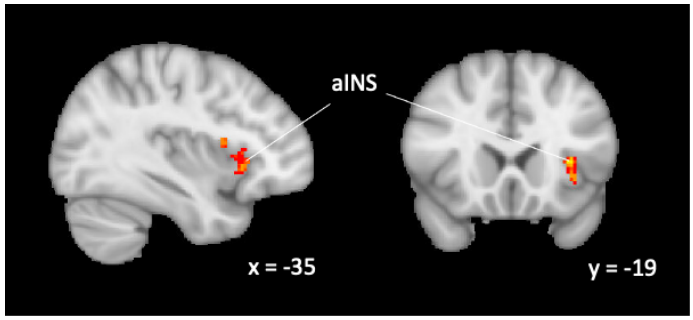

Figure 9: BOLD response during the 'end' time section for subjects who developed hyperalgesia

For the hyperalgesia group (n = 6), group mean BOLD activation was significantly increased during the 'end' time section in the capsaicin scan vs. placebo scan (mixed effects analysis, $Z > 2.3$, $p < 0.05$) in the anterior insula cortex (aINS). MNI-512 co-ordinates are shown. There were no areas of significantly increased activation in the beginning or middle time sections for the capsaicin vs. placebo comparison.

Change in BOLD response in selected brain regions for all subjects (n = 14), for those who developed hyperalgesia (n = 6) and for those who did not develop hyperalgesia (n = 8) was also explored using extracted BOLD parameter estimates for the dpIns, vlPAG, RVM and NCF.

Dorsal-posterior insula cortex (dpIns):

For the dpIns, the BOLD response was higher when averaged across all subjects and for the subjects who developed hyperalgesia across all time sections (beginning, middle and end), but not for the subjects who did not develop hyperalgesia until the end time section. Two-way repeated measures ANOVA showed that there was no statistically significant interaction between condition and time section or main effect of either factor individually for any group (all, those who developed hyperalgesia or those who did not develop hyperalgesia) and Bonferroni's multiple comparisons showed that there was no statistically significant difference between capsaicin and placebo conditions for any time sections, as shown in Figure 10.

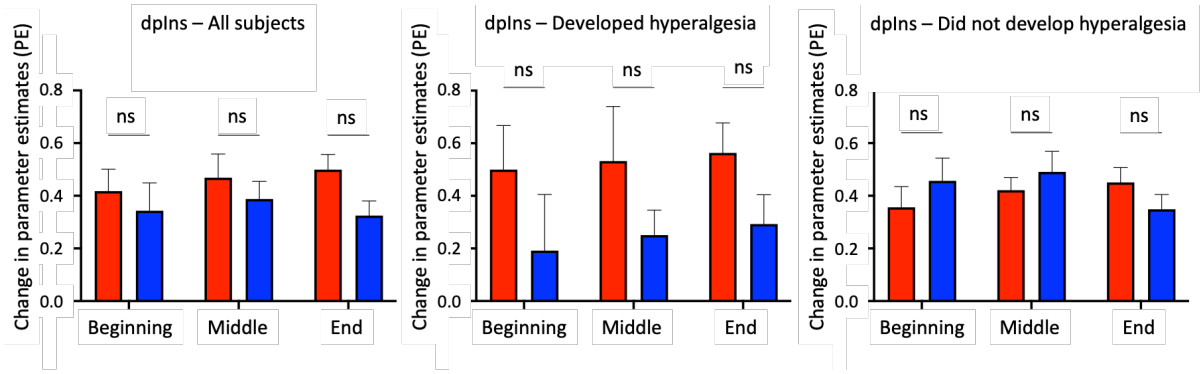

Figure 10: BOLD response in the left dorsal posterior insula cortex (dpIns) for beginning, middle and end time sections

The stimulus-evoked BOLD parameter estimates were extracted using Featquery from the left dorsal posterior insula cortex (dpIns) and plotted for the three time periods for all subjects (left, n = 14), subjects who developed hyperalgesia (centre, n = 6) and subjects who did not develop hyperalgesia (right, n = 8). A two-way ANOVA was performed to analyse the effect of the condition (capsaicin or placebo) and time section (beginning, middle or end). There was no interaction between these factors or main effect of either factor individually. Bonferroni's multiple comparison tests for each group showed there was no statistically significant difference between the capsaicin and placebo groups in any time section for any group.

Ventrolateral periaqueductal grey (vlPAG):

For the vlPAG, similar to the dpIns, there was a higher BOLD response in the capsaicin condition for all time sections for all subjects and for the hyperalgesia group, whereas for the no-hyperalgesia group this was reversed. Again, a two-way repeated measures ANOVA showed that there was no statistically significant interaction between condition and time section or main effect of either factor individually for any group (all, those who developed hyperalgesia or those who did not develop hyperalgesia) and Bonferroni's multiple comparisons showed that there was no statistically significant difference between capsaicin and placebo conditions for any time sections, as shown in Figure 11.

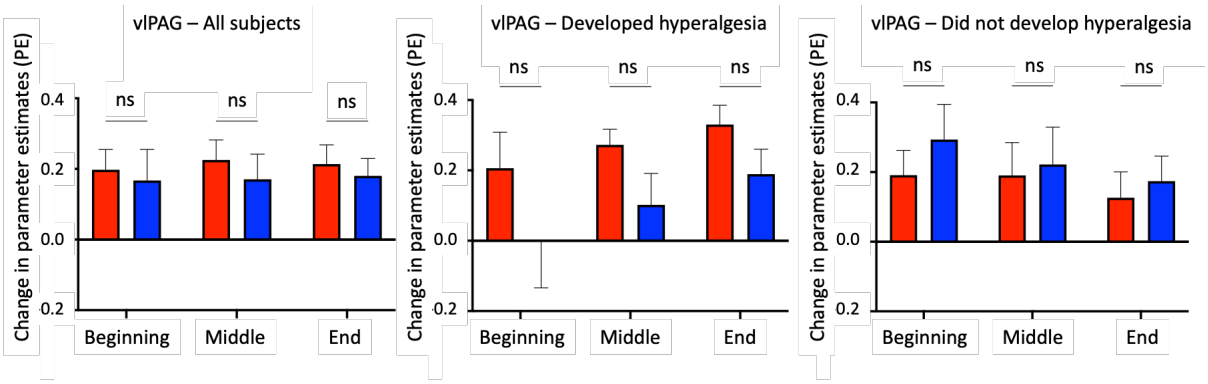

Figure 11: BOLD response in the ventrolateral periaqueductal grey (vlPAG) for beginning, middle and end time sections

The stimulus-evoked BOLD parameter estimates were extracted using Featquery from the ventrolateral periaqueductal grey (vlPAG) region and plotted for the three time periods for all subjects (left, n = 14), subjects who developed hyperalgesia (centre, n = 6) and subjects who did not develop hyperalgesia (right, n = 8). A two-way ANOVA was performed to analyse the effect of the condition (capsaicin or placebo) and time section (beginning, middle or end). There was no interaction between these factors or main effect of either factor individually. Bonferroni's multiple comparison tests for each group showed there was no statistically significant difference between the capsaicin and placebo groups in any time section for any group.

Rostral ventromedial medulla (RVM):

For the RVM, the response in all time sections for all subjects together was very similar between capsaicin and placebo conditions. However, once the subjects were split into hyperalgesia and no-hyperalgesia groups, it was shown that underlying this similarity was a polarised response; with the group who developed hyperalgesia having a higher BOLD response during the capsaicin condition and

the group who did not develop hyperalgesia having a higher BOLD response during the placebo condition. A two-way repeated measures ANOVA showed that there was no statistically significant interaction between condition and time section, or main effect of either factor individually, for any group (all, those who developed hyperalgesia or those who did not develop hyperalgesia). Bonferroni's multiple comparisons showed that for the hyperalgesia group, there was a statistically significant difference between the capsaicin and placebo conditions for the beginning and middle time sections ($p = 0.0125$ and $p = 0.0209$, respectively). There was no statistically significant difference between capsaicin and placebo conditions for the end time section or for any time sections for all subjects or for the no-hyperalgesia group, as shown in Figure 12.

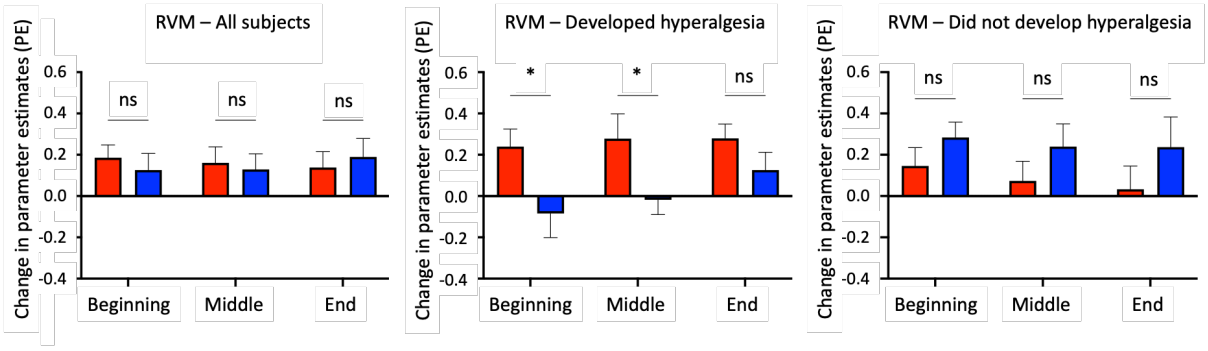

Figure 12: BOLD response in the rostral ventromedial medulla (RVM) for beginning, middle and end time sections

The stimulus-evoked BOLD parameter estimates were extracted using Featquery from the rostral ventromedial medulla (RVM) region and plotted for the three time periods for all subjects (left, n = 14), subjects who developed hyperalgesia (centre, n = 6) and subjects who did not develop hyperalgesia (right, n = 8). A two-way ANOVA was performed to analyse the effect of the condition (capsaicin or placebo) and time section (beginning, middle or end). There was no interaction between these factors or main effect of either factor individually. Bonferroni's multiple comparison tests for each group showed there was a statistically significant difference between the capsaicin and placebo conditions for the beginning and middle time sections ($p = 0.0125$ and $p = 0.0209$, respectively) for the hyperalgesia group, but not for the end section ($p = 0.3324$). There was no statistically significant difference between capsaicin and placebo conditions for any time sections for all subjects or for the group who did not develop hyperalgesia.

Nucleus cuneiformis (NCF):

For the left NCF, there was again a polarised response in the group who developed hyperalgesia vs. the group who did not develop hyperalgesia, with the hyperalgesia group having a higher BOLD

response in this region during the capsaicin condition and the no-hyperalgesia group having the opposite. A two-way repeated measures ANOVA showed that there was no statistically significant interaction between condition and time section, or main effect of either factor individually, for any group (all, those who developed hyperalgesia or those who did not develop hyperalgesia). Bonferroni's multiple comparisons showed that for the hyperalgesia group, there was a statistically significant difference between the capsaicin and placebo conditions for all time sections (beginning, $p = 0.0428$; middle, $p = 0.0066$; and end, $p = 0.0423$). There was no statistically significant difference between capsaicin and placebo conditions for any time sections for all subjects or for the group who did not develop hyperalgesia, as shown in Figure 13.

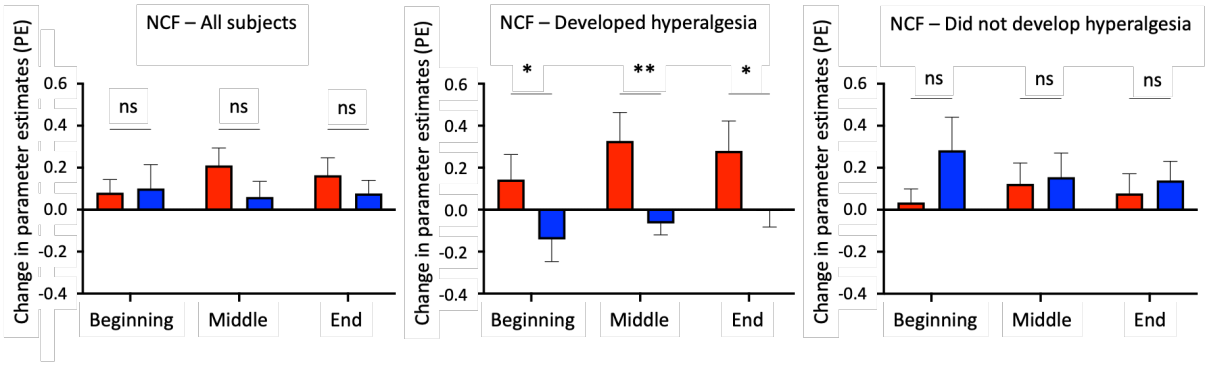

Figure 13: BOLD response in the left nucleus cuneiformis (NCF) for beginning, middle and end time sections

The stimulus-evoked BOLD parameter estimates were extracted using Featquery from the left nucleus cuneiformis (NCF) region and plotted for the three time periods for all subjects (left, n = 14), subjects who developed hyperalgesia (centre, n = 6) and subjects who did not develop hyperalgesia (right, n = 8). A two-way ANOVA was performed to analyse the effect of the condition (capsaicin or placebo) and time section (beginning, middle or end). There was no interaction between these factors or main effect of either factor individually. Bonferroni's multiple comparison tests for each group showed there was a statistically significant difference between the capsaicin and placebo conditions for the beginning, middle and end time sections (p = 0.0428, p = 0.0066, and p = 0.0423, respectively) for the hyperalgesia group. There was no statistically significant difference between capsaicin and placebo conditions for any time sections for all subjects or for the no-hyperalgesia group.

2.5 Discussion

Topical and intradermal capsaicin models have been extensively used in research studies to investigate both peripheral and central sensitisation (O'Neill et al. 2012). They have also been used in many experiments alongside fMRI in order to investigate the brain responses during the sensitised state. In these studies, it has been shown that during capsaicin-induced secondary mechanical hyperalgesia there is increased BOLD response in several cortical and sub-cortical brain regions including the prefrontal cortex, primary and secondary somatosensory cortices, posterior insula cortex, anterior and posterior cingulate cortices, parietal association cortex, thalamus and in the brainstem (Baron et al. 1999; Zambreanu et al. 2005). However, these brain regions are intrinsically linked to pain perception and increased activity during capsaicin-induced hyperalgesia could be attributed to increased pain intensity rather than as a result of the sensitisation specifically. One study aimed to address this by using a stimulus intensity matched design to identify activity that was specifically related to maintenance of the centrally sensitised state, and showed that activity in the brainstem (specifically the mesencephalic pontine reticular formation) fit this specificity criteria (Lee et al. 2008). No previous studies have aimed to investigate the onset of capsaicin-induced secondary mechanical hyperalgesia, which was the primary aim of this study in order to increase our understanding of the role of supraspinal activity during the development of central sensitisation.

Overall, the study shows that pain intensity rating data indicate a steady increase in pain intensity throughout the 37 poke stimuli during the capsaicin condition, with a significant difference compared to the placebo condition from poke 28 onwards (Figure 5A). This increasing trend is also seen in imaging data in the left dpIns, although this increase is not significant, potentially due to a low number of participants who developed hyperalgesia (only 6 within the group of 14). This is consistent with existing literature that has shown a specific role of this region of the dpIns in tracking the intensity of pain (Segerdahl et al. 2015).

During analysis of the data, it was noted that only a sub-set of subjects developed hyperalgesia during the time course of the imaging session. As a result, further exploratory analysis was conducted to explore the vulnerability of individual subjects to developing a sensitised state. There is variability in the response of healthy human subjects to capsaicin (i.e. variability in the development of central sensitisation), this could be related to many mechanisms such as differences in enzymes that breakdown the capsaicin or in the TRPV1 receptors (O'Neill et al. 2012). A recent systematic literature review of experimental hyperalgesia models reported that response rates to topical capsaicin range

between 80-100%, but importantly the response rate was only reported in 11 out of the 47 studies included that used the model (Quesada et al. 2021). This is similar for intradermal capsaicin, for which the response rate for developing secondary hyperalgesia was 75-100%, with response rate reported in 28 out of 61 studies (Quesada et al. 2021). It has been shown that the development of hyperalgesia induced by capsaicin varies depending on temperature, with reduced hyperalgesia on cooling (Grönroos and Pertovaara 1993). It has also been reported that females and older subjects have a larger hyperalgesia response compared to males and younger subjects (Gazerani, Andersen, and Arendt-Nielsen 2005; Morris, Cruwys, and Kidd 1997). Further, a study showed that red haired women had a reduced secondary hyperalgesia response to topical capsaicin compared to blonde or dark haired women, likely linked to a mutation in the melanocortin-1 receptor (MC1R) gene which can result in red hair in humans and may modulate pain responses (Andresen et al. 2011). In the current study, only 6 out of 14 subjects developed hyperalgesia (defined as those who had a significant increase in the pain intensity rating in the capsaicin treatment phase compared to the baseline phase), which is a response rate of only 43%. This is far lower than the 80-100% reported by Quesada *et al*.

The variability in response to capsaicin is a key factor that must be accounted for in study designs. To optimise experimental designs, a set definition of an adequate response to the model should be stated and subjects should only be included if they reach this threshold (O'Neill et al. 2012). For example, a study looking at the analgesic effects of neramexane and flupirtine using the intradermal capsaicin model included only subjects whose pain ratings to pin-prick stimuli increased 2-fold following capsaicin injection, which was 78% of the original subject cohort (Klein, Magerl, et al. 2008).

When the cohort of subjects included in the study are split into subjects who developed hyperalgesia (defined as those who had a significant increase in the pain intensity rating in the capsaicin treatment phase compared to the baseline phase) and subjects who did not develop hyperalgesia (those who did not), there was a significant increase in BOLD response in the anterior insular cortex during the end time section in the whole-brain analysis. When looking at selected brain regions using extracted parameter estimates, the BOLD responses in the RVM were significantly higher during the beginning and middle time sections, and the BOLD responses in the NCF were significantly higher during all time sections. This may indicate a potential role of these brainstem regions in driving the development of central sensitisation seen in the pain intensity rating data for the group who did develop hyperalgesia.

Interestingly, in the selected brainstem regions (vlPAG, RVM and NCF), the hyperalgesia group have higher BOLD responses to the pin-prick stimuli in the capsaicin condition and lower BOLD responses

in the placebo condition, compared to the no-hyperalgesia group who have higher BOLD responses in the placebo condition and lower BOLD responses during the capsaicin condition. The higher responses during the placebo condition of the group who did not develop hyperalgesia may indicate that the descending pain inhibitory system is more active in these subjects, so they have a lower 'vulnerability' to pain. The group who developed hyperalgesia may have a weaker inhibitory system (shown by the low BOLD response in the brainstem regions in the placebo condition), so they are more vulnerable to developing pain.

Frustratingly, many of the results discussed above are below the threshold for statistical significance. A key limitation of the study is that the number of subjects included is too low. The subject number of 14 for analysis may have been sufficient if all subjects had responded to the model to only look at the amplification of neural activity during the onset of central sensitisation. Previous studies have used similar group sizes of 12-15 subjects (Zambreanu et al. 2005; Lee et al. 2008). However, the fact that only a small number of subjects developed hyperalgesia means that this study was significantly underpowered for investigation of this primary objective, as only 6 subjects could be included to look at amplification of neural responses while the remaining 8 subjects did not respond. For the further exploratory analysis investigating vulnerability to developing a sensitised state, by comparing the responses of subjects who responded with the responses of those who did not, both groups are too small to make any firm conclusions. It would be very interesting to conduct a further experiment, utilising this early data to conduct a full power analysis and identify the minimum group size to detect differences in neural responses between those who develop hyperalgesia during the experiment and those who do not.

The great advantage of the within-subject design used in this study is that it controls for variability between individuals, enabling paired statistical comparison of the capsaicin and placebo conditions in the same person. However, a major disadvantage of within-subject designs is that an order effect can occur, where subject responses in the first condition can impact their responses in the second condition (Price et al. 2017). Although the order of the visits was randomised, the possibility of an order effect is a limitation in the comparison between the hyperalgesia and no-hyperalgesia groups that was conducted as part of the study. Subjects who experienced the capsaicin condition at the first visit were potentially more likely to develop hyperalgesia due to enhanced attentiveness and anxiety relating to the pain paradigm. To assess this, the randomisation order was compared for the hyperalgesia and no-hyperalgesia groupings. There were 4 subjects in the hyperalgesia group who received capsaicin at visit 1, and 2 who received placebo at visit 1, whereas there were 3 subjects in

the no-hyperalgesia group who received capsaicin at visit 1 and 5 subjects who received placebo at visit 1, therefore there was a higher proportion of subjects who had capsaicin at visit 1 who also developed hyperalgesia (and vice versa). To test if there was a significant order effect in the data, a three-way ANOVA was performed with the factors: stimulus number, treatment (capsaicin or placebo) and treatment order (capsaicin visit 1 or capsaicin visit 2). This showed that there was no significant effect of the treatment order ($F(1,12) = 0.6922$, $p = = 0.4217$), or of the stimulus number ($F(9, 108) = 1.685$, $p = 0.1013$), but that there was a significant effect of treatment ($F(1,12) = 11.19$, $p = 0.0058$).

To entirely overcome the issue of order effect if the experiment were to be repeated, the treatment order for subjects in each group (hyperalgesia and no-hyperalgesia) should be completely counterbalanced, with an equal number of subjects in each group receiving capsaicin first to the number who receive placebo first. This would be complex, and would likely require a screening visit to take place before the treatment visits to classify subjects as 'responders' or 'non-responders' prior to their participation in the treatment visits, which would allow the treatment orders for 'responder' and 'non-responder' groups to be planned in advance. The counterbalancing would need to be completed by a third party who could be unblinded, and the subjects would need to be randomly assigned to different orders.

Prior to application of the capsaicin or placebo cream, there were pin-prick stimuli applied in the scanner in order to characterise the baseline responses to the stimuli. As discussed in the methods, a technical issue with the stimulus timing files provided for the baseline data meant that these data could not be included for analysis. Ideally, it would have been valuable to include analysis of the responses at baseline, specifically it would have been interesting to understand whether the baseline responses are predictive of the response status for individual subjects.

2.6 Conclusion

In conclusion, the results of this study hint towards some very interesting findings about neural activity that occurs during the onset of central sensitisation induced by topical capsaicin, and the difference in responses of subjects who respond to the model (i.e. develop hyperalgesia) and those who do not respond. The results in the RVM and NCF brainstem regions are particularly notable given previous literature showing a specific role for the brainstem in the maintenance of central sensitisation, indicating that these regions may also play a key role in its development for those who respond. For

those who don't respond there could even be a protective role of descending inhibition from these regions. However, limitations in the study design, especially the fact that subject numbers are too low, mean that the overall conclusions of the experiment remain speculative. Further studies are required to verify these results, with larger subject numbers and an optimised study design.

EXPERIMENTAL CHAPTER 3

Characterisation of the neural correlates underlying the secondary hyperalgesia induced by the high frequency stimulation (HFS) model using fMRI

3.1 Abstract

Aims: Central sensitisation is characterised by an increase in pain response to noxious stimuli (hyperalgesia). Experimental central sensitisation models can elicit hyperalgesia in healthy humans. This study aimed to characterise how central sensitisation induced by one such model – high frequency stimulation (HFS) - modulates brain activity measured by fMRI. Based on previous fMRI studies with other experimental models, it was hypothesised that the response to pin-prick stimulation would be increased in the pain-related cortical regions and brainstem regions such as the nucleus cuneiformis, and that resting-state functional connectivity to selected seed-regions within the descending pain modulatory system (DPMS) would be increased, following HFS. The HFS model has been shown to modulate electroencephalogram (EEG) recordings and RIII reflex variables reflecting central sensitisation. Data were collected during the screening visit of the IMI-PainCare-BioPain-RCT4 trial; a multicentre trial investigating biomarkers of analgesic efficacy. This preliminary dataset was collected from 18 subjects, at the Oxford site (REC Reference 20/SW/0017).

Methods: After an initial baseline MRI scan, HFS was applied to the left lower leg of 18 healthy subjects. A second MRI scan was conducted 20 minutes after HFS application. HFS consisted of five 1s trains of 100 Hz electrical pulses separated by 9s intervals. Scans measured blood oxygen level dependent (BOLD) signal during 18 punctate mechanical stimuli applied 1cm outside the HFS site (secondary hyperalgesia area), and during rest. A whole brain, mixed effects analysis with cluster-based correction for multiple comparisons was performed to identify differences in stimulus evoked neural activity post-HFS vs. baseline. To investigate functional connectivity during rest a seed-based analysis was completed using three seed regions involved in pain processing; thalamus, anterior cingulate cortex (ACC) and periaqueductal grey (PAG).

Results: Following HFS, reported mean pain intensity and unpleasantness significantly increased during punctate mechanical stimulation. This was associated with significantly increased activation during the post-HFS scan vs. baseline (mixed effects analysis, $Z > 3.1$, $p < 0.05$) in areas involved in pain perception such as the posterior insula cortex, mid-anterior cingulate cortex, amygdala, hippocampus, thalamus, secondary somatosensory cortex and nucleus cuneiformis (NCF). Seed-based analysis showed functional connectivity between the periaqueductal grey and anterior cingulate cortex seed-regions and pain-related cortical regions such as the secondary somatosensory cortex and insula cortex was altered, while there were no regions that showed altered functional connectivity with the thalamus.

Conclusions: Compared to baseline, mechanical stimulation applied after HFS resulted in increased neural activity in cortical and sub-cortical pain processing areas and key brainstem nuclei such as the nucleus cuneiformis – an area shown to be implicated in both human and animal models of central sensitisation. In addition, functional connectivity was altered between brain regions involved in the descending pain modulatory system. This is consistent with other experimental central sensitisation models that have been widely studied using fMRI.

3.2 Introduction

There have been many experimental models of certain features of pain conditions, including peripheral and central sensitisation, that have been used in neuroimaging studies to study pain responses and the effects of analgesics in humans. The systematic literature review and meta-analysis in Chapter 1 of this thesis covered this topic in detail. The most commonly used experimental model in imaging studies has been topical capsaicin. Other models such as thermal stimulation (thermode-induced heat-injury), low-frequency electrical stimulation, ultraviolet-B radiation and intradermal capsaicin have also been used in imaging studies.

A recent comprehensive review of human models of central sensitisation outlined that out of over twelve models identified, there were five models that reliably induced secondary hyperalgesia to mechanical pin-prick stimuli and had been used independently by multiple research groups. These five models were topical capsaicin, intradermal capsaicin, thermode-induced heat-injury, low frequency electrical stimulation and high frequency stimulation (HFS) (Quesada et al. 2021). Therefore, the HFS model is an established model of the features of central sensitisation that has been used in multiple pain research studies, but unlike the others, there are no imaging studies showing the neural correlates of the model.

The HFS model involves delivery of electrical stimulation to the skin via surface electrodes. The stimulation is commonly delivered using a circular array of pin-electrodes, with five 1 second trains of 100Hz (high-frequency) stimulation at an interval of 10 seconds, with an intensity 10–20 times the electrical detection threshold to single pulses (Klein et al. 2004; Klein, Magerl, and Treede 2006; Klein, Stahn, et al. 2008). HFS rapidly induces an area of increased sensitivity to mechanical pin-prick stimuli in the skin surrounding the electrode pins, that lasts for several hours (Klein et al. 2004; Klein, Stahn, et al. 2008; Pfau et al. 2011; van den Broeke and Mouraux 2014). The human protocol for the HFS model was developed on the basis of animal study protocols which used electrical stimulation to produce long term potentiation of spinal nociceptive pathways (Klein et al. 2004). All types of nociceptors have been shown to contribute to the HFS induced response; with C-fibres having a larger contribution than Aδ-fibres, and the highest contribution from TRPV1-positive C-fibre nociceptors, as predicted based on animal studies (Henrich et al. 2015).

The protocol for the HFS model continues to evolve and it has been reported that there are differences in the response when the frequency of the stimulation is varied (Xia, Mørch, and Andersen 2016; van

den Broeke et al. 2019). One such study identified that an intermediate frequency 42Hz resulted in the strongest increase in sensitivity to pin-prick stimuli (van den Broeke et al. 2019) compared to 5Hz (low-frequency), 20Hz and 100Hz (high frequency) stimulation. A further study aimed to characterise the reliability of the response to the HFS model, both within- and between-session, and reported that there was good relative reliability of the area of hyperalgesia and the sensitivity to pin-prick stimuli between-sessions, concluding that the model is suitable to compare between subjects. However, the study reported there was lower absolute reliability with fluctuations in response when measures were repeated, concluding that the model may be less suitable for a within-subject design, such as an intervention study (Cayrol et al. 2020).

Although it has not been applied in an MRI study, use of the HFS model to induce central sensitisation in healthy humans has been investigated in conjunction with other measurements of pain responses. One example of this is the analysis of pin-prick evoked brain potentials (PEPs) measured using electroencephalogram (EEG), which have been shown to be altered in the sensitised (post-HFS) state compared to the non-sensitised state. Pin-prick stimulation of non-sensitised skin resulted in a low-frequency response followed by a decrease in alpha-band oscillations, and that during secondary mechanical hyperalgesia induced by HFS, there was a significant increase in the low-frequency response, but no increase in the alpha-band oscillations (van den Broeke et al. 2017). A second example is the use of the RIII nociceptive reflex of the lower limb. In a recent study investigating the response of RIII reflex variables reflecting central sensitization induced by the HFS and topical capsaicin models, it was shown that both models significantly reduced the RIII reflex threshold (by 20% and 18% respectively) and that neither model affected the size of the RII reflex (Leone et al. 2021). These studies therefore show that the HFS model is modulating the pain response as measured by multiple pain biomarkers, and that the modulation of the reflex variables reflecting central sensitisation is consistent with that of the topical capsaicin model.

As discussed in Chapter 1 of this thesis, imaging experiments using other experimental models to elicit hyperalgesia have shown that these techniques result in modulation of cortical and subcortical activity. In the centrally sensitised state, it was commonly reported that noxious mechanical stimuli applied to the area of secondary hyperalgesia induced increased activation in the somatosensory cortex, prefrontal cortex, insula cortex, anterior cingulate cortex (ACC), thalamus, and brainstem regions such as the nucleus cuneiformis (NCF) and periaqueductal grey (PAG), compared to the non-sensitised state (Maihöfner and Handwerker 2005; Zambreanu et al. 2005; Lee et al. 2008). This is consistent with animal studies which have shown that there is a significant contribution of supraspinal

sites to the development and maintenance of central sensitisation, with a particular contribution from brainstem nuclei (Urban and Gebhart 1999). Changes in the spinal cord have also been investigated using MRI, demonstrating increased activity in the ipsilateral dorsal horn during secondary mechanical hyperalgesia compared to stimulation prior to sensitisation (Rempe et al. 2014).

More recently, imaging techniques have also been applied to investigate changes in resting state activity associated with experimental models of central sensitisation. A recent study reported that resting-state functional connectivity of the descending pain modulatory system (DPMS), including the amygdala, PAG, parabrachial nucleus and ACC, was altered during tonic pain induced by the capsaicin-heat pain model compared to pain-free rest (Meeker et al. 2022).

The DPMS has been well-characterised in studies investigating the placebo effect, which have demonstrated that functional connectivity between the rostral ACC and the PAG and bilateral amygdalae is enhanced during placebo analgesia and that this coupling is stopped by naloxone (an opioid antagonist) (Bingel et al. 2006; Eippert et al. 2009). This evidences the key role of the endogenous opioid system in descending modulation of pain perception. Crucially, the influence of the DPMS is bidirectional, enabling both the alleviation of pain as in the placebo effect, and also the facilitation of pain (Bingel and Tracey 2008). The hyperalgesia and allodynia effects induced by central sensitisation following tissue damage due to injury is one example where the DPMS has an opposite role in facilitating increase pain perception. Imaging techniques have been used to interrogate the role of key brainstem areas involved in pain modulation in the facilitation of pain perception in a sensitised state. The PAG and NCF regions of the mesencephalic reticular formation have been shown to be activated during capsaicin-induced mechanical hyperalgesia (Zambreanu et al. 2005) and the involvement of brainstem regions in sensitisation was further illustrated in a study that mapped changes in activity in brainstem nuclei in response to primary and secondary dynamic mechanical allodynia (Mainero et al. 2007). Activity in the NCF brainstem region has been demonstrated to be specifically related to the pain perception in the centrally sensitised state, as this activity was specific to the centrally sensitised state when the intensity of pain stimuli were matched in the sensitised and non-sensitised states (Lee et al. 2008). Furthermore, there is growing evidence that development of chronic neuropathic pain states is due to dysregulation or the loss of control of the DPMS (Drake et al. 2021; Ossipov, Morimura, and Porreca 2014), making this system highly relevant in the understanding of chronic pain development and the identification of therapeutic targets.

The current study aimed to characterise how central sensitisation induced by HFS modulates brain activity as measured by functional magnetic resonance imaging (fMRI). Specifically, it aimed to:

1. Compare the whole-brain blood-oxygen level dependent (BOLD) response evoked by mechanical pin-prick stimuli before and after inducing hyperalgesia by the application of HFS, with a specific focus on characterising the change in BOLD response in the posterior insula cortex and the NCF.
2. Compare the whole-brain resting-state functional connectivity to selected seed-regions within the DPMS – the ventrolateral PAG (vlPAG), subgenual ACC (sACC), amygdala and NCF – in a centrally sensitised state (post-HFS) compared to baseline (pre-HFS).

It was hypothesised that the HFS-induced secondary mechanical hyperalgesia would increase the BOLD response to pin-prick stimulation in the brain regions that have been shown to have increased activity with other experimental models of central sensitisation, including the insula cortex, ACC, secondary somatosensory cortex, thalamus, and brainstem regions such as the NCF (Maihöfner and Handwerker 2005; Zambreanu et al. 2005; Lee et al. 2008). Further, it was hypothesised that the BOLD response in the NCF region of the brainstem would increase in the post-HFS condition too, as this region has been shown in a previous study to have a specific role in the maintenance of the centrally-sensitised state (Lee et al. 2008), which should be consistent with the induction of central sensitisation with the HFS model.

Secondly, it was hypothesised that functional connectivity between selected seed-regions within the DPMS (vlPAG, sACC, amygdala, and NCF) would be altered with similar pain-related brain regions as above, particularly with regions of the DPMS as demonstrated with the capsaicin-heat pain model (Meeker et al. 2022). The vlPAG seed-region was chosen due to the role of the vlPAG in activating descending modulation of neuropathic pain, for example evidenced in a recent optogenetic study in mice (Huang et al. 2019). In a study using the capsaicin heat-pain model, it was demonstrated that deactivation of the vlPAG occurred during primary allodynia, and that this decrease in activity was inversely correlated with pain ratings meaning that higher deactivation was associated with higher subject-reported pain intensity (Mainero et al. 2007). In addition, it has been shown that functional connectivity between the PAG and sACC is altered during tonic pain and that this functional connectivity is positively correlated with pain intensity ratings (Meeker et al. 2022). These findings indicate the PAG region has a role in the intensity of pain perceived during sensitisation, and therefore we aim to investigate whether this role is underpinned by changes in functional connectivity at rest

between this region and other regions involved in pain perception during central sensitisation. The altered connectivity between the PAG and sACC was also one reason that the sACC seed-region was chosen. The rostral area of the ACC plays a key role in the DPMS and connectivity between this region and the PAG and bilateral amygdalae has been shown to be increased during placebo analgesia (Bingel et al. 2006; Eippert et al. 2009), demonstrating its role in modulating the perception of pain. The amygdala seed-region was chosen due to the role of the amygdala in the DPMS, as specifically it has been shown in whole-brain analysis that functional connectivity (either in pain-free rest or during pain) between the amygdala seed-regions and several areas, including the right superior parietal lobule, caudate nucleus, right inferior temporal gyrus, right claustrum, right primary visual cortex and right temporo-occipitoparietal junction, is correlated with subsequent pain intensity ratings (Meeker et al. 2022). Finally, the NCF seed-region was chosen due to the evidence that the NCF plays a key role in the maintenance of the centrally sensitised state in human studies using the capsaicin model (Lee et al. 2008; Zambreanu et al. 2005), therefore it is a key region to include to interrogate whether changes in functional connectivity with this region during rest are underpinning the changes in BOLD response to mechanical stimulation that have been shown in previous studies.

3.3 Methods

3.3.1 Study participants and ethical approval

Data was collected as part of the IMI-BioPain RCT4 trial. The aim of the IMI-BioPain RCT4 trial focusses on the use of fMRI to assess analgesic efficacy in healthy human participants. It includes an initial screening visit, during which no analgesics are administered. The data shown here were collected during this initial screening visit.

This preliminary dataset was collected from 18 healthy subjects (mean age 25.7, range 21 to 38, 9 female), at the Oxford site (REC Reference 20/SW/0017). All subjects were right-handed as assessed by the Edinburgh Handedness Inventory, and defined as a score ≥60. Written informed consent was obtained from all participants.

3.3.2 Study design

To investigate how HFS-induced central sensitisation affects brain activity at rest and in response to mechanical pin-prick stimuli, we compared fMRI data collected before HFS (baseline) and approximately 20 minutes after the application of HFS. The study design is shown in Figure 1.

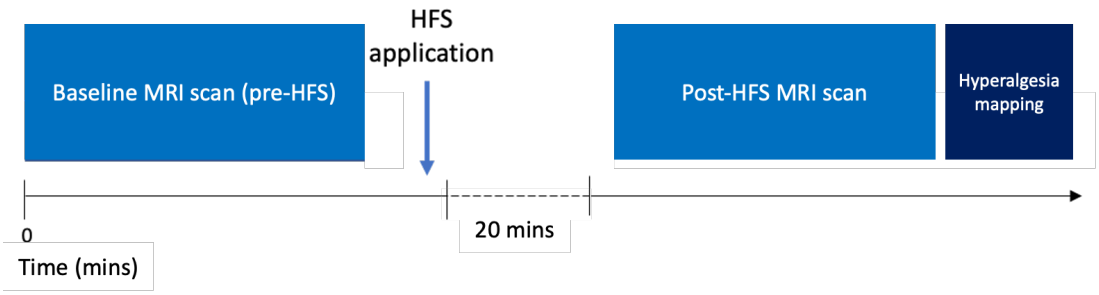

Figure 1: Overview of study design.

The study design consisted of a baseline MRI scan (pre-HFS), followed by the application of HFS. After a period of 20 minutes, a second post-HFS MRI scan was completed. Hyperalgesia mapping was completed after the second MRI scan.

3.3.3 High frequency stimulation (HFS)

In order to induce hyperalgesia, HFS was delivered to the skin of the left lower leg using the multi-pin HFS Electrode "EPS-P10" manufactured by *MRC Systems GmbH*. The pulses delivered by the electrode were generated by the Digitimer DS7A constant current stimulator. The HFS application consisted of 5 trains of electrical pulses delivered at 100 Hz. Train duration was 1s, with an interval of 9s between each train, and the stimulation intensity was set to 20x the detection threshold for each subject. After HFS application the position of the cathode pins was marked on the subject's leg with a pen. The HFS electrode and electrode placement are illustrated in Figure 2.

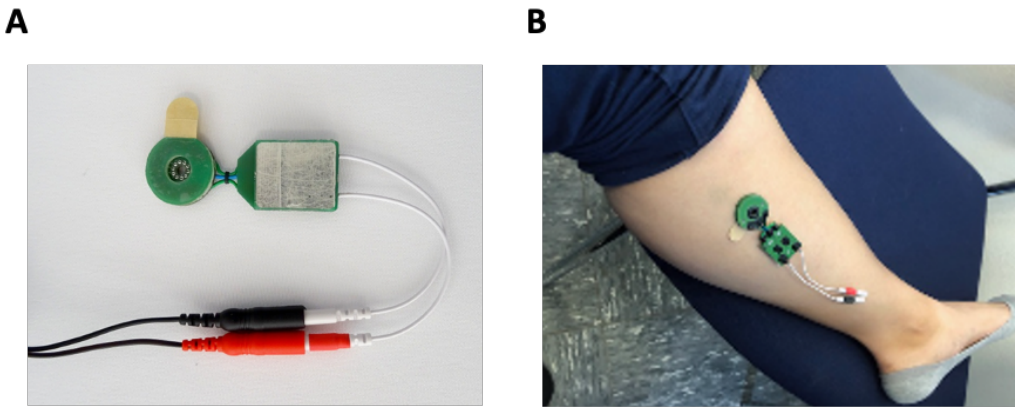

Figure 2: HFS Electrode "EPS-P10" and electrode positioning

A: The HFS electrode used is shown. It consists of a circular cathode, with 10 needle pins arranged on a circle with a diameter of 5 mm, and a rectangular anode with area 24x20mm^2. The cathode is secured to the skin with a double adhesive ring and the anode is secured to the skin with an adhesive electrolytic gel pad. It is attached to two connecting cables (shown) which are connected to the Digitimer DS7A constant current stimulator (not shown).

B: The HFS electrode was positioned on the medial aspect of the left lower leg. The electrode was not placed too close to the tibia, as shown in the figure. The rectangular anode was positioned towards the ankle and the circular cathode was placed towards the knee.

The HFS model is a validated and non-invasive procedure to induce a stable secondary hyperalgesia surrounding the location where HFS was applied due to central sensitization lasting at least four hours (Klein et al. 2004; Pfau et al. 2011; van den Broeke and Mouraux 2014). The electrode is designed to preferentially activate cutaneous nociceptors and the application of HFS induces a local skin flare response, but does not cause long-lasting spontaneous pain.

3.3.4 Magnetic resonance imaging (MRI) protocol and acquisition

Each MRI scan included a blood oxygen level dependent (BOLD) scan during resting state, a BOLD scan during mechanical punctate stimuli in the area of secondary hyperalgesia, an arterial spin labelling (ASL) scan during rest, and a field map. The first MRI scan (pre-HFS) also included a T1 structural scan acquired at the end. During the mechanical punctate stimuli scan, BOLD signal changes were measured in response to 18 mechanical stimuli each with a 1s duration, applied using a 512nM weighted non-skin penetrating punctate probe.

Participants rated the pain intensity of each mechanical stimulus, and provided an average rating of pain unpleasantness following all 18 stimuli, both using a visual analogue scale from 0 (no pain at all/not unpleasant at all) to 100 (most intense pain imaginable/extremely unpleasant). The total duration of each punctate scan was 10 minutes. Punctate stimuli were applied in the area of secondary hyperalgesia, 1cm outside the site of the HFS cathode pins. The MRI protocol is outlined in Figure 3.

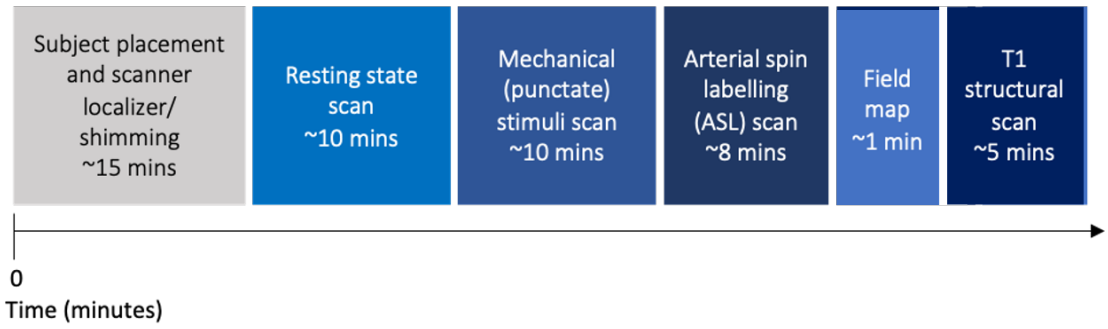

Figure 3: Overview of MRI scan protocol.

For the baseline scan, following subject placement in the scanner and completion of localizer scans and shimming, the protocol consisted of a resting state BOLD scan (10 minutes), a mechanical stimuli BOLD scan (10 minutes), an arterial spin labelling (ASL) scan, a field map and a structural T1 scan. The scan protocol for pre- and post-HFS scans were identical, except the T1 scan was only completed in the pre-HFS scan.

MRI data was collected using a 3T Siemens PRISMA scanner with a 32-channel head-coil. All BOLD data (mechanical stimulation task and rest) were acquired with a whole brain echo-planar imaging sequence with an echo time of 36ms, field of view 192mm x 192mm, voxel size 2mm x 2mm x 2mm and multiband acceleration factor 6. The mechanical stimulation task scan had 531 volumes and the rest scan had 513 volumes, both with a repetition time of 1.17 seconds. The ASL data are not included in this thesis and acquisition of this data is therefore not described here. A field map was acquired to after the functional scans to enable correction of field inhomogeneity during analysis, with voxel size 2mm x 2mm x 2mm and field of view 192 mm x 192mm. Finally, in the pre-HFS scan the T1-weighted structural scan was acquired with voxel size 1mm x 1mm x 1mm for registration of the functional BOLD scans to standard space for group-level analysis.

3.3.5 Hyperalgesia mapping

Hyperalgesia mapping was completed after the second MRI scan, approximately 90 minutes after the HFS was applied. To map the area of hyperalgesia, mechanical pin-prick stimuli were applied with the 512nM stimulator in 8 radii around the position HFS was applied, as shown in Figure 4. The stimuli were applied from the outermost point working in towards the centre at irregular time intervals. Subjects were instructed to close their eyes, and asked to report when/if the stimulus intensity felt "different" - more intense, or a stronger pricking or stinging sensation. The region between the more intense stimulus placement and the previous stimulus was marked with pen and the radii were measured from the pen mark to the marked edge of the cathode pins, allowing a mean to be

calculated. Following the mapping, subjects were asked to provide a verbal average pain intensity score for the pin-prick stimuli that were applied during the mapping exercise, using a scale from 0 (no pain at all) to 100 (most intense pain imaginable).

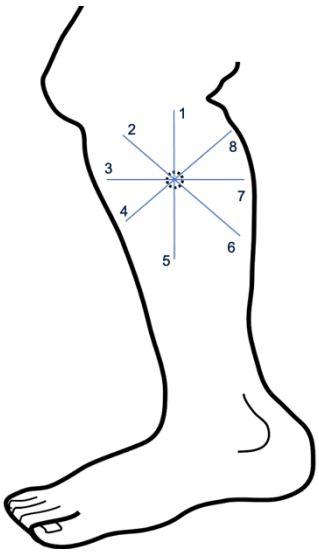

Figure 4: Hyperalgesia mapping protocol.

Mechanical pin-prick stimuli were applied with the 512nM stimulator in 8 radii around the marked area of skin where the HFS cathode pins were situated. Starting at the position closest to the knee (marked '1' in the figure) stimuli were applied from the outermost point working in towards the centre at irregular time intervals. This was repeated for each radius in the order labelled 1 to 8 in the figure. Subjects were instructed to close their eyes, and asked to report when/if the stimulus felt "different" - more intense, or stronger pricking/stinging. The region between the more intense stimulus placement and the previous stimulus was marked, and radii were measured to the marked edge of the cathode pins.

3.3.6 Statistical analysis

Statistical analysis for all behavioural data was completed using GraphPad PRISM version 9.4.1 (GraphPad Software, LLC). Statistical significance is reported with the following symbols; ns for $P > 0.05$; * for $P \leq 0.05$, ** for $P \leq 0.01$, *** for $P \leq 0.001$, and **** for $P \leq 0.0001$.

Imaging data were analysed using tools in FMRIB Software Library v6.0 (FSL) (Woolrich et al. 2009; Smith et al. 2004; Jenkinson et al. 2012). For analysis of BOLD data, structural and magnitude images were brain extracted (Smith 2002) and a calibrated field map image was prepared as required for B0 unwarping. Registration to the structural image and B0 unwarping were performed using FEAT (Woolrich et al. 2001). Motion correction, spatial smoothing (5mm for mechanical pin-prick stimulation scan and 3mm for resting state scan) and high-pass temporal filtering were applied. Independent component analysis was conducted with the MELODIC tool and data from the first 10 subjects was hand classified into signal and noise components. This training dataset was then used to remove noise components from the remaining 8 subjects using FIX (Griffanti et al. 2014; Salimi-Khorshidi et al. 2014).

For the mechanical pin-prick stimulation scan, once each subject's data had been denoised an individual statistical map for the response to the pin-prick stimuli was generated using the general linear model (GLM) approach implemented with FEAT (Woolrich et al. 2001). Finally, a group-level whole brain, mixed effects analysis with a cluster-based correction for multiple comparisons was performed using FEAT to search for differences in stimulus evoked neural activity post-HFS when compared to pre-HFS (Woolrich et al. 2004). The Featquery tool in FSL was used to extract mean percentage change in BOLD parameter estimates for the posterior insula and NCF regions.

For the resting state analysis, the time course for activity in each of the selected seed-regions (vlPAG, sACC, right amygdala and left NCF) was extracted and used to generate individual statistical maps of the functionally correlated activity across the whole brain for each subject, using the GLM approach implemented with FEAT (Woolrich et al. 2001). Individual maps were constrained to grey matter only by regressing out activity in white matter and cerebrospinal fluid, using time courses for this activity in the GLM which were generated from the anatomical segmentations for each tissue type. A group-level whole brain analysis was conducted with the same methodology applied for the pin-prick data, to identify differences in the seed-based functional connectivity between the pre-HFS and post-HFS conditions (Woolrich et al. 2004). All seed-regions are shown in Figure 5 and are described below.

The ventrolateral PAG (vlPAG) seed-region was defined in a previous study using a connectivity-based segmentation approach. Diffusion MRI optimised for the brainstem was used with probabilistic tractography to elucidate connectivity profiles of the voxels within the PAG, enabling it to be segmented into four clusters, one of which being the ventrolateral PAG (Ezra et al. 2015; Faull and Pattinson 2017).

The subgenual ACC seed-region was anatomically defined using bilateral 5mm radius spheres in the voxel location corresponding to the subgenual ACC described by Meeker et al., with MNI co-ordinates x=±5, y=31, z=-9 (Meeker et al. 2022).

The right amygdala seed-region was anatomically defined using the Harvard-Oxford Subcortical Structural Atlas applied in FSL (Desikan et al. 2006), with a mask created by thresholding to 50% and binarizing the image.

The NCF seed-region was functionally defined using the area of increased BOLD response to mechanical pinprick stimulation identified in the whole-brain analysis of the post-HFS condition

compared to the pre-HFS (baseline) condition that was consistent with this region. The thresholded z-statistic image generated in the whole-brain analysis was constrained to the brainstem only (defined using the Harvard-Oxford Subcortical Structural Atlas applied in FSL (Desikan et al. 2006)), and binarized to produce the seed-region mask.

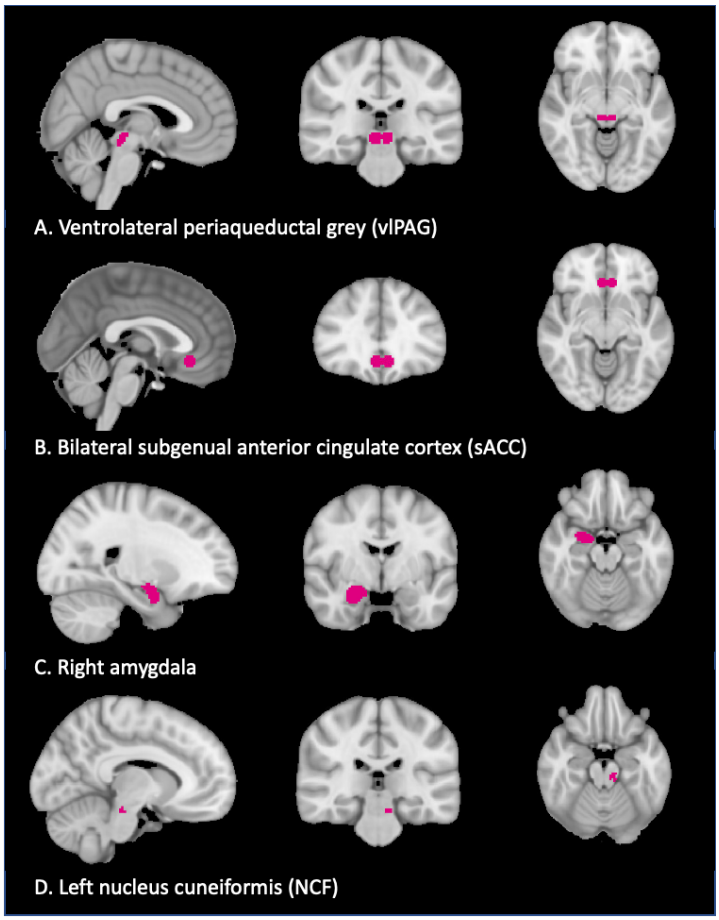

Figure 5: Masks used to define seed regions for seed-based functional connectivity analysis

Seed-based functional connectivity analysis was carried out using four seed-regions; the ventrolateral periaqueductal grey (vlPAG - A), the bilateral subgenual anterior cingulate cortex (sACC - B), the right amygdala (C), and the left nucleus cuneiformis (NCF - D). The vlPAG was defined using a connectivity-based segmentation approach (Ezra et al. 2015). The sACC was defined using a 5mm sphere mask with voxel co-ordinates corresponding to this region from a previous study (Meeker et al. 2022). The right amygdala was anatomically defined using the Harvard-Oxford Subcortical Structural Atlas applied in FSL (Desikan et al. 2006). The NCF was functionally defined as the area of increased BOLD response to mechanical stimulation in the post-HFS condition compared to baseline (pre-HFS) that corresponded to the NCF region in the brainstem.

3.4 Results

3.4.1 Hyperalgesia mapping results

Hyperalgesia mapping completed 90 minutes after the HFS was applied demonstrated that all subjects developed a discrete area of increased sensitivity to mechanical stimuli which could be mapped. The average radius of the area of hyperalgesia was 40.5mm (range from 12.6mm to 72mm). Subjects rated the average pain intensity of the mapping stimuli on a scale from 0 (no pain at all) to 100 (most intense pain imaginable), and the average pain intensity score for the hyperalgesia mapping was 36.9 (range from 5 to 75).

3.4.2 Mechanical pin-prick stimuli responses

Subject reported pain intensity and pain unpleasantness measured using the visual analogue scale from 0 (no pain at all/not unpleasant at all) to 100 (most intense pain imaginable/extremely unpleasant) both increased during the post-HFS stimulation compared to baseline (pre-HFS). During the post-HFS scan, the mean pain intensity ratings increased from 14.73 to 32.31 ($p < 0.0001$, paired t-test) compared to baseline (pre-HFS), and mean pain unpleasantness ratings increased from 16.06 to 39.78 ($p < 0.0001$, paired t-test). On an individual subject level, the ratings were higher in the post-HFS scan compared to baseline (pre-HFS) in 17 subjects out of the total 18 subjects for pain intensity, and in all 18 subjects for pain unpleasantness.

Pain intensity and pain unpleasantness ratings are shown in Figure 6, plotted for both individual subjects (Figure 6A and 6C) and as the mean for all 18 subjects (Figure 6B and 6D).

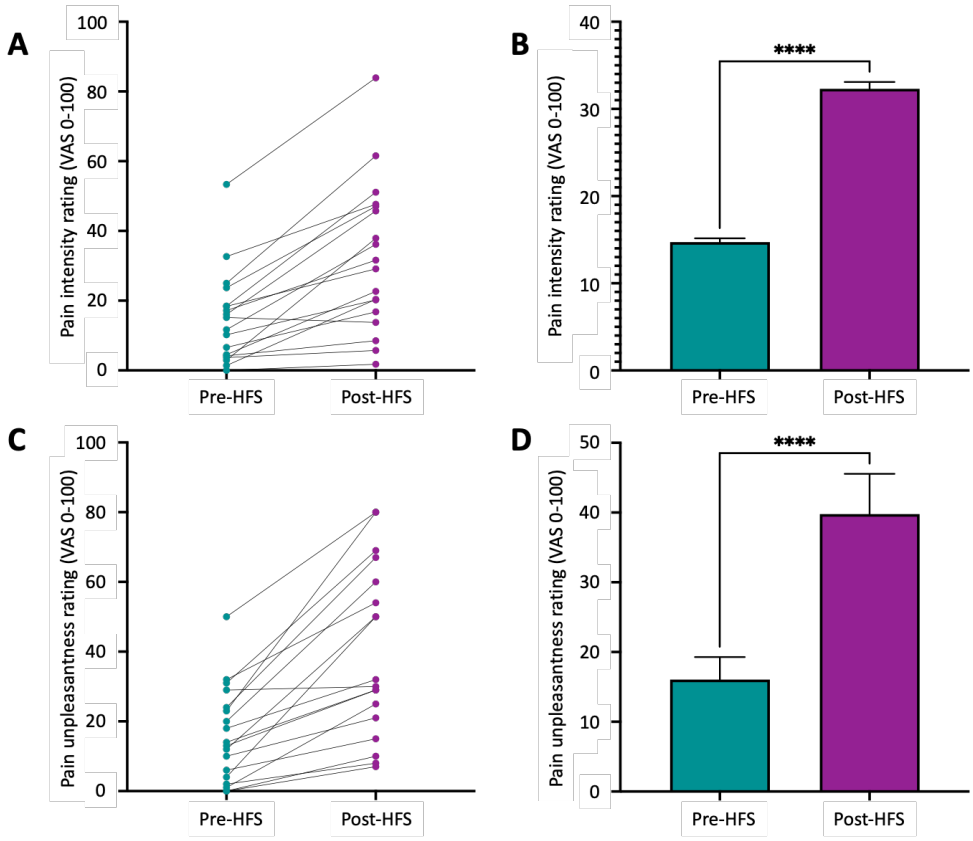

Figure 6: Pain intensity and pain unpleasantness ratings for pre-HFS and post-HFS scans.

Top panels A and B show mean pain intensity ratings for individual subjects, both plotted for individual subjects (A) and as a mean for all 18 subjects (B). Compared to baseline (pre-HFS), the mean pain intensity increased for post-HFS for 17 out of 18 subjects, and the mean pain intensity for all 18 subjects increased from 14.73 to 32.31 ($p < 0.0001$, paired t-test). Bottom panels C and D show average pain unpleasantness ratings for individual subjects (C) and unpleasantness ratings for all 18 subjects (D). Average unpleasantness ratings increased in the post-HFS scan for all 18 subjects, and the mean pain unpleasantness ratings increased from 16.06 to 39.78 ($p < 0.0001$, paired t-test). Error bars show the SEM.

The BOLD response during hyperalgesia was significantly increased compared to baseline (pre-HFS) in areas involved in pain perception and in descending pain modulation, including the posterior insula cortex, mid-anterior cingulate cortex, amygdala, hippocampus, NCF, thalamus and secondary somatosensory cortex (mixed effects analysis, $Z > 3.1$, $p < 0.05$). The whole-brain BOLD response for the pre-HFS vs. post-HFS comparison in shown in Figure 7.

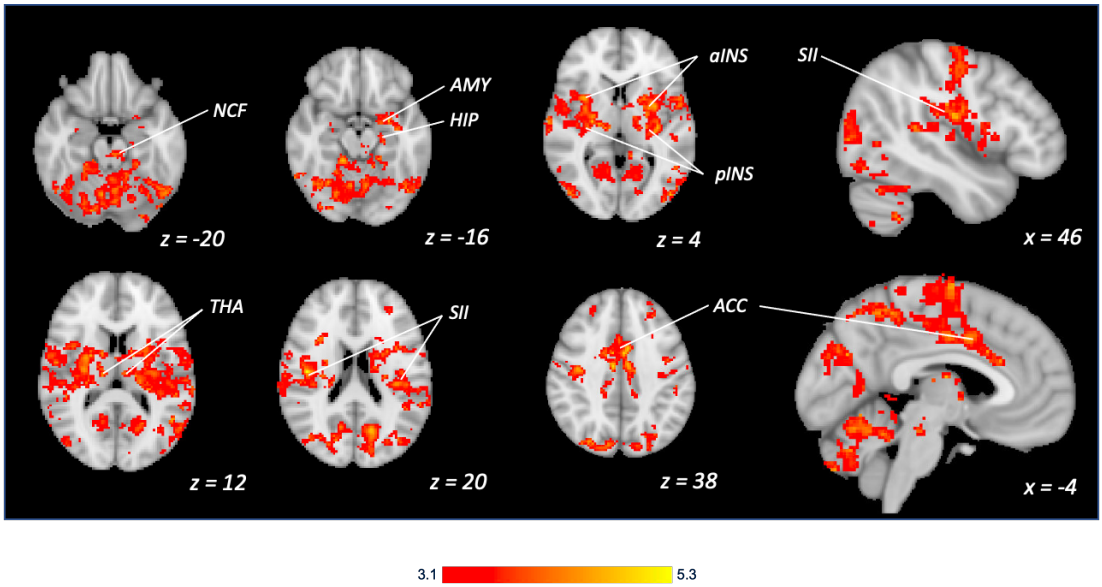

Figure 7: Whole-brain BOLD response to mechanical stimulation during hyperalgesia (post-HFS) compared to baseline.

BOLD activation was significantly increased during the post-HFS scan vs. baseline (mixed effects analysis, Z > 3.1, p < 0.05) in areas involved in pain perception such as the anterior and posterior insula cortices (aINS and pINS), anterior cingulate cortex (ACC), amygdala (AMY), hippocampus (HIP), nucleus cuneiformis (NCF), thalamus (THA) and secondary somatosensory cortex (SII). MNI-512 co-ordinates are shown.

The posterior insula cortex is an area of particular interest in this study as BOLD activation in this region has been shown to be modulated by other experimental hyperalgesia models and by analgesics (Wanigasekera et al. 2016). Based on this, the region has been selected as one of the primary endpoints for the BioPain RCT4 trial, therefore it was important to characterise the response to the HFS model in the posterior insula cortex. The endpoint did not specify the ipsilateral or contralateral insula cortex; therefore, both sides are explored here. In previous studies, it has been shown that change in cerebral blood flow in the contralateral dorsal-posterior insula cortex is strongly correlated to pain intensity ratings (Segerdahl et al. 2015), so the contralateral (right) side is most relevant.

Figure 8 shows the change in BOLD response in the left (ipsilateral to the stimulus applied) and right (contralateral to the stimulus applied) insula cortex. An anatomical mask was used to constrain the post-HFS vs. baseline (pre-HFS) whole brain result (mixed effects analysis, $Z > 3.1$, $p < 0.05$), creating a functional mask for each side representing the area of the insula that was significantly more activated during mechanical stimulation post-HFS. Mean percentage change in parameter estimates were extracted from these regions and are shown plotted in the figure, demonstrating a clear increase post-HFS compared to baseline (pre-HFS) on both sides.

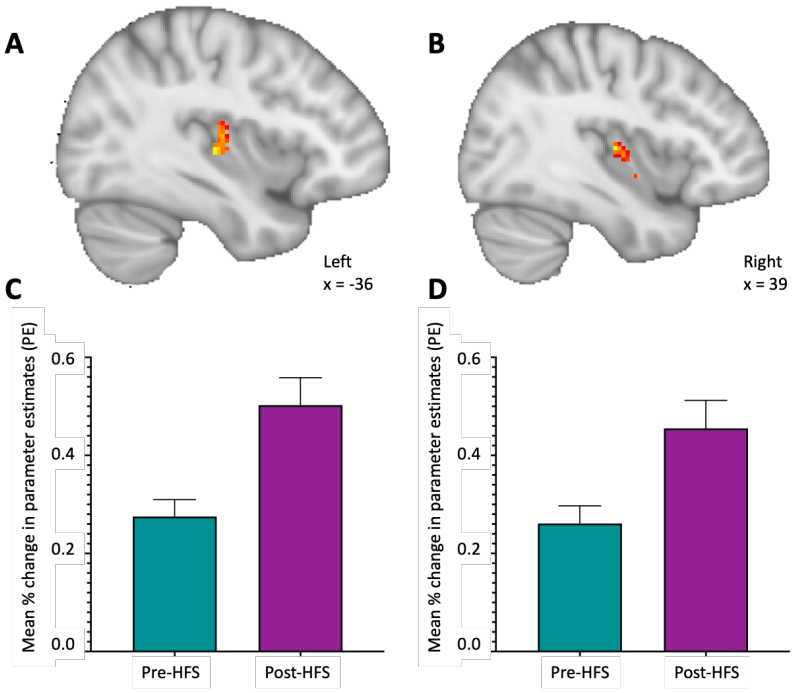

Figure 8: Illustration of change in BOLD response in the posterior insula cortex in the post-HFS condition compared to baseline (pre-HFS) from the whole-brain analysis.

Areas of significant activation in the posterior insula cortex from the whole-brain analysis (mixed effects analysis, $Z > 3.1$, $p < 0.05$) are shown in the top panels for the left (A) and right (B) posterior insula. The mean percentage change in BOLD parameter estimates was extracted from these areas using the Featquery tool in FSL. The extracted parameter estimates are shown as a bar graph for each area of activation for the left (C) and right (D) sides. Error bars show the SEM. MNI-512 co-ordinates are shown for images. An anatomical posterior insula cortex mask was used to ensure that the significant activity illustrated in the figure came from the posterior insula.

A correlation analysis showed that the change in pain intensity and unpleasantness ratings between the pre-HFS and post-HFS conditions was significantly correlated with the change in the BOLD parameter estimate in the right (contralateral) posterior insula cortex. This is shown in Figure 9.

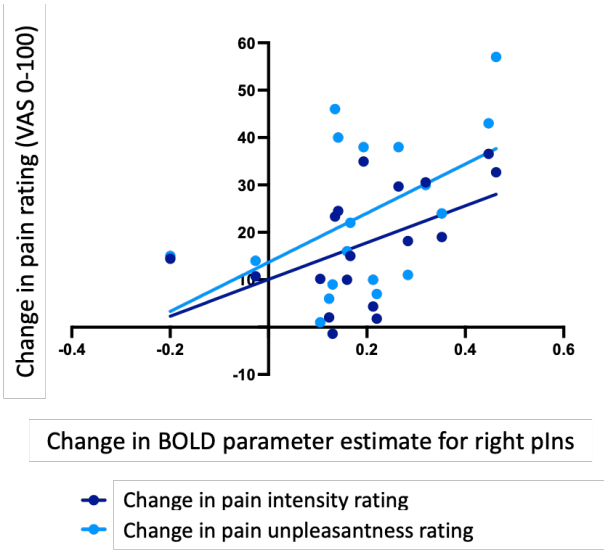

Figure 9: Correlation between pain ratings and the BOLD response in the right (contralateral) posterior insula cortex.

Change in pain intensity and unpleasantness ratings between the pre-HFS and post-HFS condition are plotted against the change in BOLD parameter estimate for the right posterior insula (pINs). Calculation of a Pearson correlation coefficient showed there was a positive correlation between the two variables with both pain intensity and unpleasantness, r(df) = 0.5041 and 0.4954, p = 0.0165 and 0.0183, respectively.

The NCF is also an area of particular interest as this region of the brainstem has been shown to have a specific role in the maintenance of central sensitisation (Lee et al. 2008; Zambreanu et al. 2005). In the whole-brain analysis comparing the sensitised (post-HFS) condition compared to baseline (pre-HFS) there was an area of the brainstem that showed significantly increase activation in the post-HFS condition. This area corresponded to the NCF, an area that has been previously reported to be significantly active when comparing a secondary hyperalgesia condition induced by topical capsaicin compared with the control condition (Zambreanu et al. 2005). This is shown in Figure 10A, which shows the brainstem area of increased activation in the post-HFS vs. pre-HFS whole-brain comparison (mixed effects analysis, $Z > 3.1$, $p < 0.05$) in red/yellow, and a 5mm spherical mask (constrained to the brainstem only) with its centre at the reported peak MNI co-ordinates for the NCF region ($x = -10$, $y = -28$, $z = -18$) in blue (Zambreanu et al. 2005). There is considerable overlap in the areas shown, though the result from the HFS model also extends more centrally across the brainstem too. Parameter estimates extracted from the NCF region mask (as described above, generated from peak voxel co-ordinates for the activation cluster reported by Zambreanu et al.) show that the BOLD response in the NCF is increased during the post-HFS condition compared to baseline (pre-HFS). It also changes from a small deactivation in the pre-HFS condition in response to the pin-prick stimuli, to a larger activation in the sensitised (post-HFS) condition in response to the same stimuli. This is shown in Figure 10B. There was a positive relationship between the hyperalgesia radius and the change in BOLD response in the NCF between the pre-HFS and post-HFS conditions, with subjects who had the largest hyperalgesia area also having the largest increase in BOLD response in this brainstem region. This relationship was not significant at the $p < 0.05$ level with a Pearson correlation coefficient. The correlation analysis is shown in Figure 10C.

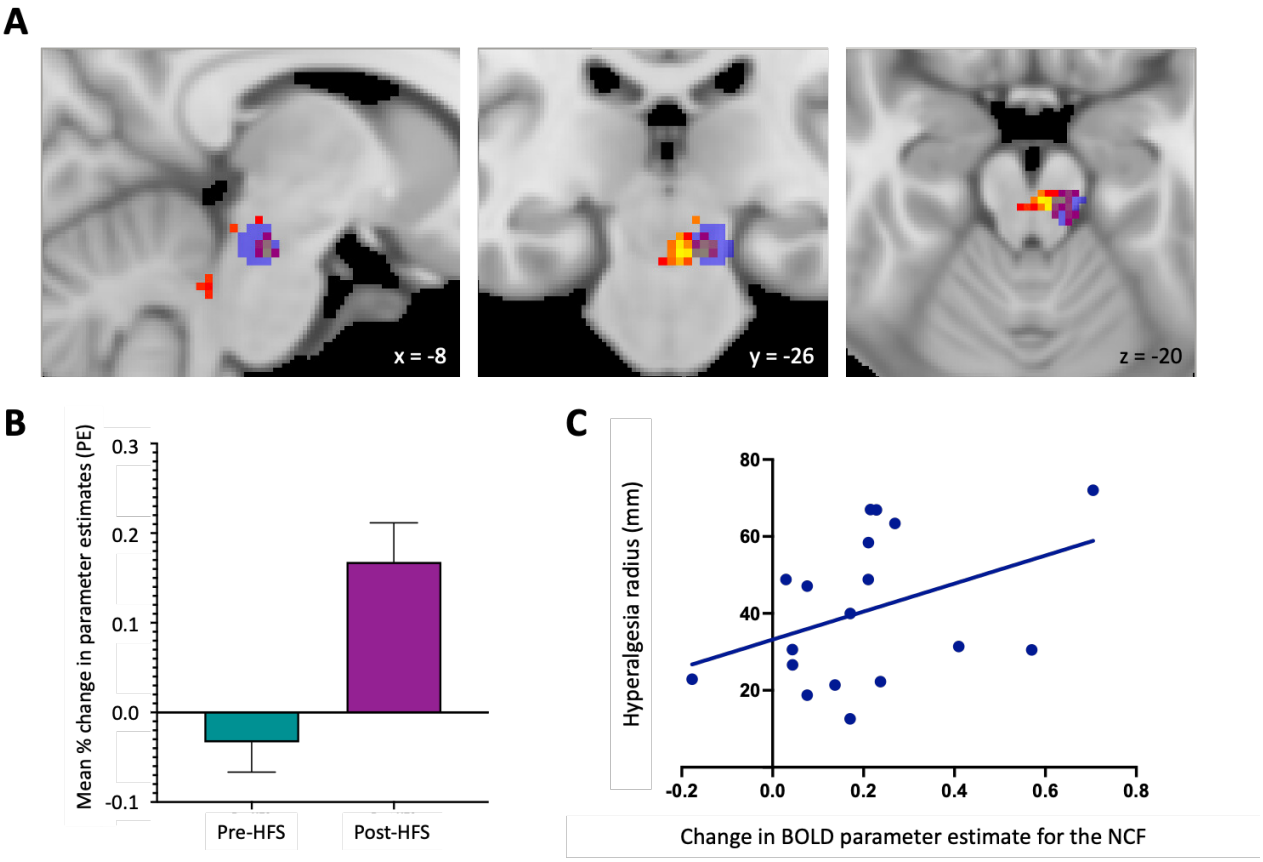

Figure 10: Illustration of change in BOLD response in the NCF in the post-HFS condition compared to baseline (pre-HFS).

A: The post-HFS vs. baseline (pre-HFS) whole-brain analysis (mixed effects analysis, $Z > 3.1$, $p < 0.05$) resulting in a cluster of activation in the brainstem region that corresponds to the NCF. This is shown in red/yellow, with the thresholded z-statistic image generated in the whole-brain analysis constrained to the brainstem only (defined using the Harvard-Oxford Subcortical Structural Atlas applied in FSL (Desikan et al. 2006)). In blue, a 5mm spherical mask of the peak activation voxel reported by Zambreanu et al. for the NCF region is shown, also constrained to the brainstem as defined above. MNI-512 co-ordinates are shown.

B: Mean percentage parameter estimates for the BOLD response in the pre-HFS and post-HFS conditions are plotted. Parameters estimates were extracted from the whole-brain analysis for the area of the NCF defined using the blue mask (generated using the peak activation voxel reported for the NCF region). Error bars show the SEM.

C: Hyperalgesia radius (mm) is plotted against the change in BOLD parameter estimate for the NCF between the pre-HFS and post-HFS condition. Calculation of a Pearson correlation coefficient showed there was not a significant correlation between these variables, $r(df) = 0.3886$, $p = 0.0555$.

3.4.3 Resting state seed-based functional connectivity results

Ventrolateral PAG seed region:

Whole-brain analysis showed functional connectivity was significantly increased between the ventrolateral PAG seed-region and clusters corresponding to the right thalamus and the bilateral secondary somatosensory cortex (whole-brain mixed effects analysis, $Z > 3.1$, $p < 0.05$). This is shown in Figure 11. There were no areas of decreased connectivity.

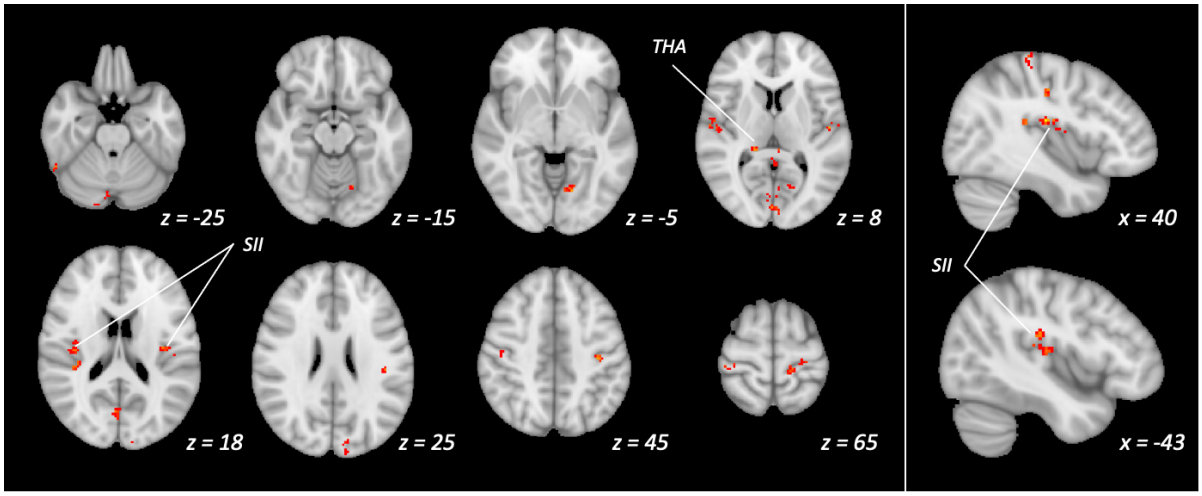

Figure 11: Whole-brain resting seed-based functional connectivity during hyperalgesia (post-HFS) compared to baseline for ventrolateral periaqueductal grey (vlPAG) seed region.

With the vlPAG seed region there was significantly increased connectivity during the post-HFS scan vs. baseline (mixed effects analysis, $Z > 3.1$, $p < 0.05$) in areas involved in pain perception such as the right thalamus (THA) and the secondary somatosensory cortex (SII). MNI-512 co-ordinates are shown below each image slice.

To further illustrate this result, the SII region is shown in a larger size in Figure 12A and 12B, and extracted functional connectivity coefficients are plotted in Figure 12C and 12D. The plotted functional connectivity coefficients extracted from these areas of activation within an anatomical mask of the left and right SII regions illustrate that this 'increase' reflects a change from negative functional connectivity to a less negative value (close to zero) from the pre-HFS scan to the post-HFS scan. The secondary somatosensory cortex region was anatomically defined using the Juelich Histological Atlas applied in FSL, combining the parietal operculum OP1, OP3 and OP4 regions, with a threshold of 50% (Eickhoff, Schleicher, et al. 2006; Eickhoff, Amunts, et al. 2006).

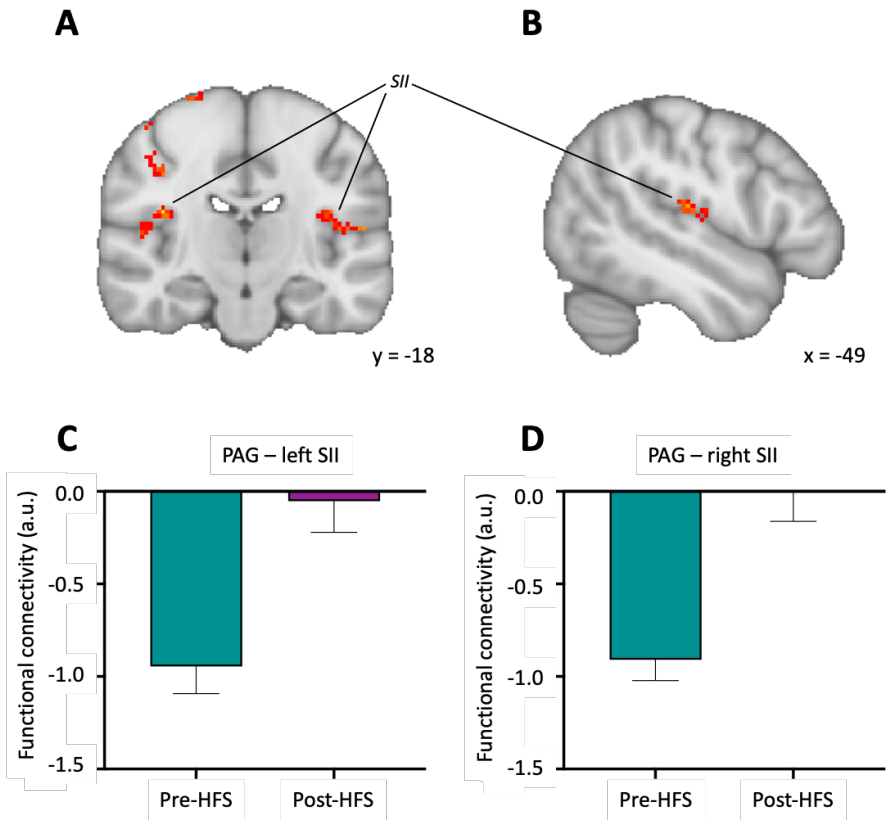

Figure 12: Seed-based functional connectivity between ventrolateral periaqueductal grey (seed-region) and the secondary somatosensory cortex (SII).

When using the ventrolateral periaqueductal grey as a seed-region there was significantly increased functional connectivity with the secondary somatosensory cortex (SII) during hyperalgesia (post-HFS) compared to baseline, as shown in the coronal image slice (A) and the sagittal image slice (B), which shows the left side as an example. Functional connectivity coefficients extracted from these areas of activation within an anatomical mask of the left and right SII regions are plotted in the bar charts below (C and D), illustrating that this 'increase' reflects a change from negative functional connectivity to a less negative value (close to zero) from the pre-HFS scan to the post-HFS scan. Error bars show the SEM. MNI-512 co-ordinates are shown.

Region-of-interest analysis was carried out to interrogate the relationship between the vlPAG seed-region and the right posterior insula cortex. An anatomical mask of the right posterior insula was used to carry out a small-volume correction using non-parametric permutation testing with 5,000 permutations and threshold-free cluster-enhancement, with family-wise error corrected to 0.05 (Winkler et al. 2014). This showed that functional connectivity between the vlPAG and right posterior insula was significantly increased during rest in the post-HFS condition compared to baseline (pre-HFS). This is shown in Figure 13A. Extracted functional connectivity coefficients show that this

significant increase is caused by a change from negative connectivity to positive connectivity from the pre-HFS condition to the post-HFS condition, as shown in Figure 13B. This change in functional connectivity coefficients was found to have a negative relationship with the change in pain intensity and unpleasantness ratings when the two variables were plotted (as shown in Figure 13C), though this was not significant at the $p > 0.05$ level with calculation of a Pearson correlation coefficient. Correlation with pain ratings was investigated as it has been previously shown in studies using the capsaicin heat-pain model that deactivation of the vlPAG during primary allodynia is inversely correlated with pain ratings (Mainero et al. 2007), and that activation in the contralateral dorsal-posterior insula is positively correlated with pain ratings during tonic pain (Segerdahl et al. 2015). Interestingly, there does seem to be a relationship between the vlPAG – right posterior insular functional connectivity and the pain ratings here, though it is not significant.

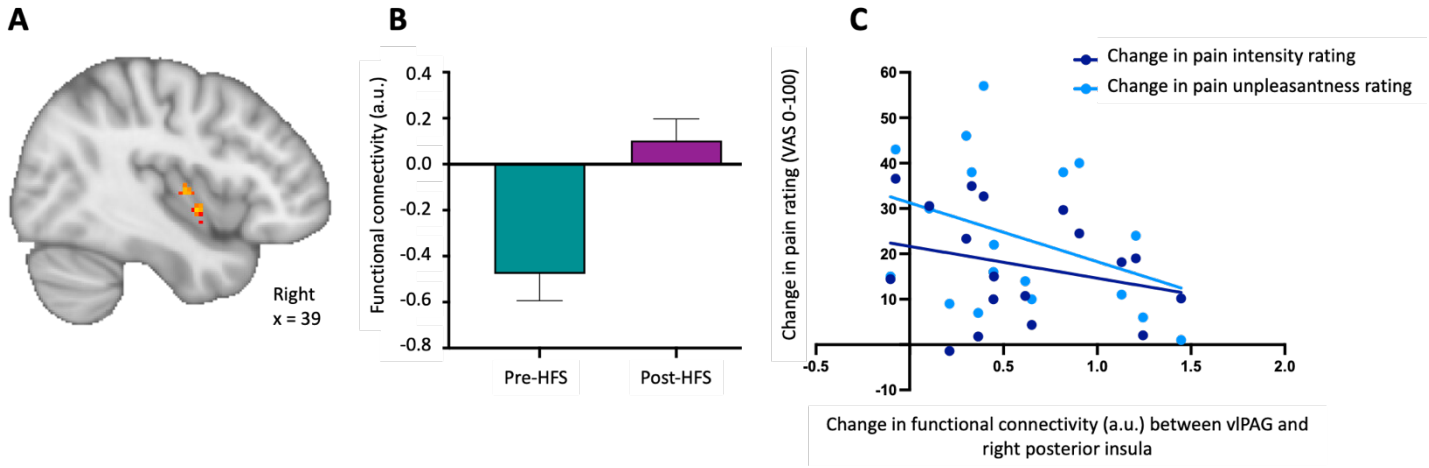

Figure 13: Region of interest (ROI) analysis of the right posterior insula with the vlPAG seed-region

A: The region of the right posterior insula found to have significantly increased functional connectivity with the vlPAG seed-region in the post-HFS condition compared to baseline (pre-HFS). Connectivity between these regions was evaluated with a small-volume correction using non-parametric permutation testing with 5,000 permutations and threshold-free cluster-enhancement, with family-wise error corrected to 0.05. MNI-512 co-ordinates are shown below the image slice.

B: Functional connectivity coefficients were extracted for the connectivity between the right posterior insular and the vlPAG and are plotted as a bar chart. The mean functional connectivity coefficient is increased in the post-HFS condition compared to baseline (pre-HFS) and also changes from negative connectivity to positive connectivity. Error bars show the SEM.

C: Change in pain intensity and unpleasantness ratings between the pre-HFS and post-HFS conditions is plotted against the change in the functional connectivity coefficient between the right posterior insula and the vlPAG, and shows there is a negative relationship; as change in ratings decreases the change in functional connectivity increases. Calculation of a Pearson correlation coefficient showed the relationship was not statistically significant between the two variables with both pain intensity and unpleasantness, r(df) = -0.2658 and -0.3612, p = 0.1432 and 0.0704, respectively.

Right amygdala seed region:

Whole-brain seed-based functional connectivity analysis using the right amygdala as the seed region showed that functional connectivity increased between the right amygdala and the frontal orbital cortex and the precentral gyrus in the post-HFS condition compared to the pre-HFS condition (whole-brain mixed effects analysis, $Z > 3.1$, $p < 0.05$), as shown in Figure 14. There were no areas of decreased connectivity.

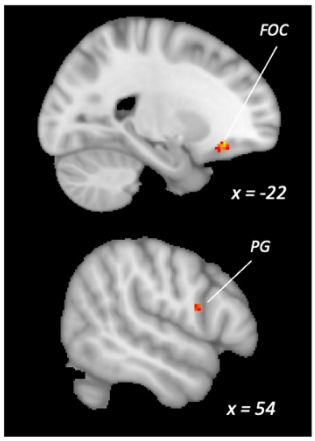

Figure 14: Whole-brain resting seed-based functional connectivity during hyperalgesia (post-HFS) compared to baseline for right amygdala seed region.

With the right amygdala seed region there was significantly increased connectivity during the post-HFS scan vs. baseline (mixed effects analysis, $Z > 3.1$, $p < 0.05$) in the frontal orbital cortex (FOC) and the precentral gyrus (PG) regions. Image slices taken at MNI-512 co-ordinate x = -22 (top) and x = 54 (bottom).

Bilateral subgenual anterior cingulate cortex (sACC) seed region:

Whole-brain seed-based functional connectivity analysis using the bilateral sACC as the seed region showed that functional connectivity decreased between the sACC and a more central part of the ACC and the SII region in the post-HFS condition compared to the pre-HFS condition (whole-brain mixed effects analysis, $Z > 3.1$, $p < 0.05$), as shown in Figure 15. These 'decreases' reflected a change from positive or close to zero connectivity in the pre-HFS condition to negative connectivity in the post-HFS condition. There were no areas of increased connectivity.

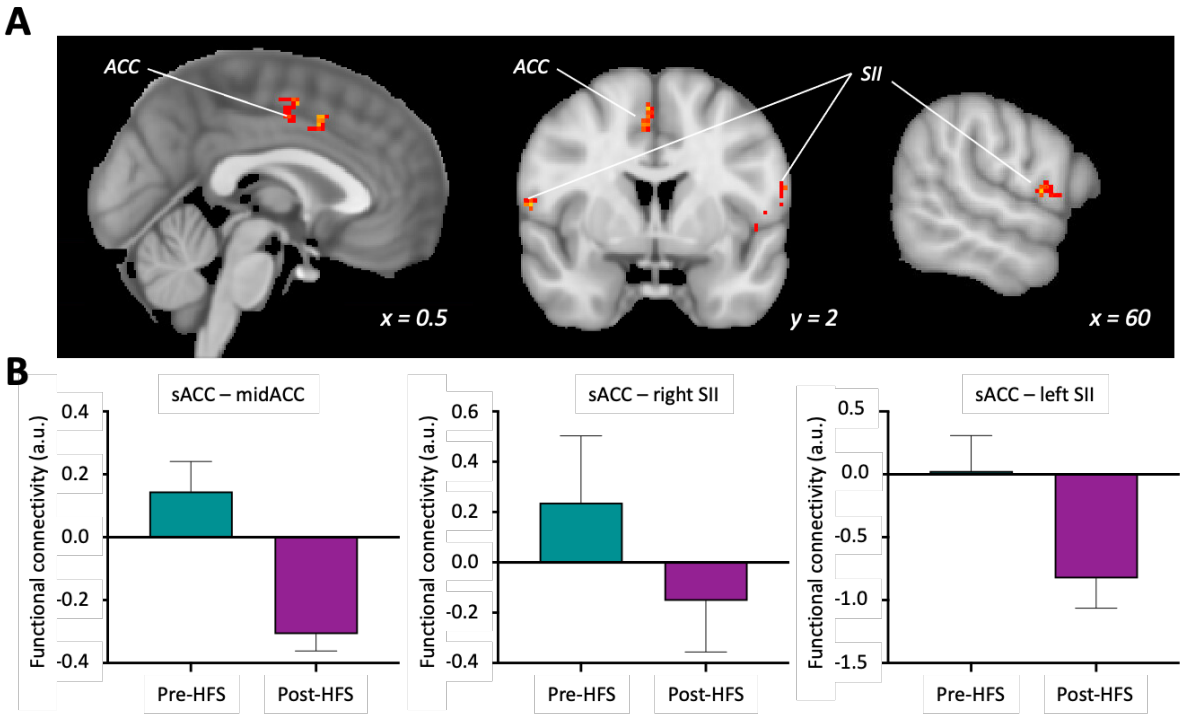

Figure 15: Whole-brain resting seed-based functional connectivity during hyperalgesia (post-HFS) compared to baseline for subgenual anterior cingulate cortex (sACC) seed region.

A: With the sACC seed region there was significantly decreased connectivity during the post-HFS scan vs. baseline (mixed effects analysis, Z > 3.1, p < 0.05) in the ACC and SII regions. Image slices taken at MNI-512 co-ordinate x = 0.5 (left) and y = 2 (middle) and x = 60 (right).

B: To further illustrate this result, functional connectivity coefficients were extracted for the connectivity between the sACC and the regions with significantly decreased functional connectivity (mid-ACC, right SII and left SII) and are plotted as bar charts. These show that there was a change from positive or close to zero connectivity in the pre-HFS condition to negative connectivity in the post-HFS condition. Error bars show the SEM.

Nucleus cuneiformis (NCF) seed region:

Whole-brain seed-based functional connectivity analysis using the NCF as the seed region showed that functional connectivity decreased between the NCF and the posterior cingulate cortex (PCC) in the post-HFS condition compared to the pre-HFS condition (whole-brain mixed effects analysis, Z > 3.1, p < 0.05), as shown in Figure 16. There were no areas of increased connectivity.

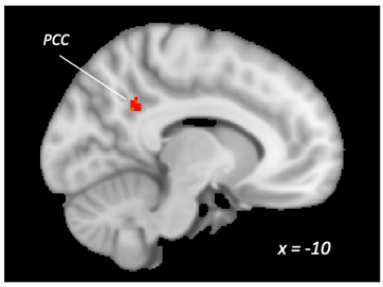

Figure 16: Whole-brain resting seed-based functional connectivity during hyperalgesia (post-HFS) compared to baseline for the NCF seed region.

With the NCF seed region there was significantly decreased connectivity during the post-HFS scan vs. baseline (mixed effects analysis, $Z > 3.1$, $p < 0.05$) in the posterior cingulate cortex (PCC) region. Image slice taken at MNI-512 co-ordinate x = -10.

3.4.4 Summary of key results

Overall this chapter has outlined many changes in punctate-evoked responses and functional connectivity following sensitisation with the HFS model compared to baseline. In order to consolidate these findings, the key results of this chapter are summarised in Figure 17. During mechanical stimulation, there was increased BOLD activity in the ACC, SII, insula cortex and in the brainstem, specifically the NCF, as shown in Figure 17A. The extracted BOLD parameter estimates are plotted for the posterior insula cortex and NCF in Figure 17B to illustrate this change. These changes in brain activity were accompanied by changes in behavioural data, with subject-reported pain intensity ratings significantly increased in the post-HFS condition compared to the pre-HFS condition, and a significant correlation between the change in pain intensity ratings and the change in BOLD response in the posterior insula cortex, as shown in Figure 17C. Functional connectivity was shown to be altered between the SII region, shown to have an increased BOLD response during mechanical stimulation following HFS, and the vlPAG, a key region of the brainstem involved in the descending pain modulatory system, as shown in Figure 17D.

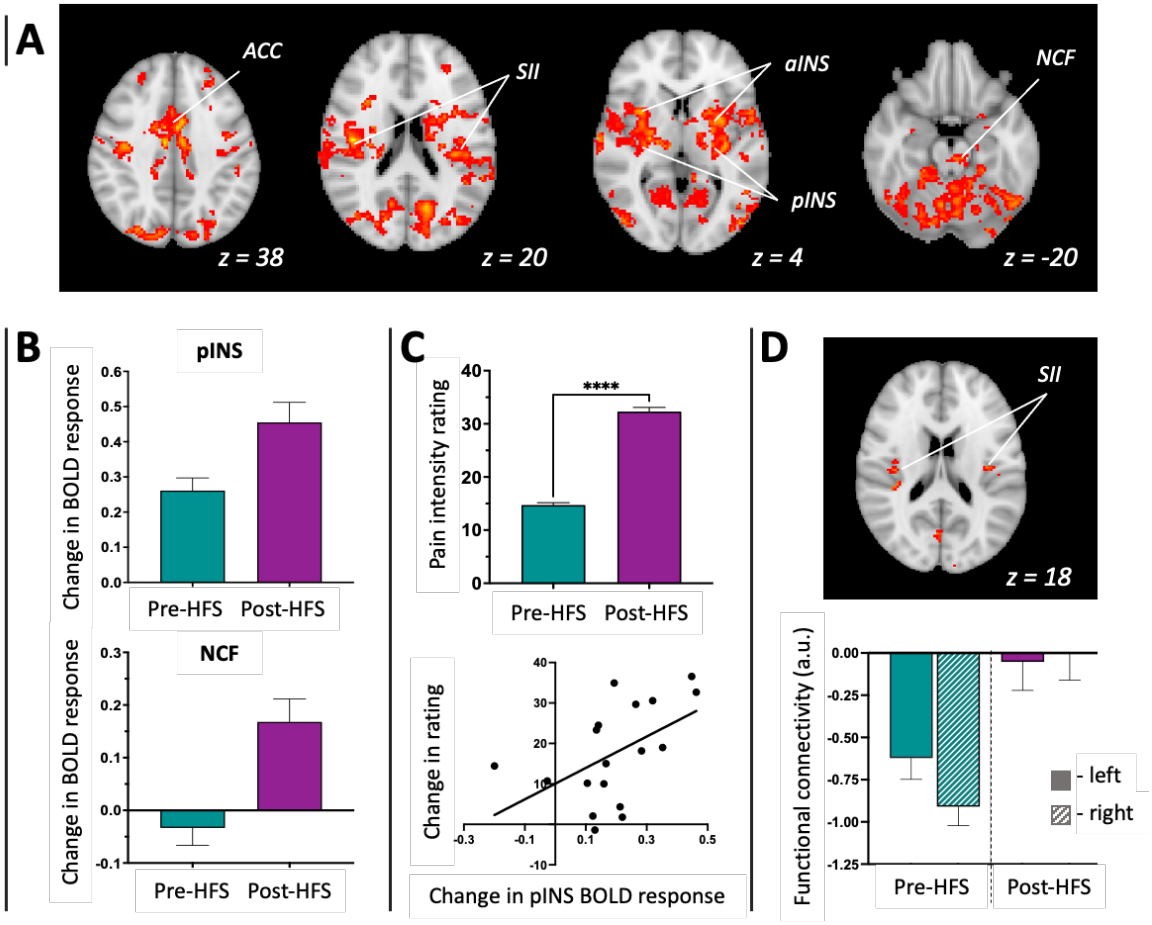

Figure 17: Summary of key results.

A: BOLD activation was significantly increased during the post-HFS scan vs. baseline (mixed effects analysis, $Z > 3.1$, $p < 0.05$) in areas involved in pain perception such as the anterior cingulate cortex (ACC), secondary somatosensory cortex (SII), anterior and posterior insula cortices (aINS and pINS) and nucleus cuneiformis (NCF). MNI-512 co-ordinates are shown.

B: Extracted mean percentage change in BOLD parameter estimates are shown as a bar graph for the pINS (contralateral) and NCF (ipsilateral) regions, illustrating the increase in activity during the post-HFS condition compare to the pre-HFS baseline. Error bars show the SEM.

C: Mean pain intensity increased during the post-HFS condition compared to the pre-HFS baseline from 14.73 to 32.31 ($p < 0.0001$, paired t-test). This change in pain intensity ratings was significantly correlated with the change in punctate-evoked BOLD response in the contralateral posterior insula cortex ($r(df) = 0.5041$, $p = 0.0165$).

D: There was significantly increased functional connectivity between the vlPAG seed region and bilateral SII during hyperalgesia (post-HFS) compared to baseline (pre-HFS) as shown in the top panel (mixed effects analysis, $Z > 3.1$, $p < 0.05$). MNI-512 co-ordinates are shown. Functional connectivity coefficients are plotted showing functional connectivity was altered from negative connectivity (pre-HFS) to around zero connectivity (post-HFS). Error bars show the SEM.

3.5 Discussion

The use of fMRI in conjunction with experimental models of central sensitisation in healthy humans has been shown to be a valuable tool for investigation of the neural correlates of central sensitisation and its modulation by analgesics (Lee et al. 2008; Zambreanu et al. 2005; Iannetti et al. 2005; Lee et al. 2013; Wanigasekera et al. 2016). However, the HFS model had not previously been studied in conjunction with fMRI. This study has used fMRI to show that the state of central sensitisation induced by HFS consists of increased neural activity in cortical and sub-cortical pain processing areas and key brainstem nuclei such as the NCF during mechanical stimulation. It has also shown that the functional connectivity between brain regions involved in the DPMS is altered during rest following application of HFS compared to the non-sensitised state.

Overall, the study demonstrates that HFS induced central sensitisation results in modulation of brain activity that is consistent with other central sensitisation models that have been widely studied using fMRI, namely capsaicin, which has been well-characterised in imaging studies. Two studies that aimed to characterise the neural correlates of central sensitisation using capsaicin models (topical capsaicin and intradermal capsaicin) reported activity in the brainstem (Lee et al. 2008; Zambreanu et al. 2005). This result has been replicated in this study with the HFS model, where there is a significant change in activation in the NCF following HFS compared to baseline. Modulation of activity in cortical regions such as the insula cortex, ACC, thalamus and secondary somatosensory cortex has been reported consistently in imaging studies using other experimental models, as discussed in detail in Chapter 1 of this thesis, and this is also consistent with the results of this study. Furthermore, the study demonstrated that the increase in pain ratings and BOLD response in the contralateral posterior insula in the pre-HFS condition vs. the post-HFS condition were positively correlated, which is consistent with evidence from a 3T study using the topical capsaicin model which also showed that pain ratings were correlated with the imaging result in the contralateral dorsal-posterior insula cortex (Segerdahl et al. 2015). During rest, seed-based functional connectivity analysis demonstrated there were changes in connectivity between seed-regions in the DPMS and a number of brain regions, which is consistent with a recent study that showed modulation of the functional connectivity of DPMS dyads during tonic pain induced by the capsaicin model (Meeker et al. 2022). Interestingly, the changes in functional connectivity observed in these analyses involved a change in the sign of the functional connectivity measure. The vlPAG seed-region showed negative functional connectivity with the bilateral SII and right posterior insula cortex regions in the pre-HFS baseline condition, which switched to a close to zero or positive connectivity in the post-HFS condition. The sACC seed-region showed positive or close

to zero functional connectivity with the mid-ACC and bilateral SII regions in the pre-HFS condition, which switched to a negative connectivity in the post-HFS condition. Functional connectivity is a measure of how synchronous fluctuations in the BOLD response in two brain regions is, during rest (Lee, Smyser, and Shimony 2013). Positive functional connectivity between two regions means that responses are synchronised or correlated, functional connectivity of zero means responses are not synchronised, and negative functional connectivity means that responses are anticorrelated (Fox et al. 2005; Liang, King, and Zhang 2012; Martinez-Gutierrez et al. 2022). Previously, negative connectivity has been less well studied and interpretation of such findings is debated, but evidence is growing that it likely does have a physiological basis (Martinez-Gutierrez et al. 2022). Negative functional connectivity has been previously shown between the PAG (a key region involved in pain modulation) and the posterior insula cortex during rest (Kong et al. 2010). The switch from negative connectivity (during rest) to positive connectivity (during hyperalgesia) may reflect modulation of pain responses during the hyperalgesic state mediated by the PAG. Overall, it is not possible to conclude the exact basis for the changes in functional connectivity observed in this chapter, and further studies are needed to elucidate the meaning of these results.

There are various advantages and disadvantages of the different experimental models of central sensitisation. HFS notably offers a long and stable duration of central sensitisation (Henrich et al. 2015; Klein et al. 2004; Pfau et al. 2011). This is advantageous in imaging studies as MRI data acquisition protocols can be up to 1.5 – 2 hours long. In addition, it allows flexibility in study designs where imaging data may be collected at multiple time points, for example multiple time points after an analgesic intervention has been administered to understand the effect over time. The rapid and consistent onset of the sensitised state also enables the model to be used for assessing the efficacy of analgesics which are administered after the establishment of the sensitised state (post-HFS), more closely mimicking the scenario for treating patients who already have developed chronic pain. In previous studies using the capsaicin models the analgesics are often given prior to the model set-up, therefore confounding interpretation of whether the effect of the drug is modulating the establishment or maintenance of the sensitised state. A further benefit of the HFS model is that it has been shown to have a high response rate. In this study, 17 out of 18 subjects reported increased pain intensity and unpleasantness in response to pin-prick stimuli, a response rate of 94.4%. This is consistent with previous studies which have reported response rates of 79-100% (Klein, Magerl, and Treede 2006; Klein, Stahn, et al. 2008; Pfau et al. 2011; Biurrun Manresa et al. 2018; Quesada et al. 2021). This is advantageous as it maximises the effect size within the data set and reduces the likelihood for individual subjects' data to need to be excluded if they did not develop sufficient

hyperalgesia. As data acquisition for imaging studies is expensive and resource intensive, this is an important consideration when designing imaging studies. These advantages mean that the HFS model is a valuable tool for use in conjunction with neuroimaging.

A potential disadvantage of the HFS model has been raised in a recent study that reported large between-subject variability and significant fluctuations in the within-subject response across repeated measures, when assessed using hyperalgesia area and pain intensity ratings (Cayrol et al. 2020). The current study is consistent with this result, with high level of variability in the change in the radius of the hyperalgesia area and in pain intensity ratings between subjects, which ranged from 12.6mm to 72mm and -1.39 to 39.56, respectively. There was a high level of variability in the imaging results between subjects as well, shown by the change in the BOLD parameter estimate in the right posterior insula which ranged from -0.19963 to 0.4626. The study design did not enable evaluation of consistency of within-subject repeated measures as HFS was applied once in each subject. It would be valuable to investigate the within-subject response variability further, as the Cayrol et al. study only looked at hyperalgesia area and subject ratings of pain intensity. However, if this finding was replicated in further studies and also validated using more objective pain biomarkers such as MRI, it would be an important consideration for the design of future studies. Interventional studies that involve repeated measures under different conditions, for example placebo-controlled drug studies, would need to ensure the effect size of the response and the number of subjects included was high enough to mitigate any variability in the magnitude of the hyperalgesia response to the HFS model itself.

A key limitation with the methodology of this study was that it was not conducted in a blinded and randomised manner. In order to achieve this, the design should have included a sham stimulation arm and have involved two visits (one for HFS and one for sham), which subjects would have attended in a randomised order with the researchers and subjects blinded to the condition. Unfortunately, this would not have been possible due to the fact that the data were from the screening visit of the BioPain study – the protocol of which was optimised for the primary endpoint of the trial (i.e. understanding the effects of the analgesics) and not for this HFS model characterisation. To enable the blinding and randomisation, it would have required an additional visit, and since the study already required a high number of visits (5 in total) and also already involved high costs due to the high number of scans included, therefore this would not have been feasible.

3.6 Conclusion

In conclusion, this study has shown that the neural correlates of HFS-induced central sensitisation are aligned to those induced by other models of central sensitisation, as measured with fMRI. The HFS model has promising characteristics that make it a valuable tool for use in future studies. However, there remains a need to further characterise the response to HFS, particularly it's consistency across within-subject repeated measures. It is important that the advantages and potential disadvantages associated with the HFS model are carefully considered when designing experiments that utilise this tool, as with any other experimental model that is applied in a research setting.

EXPERIMENTAL CHAPTER 4

BioPain Trial: A randomised, double-blind, placebo-controlled, cross-over trial in healthy subjects to investigate the effects of lacosamide, pregabalin and tapentadol on biomarkers of pain processing observed by fMRI of the brain

4.1 Abstract

Introduction and aims: There is an unmet need for effective analgesics for chronic pain patients. Challenges in bridging the gap between pre-clinical and clinical trials during drug development highlights a need for objective pain biomarkers, to verify target engagement and efficacy. Functional magnetic resonance imaging (fMRI), used in conjunction with experimental models of chronic pain features such as hyperalgesia, is a promising tool in this area. This multi-site study aimed to profile biomarkers derived from fMRI measures, after administration of drugs with known analgesic efficacy.

Methods: Data was collected from 29 healthy human subjects in total, across 3 sites (in the UK, France and Denmark). Local regulatory and ethics approvals were granted at all three sites, as applicable. The trial applied a 4-way cross-over, placebo-controlled, double-blind, randomised design. At each of four study days, hyperalgesia was induced in the left lower limb using high-frequency electrical stimulation (HFS). Subjects then received an oral dose of lacosamide, pregabalin, tapentadol, or placebo. FMRI measures of blood oxygen level dependent (BOLD) signal during 18 punctate mechanical stimuli applied 1cm outside the HFS site (secondary hyperalgesia area), and during rest, were obtained at 1-hour post-drug and 3-hours post-drug time points. Two primary endpoints were assessed; the change in BOLD response to mechanical stimulation in the posterior insular cortex, and the change in functional connectivity between the thalamus (seed-region) and the secondary somatosensory cortex, both for the pregabalin vs. placebo comparison at the 3-hour timepoint.

Results: The trial result was negative for both primary endpoints; which were tested in parallel, splitting the overall α (0.05) equally between them, thus requiring a p-value of less than 0.025 to reach significance. For the difference in BOLD response in the posterior insula at the 3-hour time point between pregabalin and placebo the p value was p=0.0408 (paired t-test) and for the difference in functional connectivity between the thalamus and SII at the 3-hour time point between pregabalin and placebo the p value was p=0.4666 (paired t-test). Thus, the alpha-level 0.025 was not reached. Further exploratory analysis showed that the BOLD response to mechanical pin-prick stimulation was reduced in the right (contralateral) posterior insular cortex with both pregabalin and tapentadol at the 1-hour time point, and with pregabalin at the 3-hour time point, compared to placebo. During rest, lacosamide was shown to decrease connectivity between the right thalamus and the right secondary somatosensory cortex at both the 1-hour and 3-hour time points, compared to placebo.

Conclusions: Drugs of known analgesic efficacy are shown to modulate fMRI pain biomarkers during experimentally induced hyperalgesia, as expected based on evidence from previous studies. The standardised protocol and multi-site approach mean that this work contributes valuable additional evidence on the utility of fMRI measures in evaluating analgesic efficacy, especially as two of the three compounds (lacosamide and tapentadol) had not been previously studied using fMRI. It does highlight that selection of narrowly defined trial endpoints needs careful consideration in future fMRI trial designs, as the results of this study show good target engagement of these drugs with pain related brain regions, despite failing to show statistical significance in the primary endpoint measures. Overall, the results of this trial further support the use of fMRI in conjunction with experimental pain models as a valuable tool for assessing modulation of the neural correlates of the pain response by analgesics.

4.2 Introduction

Chronic pain represents a major challenge for healthcare systems, associated with a significant social and economic impact. 10-14% of the population suffer from moderate to severely disabling chronic pain (Fayaz et al. 2016). There remains a significant unmet need for effective analgesic treatments, as the success rate for analgesics treating chronic pain is only around 30% (Borsook, Becerra, and Hargreaves 2011a). Development of improved analgesics is hindered by the lack of objective outcome measures to support the subjective and behavioural measures currently used in animal studies and clinical trials. Advances in functional imaging offer hope that identification of chronic pain neural signatures, and crucially of analgesic efficacy, could offer an objective biomarker for use in analgesic development (Borsook, Becerra, and Hargreaves 2011a; Tracey, Woolf, and Andrews 2019).

FMRI has been used in many studies to investigate the effects of analgesics on the brain. In healthy humans, it has been used in conjunction with experimental models of features of chronic pain, such as central sensitisation, to investigate the mechanism of action of pharmacological interventions, as discussed in detail in Chapter 1 of this thesis. Pharmacological interventions studied include gabapentin (Iannetti et al. 2005; Wanigasekera et al. 2016), cyclooxygenase inhibitors (Maihöfner et al. 2007), lidocaine (Seifert et al. 2009), and cannabinoids (Lee et al. 2013). All studies report that fMRI measures are modulated by the analgesics studied. Furthermore, evoked and resting BOLD responses to noxious stimulation have been used for characterising analgesic effects at a neural level for other drug classes including opioids and ketamine (Rogers et al. 2004; Wise et al. 2002; Wise, Williams, and Tracey 2004). The technique has also been used to characterise analgesic efficacy in patients with pain conditions such as fibromyalgia (Kim et al. 2013) and post-traumatic neuropathic pain (Wanigasekera et al. 2018). Specifically, fMRI has been proposed as a useful measure to complement existing tools for evaluating neural mechanisms of action and target engagement of candidate treatments during drug development. It has been shown that fMRI measures, such as evoked-pain BOLD responses and functional connectivity measures, are effective in distinguishing drugs with and without clinical efficacy in small cohort studies (Upadhyay et al. 2011; Wanigasekera et al. 2016).

Although fMRI is a well-established tool for assessing analgesic efficacy in a research setting, with potential to be a biomarker of efficacy in drug development, additional evidence and further standardisation is needed for use in clinical trials (Smith et al. 2017). This trial aims to profile reliable biomarkers of analgesic efficacy observed using fMRI, which could then be used in future clinical trials to ascertain potential efficacy of analgesic drug candidates in humans, to improve the translatability

of promising drug candidates from animal studies to human studies. In order to focus primarily on profiling fMRI as a biomarker of analgesic efficacy, the double-blind, randomised and placebo-controlled trial assessed three drugs with known analgesic or anti-hyperalgesic action. These were lacosamide, pregabalin and tapentadol, given at doses know to have a clinically relevant analgesic effect. All drugs have marketing authorisation in the EU; lacosamide for treatment of epilepsy (it has also been assessed and rejected for painful diabetic polyneuropathy, with these trials evidencing its analgesic efficacy), pregabalin and tapentadol both for peripheral and central neuropathic pain. Interestingly, lacosamide and tapentadol have not been previously studied in a study using an experimental pain model of central sensitisation and fMRI together. Gabapentin (in the same class as pregabalin) has been previously studied, therefore primary and secondary trial outcomes focus on the specific fMRI measures that have been shown to be modulated by this drug (Wanigasekera et al. 2016). They are:

Primary objectives:

1. To test if the punctate evoked BOLD response in the posterior insula at 3-hours post-drug administration differs in pregabalin period as compared to the placebo period, at the sensitized leg.
2. To test if the resting state connectivity between the secondary somatosensory cortex (SII) and thalamus at 3-hours post-drug administration in the presence of sensitization differs in the pregabalin period as compared to the placebo period.

Secondary objectives:

1. To test if the punctate evoked BOLD response in the posterior insula at 1-hour post-drug administration differs in at least one analgesic treatment period as compared to the placebo period, at the sensitized leg.
2. To test if the resting state connectivity between SII and thalamus at 1-hour post-drug administration in the presence of sensitization differs in at least one analgesic treatment session as compared to the placebo session.

It is hypothesised that in this study the punctate evoked BOLD response in the posterior insula and the resting state functional connectivity between the right thalamus seed-region and the SII will be decreased with pregabalin compared to placebo, as has been previously shown with gabapentin

(Wanigasekera et al. 2016). It is hypothesised that the other two drugs, lacosamide and tapentadol, may also modulate these measures through their analgesic efficacy. In addition to the primary and secondary outcome measures, this trial also aimed to compare the whole-brain BOLD responses during mechanical stimulation of the area of secondary hyperalgesia and during rest between the drug and placebo conditions, to understand the full picture of the neural correlates of the analgesic efficacy of each drug. Lastly, the trial also aimed to compare the BOLD response in the nucleus cuneiformis (NCF) area of the brainstem with each drug compared to placebo, as the BOLD response to pin-prick stimulation during central sensitisation in this region has been shown to be modulated by gabapentin (Wanigasekera et al. 2016).

This trial (known as BioPain RCT4) is related to 3 similarly designed trials which investigate different biomarkers of analgesic efficacy in humans, using a harmonised protocol. The first (BioPain RCT1) investigates biomarkers derived from nerve excitability testing using threshold tracking of the peripheral nervous system (Nochi et al. 2022). The second (BioPain RCT2) investigates spinal cord and brainstem activity using biomarkers derived from non-invasive neurophysiological measurements (the RIII flexion reflex, the N13 component of somatosensory evoked potentials and the R2 component of the blink reflex) (Leone et al. 2022). The third (BioPain RCT3) investigates biomarkers derived from non-invasive electroencephalographic (EEG) measures of brain activity (Mouraux et al. 2021). Each of the four trials involved data collection from multiple sites in Europe.

4.3 Methods

4.3.1 Study participants and ethical approval

Data was collected as part of the IMI-BioPain RCT4 trial. The aim of the IMI-BioPain RCT4 trial focusses on the use of fMRI to assess analgesic efficacy in healthy human participants. Written informed consent was obtained from all participants. Subjects were recruited at three sites; University of Oxford, UK, Aarhus University, Denmark, and Clermont Auvergne University, Clermont-Ferrand, France. The RCT4 protocol is registered in the Clinical Trials Register (EudraCT registration number: 2019-000908-15; https://www.clinicaltrialsregister.eu/ctr-search/trial/2019-000908-15/DK). Local regulatory and ethics approvals were granted for the final protocol versions at all three sites in RCT4, as applicable.

4.3.2 Study design

IMI2-PainCare-BioPain-RCT4 is a multi-site, single dose, placebo-controlled double-blind, randomized 4-way cross-over pharmacodynamics and pharmacokinetic study in healthy subjects. Subjects initially attended a screening visit, followed by four study periods and a follow-up telephone contact. Subjects were contacted after the screening visit and before the first study period to confirm arrangements.

At the screening visit, the purpose of the research and extent of the assessments was explained, and informed consent was obtained. Inclusion and exclusion criteria were assessed, including assessing body-mass index (BMI), blood pressure and respiratory rate, performing a 12-lead electrocardiogram (ECG), a urine drug test, a urine pregnancy test and a blood test to verify normal hepatic and renal function. Subjects were then instructed on the study-specific procedures, including how to use the rating scales. At the screening visit, participants completed two MRI scans, the first before HFS was applied and the second 20 minutes after induction of HFS. Completion of these scans allowed familiarization of the subject with the scanner environment, and assessment of their tolerability of staying in the scanner and the study procedures. It also allowed characterization of the evoked and resting central neural response to HFS induced central sensitization, which was discussed in detail in the previous chapter.

After screening, subjects attended four study periods. At each, subjects were re-screened for certain absolute exclusion criteria, including performing a urine drugs test and urine pregnancy test, in addition to a set of temporary exclusion criteria. Temporary exclusion criteria included alcohol consumption in the past 48 hrs, intake of any drug (except oral contraceptives, or paracetamol/ibuprofen with last intake >4 days prior to the study period), changes in physical exercise activities, current pain within 4 days of the study period and any transient clinically-relevant illnesses within 4 days of the study period. If screening of exclusion criteria for eligibility for study period 1 showed that one or more temporary exclusion criteria are met, the start of period 1 could be postponed and re-scheduled.

There were set minimum and maximum intervals between each visit. There was a minimum of 2 days and maximum of 6 weeks between the screening visit and study period 1, then a minimum of 1 week between each study period. There was a maximum limit of 8 weeks to complete all 4 study periods. Between 7 and 14 days after the last period the absence of untoward medical sequelae of the study was ascertained in a follow-up telephone call with the subject. Figure 1 summarises the timeline of the study visits.

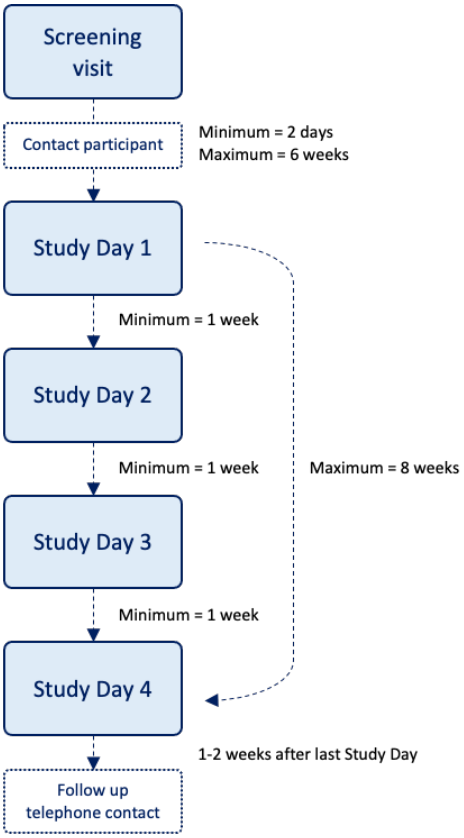

Figure 1: Timeline of screening and study visits.

Participants first attended a screening visit to assess eligibility and conduct baseline MRI scans pre- and post-HFS. Subsequently, the participants attended 4 study periods, which consisted of the study day followed by a short next-day visit to collect the 24hr PK blood sample. On each study day, participants received a dose of either lacosamide, pregabalin, tapentadol or placebo. The interval between the screening visit and first study day was a minimum of 2 days and maximum of 6 weeks. Thereafter, the minimum interval between study days was 1 week, with a maximum time period in which to complete all 4 study days of 8 weeks. After the participant had completed the study days, they were contacted for a follow-up telephone call.

The schedule for each study period was identical, and is shown in Figure 2. Subjects arrived at 8am, having fasted overnight, and were screened for absolute and temporary exclusion criteria as above. Patient reported outcome measures (PROMs) were recorded for assessment of the subject's level of anxiety and expectation of pain. Then, HFS was applied to the left lower limb. Following HFS application, there were three pharmacodynamic (PD) assessments – the first (PD1) took place 30 minutes after HFS (prior to dosing) and consisted of 18 mechanical pin-prick stimuli only. Subjects were asked to rate the pain intensity of each stimulus and the average unpleasantness of the stimuli at the end. After PD1, subjects completed a further PROM assessment of their expectation of pain relief, and then were given an oral dose of the study drug, with water. The second and third PD sessions (PD2 and PD3) were both MRI scans, which were started one-hour after dosing and three-hours after dosing, respectively. The MRI scan protocol is outlined in detail below. Hyperalgesia mapping was completed in the time between the two scans, and is also discussed in more detail below. In addition, blood samples were taken at four time points during the Study Day and a fifth sample was taken during the following day, to measure plasma drug levels. During the afternoon, two further PROMS were collected for tiredness and anxiety.

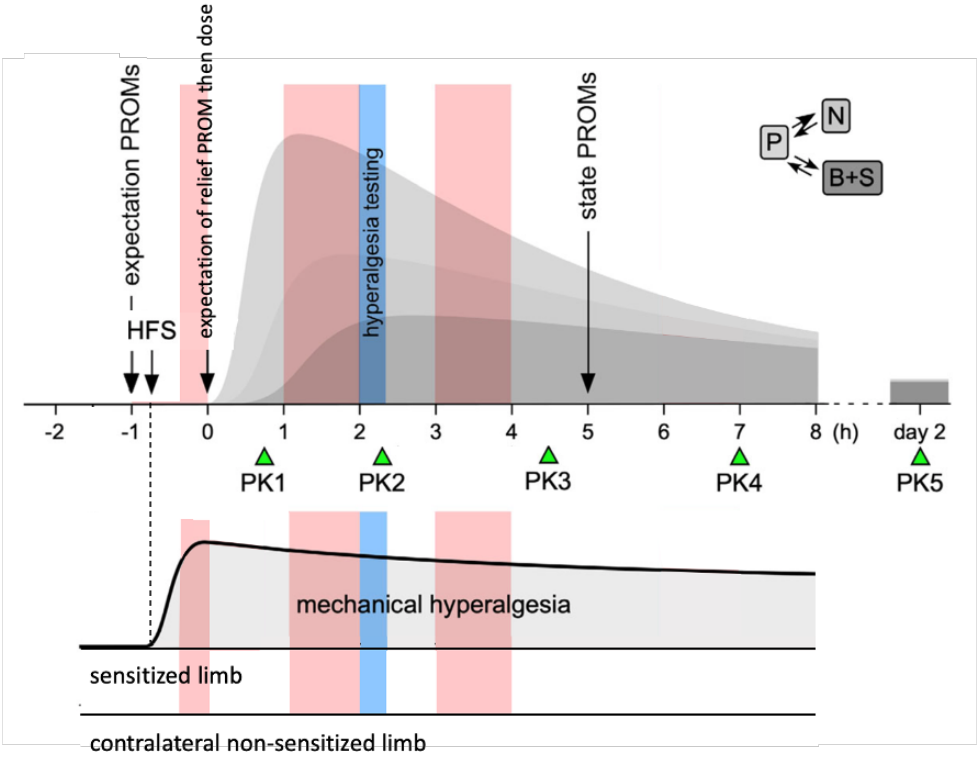

Figure 2: Trial design of each study period.

At the start of each study period, patient-reported outcomes (PROMs) were collected to assess the subject's expectations of pain and anxiety (expectation PROMs), and the HFS was applied. After HFS, one pre-dose and 2 post-dose pharmacodynamic (PD) assessments were made, as shown in light red in the figure. The first consisted of mechanical pin-prick stimuli only, after which a further PROM for subject's expectation of pain relief was obtained and the drug was administered. The second and third PD assessments consisted of neuroimaging assessments (MRI scans), which included resting state and task (mechanical pin-prick stimuli) sessions. Five blood samples were taken to measure plasma drug levels (indicated by PK) and to model the PK profiles in the plasma (P), peripheral nerves (N), spinal (S), and brain (B) compartments. Tiredness and state anxiety (state PROMs) were collected. Assessment of hyperalgesia was done once in the period between the two neuroimaging sessions (light blue). Adapted from (Mouraux et al. 2021) and (Nochi et al. 2022) for the RCT4 protocol.

4.3.3 Study drugs and dosing

The three study drugs used in the trial were lacosamide (Vimpat®), pregabalin (Lyrica®) and tapentadol (Palexia®). The dose was 200mg for lacosamide (2 x 100mg tablets), 150mg for pregabalin (2 x 75mg tablets) and 100mg for tapentadol (2 x 50mg tablets). All drugs are registered medications in the UK

and were over-encapsulated by Cardiff and Vale University Health Board pharmacy (UK-based due to import restrictions) and randomisation lists were provided by Heidelberg University pharmacy (centralised for the multi-site trial). All doses (including placebo) were encapsulated in identical capsules to ensure subjects and researchers remained blinded.

4.3.4 High frequency stimulation (HFS)

The method for application of HFS and the rationale for its use was described in detail in the previous chapter of this thesis. Briefly, HFS was applied using the HFS Electrode "EPS-P10" manufactured by *MRC Systems GmbH*. The pulses delivered by the electrode were generated by the Digitimer DS7A constant current stimulator. HFS application consisted of 5 trains of electrical pulses delivered at 100 Hz. Train duration was 1s, with an interval of 9s between each train, and the stimulation intensity was set to 20x the detection threshold for each subject. This model is shown to induce increased sensitivity to mechanical pin-prick stimuli in the area of skin surrounding the electrode pins (area of secondary hyperalgesia), which develops rapidly and lasts for several hours (Klein et al. 2004; Klein, Stahn, et al. 2008; Pfau et al. 2011; van den Broeke and Mouraux 2014).

4.3.5 Magnetic resonance imaging (MRI) protocol

On the study days, each MRI scan included a blood oxygen level dependent (BOLD) scan during resting state, a BOLD scan during mechanical punctate (pin-prick) stimuli in the area of secondary hyperalgesia, an arterial spin labelling (ASL) scan during rest, a BOLD scan during a visual stimulus (flashing black and white checkerboard) and a field map. During the mechanical punctate stimuli scan, BOLD signal changes were measured in response to 18 mechanical stimuli each with a 1s duration, applied using a 512nM weighted non-skin penetrating punctate probe. Stimuli were jittered with an inter-stimulus interval of 31 to 35 seconds.

Participants rated the pain intensity of each mechanical stimulus, and provided an average rating of pain unpleasantness following all 18 stimuli, both using a visual analogue scale from 0 (no pain at all/not unpleasant at all) to 100 (most intense pain imaginable/extremely unpleasant). The total duration of each punctate scan was 10 minutes. Punctate stimuli were applied in the area of secondary hyperalgesia, 1cm outside the perimeter of the circular HFS cathode pin area. The MRI protocol is outlined in Figure 3.

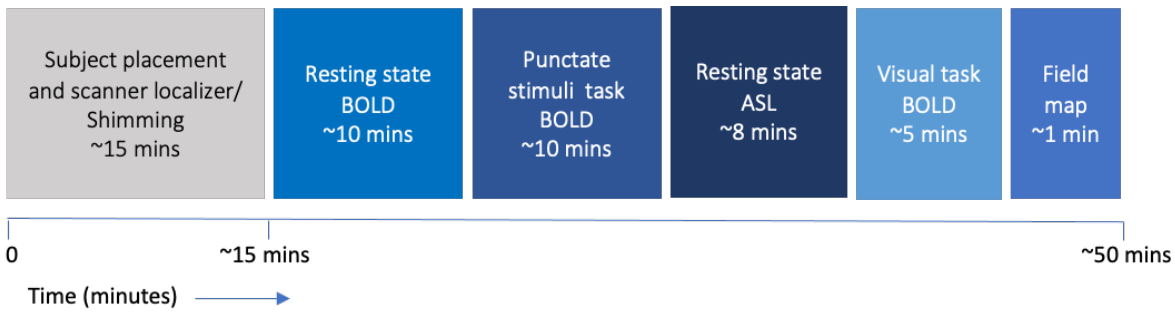

Figure 3: Overview MRI scan protocol.

For the two MRI scan sessions, there was approximately 15 minutes of set-up time at the start, during which the subject was positioned in the scanner and initial localizer and shimming scans were conducted. Following this, the first main scan was a blood oxygen-level dependent (BOLD) scan during rest – 'Resting state BOLD' in the diagram above. Then, the second main scan was a BOLD scan during punctate mechanical stimuli, which consisted of 18 pin-prick stimuli applied to the area of secondary hyperalgesia on the left lower leg – 'Punctate stimuli task BOLD'. The third scan was an arterial spin labelling (ASL) scan conducted during rest – 'Resting state ASL'. Then the next scan was a BOLD scan during a visual stimulation task (flashing black and white chequerboard) which acts as a control task for the drug activity – 'Visual task BOLD'. Finally, a field map scan was completed at the end – 'Field map'. In total, each scan session lasted approximately 50 minutes.

The specific scanner protocols were harmonised between the three sites, but there were differences in the scanner model at each site and site-specific protocols used. At the Oxford site, MRI data was collected using a 3T Siemens PRISMA scanner with a 32-channel head-coil. All BOLD data (resting state, mechanical stimulation task and visual task) were acquired with a whole brain echo-planar imaging sequence with an echo time of 36ms, field of view 192mm x 192mm, voxel size 2mm x 2mm x 2mm, multiband acceleration factor 6, echo spacing of 0.62ms and bandwidth of 2084 Hz/Px. The resting state scan had 513 volumes, the mechanical stimulation task scan had 531 volumes and the visual task scan had 257 volumes, each with a repetition time of 1.17 seconds. The ASL data are not included in this thesis and acquisition of this data is therefore not described here. A field map was acquired to after the functional scans to enable correction of field inhomogeneity during analysis, with voxel size 2mm x 2mm x 2mm and field of view 192 mm x 192mm. For each subject, a T1 structural scan was also acquired at the end of the first MRI scan conducted during the screening visit, before HFS is applied. This T1-weighted structural scan was acquired with voxel size 1mm x 1mm x 1mm for registration of the functional BOLD scans to standard space for group-level analysis.

At the Clermont-Ferrand site, MRI data was collected using a 3T Siemens MAGNETOM VIDA scanner with a 32-channel head-coil. The BOLD scan protocol (for resting state, mechanical stimulation task and visual task scans) was aligned to Oxford's, with the same repetition time (1.17 seconds), echo time (36ms), field of view (192mm x 192mm), voxel size (2mm x 2mm x 2mm) and multiband acceleration factor (6), echo spacing (0.62ms) and bandwidth (2084 Hz/Px). The number of volumes collected per scan was slightly different, with 520 volumes for resting state scans, 700 volumes for the mechanical stimulation task scans and 280 volumes for the visual task scans. The protocol for the field maps and T1 structural scan were also aligned.

At the Aarhus site, MRI data was collected using a 3T Siemens PRISMA scanner (the same scanner model as in Oxford). The BOLD scan protocol (for resting state, mechanical stimulation task and visual task sans) was slightly different to the protocol used in the other two sites due to differences in local practices. BOLD data were acquired with a whole brain echo-planar imaging sequence with an echo time of 29.6ms, field of view 200mm x 200mm, voxel size 1.8mm x 1.8mm x 1.8mm, multiband acceleration factor 4, GRAPPA in-plane acceleration with factor 2, echo spacing of 0.72ms and bandwidth of 1594 Hz/Px. The resting state scan had 450 volumes, the mechanical stimulation task scan had 480 volumes and the visual task scan had 224 volumes, each with a repetition time of 1.34 seconds. Overall, the differences in the protocol used at this site result in a reduced signal-to-noise ratio compared to the other two sites.

4.3.6 Hyperalgesia mapping

Hyperalgesia mapping was completed after the first MRI scan, approximately 2 hours post-drug and approximately 2 hours and 45 minutes after the HFS was applied. To map the area of hyperalgesia, mechanical pin-prick stimuli were applied with the 512nM stimulator in 8 radii around the position HFS was applied, as described in detail in Chapter 3 of this thesis.

4.3.7 Statistical analysis

Statistical analysis for all behavioural data was completed using GraphPad PRISM version 9.4.1 (GraphPad Software, LLC). Statistical significance is reported with the following symbols; ns for $P > 0.05$; * for $P \leq 0.05$, ** for $P \leq 0.01$, *** for $P \leq 0.001$, and **** for $P \leq 0.0001$.

All imaging data were analysed at the Oxford site, with a standardised pipeline using tools in FMRIB Software Library v6.0 (FSL) (Woolrich et al. 2009; Smith et al. 2004; Jenkinson et al. 2012). For each scan, structural and magnitude images were brain extracted (Smith 2002) and a calibrated field map

image was prepared as required for B0 unwarping. For BOLD data, registration to the structural image and B0 unwarping were performed using FEAT (Woolrich et al. 2001). Motion correction, spatial smoothing (5mm for mechanical pin-prick stimulation and visual task scans, and 3mm for resting state scan) and high-pass temporal filtering were applied. The 3mm smoothing was used for resting state to aid identification of small brain regions such as the brainstem. Independent component analysis was conducted with the MELODIC tool and noise components were removed using the FIX auto-classifier (Griffanti et al. 2014; Salimi-Khorshidi et al. 2014). The existing training dataset developed during analysis of the screening data, described in Chapter 3 of this thesis, was used for this. The training dataset was developed by hand classifying components as signal or noise in the screening scans of the first 10 subjects at the Oxford site (and study day scans for the visual task data). For a sample of scans from each site and each scan type (resting state, mechanical stimuli task and visual task), components were hand classified and checked against the auto-classified result, to verify that the training dataset was accurately identifying the noise components.

After pre-processing and noise removal, a three-level analysis approach was used for all BOLD data in order to account for different variances, as due to the nature of the multi-site study there are two sources of variance; the variance between individual subjects and the variance between the three sites. The first level analysis was completed separately for each scan, with the output of this stage being the average response of that subject to the stimulus (or the time course of activity correlated to the seed region for the resting state scans). The second level analysis was then completed separately for each site, using mixed effects analysis with a paired t-test design, with the three output contrasts of this stage being the combined difference between each drug condition (lacosamide, pregabalin and tapentadol) and the placebo condition. This stage was repeated for each time point (PD2; 1-hour post-drug and PD3; 3-hours post-drug). Finally, the third level analysis was a fixed effects analysis taking a simple average of the three individual site analyses for each comparison. This format was used to effectively account for any differences in variance at each site. The analysis steps for each type of scan (resting, mechanical stimuli and visual task) are described in detail below.

For the resting state scans, in the first level analysis the time course for activity in the selected seed-region (right thalamus) was extracted and used to generate individual statistical maps of the functionally correlated activity across the whole brain for each subject, using the GLM approach implemented with FEAT (Woolrich et al. 2001). The right thalamus seed-region was anatomically defined using the Harvard-Oxford Subcortical Structural Atlas applied in FSL (Desikan et al. 2006), with a mask created by thresholding to 50% and binarizing the image. Individual maps were constrained to

grey matter only by regressing out activity in white matter and cerebrospinal fluid, using time courses for this activity in the GLM which were generated from the anatomical segmentations for each tissue type. The second level (site-specific) analysis was conducted using FEAT to carry out a mixed effects analysis with a cluster-based correction for multiple comparisons, to compare functional connectivity to the seed region in each drug condition (lacosamide, pregabalin and tapentadol) to the placebo condition (Woolrich et al. 2004). The third level (multi-site) analysis was carried out as above, using FEAT to conduct a fixed effects analysis to average the result from the three sites (Woolrich et al. 2004).

For the mechanical pin-prick stimulation scans and the visual task scans, in the first level analysis an individual statistical map for the response to the pin-prick or visual stimuli was generated using the general linear model (GLM) approach implemented with FEAT (Woolrich et al. 2001). The second level (site-specific) analysis was conducted using FEAT to carry out a mixed effects analysis with a cluster-based correction for multiple comparisons, to compare stimulus evoked neural activity in each drug condition (lacosamide, pregabalin and tapentadol) to the placebo condition (Woolrich et al. 2004). The third level (multi-site) analysis was carried out as above, using FEAT to conduct a fixed effects analysis to average the result from the three sites (Woolrich et al. 2004). For the mechanical pin-prick stimulation scans, the Featquery tool in FSL was used to extract mean percentage change in BOLD parameter estimates for the posterior insular cortex and the NCF. To create a mask of the posterior insular cortex, the insular cortex was first anatomically defined using the Harvard-Oxford Subcortical Structural Atlas applied in FSL (Desikan et al. 2006), applying thresholding to 50% and binarizing the image. This was then manually constrained to the area of the posterior insular only, using the central sulcus as the boundary. The NCF was functionally defined from previous studies (Zambreanu et al. 2005; Wanigasekera et al. 2016). The left NCF was defined using the peak activation voxel in this region from Zambreanu et al. 2005, and the right NCF was defined using the peak activation voxel in this region from Wanigasekera et al. 2016. Both peak voxels were used to create a 5mm spherical mask that was constrained to the brainstem using the Harvard-Oxford Subcortical Structural Atlas applied in FSL (Desikan et al. 2006).

Parameters for the primary and secondary endpoints (the BOLD response in the posterior insula cortex and the functional connectivity between the thalamus and SII region) were extracted for analysis. For primary endpoints (which are constrained to the pregabalin vs. placebo comparison), a paired t-test was used for statistical analysis. The two primary endpoints were tested in parallel with the overall alpha-level (0.05) split equally between them, so each required $P \leq 0.025$ to reach significance.

4.4 Results

In total, 37 subjects were screened for the trial across the three sites (20 at Oxford, 10 at Aarhus and 7 at Clermont-Ferrand). There were 6 subjects that did not pass screening, resulting in a total of 31 subjects enrolled in the trial. Reasons for screen failure were electrocardiogram (ECG) result abnormalities (n=2), body mass index (BMI) outside the range required for study eligibility (n=2), and subjects not willing to proceed or who did not tolerate study procedures (n=2). There were 2 subjects that dropped out of the trial following enrolment. Reasons for drop out were starting a new medication that resulted in ineligibility (n=1) and anxiety due to repeated blood samples (n=1). Therefore, there were 29 recruited subjects who completed the trial. The number of subjects screened, enrolled and completed is shown in Figure 4, as well as the number of subjects who failed screening or dropped out of the study.

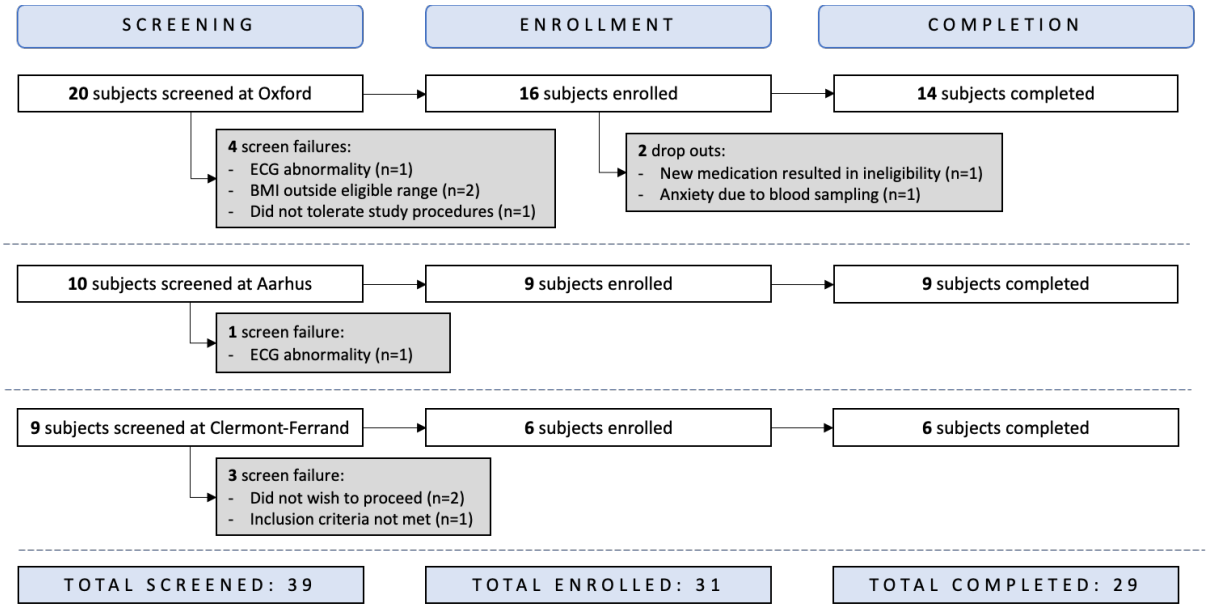

Figure 4: Flowchart of included subjects.

In total, 37 subjects were screened for eligibility across the three sites. There were 8 subjects that failed screening due to electrocardiogram (ECG) abnormality (n=2), BMI outside the eligible range (n=2), subjects not willing to proceed or who did not tolerate study procedures (n=3) and inclusion criteria (unspecified) not met (n=1). Consequently, there were 31 subjects enrolled in the study. There were 2 subjects that dropped out of the study due to starting a new medication that resulted in ineligibility (n=1) and anxiety due to blood sampling (n=1). Therefore, the total included in the final analysis was 29 subjects.

For subjects from Oxford and Aarhus (n=23), the mean age was 25.5 years, with an age range between 21-38 years. 10 subjects were female and 13 were male. Demographics data is not available from the Clermont-Ferrand site, but is likely to be a similar population.

There are some datasets missing. During one visit an issue with the scanner computer resulted in the 1-hour post-drug scan being missed. Unblinding revealed this visit was the subject's lacosamide visit. One subject experienced side effects to the drug during their final study visit, and although some MRI data was collected these datasets were not included in analysis as the subject was unable to complete the scans. Unblinding revealed this visit was the subject's tapentadol visit. Consequently, at some time points the total number of subjects included is less than 29, as shown in Table 1.

PD time point	*Placebo*	*Lacosamide*	*Pregabalin*	*Tapentadol*
PD1 (pre-drug)	n=29	n=29	n=29	n=29
PD2 (1-hour post-drug)	n=29	n=28	n=29	n=28
PD3 (3-hours post-drug)	n=29	n=29	n=29	n=28

Table 1: Datasets included for analysis.

The total number of datasets was 29 for the majority of PD time points across all drug conditions. A technical issue with the scanner computer resulted in one dataset for lacosamide at the PD2 (1-hour post-drug) time point being missed. One subject experiencing adverse events at the tapentadol visit resulted in them being unable to complete the scans at the PD2 and PD3 time points (1-hour and 3-hours post-drug), hence these datasets are excluded from analysis.

4.4.1 Hyperalgesia mapping results

Hyperalgesia mapping completed after the first MRI scan (approximately 2-hours post-drug) demonstrated that all subjects (n=29) developed a discrete area of increased sensitivity to mechanical stimuli which could be mapped at all visits. A one-way ANOVA was performed to determine whether the drugs affected the radius of the hyperalgesia area, showing that there was not a statistically significant difference in the radius between the drugs ($F(2.807, 78.59) = 0.3679$, $p = 0.7631$).

4.4.2 Behavioural responses to mechanical pin-prick stimuli

Raw data for pain intensity and unpleasantness ratings for each time point (PD1; pre-drug baseline, PD2; 1-hour post-drug, and PD3; 3-hour post-drug) are shown in Figure 5A and 5B. This shows that there was considerable variation in the baseline (PD1) ratings between the conditions (placebo, lacosamide, pregabalin and tapentadol). Two-way mixed model analysis to investigate the effect of drug and time point on the pain ratings, with Bonferroni correction for multiple comparisons, showed that there is no significant difference between the drug arms in PD1, and that there were no statistically significant differences in any of the placebo vs. drug comparisons at any of the time points. For pain intensity ratings, there was a statistically significant interaction between the effects of drug and time point ($F(1.459, 40.13) = 4.093$, $p = 0.0354$). There was no statistically significant effect of drug ($p = 0.4916$), but time point did have a statistically significant effect ($p = 0.0006$). Similarly, for pain unpleasantness ratings, there was a statistically significant interaction between the effects of drug and time point ($F(2.157, 58.96) = 3.093$, $p = 0.0491$). Again, drug did not have a statistically significant effect ($p = 0.3568$), but time point did have a statistically significant effect ($p = 0.0008$).

All pain intensity and unpleasantness ratings are also shown in a heatmap plot in Figure 6C. This plot shows trends in the data; firstly, that many subjects rated the pain on the lower end of the scale, as shown by the many dark blue rows. This was particularly the case in France and Denmark, where subjects rated lower than subjects from the UK. Where subjects are rating so low in the pre-drug baseline (PD1) session, it gives very little room for to see a drug effect in the post-drug sessions, as they are already close to the bottom of the scale. Secondly, it shows that the majority of subjects across all sites were fairly consistent in their ratings, with most rows coloured in similar colours across the visits and few dramatic colour changes.

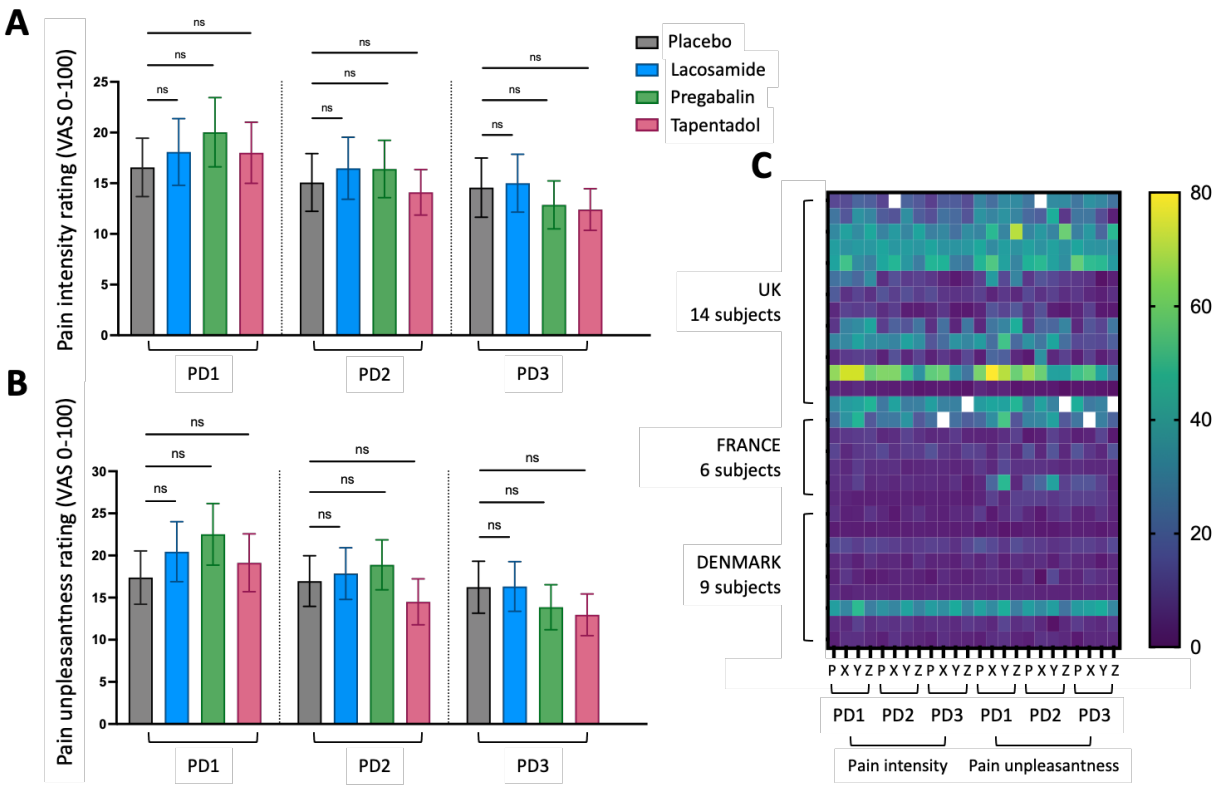

Figure 5: Pain intensity and unpleasantness ratings for all time points; PD1 (pre-drug baseline), PD2 (1-hour post-drug) and PD3 (3-hour post-drug).

A: Mean pain intensity ratings for all time-points; PD1 (pre-drug baseline), PD2 (1-hour post-drug) and PD3 (3-hour post-drug) are shown. A two-way mixed-effects analysis with Geisser-Greenhouse correction for sphericity was performed to analyse the effect of drug and time point on the pain intensity ratings. This showed that there was a statistically significant interaction between the effects of drug and time point (F (1.459, 40.13) = 4.093, p = 0.0354). Simple main effects analysis showed that drug did not have a statistically significant effect (p = 0.4916), and time point did have a statistically significant effect (p = 0.0006). Bonferroni's multiple comparison test was performed comparing each group to the placebo group, and showed there were no statistically significant differences between each drug and placebo at any time point.

B: Mean pain unpleasantness ratings for all time points; PD1 (pre-drug baseline), PD2 (1-hour post-drug) and PD3 (3-hour post-drug) are shown. A two-way mixed-effects analysis with Geisser-Greenhouse correction for sphericity was performed to analyse the effect of drug and time point on the pain unpleasantness ratings. This showed that there was a statistically significant interaction between the effects of drug and time point (F (2.157, 58.96) = 3.093, p = 0.0491). Simple main effects analysis showed that drug did not have a statistically significant effect (p = 0.3568), and time point did have a statistically significant effect (p = 0.0008). Bonferroni's multiple comparison test was performed comparing each group to the placebo group, and showed there was a no statistically significant differences between each drug and placebo at any time point.

C: Heatmap plot of all pain intensity and unpleasantness ratings for all subjects, across all sites. All ratings were given on a 0 to 100 scale. Lower ratings are coloured dark blue and higher ratings are coloured yellow, with the colour bar corresponding to the rating values shown on the right.

Due to the large variation in the pre-drug baseline (PD1) ratings, the post-dosing data from PD2 and PD3 sessions were normalised to the pre-drug baseline (PD1). The change in subject reported pain intensity and pain unpleasantness measured using the visual analogue scale from 0 (no pain at all/not unpleasant at all) to 100 (most intense pain imaginable/extremely unpleasant) showed a decrease in all conditions (placebo, lacosamide, pregabalin and tapentadol) in both post-drug time points (PD2, 1-hour post-drug; and PD3, 3-hours post-drug) when compared to the pre-drug baseline (PD1). All drugs showed a larger decrease than placebo. This is shown in Figure 6.

For pain intensity ratings, a two-way mixed model analysis to investigate the effect of drug and time point on the pain ratings showed that there was a statistically significant interaction between the effects of drug and time point ($F(2.328, 62.85) = 3.380$, $p = 0.0337$), and there was a statistically significant effect of drug and time point factors individually ($p = 0.0120$ and $p = 0.0045$, respectively). Bonferroni's multiple comparison test performed comparing each group to the placebo group showed a statistically significant difference between placebo and pregabalin at the PD3 (3-hours post-drug) time point (adjusted $p = 0.0215$).

For pain unpleasantness ratings, the same analysis showed that there was not a statistically significant interaction between the effects of drug and time point ($F(2.541, 67.75) = 2.425$, $p = 0.0829$), but there was a statistically significant effect of drug and time point factors individually ($p = 0.0284$ and $p = 0.0209$, respectively). Bonferroni's multiple comparison test performed comparing each group to the placebo group showed there was also a statistically significant difference between placebo and pregabalin at the PD3 time point (adjusted $p = 0.0075$).

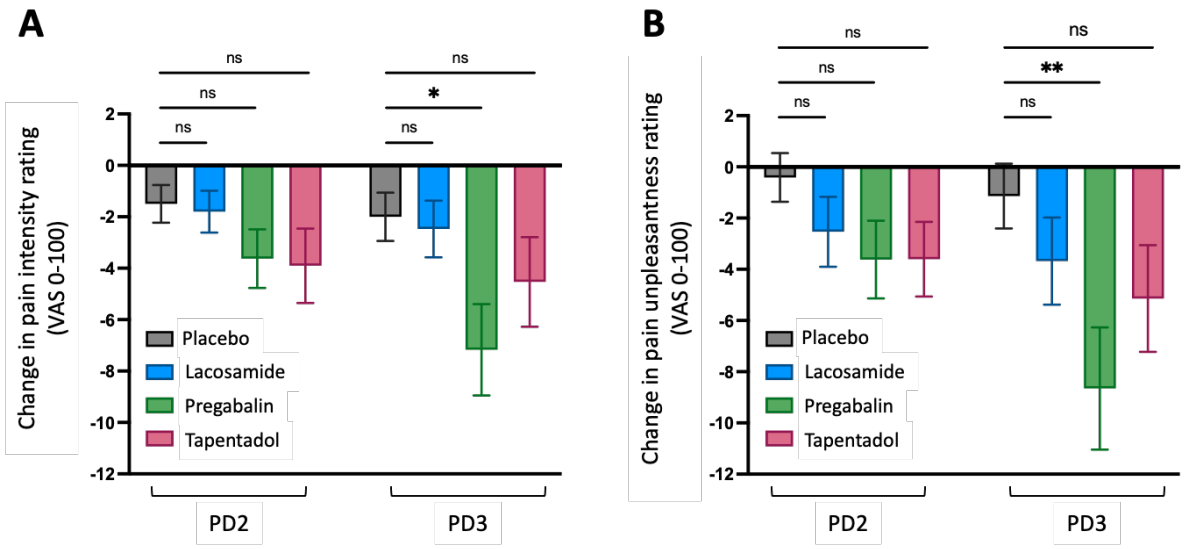

Figure 6: Change in pain intensity and unpleasantness ratings compared to pre-drug baseline.

A: Mean change in pain intensity ratings for both time-points (PD2; 1-hour post-drug, and PD3; 3-hours post-drug) normalised to pre-drug baseline (PD1) ratings are shown. A two-way mixed-effects analysis with Geisser-Greenhouse correction for sphericity was performed to analyse the effect of drug and time point on the pain intensity ratings. This showed that there was a statistically significant interaction between the effects of drug and time point ($F(2.328, 62.85) = 3.380$, $p = 0.0337$). Simple main effects analysis showed that drug and time point each had a statistically significant effect ($p = 0.0120$ and $p = 0.0045$, respectively). Bonferroni's multiple comparison test was performed comparing each group to the placebo group, and showed there was a statistically significant difference between placebo and pregabalin at the PD3 time point (adjusted $p = 0.0215$).

B: Mean change in pain unpleasantness ratings for both time points (PD2; 1-hour post-drug, and PD3; 3-hours post-drug) normalised to pre-drug baseline (PD1) ratings are shown. The same analysis was completed as above, and showed that there was not a statistically significant interaction between the effects of drug and time point ($F(2.541, 67.75) = 2.425$, $p = 0.0829$). Simple main effects analysis showed that drug and time point each had a statistically significant effect ($p = 0.0284$ and $p = 0.0209$, respectively). Bonferroni's multiple comparison test was performed comparing each group to the placebo group, and showed there was a statistically significant difference between placebo and pregabalin at the PD3 time point (adjusted $p = 0.0075$).

4.4.3 Primary and secondary endpoint outcomes

The primary and secondary endpoints of the trial focussed on two imaging measures; the punctate evoked BOLD response in the posterior insula, and the resting state connectivity between the

thalamus seed-region and SII. The two primary endpoints consisted of a difference in these two measures for only the pregabalin vs. placebo comparison, at the 3-hour post-drug time point. The secondary endpoints consisted of a difference in these two measures for at least one analgesic treatment period vs. placebo comparisons, at the 1-hour post-drug time point. For both primary and secondary endpoints the result from the right (contralateral) side was used.

The overall trial result was negative for both primary endpoints. The two primary endpoints were tested in parallel, so the overall alpha-level (0.05) was split equally between the two paired t-tests that were conducted. Subsequently, each endpoint required a p-value of less than 0.025 to reach significance. For the difference in BOLD response in the posterior insula at the 3-hour time point between pregabalin and placebo the p value was p=0.0408 (paired t-test) and for the difference in functional connectivity between the thalamus and SII at the 3-hour time point between pregabalin and placebo the p value was p=0.4666 (paired t-test). Thus, the alpha-level 0.025 was not reached. On this basis, all further analysis shown in this thesis can be considered exploratory (as the primary endpoint was not met). Exploratory analysis results for the fMRI measures included in the primary and secondary endpoints (the punctate evoked BOLD response in the posterior insula, and the resting state connectivity between the thalamus seed-region and SII) is shown below, for all drugs and at both time points. Consistent with the rest of this thesis, a significance level of $p \leq 0.05$ is used.

Endpoint 1: Punctate evoked BOLD response in the posterior insula

The punctate evoked BOLD response in the right (contralateral) posterior insula decreased for all drugs compared to placebo at the 3-hour post-drug time point. Only pregabalin resulted in a significant decrease in the BOLD response compared to placebo (two-tailed paired t-test, p=0.0408). This measure also decreased for all drugs at the 1-hour post-drug time point, at which pregabalin and tapentadol resulted in a significant decrease in the BOLD response compared to placebo (two-tailed paired t-test, p=0.0102 and p=0.0486, respectively).

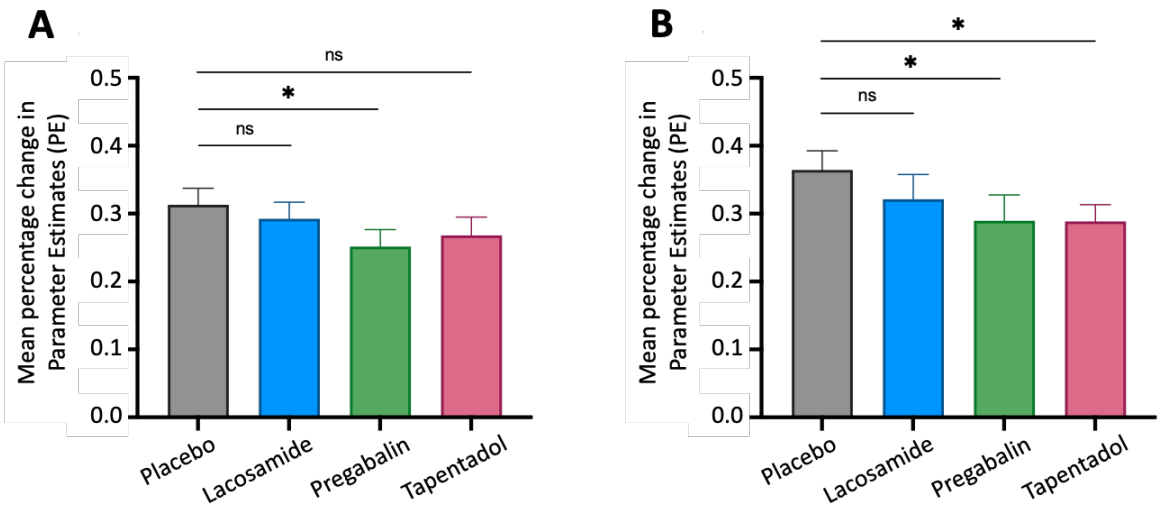

Figure 7: BOLD response in the right posterior insula cortex for each drug.

The mean percentage change in BOLD parameter estimates in response to punctate stimulation was extracted from the anatomically defined right posterior insula cortex using the Featquery tool in FSL. The extracted parameter estimates are shown for each drug, at the 3-hour (A) and 1-hour (B) time points. Error bars show the SEM. A two-tailed paired t-test was conducted for each drug vs. placebo, at each time point. At the 3-hour post-drug time point (primary endpoint 1) there was a significant difference between pregabalin and placebo (p=0.0408) and no significant difference between lacosamide or tapentadol and placebo (p=0.2864 and p=0.1764, respectively). At the 1-hour post-drug time point (secondary endpoint 1) there was a significant difference between pregabalin and tapentadol vs. placebo (p=0.0102 and p=0.0486, respectively), and no significant difference between lacosamide and placebo (p=0.1413).

Endpoint 2: Functional connectivity between the thalamus and SII

Functional connectivity during rest between the right (contralateral) thalamus seed-region and SII decreased for all drugs compared to placebo at the 3-hour and 1-hour post-drug time points. Only lacosamide resulted in a significant decrease in the functional connectivity between the two regions compared to placebo at both time points (two-tailed paired t-test, p=0.0162 at 3-hours post-drug and p=0.0228 at 1-hour post-drug).

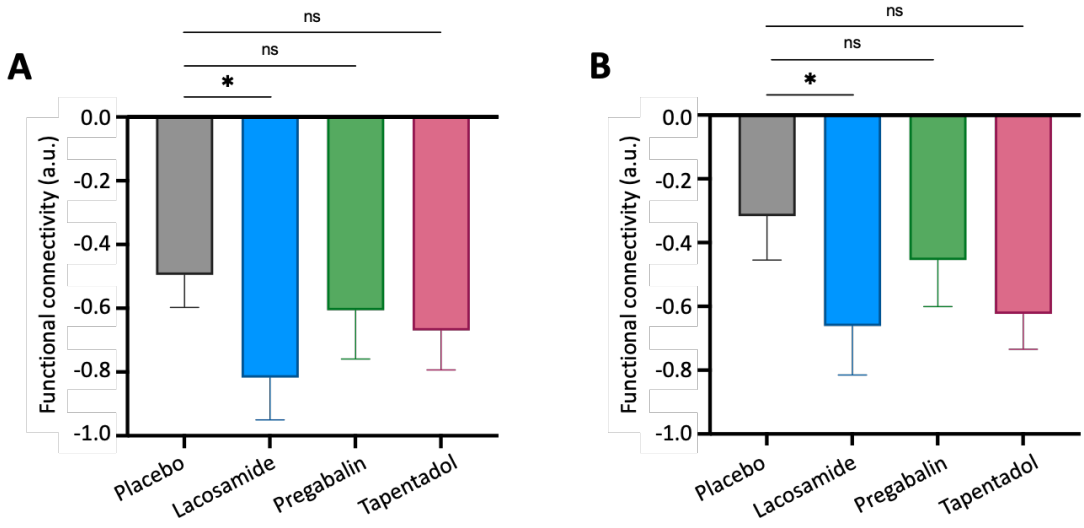

Figure 8: Functional connectivity between the right thalamus seed-region and the right secondary somatosensory cortex (SII) for each drug.

Extracted functional connectivity coefficients for connectivity between the anatomically defined right thalamus seed-region and the anatomically defined SII are plotted as a bar graph each drug, at the 3-hour time point (A) and the 1-hour time point (B). Error bars show the SEM. A two-tailed paired t-test was conducted for each drug vs. placebo. There was a significant difference between lacosamide and placebo at both time points (p=0.0162 and p=0.0228, for 3-hour and 1-hour time points respectively) and no significant difference between pregabalin and placebo (p=0.4666 and p=0.3518, for 3-hour and 1-hour time points respectively) or tapentadol and placebo (p=0.2664 and p=0.0867, for 3-hour and 1-hour time points respectively).

4.4.4 Whole-brain neural response to mechanical pin-prick stimuli

Whole-brain analysis of the punctate-evoked BOLD response showed that both pregabalin and tapentadol modulated the neural response to punctate stimulation compared to placebo. For pregabalin, at the 3-hour post-drug time point, the BOLD response was significantly decreased in the right anterior insula cortex and in the left putamen, caudate nucleus, premotor cortex and primary somatosensory cortex compared to placebo (mixed effects analysis, $Z > 3.1$, $p < 0.05$), as shown in Figure 9. Results at the 1-hour post-drug time point were aligned to the 3-hour results, with additional clusters in the anterior cingulate cortex (ACC) and SII regions (1-hour time point results not shown). There were no areas that showed increased BOLD response during the pregabalin visit compared to the placebo visit at either time point.

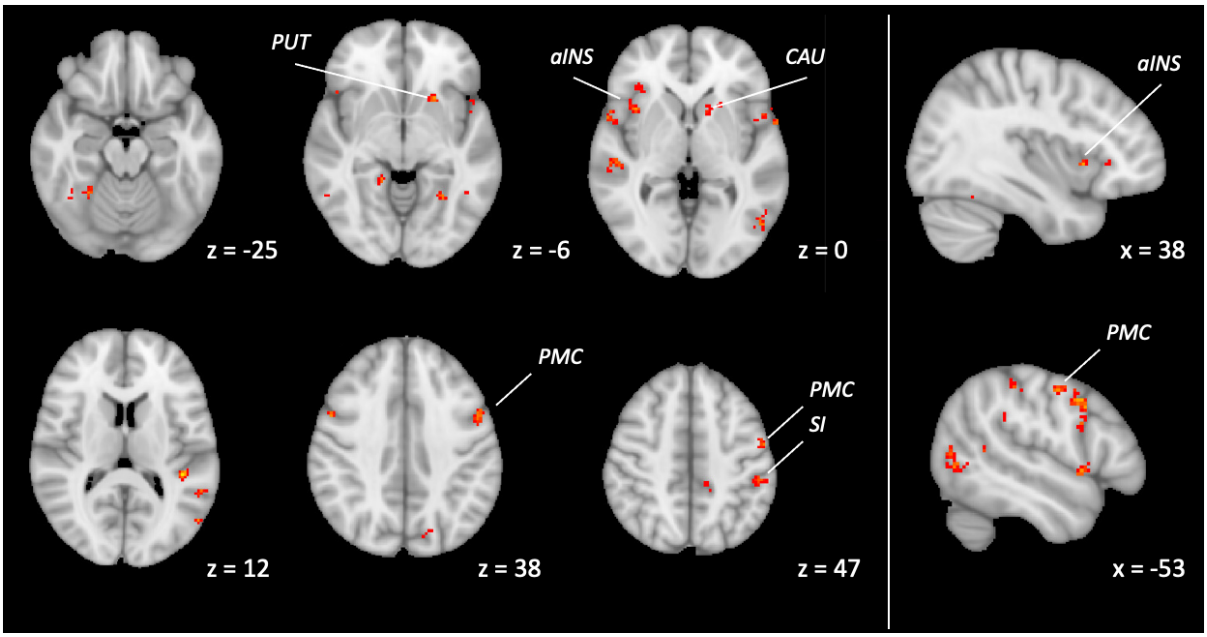

Figure 9: Whole-brain comparison between BOLD response to mechanical pin-prick stimulation following administration of placebo vs. administration of pregabalin at the 3-hour post-drug time point.

There was significantly decreased BOLD activation during the pregabalin visit compared to the placebo visit in the right anterior insula cortex (aINS) and in the left putamen (PUT), caudate nucleus (CAU), premotor cortex (PMC) and primary somatosensory cortex (SI) (mixed effects analysis, $Z > 3.1$, $p < 0.05$). MNI-512 co-ordinates are shown for images.

For tapentadol, at the 3-hour post-drug time point, the BOLD response was significantly decreased in the bilateral anterior insula cortex, amygdala, putamen, caudate nucleus, premotor cortex and primary somatosensory cortex, and left SII, compared to placebo (mixed effects analysis, $Z > 3.1$, $p < 0.05$), as shown in Figure 10. Results at the 1-hour post-drug time point were aligned to the 3-hour post-drug time point results (not shown). For tapentadol, at the 3-hour time point, there was also an area of increased BOLD response in the left thalamus in the tapentadol visit compared to placebo visit. There were no areas that showed increased BOLD response during the tapentadol visit compared to the placebo visit at the 1-hour post-drug time point.

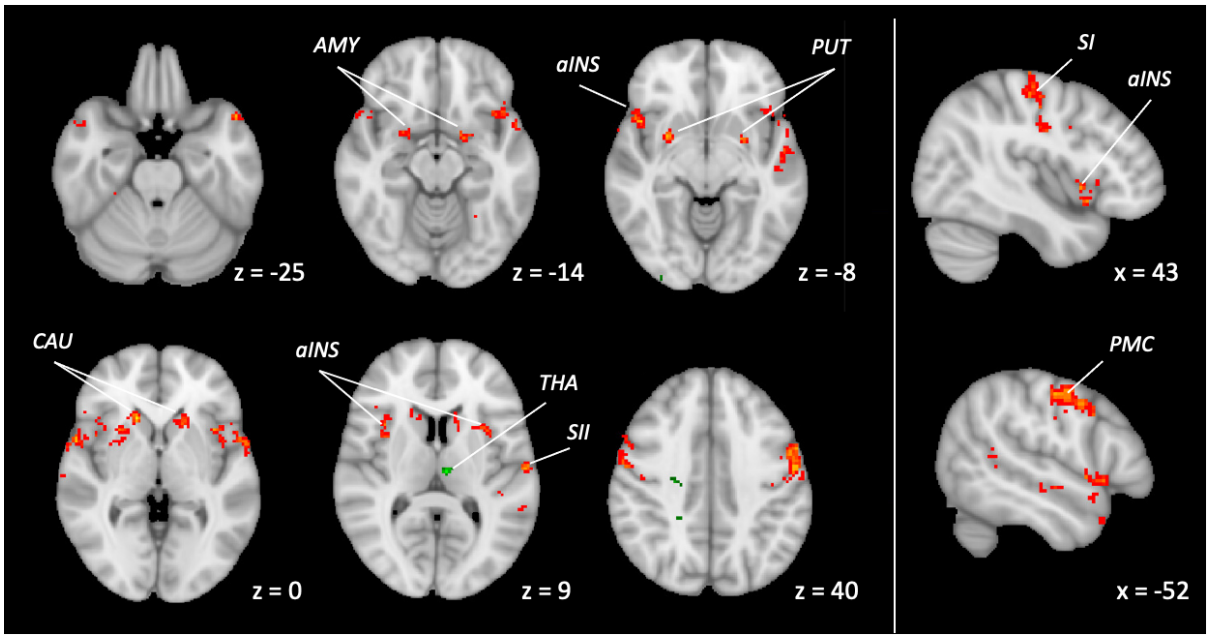

Figure 10: Whole-brain comparison between BOLD response to mechanical pin-prick stimulation following administration of placebo vs. administration of tapentadol at the 3-hour post-drug time point.

There was significantly decreased BOLD activation during the tapentadol visit compared to the placebo visit in bilateral anterior insula cortex (aINS), amygdala (AMY), putamen (PUT), caudate nucleus (CAU), premotor cortex (PMC) and primary somatosensory cortex (SI), and in the left secondary somatosensory cortex (SII) (mixed effects analysis, $Z > 3.1$, $p < 0.05$), shown in red/yellow. There was also significantly increased BOLD activation during the tapentadol visit compared to the placebo visit in the left thalamus (THA), shown in green. MNI-512 co-ordinates are shown for images.

4.4.5 Whole brain functional connectivity with right thalamus seed-region

Whole-brain functional connectivity with the right thalamus seed-region was analysed for each drug compared to placebo at both time points; 1-hour and 3-hours post-drug (mixed effects analysis, $Z > 3.1$, $p < 0.05$).

Lacosamide compared to placebo:

At the 1-hour post-drug time point, there was significantly decreased functional connectivity in the lacosamide visit compared to the placebo visit in the anterior and posterior cingulate cortices, and in the precuneous cortex. There was also significantly decreased functional connectivity with the same contrast at the 3-hour time point in the posterior cingulate cortex, and in a small part of the SII region. There was a small area of significantly increased functional connectivity in the lacosamide visit

compared to the placebo visit at the 1-hour post-drug time point in the cerebellum, and there were no areas of increased connectivity at the 3-hour time point. These results are shown in Figure 11.

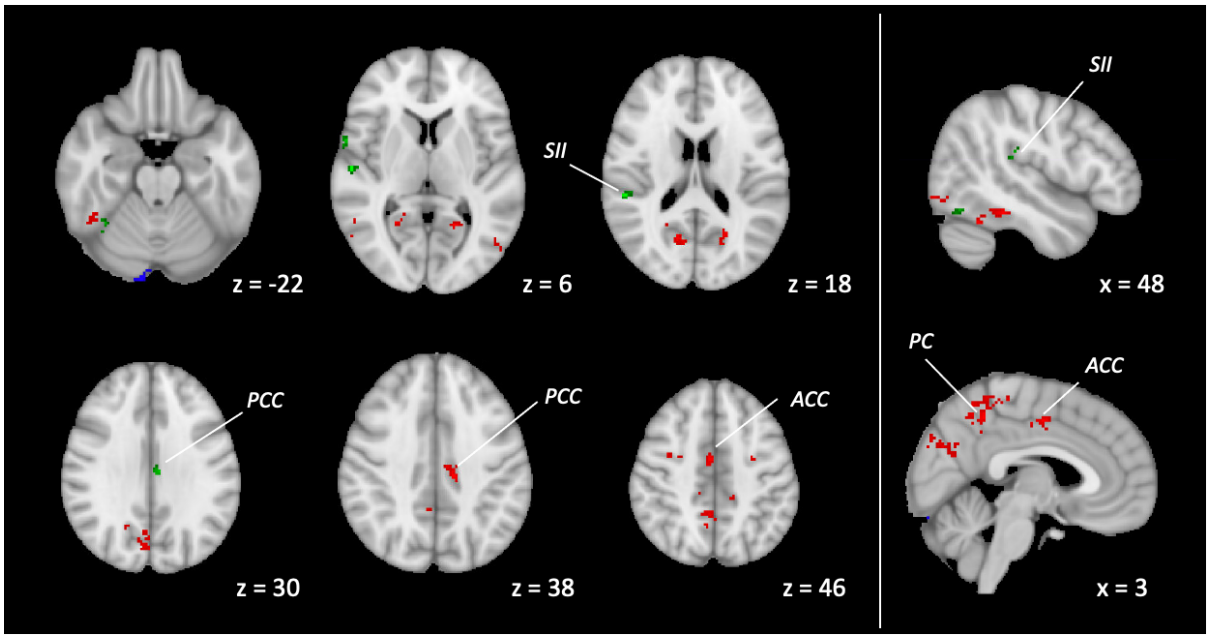

Figure 11: Whole-brain functional connectivity with right thalamus seed-region following administration of lacosamide compared to placebo.

There was significantly decreased functional connectivity in the lacosamide visit compared to the placebo visit at the 1-hour post-drug time point in the posterior cingulate cortex (PCC), anterior cingulate cortex (ACC) and in the precuneous cortex (PC), as shown in red (mixed effects analysis, $Z > 3.1$, $p < 0.05$). There was also significantly decreased functional connectivity with the same contrast at the 3-hour time point in the posterior cingulate cortex (PCC), and in a small part of the secondary somatosensory cortex (SII), as shown in green (mixed effects analysis, $Z > 3.1$, $p < 0.05$). There was a small region of significantly increased functional connectivity in the lacosamide visit compared to the placebo visit at the 1-hour post-drug time point in the cerebellum as shown in blue (mixed effects analysis, $Z > 3.1$, $p < 0.05$), and there were no areas of increased connectivity at the 3-hour time point. MNI-512 co-ordinates are shown.

Pregabalin compared to placebo:

Pregabalin did not modulate functional connectivity in brain regions associated with pain processing in this study. Compared to placebo, there was an area of decreased functional connectivity in the visual cortex at the 3-hour post-pregabalin time point. There were no areas that showed decreased functional connectivity at the 1-hour time point, and there were no areas of increased functional connectivity compared to the placebo visit at either time point, compared to placebo.

Tapentadol compared to placebo:

At the 1-hour post-drug time point, there was significantly decreased functional connectivity in the tapentadol visit compared to the placebo visit in the periaqueductal grey (PAG). There was also significantly decreased functional connectivity with the same contrast at the 3-hour time point in the superior temporal gyrus. There was significantly increased functional connectivity in the tapentadol visit compared to the placebo visit at the 1-hour post-drug time point in the middle frontal gyrus, and there were no areas of increased connectivity at the 3-hour time point. These results are shown in Figure 12.

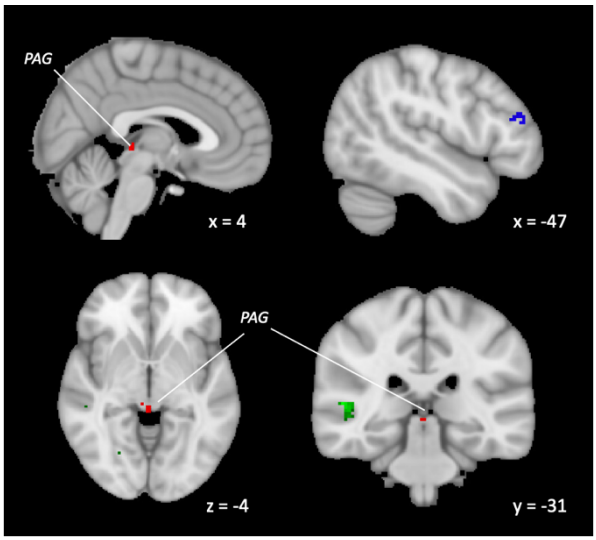

Figure 12: Whole-brain functional connectivity with right thalamus seed-region following administration of tapentadol compared to placebo.

Functional connectivity significantly decreased in the tapentadol visit compared to the placebo visit at the 1-hour time point in the periaqueductal grey (PAG), as shown in red. There was also significantly decreased functional connectivity with the same contrast at the 3-hour time point in an area of the superior temporal gyrus, as shown in green. Functional connectivity significantly increased in the tapentadol visit compared to the placebo visit at the 1-hour time point in the middle frontal gyrus as shown in blue. All were mixed effects analyses, $Z > 3.1$, $p < 0.05$. MNI-512 co-ordinates are shown.

4.4.6 Punctate evoked BOLD response in the NCF region of the brainstem

The mean percentage change in BOLD parameter estimates in response to punctate stimulation was extracted from the left and right NCF using the Featquery tool in FSL. To test for a significant effect of the drugs on this measure, a one-way mixed effects analysis with Geisser-Greenhouse correction for

sphericity was performed. This showed that drug did not have a statistically significant effect at either time point (1-hour post-drug or 3-hours post-drug) for either side (left or right).

4.4.7 Whole-brain BOLD response to visual stimulus

There were no areas of statistically significant activation or deactivation in the drug vs. placebo comparison of the response to the visual stimulus for any drugs, at either time point (mixed effects analysis, $Z > 3.1$, $p < 0.05$).

4.5 Discussion

Functional MRI has already been shown to be an effective tool for evaluating target engagement and efficacy of analgesics in small cohort studies in healthy humans (Borsook, Becerra, and Hargreaves 2011a; Smith et al. 2017). However, there remains a need to further standardise the technique and develop specific, objective fMRI biomarkers. This study has provided valuable additional data by using two specific fMRI measures (punctate-evoked BOLD response in the posterior insula and functional connectivity between the thalamus and SII at rest), a standardised protocol across multiple sites and three analgesics with known efficacy. The overall trial result was negative, as both primary endpoints failed to reach the required significance level of $P \leq 0.025$ for the pregabalin vs. placebo comparison at the 3-hour time point. However, further exploratory analysis was conducted on the trial data and showed that the drugs did alter brain activity in response to mechanical stimuli and during rest in different regions compared to placebo. The three drugs included in the trial act on different parts of the pain processing system, as outlined in Figure 13.

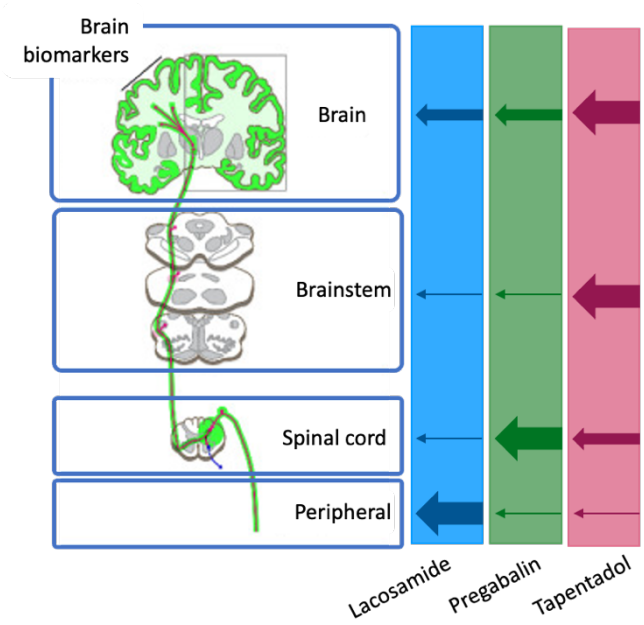

Figure 13: Schematic of the drugs used in the BioPain RCT4 trial and their sites of action.

The BioPain trial consisted of four individual trials measuring biomarkers of analgesic efficacy at different levels of the pain processing pathway, including the periphery (RCT1), spinal cord (RCT2), brainstem (RCT2 and RCT4) and brain (RCT3 and RCT4). Three drugs were used in all four studies; lacosamide (in blue), pregabalin (in green) and tapentadol (in pink). Lacosamide, pregabalin and tapentadol were selected as they were expected to respectively act predominantly on the peripheral, spinal and brain compartments of the pain processing system. However, all the drugs are known to act across multiple levels of the pathway, as outlined using the arrows of different sizes in the diagram. The larger the arrow, the stronger the drug is expected to influence that part of the pathway. Adapted from van Niel et al. 2022 (van Niel et al. 2022).

Lacosamide is an antiepileptic drug that has shown efficacy in neuropathic pain animal models. It has a dual mechanism of action; it enhances slow inactivation of sodium channels, resulting in normalised activation thresholds during pathological states of increase responsiveness, and it interacts with collapsin-response mediator protein 2 (CRMP-2), affecting neuronal growth and plasticity (Beyreuther et al. 2007). It has been assessed in clinical trials for painful diabetic neuropathy, though despite showing efficacy results were inconclusive, in part due to a large placebo effect in the studies (Carmland et al. 2019). Future patient stratification studies aim to explore whether certain patient groups have a higher response to lacosamide (Carmland et al. 2019; de Greef et al. 2019). Pregabalin acts as a voltage gated calcium channel antagonist, which results in reduced release of excitatory neurotransmitters and inhibition of synaptic transmission, a mechanism particularly relevant for pain signalling in the spinal cord. It is an effective drug used for treating neuropathic pain (Verma, Singh, and Singh Jaggi 2014). Tapentadol acts as both a μ-opioid receptor agonist, decreasing ascending pain

signalling, and as a noradrenaline reuptake inhibitor, increasing descending inhibition (Romualdi et al. 2019). It is used clinically for treating a number of chronic pain conditions (Langford et al. 2016). For the BioPain trial, these three drugs were chosen as they were expected to respectively act predominantly on the peripheral, spinal and brain compartments of the pain processing system. Using fMRI, it was expected that changes in neural activity would be observed as a marker of direct drug actions on the brain, for example tapentadol acting on μ-opioid receptor locations in the cortex, subcortical structures and brainstem, and of indirect drug actions in the periphery and the spinal cord which in turn might reduce the nociceptive transmission in to the brain.

Lacosamide did not appear to modulate the punctate-evoked BOLD response in the posterior insula, but had the greatest effect on the functional connectivity between the thalamus and SII regions than either of the other two drugs. This could reflect an overall effect of lacosamide in reducing neuronal excitability on the functional connectivity between the brain regions.

Pregabalin had the greatest effect on the punctate-evoked BOLD response in the posterior insula but did not modulate the functional connectivity between the thalamus and SII regions. This is surprising, as based on a previous study demonstrating the effects of gabapentin on these measures (Wanigasekera et al. 2016), it would be expected that pregabalin (a drug in the same class as gabapentin), would be likely to also modulate both measures. This may be due to differences between the study designs. In the previous study the topical capsaicin model was used, which is associated with ongoing pain that does not occur with the HFS model. Also, gabapentin was given pre-emptively prior to the establishment of central sensitisation, whereas in the BioPain study dosing took place after HFS, during an established state of central sensitisation. It could also be due to the specific drugs resulting in differences in the outcome, or it may have been due to limitations with the trial design that the same result was not seen here. The other two drugs (lacosamide and tapentadol) have not been studied in this type of trial using an experimental model of central sensitisation in conjunction with fMRI, so there was less evidence on which to base the hypothesis. Despite this, it was still expected that these fMRI measures would both be modulated by these effective analgesics, therefore the fact that only pregabalin and tapentadol modulated the punctate-evoked endpoint and only lacosamide modulated the functional connectivity endpoint is an interesting finding.

Tapentadol did not have a major effect on either of the primary and secondary outcome measures, with only the significant decrease seen in the punctate-evoked BOLD response in the posterior insula, at the 1-hour post-drug time point. However, tapentadol did modulate punctate-evoked BOLD activity

in other areas involved in pain processing, including the anterior insula cortex, primary and secondary somatosensory cortices, as well as components of the basal ganglia (caudate nucleus and putamen) and the amygdala. During rest, tapentadol also resulted in decreased functional connectivity between the right thalamus seed-region and the PAG at the 1-hour time point. These drug-induced effects are consistent with the dual mechanism of action of tapentadol. There is widespread expression of μ-opioid receptors in cortical and sub-cortical pain processing areas, including areas in which activity changed during the tapentadol visit compared to placebo, such as the insula cortex, amygdala and PAG (Corder et al. 2018). The PAG is also a key region involved in the descending noradrenergic pathway for pain inhibition, though the specific action of tapentadol in inhibiting noradrenaline reuptake is likely to occur in the dorsal horn of the spinal cord, where this transmitter is released (Kress 2010).

Overall, this study has provided useful information on target engagement, and showed brain activity was modulated by analgesics of different drug classes and mechanisms of action in different ways. It is worth highlighting that this is despite the result of the study being negative from a statistical point of view. This indicates that there are disadvantages associated with designing early phase imaging-based biomarker studies of pharmacodynamic efficacy based on strict RCT criteria with very narrow primary endpoints. For future early phase imaging biomarker studies, it may be better to have broader exploratory objectives and endpoints aimed at understanding target engagement and modulation.

One factor that may have implicated the effect size in the results of the study is the magnitude of the placebo response, since all comparisons are made with the placebo group for each time point. Overall, this study does highlight the importance of the placebo effect in clinical trials (Tuttle et al. 2015; Enck and Klosterhalfen 2013). The change in the placebo condition was high compared to baseline across all fMRI measures, and drug vs. placebo comparisons showed only marginal changes (or no changes). This is discussed in more detail in the next chapter of this thesis.

Further, it has been shown that there are significant within-subject fluctuations in the response to the HFS model, as measured with subject reported pain intensity to pinprick stimuli (Cayrol et al. 2020). This is likely to have a negative impact on the ability of the experiment design used in this BioPain trial to elucidate the effect of each drug. Consistent with the finding reported by Cayrol *et al.*, the behavioural responses to the pre-drug baseline pinprick stimulation session (PD1) were variable in this trial. The average individual-subject range for the pain intensity ratings across all four visits (i.e. difference between the lowest rating and highest rating) was 9.7 (on the 0–100-point scale), but for

one subject this was as high as 33.9. Cayrol *et al.* indicate that the sensitivity to pinprick stimuli is likely related to the state of central sensitization, though this is ultimately a surrogate measure of the magnitude of response rather than direct measurement, so it is not possible to conclusively conclude that the state of central sensitisation itself was variable.

Finally, while the HFS model produced a high level of pain during application of the initial electrical stimulation, the pain from the mechanical pin-prick stimuli in the area of secondary hyperalgesia during the MRI scan was rated low by the subjects. The average ratings for pain intensity and unpleasantness were all below 25 out of 100 for all treatments (drug or placebo), at all time points. This could reflect a low-level of central sensitisation (using the ratings as a surrogate measure for this), which would likely impact the drug modulation that we are investigating using the fMRI. It could be argued that for some subjects, the stimuli given are not painful at all, and therefore the drugs given cannot modulate pain (as there is no pain level below 'no pain'). Contrary to this point, in the previous chapter of this thesis, it was shown that the HFS model does result in a credible state of central sensitisation, resulting in changes in brain activity in key regions such as the nucleus cuneiformis. There may have been an order effect of the study design though, as this was shown at the first screening visit, and the response to the HFS model could diminish at subsequent visits.

One potential limitation that could have affected the results of this study is any potential sedative effects of the drugs. Tiredness scores were collected during the study days to provide an indicator for how sedation may have affected the results. Future analysis is planned to assess the relationship between the tiredness scores and the subject-reported pain ratings, which may be affected by the subject's ability to provide the rating if they are very tried, and also the relationship between the tiredness scores and the primary and secondary trial endpoints, as these may be affected by levels of sedation. This analysis would aim to exclude any confounding effects of sedation on the variables of interest. However, when collecting the data it became apparent that the timing of the collection of the tiredness score was not optimised in the study design. Many subjects did appear to become tired during the MRI scans and the earlier part of the study day at some visits, but after the lunch break the majority felt much better (potentially due to the side effects of the drug wearing off, or maybe benefitting from the lunchtime meal after the required fasting at breakfast). Therefore, the state tiredness scores that were collected after lunch may not accurately reflect the tiredness experienced during the MRI data collection. This PROM should ideally have been collected twice, straight after each MRI scan, to enable more accurate conclusions to be made about the impact of tiredness at the time of the MRI data collection.

The over-arching objective of the BioPain project focussed on bridging the gap between pre-clinical and clinical research through providing translatable and objective functional pain biomarkers, and it is therefore important that the findings of this study are clinically relevant. In patients with fibromyalgia, it has been shown using fMRI and ^{1}H-MRS techniques that pregabalin results in altered functional connectivity of the posterior insula cortex with areas of the default-mode network, and reduced glutamatergic activity in this region, compared to placebo (Harris et al. 2013). This is consistent with the current study that also showed that altered responses in the posterior insula following pregabalin administration, this time in the stimulus-evoked condition. A further fMRI study in patients with post-traumatic neuropathic pain showed that there was significantly reduced activity in the SI and SII regions and in the anterior and posterior insula cortex during dynamic mechanical allodynia with pregabalin compared to placebo (Wanigasekera et al. 2018). Again this is consistent with stimulus-evoked results in the current study, which showed changes in the anterior insula and SI in the whole-brain analysis and in the posterior insula in the analysis of extracted parameter estimates. There are no imaging studies investigating lacosamide or tapentadol in chronic pain patient cohorts so it is not possible to make the same comparisons with those drugs. One study showed that tapentadol significantly increased conditioned pain modulation (CPM) responses in patients with diabetic polyneuropathy compared to placebo, concluding that the analgesic effect of tapentadol in patients with chronic pain was due to activation of descending inhibitory pain pathways (Niesters et al. 2014). This may be reflected in the results of the current study which showed altered functional connectivity between the thalamus and the PAG; a key region involved in descending pain modulation.

4.6 Conclusion

In conclusion, this trial has provided a significant contribution to the development of standardised objective pain biomarkers that can be used in future clinical studies. Overall, the IMI-Pain Care project brings together an extensive range of preclinical and clinical measures of analgesic efficacy. Through utilising standardised protocols and a combined approach looking at subject reported outcome measures, PK/PD modelling and complex statistical analyses, it aims to provide a set of validated pharmacodynamic biomarkers which can help bridge the gap between animal studies and early phase clinical trials. This thesis chapter presents an early-stage analysis of the fMRI part of the project, demonstrating that specific fMRI measures of analgesic efficacy are modulated by three analgesics acting across the nervous system. This work builds on existing evidence of the value of fMRI measures

in understanding analgesic action and target engagement in the brain, and provides a further step towards the standardisation of these fMRI biomarkers for use in a real-world setting to support the development of novel analgesics.

EXPERIMENTAL CHAPTER 5

Characterisation of the placebo effect in the BioPain trial

5.1 Abstract

Introduction and aims: Understanding the placebo effect is vital for the interpretation of placebo controlled randomised clinical trials for pain drugs, in addition to its relevance for medical practice. Functional magnetic resonance imaging (fMRI) has been applied in research to aid understanding of the neural correlates of placebo analgesia, showing changes in activity across multiple pain-related brain regions during this phenomenon. The aim of this study was to characterise the placebo effect in the IMI-PainCare BioPain RCT4 trial; a randomised, double-blind, placebo-controlled, cross-over trial in healthy subjects to investigate the effects of lacosamide, pregabalin and tapentadol on brain biomarkers of pain processing observed by fMRI. It was hypothesised that the placebo analgesia observed in the trial would be associated with altered neural activity in pain-related brain regions.

Methods: A cohort of 14 subjects who completed both the screening and study visits of the BioPain trial at the Oxford site (REC Reference 20/SW/0017) were included. To characterise the placebo effect, a comparison between data collected during screening (no drug baseline condition) and data collected at the placebo visit was conducted. At each visit, hyperalgesia was induced in the left lower limb using high-frequency electrical stimulation (HFS). At screening, subjects then completed an MRI scan with no drug administered. At the placebo visit, subjects received an oral dose of placebo after HFS application, and then completed MRI scans at 1-hour and 3-hours post-drug. The MRI protocol was aligned, measuring blood oxygen level dependent (BOLD) signal during 18 punctate mechanical stimuli applied to the secondary hyperalgesia area, and also during rest. To compare neural activity between the no drug and placebo conditions, whole brain, mixed effects analysis with cluster-based correction for multiple comparisons was performed to identify differences in stimulus evoked neural activity, and resting-state functional connectivity with the rostral anterior cingulate cortex (rACC) and ventrolateral periaqueductal grey (vlPAG) seed-regions.

Results: During the placebo condition, mean pain intensity and unpleasantness ratings significantly decreased during punctate mechanical stimulation, compared to the no drug baseline. This was associated with significantly decreased activation in brain areas involved in pain perception and descending pain modulation including the insula cortex, anterior cingulate cortex (ACC), amygdala and primary and secondary somatosensory cortices. During rest, functional connectivity decreased between the vlPAG and the dorsolateral prefrontal cortex (DLPFC), secondary somatosensory cortex and insula cortex.

Conclusions: During placebo analgesia changes in brain activity in response to mechanical stimulation and during rest were observed in regions commonly reported in fMRI placebo research, including the insula and ACC, and those involved in the affective and cognitive aspects of pain processing such as the amygdala and DLPFC. This study contributes to understanding the neural correlates underpinning placebo analgesia in a clinical trial which remain insufficiently understood, and provides contextual information to support interpretation of the main drug vs. placebo BioPain trial results.

5.2 Introduction

Research into placebo and nocebo phenomena has expanded from initial small scale methodological studies into a broad field, with important implications for clinical practice in healthcare. Recent expert consensus from placebo researchers at a Society for Interdisciplinary Placebo Studies (SIPS) conference aims to outline how placebo and nocebo research can impact clinical practice through evidence-based and ethical recommendations. Importantly, the consensus first defines the *placebo response* and *placebo effect.* The placebo response is defined as all health changes that occur after administration of an inactive treatment, as would be seen in clinical practice or measured in clinical trials. The placebo effect is defined as *"changes specifically attributable to placebo and nocebo mechanisms, including the neurobiological and psychological mechanisms of expectancies" (*Evers et al. 2018*)*. These expectation-based mechanisms are altered by many factors, such as the external situation and verbal or non-verbal cues (Evers et al. 2018). This thesis chapter aims to characterise the placebo effect in the BioPain study data, through utilising neuroimaging data and subject-reported measures to elucidate the neural mechanisms underlying this effect.

In a clinical trial setting, placebo treatments have been used as a control, to enable researchers to differentiate the effects of expectancy from the 'true' effects of the drug being investigated. However, research into the neural mechanisms underlying this phenomenon have highlighted that placebo analgesia is a complex response involving psychological factors such as expectation, context and prior experiences. This response results in analgesia via the release of modulatory neurotransmitters across the nervous system, including opioids and non-opioids such as cannabinoids and dopamine, and the top-down modulation of pain processing via the descending pain modulatory system. (Colloca et al. 2013). This research has raised the important point that the placebo effect and drug effects in clinical trials are not simply additive (i.e. overall drug response ≠ placebo effect + drug effect), and analgesics that act on pain processing are likely to interact with the neural mechanisms underpinning placebo analgesia too (Wanigasekera et al. 2018; Petrovic et al. 2010; Wager and Roy 2010; Enck and Klosterhalfen 2013).

Endogenous opioid systems play a key role in placebo analgesia. In positron emission tomography (PET) studies it has been shown that opioid and placebo analgesia share common mechanisms, both resulting in increased activity in the rostral anterior cingulate cortex (rACC) and brainstem regions (Petrovic et al. 2002). This has been further demonstrated in functional magnetic resonance imaging (fMRI) studies which have shown changes in the BOLD response in the dorsolateral prefrontal cortex

(DLPFC) and rACC (Kong et al. 2006; Wager et al. 2004), and enhanced functional connectivity of the rACC with bilateral amygdalae and the periaqueductal grey (PAG) (Bingel et al. 2006) during placebo analgesia, indicating that activity between these regions mediates the endogenous-opioid related analgesia during the placebo effect (Bingel and Tracey 2008). Further, it has been shown that placebo-induced changes in activity in the rACC, PAG and rostral ventromedial medulla (RVM), and coupling between the rACC and the PAG during placebo analgesia, are reduced by naloxone (an opioid antagonist) (Eippert et al. 2009). Although opioid signalling is involved in both placebo analgesia mediated by endogenous opioids and analgesia induced by exogenous opioids, the neural mechanisms underpinning these responses are not identical which is an important consideration for research in this area (Petrovic et al. 2010; Zhang et al. 2020). Endogenous opioids also play a role in the relief aspect of placebo analgesia, through mediating the pleasant and rewarding feelings accompanying a reduction in pain that are important psychological mechanisms of the placebo effect (Sirucek et al. 2021). This reward aspect of the placebo effect is also mediated by endogenous dopamine release, and functional neuroimaging studies have shown that brain regions associated with dopaminergic reward processing are activated in placebo analgesia, such as the ventral striatum in the basal ganglia (de la Fuente-Fernández 2009). In addition, endogenous cannabinoids have been shown to mediate non-opioid mechanisms of placebo analgesia, specifically in circumstances when the opioid system is not involved such as after conditioning with non-steroidal anti-inflammatory drugs (NSAIDs) (Benedetti et al. 2011).

In addition to changes in brain systems involved in neurotransmitter signalling, fMRI placebo studies have also shown a reduction in activity in pain-related brain regions including the insula cortex, thalamus, mid-ACC and somatosensory cortices (Wager et al. 2004; Bingel et al. 2006; Kong et al. 2006; Koyama et al. 2005), and this has also been shown in patients (Price et al. 2007). This aspect of the placebo effect likely reflects the reduced pain perceived. Co-ordinate based meta-analyses of fMRI placebo studies have been conducted, showing decreases in activation during painful stimulation in brain regions associated with pain processing, including the ACC, insula cortex, thalamus, hypothalamus and PAG, and brain regions associated with affective aspects of pain perception, including the amygdala and striatum, during placebo analgesia (Atlas and Wager 2014; Amanzio et al. 2013). Further, a meta-analyses of individual subject fMRI data from placebo analgesia, enabling a much richer analysis than simply taking the peak activation co-ordinates, concludes that placebo analgesia results in small, widespread reductions in pain-related brain activity, in regions in the ventral attention network (such as the mid-insula cortex) and the somatomotor network (such as the posterior insula cortex). They also showed that subject reported pain ratings during placebo analgesia

correlated with reduced activity in these networks and in the thalamus, habenula, mid-cingulate, and supplementary motor area (Zunhammer et al. 2021).

Overall, previous fMRI studies on the neural basis for placebo analgesia indicate there are two elements of the effect, firstly that the response in the nociception processing networks is reduced, likely reflecting reduced pain experienced, and secondly, that there is involvement of cortical networks related to affective or emotional processing and contextual modulation (Atlas and Wager 2012; Tracey 2010; Wiech, Ploner, and Tracey 2008).

Previous neuroimaging studies investigating the placebo effect have almost exclusively involved the deliberate manipulation of subject expectations, primarily with healthy subjects in acute pain studies designed specifically for this purpose. Far fewer studies have investigated the placebo effect in a randomised clinical trial setting. One such study has shown that the neural basis for the placebo effect elucidated by acute pain imaging experiments is aligned to the neural basis for the placebo effect observed in the placebo-arm of a clinical trial in a pain patient cohort (Wanigasekera et al. 2018). The neural basis for the placebo effect in healthy human studies utilising neuroimaging in conjunction with experimental pain models to investigate drug activity is not well characterised. This is important, as if neuroimaging techniques are to be used in conjunction with experimental pain models to support early-stage assessment of novel analgesics compared to placebo, and to inform decision making in drug development, then there is a need to have a very clear understanding of the placebo effect in this setting. Assumptions that the placebo effect is equal in the drug and placebo arms and that the drug effect is additive with the placebo effect could jeopardise the ability of these techniques to reliably provide proof of efficacy in early phase clinical trials (Enck and Klosterhalfen 2013).

Therefore, the aim of the current study was to characterise the placebo effect in the BioPain trial. The BioPain trial was a randomised, double-blind, placebo-controlled, cross-over trial in healthy subjects to investigate the effects of lacosamide, pregabalin and tapentadol on brain biomarkers of pain processing observed by fMRI. The main endpoints of the trial focussed on comparing the neural activity during analgesia induced by the active drugs compared to the placebo condition, consistent with the design of many placebo-controlled studies. In addition to study visits at which drugs were administered, data was also collected at a screening visit which included a similar schedule of study procedures and data collection but did not include the administration of a drug. This enables characterisation of the placebo effect compared to the no drug baseline condition from the screening visit. Specifically, the aims of the study were to:

1. Compare the whole-brain BOLD response to mechanical pin-prick stimuli in the area of secondary mechanical hyperalgesia during the placebo condition compared to the no drug baseline condition
2. Compare the whole-brain seed-based functional connectivity with the rACC and vlPAG seed-regions during rest in the placebo condition compared to the no drug baseline condition

It was hypothesised that during the placebo condition the subject reported pain would be reduced compared to the no drug baseline condition, and that this would be associated with reduced BOLD response in brain regions shown in previous studies to have a reduced response during placebo analgesia, such as the amygdala, insula cortex and mid-ACC. It was also hypothesised that increases in the BOLD response in brain regions involved in the descending pain modulation, such as the DLPFC and the rACC, would be observed during the placebo condition, as has been shown in previous fMRI studies (Eippert et al. 2009). Placebo induced changes in functional connectivity during rest are less well defined than stimulus-evoked changes. In stimulus-evoked studies, functional connectivity between the PAG and rACC has been shown to be enhanced during placebo analgesia (Bingel et al. 2006; Wager, Scott, and Zubieta 2007; Eippert et al. 2009). More recently, it has been shown that following placebo analgesia there is a negative coupling relationship between two resting-state brain networks, the first including somatosensory regions and the posterior insula cortex and the second including brainstem, subcortical and anterior cingulate regions. Further, subjects with the most negative coupling had the strongest placebo effect (as measured by having the lowest pain intensity scores) (Wagner et al. 2020). It has been demonstrated that resting-state connectivity between the rACC and the brainstem is significantly increased during placebo compared to baseline in post-traumatic neuropathic pain patients, a relationship that was not significantly different between active treatment and baseline (Wanigasekera et al. 2018). Similar studies have shown resting state functional connectivity is predictive of the magnitude of the placebo response in chronic knee osteoarthritis patients (Tétreault et al. 2016) and fibromyalgia patients (Schmidt-Wilcke et al. 2014). Given the key role of the PAG and rACC in the stimulus-evoked placebo literature, it was hypothesised that seed-based functional connectivity between these seed-regions and brain regions involved in the placebo effect, or regions involved in sensory pain perception, would be altered. The vlPAG was selected to be used as the seed-region (rather than the entire PAG) due to evidence that this sub-region is key in implementing cognitive top-down pain modulation (Livrizzi et al. 2022).

5.3 Methods

5.3.1 Study participants and ethical approval

Data was collected as part of the IMI-BioPain RCT4 trial. This dataset includes 14 healthy subjects (mean age 26, range 21 to 38, 8 female). All data was collected at the Oxford site (REC Reference 20/SW/0017). The reason that this smaller cohort was included in this early-stage exploratory analysis was due to limited availability of data from the additional trial sites. Once all data are available from the two additional sites it is planned that similar analysis based on this initial study will be conducted with the full dataset (29 subjects). All subjects included were right-handed as assessed by the Edinburgh Handedness Inventory, and defined as a score ≥60. Written informed consent was obtained from all participants.

5.3.2 Study design

The IMI-BioPain RCT4 trial focusses on the use of fMRI to assess analgesic efficacy in healthy human participants. The trial includes an initial screening visit, during which no analgesics are administered, followed by four study visits at which subjects received an oral dose of lacosamide, pregabalin, tapentadol, or placebo. The trial was double-blind and randomised. Unblinding has taken place, and the placebo visit for each subject is known. This chapter utilises the data from the initial screening visit (no drug baseline) and the placebo visit (inert drug, orally administered). Due to the randomised order of the study days the timing of the placebo visit is variable for the subjects included in this analysis, as subjects could receive the placebo treatment at any of the 4 study visits. The study timeline and treatment administration are outlined in Figure 1.

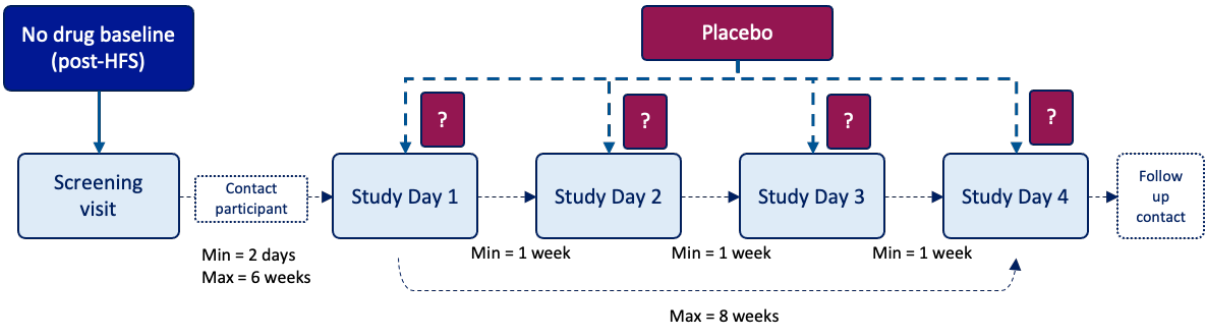

Figure 1: Study design and treatment administration.

Diagram outlining the study visits for the IMI-BioPain RCT4 trial and the visits from which data is used for this chapter. Subjects attended an initial screening visit, followed by four study days. At each study day, one of four treatments (lacosamide, pregabalin, tapentadol, or placebo) was administered orally. This chapter focusses on a comparison of the no-drug baseline condition (data collected during the screening visit) with the placebo condition (data collected at one of the four study days).

At the screening visit, eligibility criteria were first assessed. Eligible subjects then took part in an initial MRI scan, then high frequency stimulation (HFS) was applied to the left lower leg to induce secondary mechanical hyperalgesia, followed by a second MRI scan which took place approximately 20 minutes after HFS was applied. At the end of the visit, the area of hyperalgesia was mapped.

At the start of the study days, prior to application of HFS, subjects were asked to provide numeric rating scale (NRS) ratings for their anxiousness and expectation of pain, with anxiety rated from 0; not anxious at all, to 100; extremely anxious, and pain expectation rated from 0; no pain at all, to 100; pain as bad as can be imagined. Then, HFS was applied on the left lower leg. Following HFS, mechanical pin-prick stimuli were applied to the area of secondary hyperalgesia and subjects asked to rate pain intensity and unpleasantness. After this stimulation block, subjects were asked to rate their expectation of pain relief from the study medication, from 0; no relief, to 100; complete relief. Subjects then took an oral dose of the study medication. The first MRI scan started 1-hour after dosing, then hyperalgesia mapping was completed approximately 2-hours after dosing, and the second MRI scan started 3-hour after dosing. The timeline for each session is outlined in Figure 2, with the relevant data collection points for this chapter highlighted.

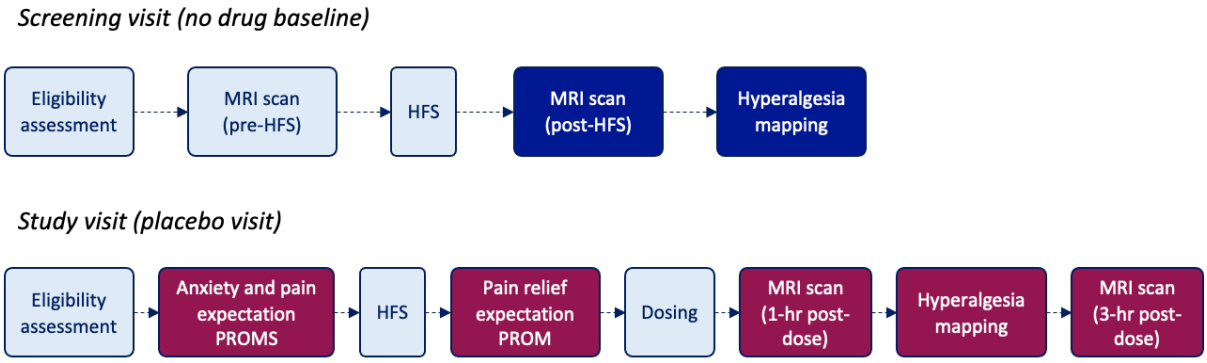

Figure 2: Outline of study procedures completed at each screening and study visit.

Diagram outlining the study procedures for each screening and study visit, with the relevant data collection points for this chapter highlighted in blue (for screening) and maroon (for the placebo visit). MRI data from the screening visit (no drug, post-HFS baseline) was compared with the MRI data from the placebo visit, at both the 1-hour post-dose and 3-hour post-dose time points. Hyperalgesia mapping data was also compared between the two conditions, and patient(subject)-reported outcome measures (PROMS) on anxiety, pain expectation and expectation of pain relief were collected during the study visits.

5.3.3 High frequency stimulation (HFS)

At the screening visit (no drug baseline) and at each study day, secondary mechanical hyperalgesia was induced on the left lower leg of the subjects using HFS. The method for application of HFS and the rationale for its use was described in detail in the previous chapters of this thesis. Briefly, HFS was applied using the HFS Electrode "EPS-P10" manufactured by *MRC Systems GmbH*. The pulses delivered by the electrode were generated by the Digitimer DS7A constant current stimulator. HFS application consisted of 5 trains of electrical pulses delivered at 100 Hz. Train duration was 1s, with an interval of 9s between each train, and the stimulation intensity was set to 20x the detection threshold for each subject.

5.3.4 Magnetic resonance imaging (MRI) protocol

At each screening visit two MRI scans were completed, one prior to application of HFS and a second after HFS-induced secondary mechanical hyperalgesia had developed. Data from the second scan (conducted during the sensitised state) was used for this study. During study visits there were also two MRI scans completed, at two post-drug administration time points (starting at 1-hour post drug and 3-hours post drug). Data from both scans during the placebo visit was used for this study.

The protocol for each MRI scan throughout the trial was very similar and has been described in detail in the previous chapters of this thesis. For this chapter, data from the first two scan blocks was used, which were a blood oxygen level dependent (BOLD) scan during resting stat and a BOLD scan during mechanical punctate (pin-prick) stimuli in the area of secondary hyperalgesia. During the mechanical punctate stimuli scan, BOLD signal changes were measured in response to 18 mechanical stimuli each with a 1s duration, applied using a 512nM weighted non-skin penetrating punctate probe. Participants rated the pain intensity of each mechanical stimulus, and provided an average rating of pain unpleasantness following all 18 stimuli, both using a visual analogue scale from 0 (no pain at all/not unpleasant at all) to 100 (most intense pain imaginable/extremely unpleasant). Punctate stimuli were applied in the area of secondary hyperalgesia, 1cm outside the site of the HFS cathode pins.

MRI data was collected using a 3T Siemens PRISMA scanner with a 32-channel head-coil. BOLD data were acquired with a whole brain echo-planar imaging sequence with an echo time of 36ms, field of view 192mm x 192mm, voxel size 2mm x 2mm x 2mm, multiband acceleration factor 6, echo spacing of 0.62ms and bandwidth of 2084 Hz/Px. The resting state scan had 513 volumes, the mechanical stimulation task scan had 531 volumes and the visual task scan had 257 volumes, each with a repetition time of 1.17 seconds. A field map was acquired to after the functional scans to enable correction of field inhomogeneity during analysis, with voxel size 2mm x 2mm x 2mm and field of view 192 mm x 192mm. For each subject, a T1 structural scan was also acquired at the end of the first MRI scan conducted during the screening visit, before HFS is applied. This T1-weighted structural scan was acquired with voxel size 1mm x 1mm x 1mm for registration of the functional BOLD scans to standard space for group-level analysis.

5.3.5 Hyperalgesia mapping

For the screening visit (no drug baseline), hyperalgesia mapping was completed after the second MRI scan. For the study visit (placebo), it was completed in the time period between the two MRI scans, approximately 2-hours post-drug and approximately 2 hours and 45 minutes after the HFS was applied. The methodology used to map the area of hyperalgesia is described in detail in Chapter 3 of this thesis. In short, mechanical pin-prick stimuli were applied with the 512nM stimulator in 8 radii around the position HFS was applied, and subjects were asked to state the position at which the stimulus felt “different”. The distance between the stated point and the HFS electrode pins was measured. Subjects were also asked to provide a verbal average pain intensity score for the pin-prick stimuli that were applied during the mapping exercise, using a scale from 0 (no pain at all) to 100 (most intense pain imaginable).

5.3.6 Statistical analysis

Statistical analysis for all behavioural data was completed using GraphPad PRISM version 9.4.1 (GraphPad Software, LLC). Statistical significance is reported with the following symbols; ns for $P > 0.05$; * for $P \leq 0.05$, ** for $P \leq 0.01$, *** for $P \leq 0.001$, and **** for $P \leq 0.0001$.

All imaging data were analysed using tools in the FMRIB Software Library v6.0 (FSL) (Woolrich et al. 2009; Smith et al. 2004; Jenkinson et al. 2012). For each scan, structural and magnitude images were brain extracted (Smith 2002) and a calibrated field map image was prepared to be used for B0 unwarping. For BOLD data, registration to the structural image and B0 unwarping were performed using FEAT (Woolrich et al. 2001). Motion correction, spatial smoothing (5mm for mechanical pin-prick stimulation, and 3mm for resting state scan) and high-pass temporal filtering were applied. Independent component analysis was conducted with the MELODIC tool and noise components were removed using the FIX auto-classifier (Griffanti et al. 2014; Salimi-Khorshidi et al. 2014), in conjunction with a training dataset that was developed by hand classifying components as signal or noise in the screening scans of the first 10 subjects (as previously described in Chapter 3 of this thesis).

For the mechanical pin-prick stimulation BOLD scan, following pre-processing and de-noising, an individual statistical map for the response to the stimuli was generated using the general linear model (GLM) approach implemented with FEAT (Woolrich et al. 2001). Then, a group-level whole brain, mixed effects analysis with a cluster-based correction for multiple comparisons was performed using FEAT to search for differences in stimulus evoked neural activity during the placebo condition compared to the no drug baseline (post-HFS) condition (Woolrich et al. 2004). The Featquery tool in FSL was used to extract mean percentage change in BOLD parameter estimates for the amygdala and insula cortex.

For the resting-state seed-based functional connectivity analysis, following pre-processing and de-noising, the time course for activity in the rACC and the vlPAG seed-regions was extracted and used to generate individual statistical maps of the functionally correlated activity across the whole brain for each subject, using the GLM approach implemented with FEAT (Woolrich et al. 2001). Individual maps were constrained to grey matter only by regressing out activity in white matter and cerebrospinal fluid, using time courses for this activity in the GLM which were generated from the anatomical segmentations for each tissue type. Then, a group-level whole brain analysis mixed effects analysis with a cluster-based correction for multiple comparisons was performed using FEAT to identify differences in the seed-based functional connectivity between the placebo condition and the

no drug baseline (post-HFS) condition (Woolrich et al. 2004). The rACC seed-region was defined using voxel co-ordinates for the rACC from a meta-analysis of brain mechanisms of placebo analgesia, which were 10, 44, 12 (x,y,z), to make a bilateral 5mm spherical mask (Atlas and Wager 2014). The vlPAG seed-region was defined in a previous study using a connectivity-based segmentation approach. Diffusion MRI optimised for the brainstem was used with probabilistic tractography to elucidate connectivity profiles of the voxels within the PAG, enabling it to be segmented into four clusters, one of which being the ventrolateral PAG (Ezra et al. 2015; Faull and Pattinson 2017).

5.4 Results

5.4.1 Hyperalgesia mapping results

Hyperalgesia mapping was completed at both the screening visit (no drug baseline) and the placebo visit. There was no significant change in the hyperalgesia radius (paired t-test, p = 0.5481) between the no drug baseline condition and the placebo condition. There was a significant decrease in the pain intensity rating for the hyperalgesia mapping in the placebo condition compared to the no drug baseline condition (paired t-test, p = 0.0097). These results are shown in Figure 3.

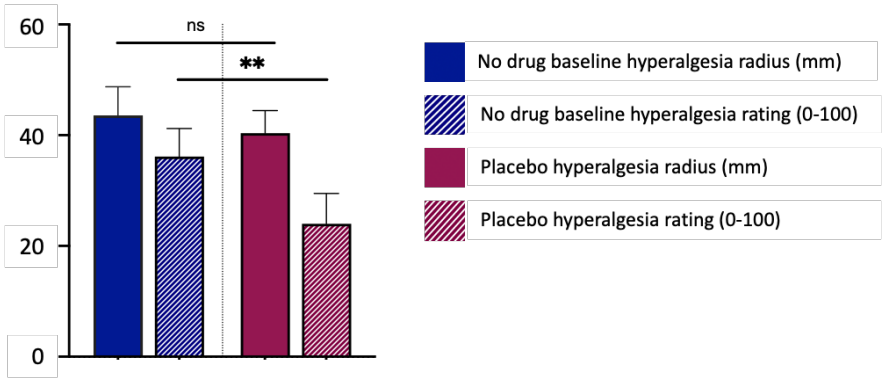

Figure 3: Hyperalgesia radius and pain intensity ratings from hyperalgesia mapping.

There was no significant difference between the hyperalgesia radius at the screening visit (no drug baseline) and the hyperalgesia radius at the placebo visit (paired t-test, p = 0.5481). However, there was a significant decrease in the pain intensity rating for the hyperalgesia mapping stimuli from the screening visit (no drug baseline) to the placebo visit (paired t-test, p = 0.0097). Due to the small sample size, determining the distribution of the hyperalgesia radius and rating data was needed to inform the choice of an appropriate statistical method. Hence, a D'Agostino-Pearson test was performed and showed that the data are normally distributed and based on this outcome parametric tests were used.

5.4.2 Subject reported anxiety and expectation measures

At the placebo visit, the mean subject reported anxiousness rating was 14.6, with a range of scores from 0 to 40. The mean subject reported pain expectation rating was 38.9, with a range of scores from 5 to 70, and the mean subject reported expectation of pain relief rating following dosing was 31.6, with a range of scores from 0 to 100. Subject ratings for expectation of pain relief, which are used later to explore correlations with changes in pain ratings and neural responses, are shown in Figure 4.

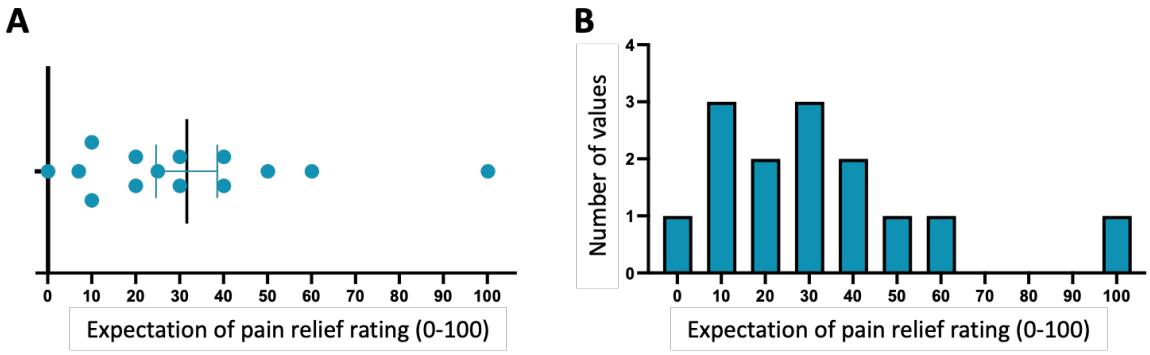

Figure 4: Expectation of pain relief ratings for the placebo visit.

A: Subject ratings for expectation of pain relief for the placebo visit. During the study visits (with drug administration), subjects were asked to rate their expectation of pain relief (0 = no relief, 100 = complete relief) prior to administration of the drug. During the placebo visit, subject ratings for expectation of pain relief ranged between 0 and 100. B: Histogram showing the frequency distribution of this data. Due to the small sample size, determining the distribution was needed to inform the choice of appropriate statistical methods in later analyses. Hence, a D'Agostino-Pearson test was performed and showed that the data are not normally distributed and based on this outcome non-parametric tests were used.

5.4.3 Response to mechanical pin-prick stimuli (pain ratings and BOLD MRI)

Mean pain intensity ratings provided during mechanical pin-prick stimulation were significantly decreased in the post-HFS (no drug baseline) condition compared to the placebo condition at both the 1-hour post-placebo and 3-hr post-placebo time points (paired t-tests, $p = 0.0144$ and $p = 0.0189$, respectively). The pain unpleasantness ratings were also significantly decreased from the post-HFS condition to the placebo condition at both time points (paired t-tests, $p = 0.0104$ and $p = 0.0215$, respectively). The majority of individual subjects had a decrease in the pain ratings between the post-HFS no drug baseline condition and the placebo condition. The group and individual pain intensity and unpleasantness ratings are shown in Figure 5.

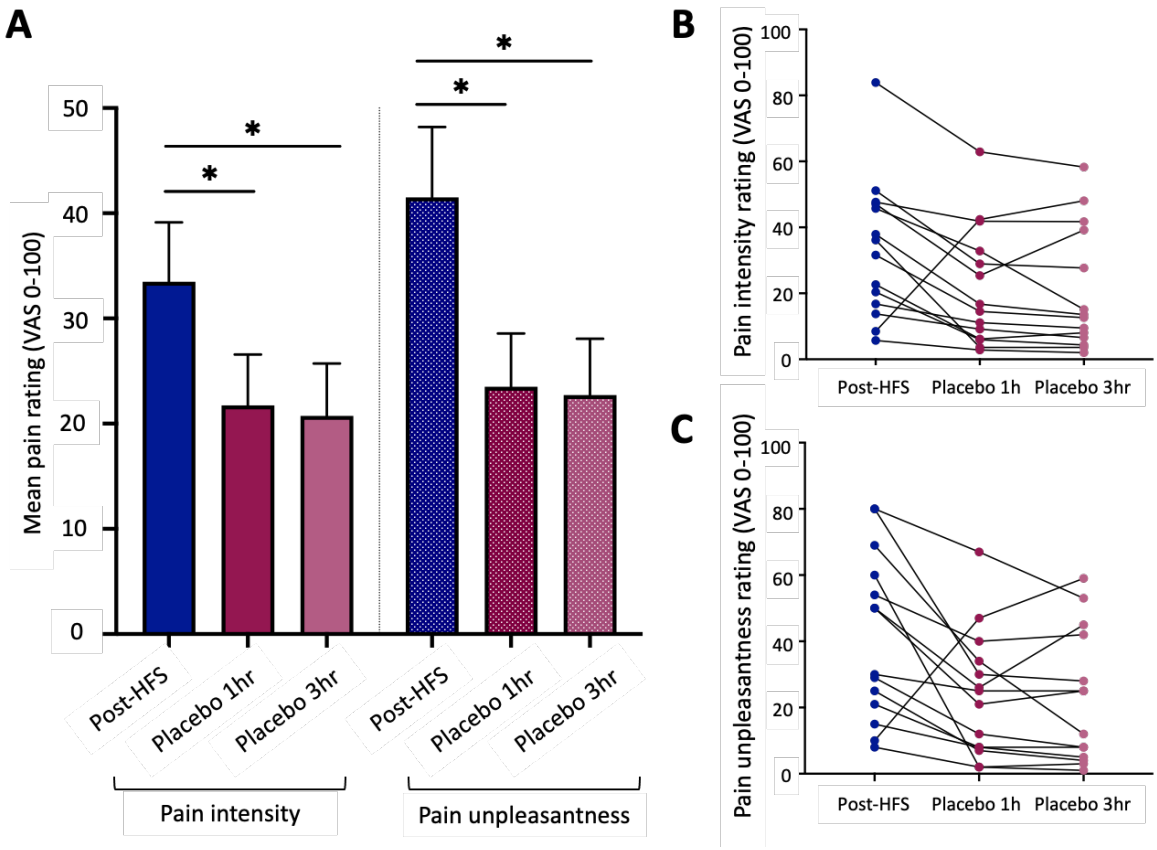

Figure 5: Subject pain intensity and unpleasantness ratings for post-HFS and placebo conditions.

A: There was a significant decrease in the mean pain intensity scores from the post-HFS (no drug baseline) condition to the placebo condition at both the 1-hour post-placebo and 3-hr post-placebo time points (paired t-tests, p = 0.0144 and p = 0.0189, respectively). This change in pain scores was mirrored in the pain unpleasantness scores, which also showed a significant decrease from the post-HFS condition to the placebo condition at both time points (paired t-tests, p = 0.0104 and p = 0.0215, respectively). Error bars show the SEM. B and C: For both pain intensity and unpleasantness, the majority of subjects' ratings decreased from the post-HFS scan to the 1-hour placebo scan, and then had a further small decrease again at the 3-hour placebo scan. For one subject, there was a larger increase in ratings, however this subject did not fully understand the use of the rating scale at screening and this was clarified to them prior to the first study visit, so this result is likely to be inaccurate for this individual. Due to the small sample size, determining the distribution of the data was needed to inform the choice of an appropriate statistical method. Hence, a D'Agostino-Pearson test was performed and showed that the data are normally distributed and based on this outcome parametric tests were used.

A correlation analysis was conducted to investigate whether there was a relationship between the subject's expectation of pain relief and the decrease in subject-reported pain intensity ratings during the placebo treatment session compared to the no-drug baseline session. This showed that there was a slight negative relationship; subjects who had the highest expectation for pain relief experienced the largest reduction in subject-reported pain intensity ratings during placebo analgesia, as shown in Figure 6. Calculation of a one-tailed Spearman correlation coefficient showed that this relationship was not significant at the 1-hour time point (r(df) = -0.3564, p = 0.1154) or at the 3-hour time point (r(df) = -0.3122, p = 0.1485).

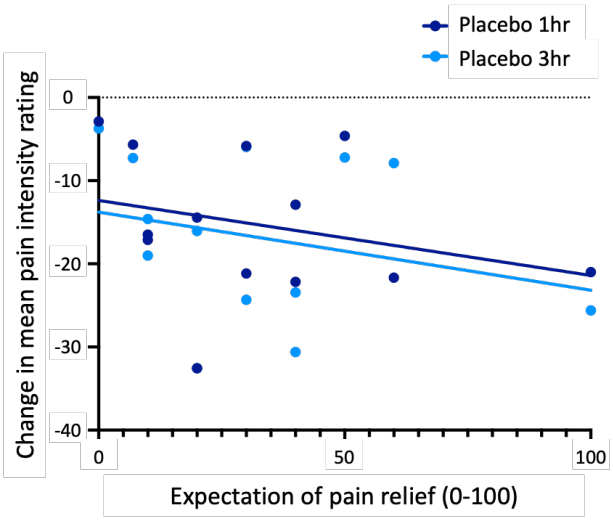

Figure 6: Relationship between expectation of pain relief and change in pain intensity ratings for mechanical stimulation during placebo analgesia

Expectation of pain relief PROMs plotted against the change in mean pain intensity ratings (the difference between the ratings during the placebo condition and the no-drug baseline condition). Calculation of a Spearman correlation coefficient showed there was no significant relationship between the two variables at the 1-hour time point (r(df) = -0.3564, p = 0.1154) or at the 3-hour time point (r(df) = -0.3122, p = 0.1485).

There were consistent decreases in the BOLD response during the 1-hour and 3-hour placebo condition time points compared to the post-HFS no drug baseline condition, therefore, for simplicity only the 3-hour time point is shown. The 3-hour time point was selected as this later time point allows more time for responses to have stabilised. There were no areas with increased BOLD response during placebo compared to the post-HFS no drug baseline condition. The BOLD response was significantly decreased in the placebo condition compared to the post-HFS no drug baseline condition in areas involved in pain perception and in descending pain modulation, including the insula cortex, mid-anterior cingulate cortex (ACC), amygdala, primary and secondary somatosensory cortices, orbitofrontal cortex and the putamen (mixed effects analysis, $Z > 3.1$, $p < 0.05$). The whole-brain BOLD response for the placebo (3-hour) vs. post-HFS no drug baseline comparison in shown in Figure 7.

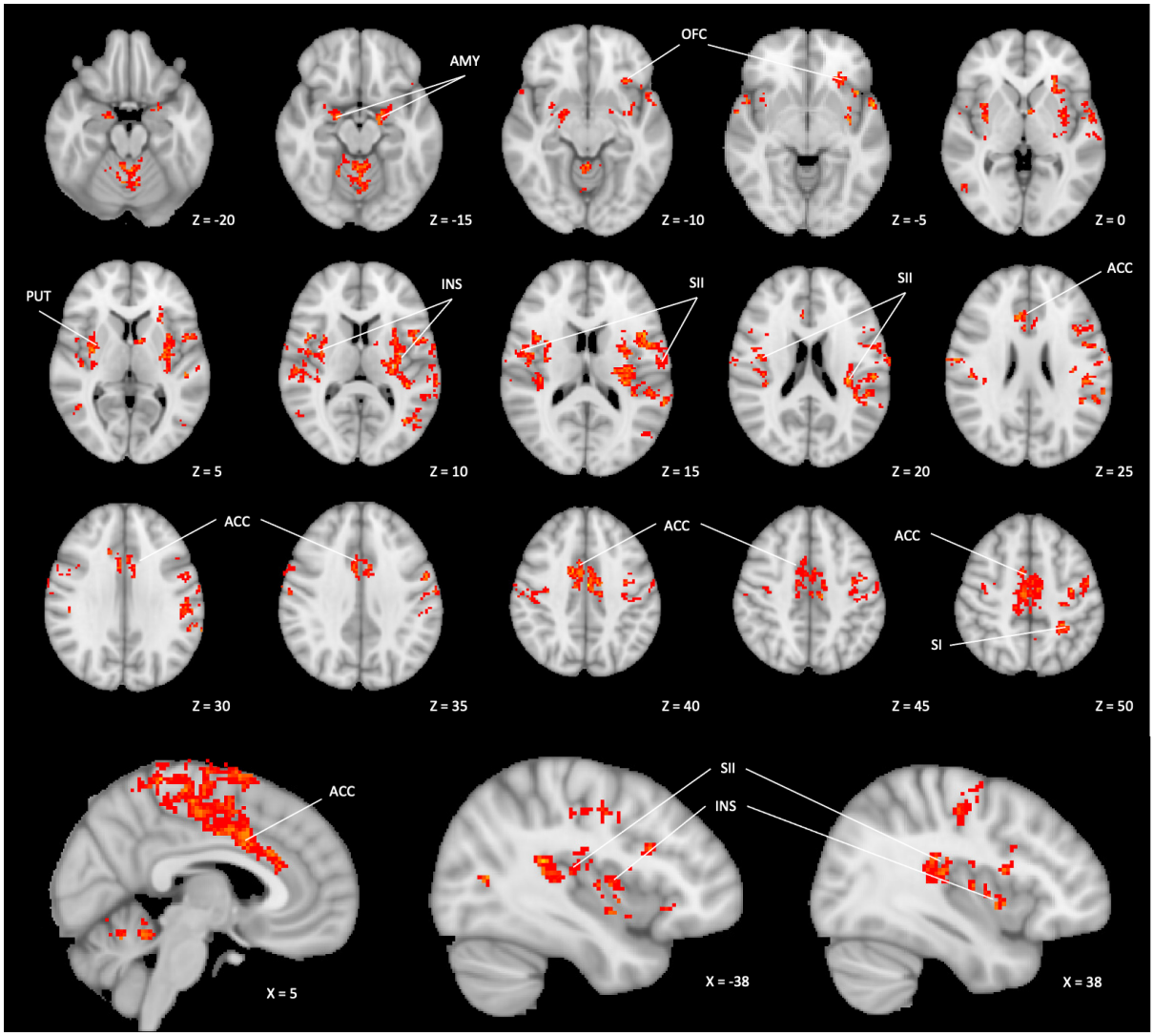

Figure 7: Whole-brain BOLD response during mechanical pin-prick stimuli for post-HFS baseline condition compared to placebo condition

There was a significant decrease in the BOLD response from the post-HFS (no drug baseline) condition to the placebo condition (mixed effects analysis, $Z > 3.1$, $p < 0.05$) in areas involved in pain perception such as the insula cortex (INS), mid anterior cingulate cortex (ACC), amygdala (AMY), primary and secondary somatosensory cortices (SI and SII), putamen (PUT) and the orbitofrontal cortex (OFC). MNI-512 co-ordinates are shown for images.

Previous research into the neural basis for the placebo effect has highlighted an important role for the amygdala, due to its contributions to the cognitive and descending pain modulatory networks and to the release of endogenous opioids during placebo analgesia (Tracey 2010), hence this region was an area of particular interest in this study. The whole-brain BOLD responses shown in Figure 7 above demonstrated that there was a decrease in BOLD activity in the amygdala during placebo analgesia. To understand this result more fully, BOLD parameter estimates were extracted from the left and right

amygdala during each condition. This showed that the BOLD response to mechanical stimulation in the amygdala was positive during the post-HFS no drug baseline condition, but switched to a negative deactivation during the placebo condition (at both the 1-hour and 3-hour time points). This result is shown in Figure 8.

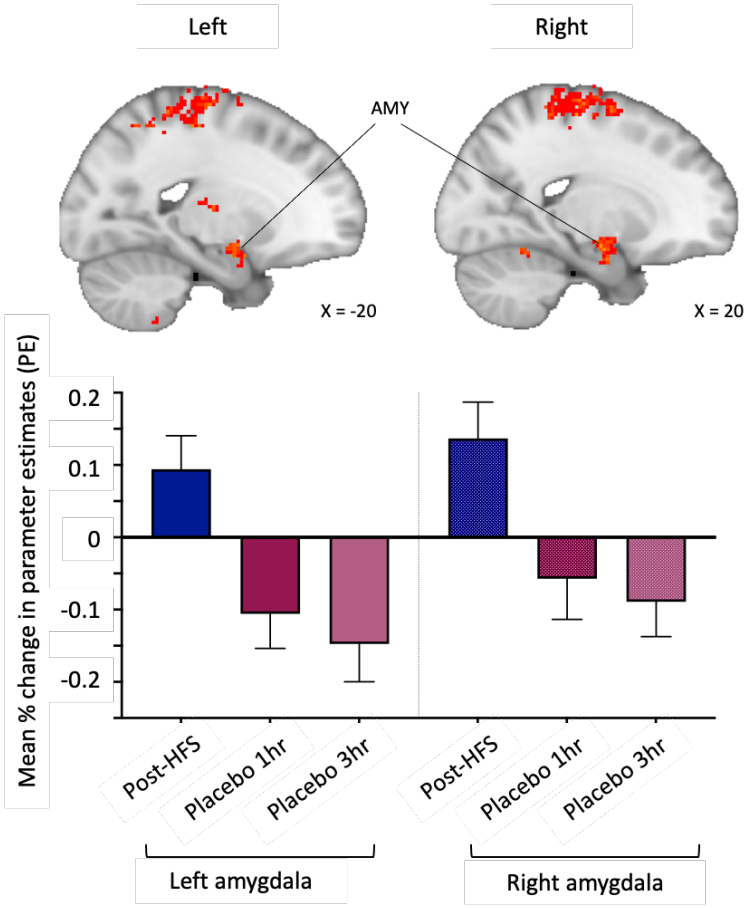

Figure 8: Change in BOLD response in the amygdala during placebo analgesia.

There was a significant decrease in the BOLD response in the left and right amygdalae from the post-HFS (no drug baseline) condition to the placebo condition. This is illustrated in the top panel with left and right amygdalae shown in the whole brain BOLD response (for the 3-hour post-dose placebo time point). BOLD parameter estimates were extracted from these areas of decreased activation during the placebo condition that corresponded to the anatomical amygdalae defined using the Harvard-Oxford atlas. These are plotted in the bottom panel, showing that the BOLD response to the mechanical stimuli during the post-HFS (no drug baseline) condition was positive, whereas during the placebo condition it is negative. Error bars show the SEM. MNI-512 co-ordinates are shown for images.

As there were no brain areas with increased BOLD response during the placebo condition compared to the post-HFS no drug baseline condition in this whole-brain analysis, region of interest (ROI) analysis was completed to investigate whether there were any changes in activity in the rACC or vlPAG – both key regions expected to show an increase in BOLD activity during the placebo condition compared to baseline. An anatomical mask of the each region was used to carry out a small-volume correction using non-parametric permutation testing with 5,000 permutations and threshold-free cluster-enhancement, with family-wise error corrected to 0.05 (Winkler et al. 2014). This analysis showed that there was no statistically significant increase in the BOLD response in each region in the placebo condition compared to the baseline condition.

5.4.4 Changes in resting state functional connectivity during placebo analgesia

For the rACC seed region, whole-brain analysis showed there were no changes in resting state functional connectivity with this region in the no drug baseline condition compared to the placebo condition at the 1-hour or 3-hour time points (whole-brain mixed effects analysis, $Z > 3.1$, $p < 0.05$).

For the vlPAG seed region, whole-brain analysis showed functional connectivity was significantly decreased between the vlPAG seed-region and the DLPFC at the 1-hour placebo time point compared to the post-HFS no drug baseline (whole-brain mixed effects analysis, $Z > 3.1$, $p < 0.05$). The DLPFC was identified anatomically using the Harvard-Oxford Cortical Structural Atlas, as the location of this area of activation was consistent with the middle frontal gyrus (JeYoung, Matthew, and Rebecca 2022; Desikan et al. 2006). At the 3-hour placebo time point, there was significantly decreased functional connectivity between the vlPAG seed-region and the insula cortex, secondary somatosensory cortex and the motor cortex (whole-brain mixed effects analysis, $Z > 3.1$, $p < 0.05$). At both time points there were no areas of increased connectivity. To further investigate the changes in functional connectivity in the DLPFC and insula cortex, functional connectivity measures were extracted and plotted. These measures show that in both regions the functional connectivity changed from a positive measure in the post-HFS no drug baseline condition, indicating that the time courses for activity in these two regions were correlated, to a negative measure, indicating that during the placebo condition the time courses for activity are anticorrelated. The whole-brain functional connectivity findings and the plots of functional connectivity measures are shown in Figure 9.

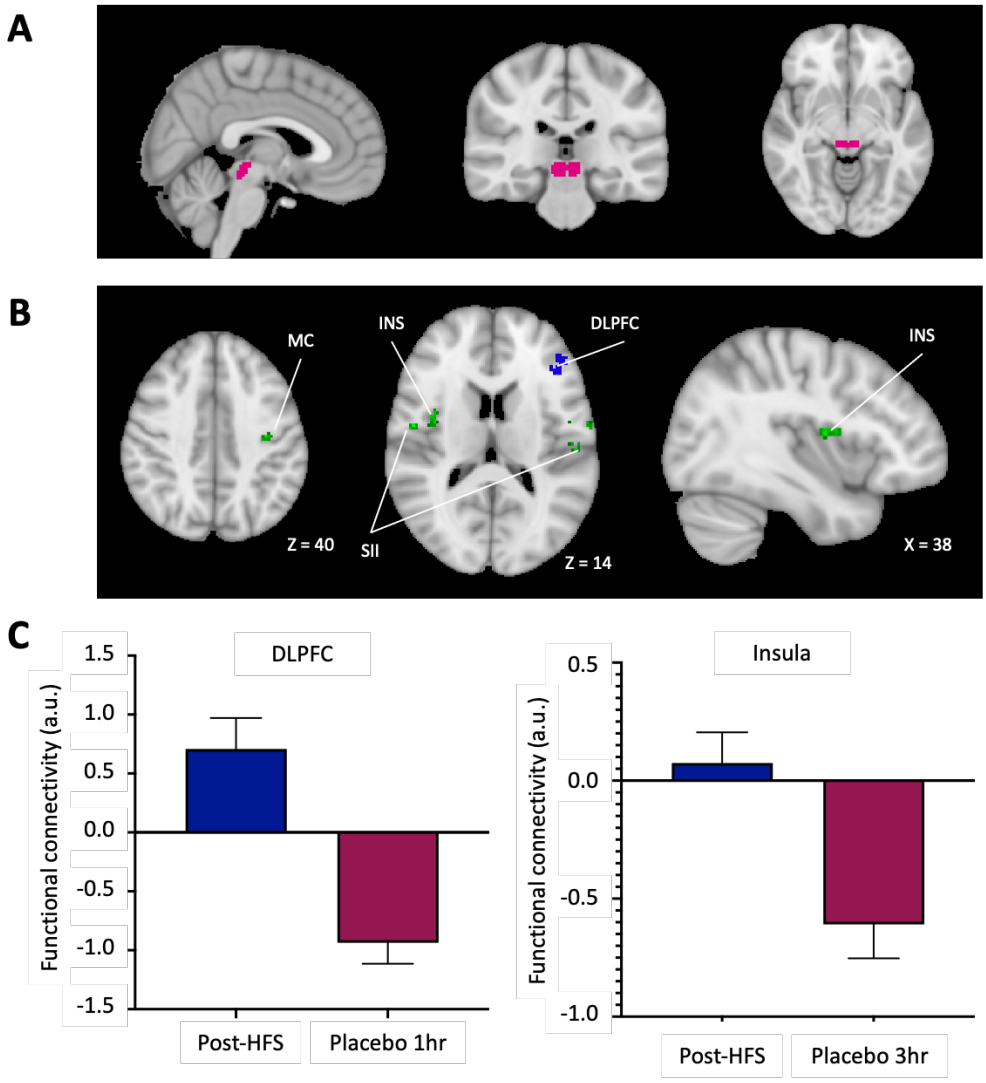

Figure 9: Functional connectivity with the ventrolateral periaqueductal grey (vlPAG) seed-region during rest for post-HFS baseline condition compared to placebo condition

A: Mask used to define the ventrolateral periaqueductal grey (vlPAG) seed region, which was defined using a connectivity-based segmentation approach in a previous study (Ezra et al. 2015). B: Whole-brain functional connectivity maps show that at the 1-hour time point (in blue) there was significantly decreased functional connectivity between the vlPAG seed-region and the dorsolateral pre-frontal cortex (DLPFC), and at the 3-hour time point (in green) there was significantly decreased functional connectivity between the vlPAG seed-region and the anterior insula cortex, secondary somatosensory cortex and the motor cortex, both during the placebo condition compared to the post-HFS no drug baseline (whole-brain mixed effects analysis, $Z > 3.1$, $p < 0.05$). MNI-512 co-ordinates are shown for images. C: Extracted functional connectivity measures for DLPFC at the 1-hour time point and the right insula at the 3-hour time point illustrate these changes. Functional connectivity measures for both regions were positive during the post-HFS no drug baseline condition and changed to negative during the placebo condition.

Correlation analyses were conducted to investigate relationships of interest between changes in resting-state functional connectivity during placebo analgesia and behavioural measures reflecting expectancy or placebo analgesia. Firstly, a two-tailed Spearman correlation analysis was conducted to investigate whether there was a relationship between the change in functional connectivity between the vlPAG and the DLPFC and the subject-reported expectation of pain relief. Secondly, a two-tailed Pearson correlation analysis was conducted to investigate whether there was a relationship between the change in functional connectivity between the vlPAG and the insular cortex with the change in pain intensity ratings to mechanical stimuli. Finally, a two-tailed Pearson correlation analysis was conducted to investigate whether there was a relationship between the change in functional connectivity between the vlPAG and the rACC with the change in pain intensity ratings to mechanical stimuli. Calculation of the respective correlation coefficients for each relationship showed that there was not a significant correlation between any of these pairs of variables ($r(df) = -0.0584$, $p = 0.8509$; $r(df) = -0.3136$, $p = 0.2967$; and $r(df) = 0.1223$, $p = 0.6906$, respectively).

5.5 Discussion

This chapter has characterised the placebo effect in a placebo-controlled clinical trial. The aim of the BioPain trial was to investigate the effects of lacosamide, pregabalin and tapentadol on brain biomarkers of pain processing observed by fMRI. The trial design consisted of a randomised, double-blind, placebo-controlled, cross-over trial in healthy subjects, utilising the HFS model to induce secondary mechanical hyperalgesia at each visit. Crucially, the study also included collection of fMRI data during an initial screening visit (at which no drug was administered), enabling the characterisation of the placebo effect through comparison of the neural responses during the no-drug baseline condition and the placebo condition.

Previous studies using fMRI have been instrumental in elucidating the neural basis for the placebo effect, enabling researchers to identify the key mechanisms underlying this reduction in pain perception during experiments in which subjects have been instructed to expect a reduction in pain. The existing evidence indicates that the placebo effect consists of two main parts; the reduction in activity in brain areas involved in pain perception – likely reflecting the reduction in pain – and the modulation of activity in brain areas involved in cognitive and emotional processing which recruit the endogenous descending pain modulatory system – reflecting top-down modulation of pain signalling during placebo analgesia (Bingel et al. 2006; Wager et al. 2004; Eippert et al. 2009; Tracey 2010). The

majority of previous fMRI studies on the placebo effect in healthy humans have utilised stimulus-evoked designs, with less existing work conducted using fMRI data collected during rest.

In the BioPain trial, the BOLD response to punctate mechanical stimuli in the placebo condition was reduced compared to the baseline condition in brain regions consistent with previous studies, notably the insula cortex, mid anterior cingulate cortex, primary and secondary somatosensory cortices (SI and SII). These brain regions are involved in pain perception and therefore this reduction in activity here is likely to be reflecting the reduced pain perception during placebo analgesia shown in the subject-reported pain ratings and not mere reporting bias. There was also a reduction in the stimulus-evoked BOLD response in the amygdala. This result is consistent with previous fMRI studies, which have shown that activity in the amygdala is reduced during placebo analgesia (Eippert et al. 2009; Atlas et al. 2012). A positron-emission tomography (PET) study has also demonstrated modulation of the amygdala activity during placebo, showing that placebo treatment potentiated opioid release in the amygdala during painful stimulation (Wager, Scott, and Zubieta 2007).

Surprisingly, in the whole-brain analysis conducted, there were no brain areas that showed increased BOLD response to mechanical stimulation during placebo analgesia. Previous studies have reported increased activation in cortical regions involved in the top-down modulation of pain during placebo analgesia, including the DLPFC and the rACC (Petrovic et al. 2002; Wager et al. 2004; Kong et al. 2006; Bingel et al. 2006). In addition, previous studies have reported activation in brainstem regions involved in the descending modulatory pain system, including the PAG and RVM (Petrovic et al. 2002).

It was also surprising that the seed-based functional connectivity during rest with the rACC seed-region was not altered during placebo. During placebo analgesia, functional connectivity has been demonstrated to be altered during rest between the rACC and the brainstem (Wanigasekera et al. 2018), and functional connectivity between the rACC and various other brain regions involved in the placebo response such as the PAG and amygdalae has been shown in response to pain stimuli (Bingel et al. 2006). In this study, there was a decrease in functional connectivity between the vlPAG and the DLPFC, with the plotted functional connectivity measures showing this reflected a change from positive connectivity at baseline to negative connectivity during placebo. This is consistent with a previous study that showed decreased functional coupling between the PAG and DLPFC in a dynamic causal modelling study (Sevel et al. 2015). Another placebo study also reported increased functional connectivity between the PAG and DLPFC (Wager et al. 2004), indicating this may not be an entirely simple change in coupling between the regions during placebo analgesia. Overall the DLPFC is a key

region in placebo analgesia, confirmed in a study that showed placebo analgesia was abolished following rTMS of the DLPFC (Krummenacher et al. 2010).

It has been previously shown that the neural basis for the placebo effect elucidated by acute pain imaging experiments is aligned to the neural basis for the placebo effect observed in the placebo-arm of a clinical trial in a pain patient cohort (Wanigasekera et al. 2018). Overall, the results here add to this work by verifying that the neural basis of the placebo effect in the placebo-arm of a clinical trial in healthy humans during a state of experimentally-induced sensitisation is also fairly consistent (though with some differences as discussed above). This is despite the differences in study designs, as the results here show consistencies with many specific placebo studies despite not having explicit manipulation of subject expectancies as part of the design, but rather an implicit change in subject expectancies within the placebo-controlled and randomised clinical trial design.

There are a number of limitations with the analysis conducted in this chapter, which may be the reason why some results hypothesised based on previous literature were not shown. The screening visit (no drug baseline condition) always occurred before the placebo visit, so it is very likely that there is a significant order effect in these results. Furthermore, the responses in the placebo condition are likely to be more variable as the placebo visit occurred at different time points for different subjects; for some subjects it was the second visit whereas for others it was the fifth visit. The BioPain study design was not optimised to conduct this exploratory analysis of the placebo effect, and the data required were only available for the 14 subjects collected at the Oxford site at the time this analysis was conducted, hence the sample size is too small to make definitive conclusions. It would be very interesting to repeat this analysis with a larger sample size, as even with the small initial sample there were promising changes in the neural activity that were consistent with previous studies. One of the reasons that some expected neural effects of placebo analgesia were not observed in this study may be due to the changes being too small to detect with the analysis methods used. Sevel et al. 2015 raise the point that, in their study, the traditional general linear model approach did not show any significant differences between the conditions. They propose that small placebo effects could be better characterized by analysing changes in the temporal dynamics among pain modulatory regions using the dynamic causal modelling approach they applied, rather than only comparing changes in the magnitude of BOLD response (Sevel et al. 2015). It would be interesting to expand the analysis conducted so far to include an approach such as dynamic causal modelling, with higher sensitivity to temporal dynamics of pain-related processes. This type of approach may show changes in functional

connectivity between the rACC and vlPAG (for example), which may have been present in the current study but too small to detect with the analysis methodology used.

There is growing evidence that the placebo effects are not solely additive to the effects of the active treatment, but that there is also interaction between placebo and drug effects (Boussageon et al. 2022; Coleshill et al. 2018). In future work, the BioPain trial data provides a valuable opportunity to explore these additive and interactive effects due to its within-subject crossover design, inclusion of a no treatment condition and collection of subject expectancy ratings at each treatment visit. Further analyses conducted with this dataset would allow exploration drug and placebo effects, and potential interactions. Comparison of each individual treatment (drug and placebo) to the no-treatment baseline session would allow more in-depth review of drug and placebo effects or interactions than the standard drug vs. placebo comparisons. For example, a previous study showed functional connectivity between the rACC and the brainstem (key areas involved in placebo analgesia) was significantly increased during placebo compared to baseline but not during active drug treatment compared to baseline, which may indicate that the neural basis for expectation-induced analgesia may be different with an active drug compared to placebo (Wanigasekera et al. 2018). Further, the relationship between subject-reported expectation of pain relief and the changes in neural response compared to the no drug baseline condition can be explored in each treatment condition. If this relationship was altered it could indicate that the drug has disrupted the placebo effect.

5.6 Conclusion

In conclusion, this chapter characterises the neural changes that occur during placebo analgesia in the placebo-controlled BioPain RCT4 clinical trial. The results show that the brain responses to painful mechanical stimuli and brain activity during rest are modulated by the subjects' altered pain expectancy during the placebo condition. These changes demonstrate an important consideration in the interpretation of the results of the BioPain RCT4 trial (and for any randomised controlled trial with a placebo control). The changes in neural response seen in the drug-arms of the trial are likely not a simple combination of the placebo effect plus the drug effect, as the drugs may modulate the placebo effect that is observed here in the comparison between the no drug baseline condition vs. placebo condition.

DISCUSSION AND FUTURE WORK

This thesis presents work using experimental pain models in healthy humans in conjunction with fMRI to develop and characterise biomarkers of pain and analgesia. The first experimental chapter comprises a systematic review and meta-analysis that summarises existing research findings from the literature in this field. The second chapter presents results from an early-stage experiment utilising ultra-high field 7T MRI to explore the onset of central sensitisation with the topical capsaicin model, showing interesting preliminary findings with amplification of neural responses in key pain processing brain regions as the state of central sensitisation develops. The third, fourth and fifth experimental chapters present results from the BioPain RCT4 trial. The trial utilised the HFS pain model to generate central sensitisation, the neural correlates of which had not previously been characterised using MRI. The third chapter characterised the neural changes in responses to mechanical stimulation and during rest following application of the HFS model. This showed that the HFS model produces centrally sensitised state consistent with that shown for established models used in imaging studies, notably capsaicin-based models. The next chapter presented the main results from the BioPain RCT4 trial. This included primary and secondary endpoints focussing on specific biomarkers of analgesic efficacy; the BOLD response in the posterior insula cortex during mechanical stimulation and the functional connectivity between the thalamus and SII during rest. These biomarkers were modulated by pregabalin and lacosamide, respectively. Whole-brain analysis also demonstrated that all drugs modulated the stimulus-evoked or resting state brain activity in pain-related brain regions, with more extensive modulation of pain responses by pregabalin and tapentadol during mechanical stimulation and by tapentadol and lacosamide during rest. Finally, the last experimental chapter presents analysis of the placebo response in the BioPain trial, comparing responses during the placebo condition of the trial to data collected during the no-drug baseline condition. This chapter shows significant changes in the placebo conditions that reflect both the reduction in magnitude of the pain response and the cortical processing underpinning this placebo analgesia.

Overall, this thesis improves our understanding of imaging biomarkers for pain and analgesia, which is important for furthering research into mechanisms of chronic pain conditions and the development of new pain treatments. In particular, the BioPain RCT4 study provides novel and valuable insights into the use of imaging biomarkers to evaluate analgesics by profiling three commonly used drugs with known efficacy. By conducting this multi-site study with a standardised and comprehensive protocol, the information gained provides unique insights into the utility of imaging biomarkers to assess neural modulation by different analgesics. Two out of the three drugs had not previously been studied in

imaging studies utilising experimental pain models in healthy humans, hence the study adds additional understanding of how analgesics with different mechanisms of action modulate neural activity.

There were challenges and limitations associated with the research presented in each chapter of this thesis, however these are discussed in detail in each individual chapter discussion and are therefore not included here.

The work presented in this thesis presents many opportunities for future work, including further analyses of this data and informing the design of future studies. Specifically, the early-phase 7T study presented in the second experimental chapter outlines some very interesting preliminary results. There are two avenues through which this could be further explored in a full-scale imaging experiment. Firstly, the results showed amplification in the neural response in many brain regions associated with pain processing as well as brainstem regions specifically related to central sensitisation. However many of these results did not reach statistical significance, likely due to the small sample size and limitations in the experiment design. The experiment could be repeated with a larger sample size, informed by a full power calculation based on these preliminary effect sizes, and also with an optimised experimental design; particularly, leaving the capsaicin cream on for a longer duration to allow the centrally sensitised state to fully develop. Secondly, the results showed differences in the neural responses for subjects that did develop hyperalgesia compared to those who did not, particularly in the brainstem regions that were investigated. Due to the small number of subjects in each group it was not possible to make conclusions based on these differences, but conducting a larger scale study with the design optimised to detect differences between those who develop hyperalgesia and those who do not would be very interesting. These further studies would provide valuable insights into the neural activity that occurs during development of central sensitisation and differences between individuals that may indicate an individual's vulnerability for developing central sensitisation. These findings would be highly relevant for chronic pain research, as central sensitisation is a key feature of many chronic pain conditions, and the factors that influence an individual's vulnerability to developing chronic pain are not fully understood. Existing evidence from human and animal studies indicate that imbalances in facilitation and inhibition controlled by the descending pain modulatory system (DPMS), which involves brainstem regions such are the PAG and RVM, could create vulnerability to developing a chronic pain state (Denk, McMahon, and Tracey 2014). Understanding the development of central sensitisation and the role of the DPMS in different individuals could provide additional targets for analgesic drug development and further clues into an individual's vulnerability for the development of chronic pain conditions.

The BioPain RCT4 study provides a rich dataset that can be further explored in many ways. One specific area that warrants future work is to apply the multivariate pattern analysis (MVPA) and machine learning techniques, which have been used in previous pain biomarker research (van der Miesen, Lindquist, and Wager 2019), to this data. Duff *et al.* recently developed a protocol for assessing analgesic efficacy in placebo-controlled fMRI studies that utilises MVPA techniques to identify evidence for pharmacodynamic modulation of brain activity and discriminate drug effects from placebo (Duff et al. 2015). The protocol includes eight different studies with six analgesic compounds. Although pregabalin was already included in the protocol development, the BioPain RCT4 study produced comparable placebo-controlled data for two new analgesics that are not previously included (lacosamide and tapentadol). This data could be aligned to the protocol in two ways; firstly, the classifier could be applied to the datasets for lacosamide and tapentadol as a further proof-of-concept test to understand whether the classifier is able to detect pharmacodynamic affect and clinical efficacy with these known analgesic compounds. Secondly, these datasets could be incorporated into the existing study database to further improve the ability of the MPVA algorithm in identifying brain responses of established analgesics, thus improving the sensitivity of this algorithm for future applications to testing novel analgesics.

In some ways, the nature of the BioPain RCT4 study contrasted with the methods outlined above. The study was a randomised clinical trial design, and, as such, had very specific and pre-determined primary and secondary endpoints. This is a key requirement for clinical trials – it allows an accurate power analysis to be conducted based on the effect size of the primary endpoint and ultimately facilitates objective assessment of the trial outcome. The BioPain trial also consisted of four RCTs investigating different biomarkers, and a core element of the project was to harmonise the trial protocols in order to facilitate collection of comparable datasets. The other three biomarkers involve the collection of discrete numerical variables and therefore are more suited to this type of design than fMRI. For RCT4, the primary and secondary endpoints of the trial included two specific imaging parameters for each drug compared to placebo; the BOLD response to mechanical stimulation in the posterior insula cortex and the functional connectivity between the thalamus and secondary somatosensory cortex. These endpoints were analysed using extracted parameters for each measure taken from the 4D imaging results. Whilst this approach makes sense in the context of a traditional RCT design, it overlooks much of the richness that imaging data offers. The results of the BioPain trial show clear modulation of neural activity relevant to pain processing with all of the analgesics tested, but not all of the analgesics modulated the specific measures included in the primary endpoint. These results demonstrate that when applying fMRI to assess analgesic activity and verify target engagement

it may be more valuable to consider whole-brain results and obtain a detailed picture of how the brain activity is modulated by the individual drug rather than assessing extracted endpoint parameters. In addition, approaches such as the MVPA technique discussed above that evaluate an overall neural signature of analgesic activity, rather than a single measure from one region, are likely to be more sensitive as imaging biomarkers for analgesia. This is an important consideration for design of future clinical trials.

The final chapter of the thesis, which explores the placebo effect in the BioPain trial, also provides opportunities for further research. The placebo effect has a big impact on the interpretation of trial results. In order for a new pain drug to be approved it is required to show higher efficacy than placebo in a randomised clinical trial. This traditional model for trial designs is increasingly being questioned, with a number of challenges being raised (Benedetti, Carlino, and Piedimonte 2016; Rief et al. 2011; Vase and Wartolowska 2019). There is evidence that the magnitude of placebo responses is increasing over time, making it more difficult for a drug to demonstrate superiority (Tuttle et al. 2015). Also, emerging literature has questioned the additive model, where the drug response is elucidated by subtracting the placebo response from the overall treatment response. This is a particular issue in patients or subjects with a large placebo response (Lund et al. 2014). There are also factors that have not previously been accounted for, such as sex differences which is often not explored as a variable in placebo or nocebo studies, but does seem to influence responses (Enck and Klosterhalfen 2019; Shafir, Olson, and Colloca 2022). The analyses conducted so far as part of this thesis focusses on characterising the placebo effect compared to a no-treatment control condition (in chapter 5), and on characterising the responses to each drug compared to the placebo condition (in chapter 4). In chapter 5, only a sub-set of 14 subjects were included from one site. The full BioPain RCT4 dataset offers opportunities for further analyses to be conducted with the larger sample size, focussing on understanding drug effects and placebo effects, and potential interactions between these responses. These further analyses conducted with the BioPain RCT4 dataset would be valuable to explore trends in this data in order to develop hypotheses for adequately powered studies in the future. Firstly, it would be interesting to study the drug induced effects relative to the no-treatment baseline session and then explore these in relation to effects induced by the placebo session. For example, a previous fMRI study has shown that functional connectivity between the rACC and the brainstem (key areas involved in placebo analgesia) was significantly increased during placebo compared to baseline but not during active drug treatment compared to baseline, which could indicate that the neural basis for expectation-induced analgesia may be different with an active drug compared to placebo (Wanigasekera et al. 2018). Secondly, it would also be interesting to explore whether any relationship

between subject-reported expectation of pain relief and the changes in neural response compared to the no drug baseline condition is the same in all treatment conditions. If this relationship was altered it could indicate that the drug has disrupted the placebo effect. Many fMRI studies focussed on the neural responses to pharmacological analgesics do not assess subject expectations related to treatment, despite the fact that subject expectations are likely to influence pain responses during the study (Bingel, Tracey, and Wiech 2012). As subject-reported ratings for expectation of pain relief were collected at each visit of the BioPain RCT4 trial it enables this data to be used to assess the impact of subject expectancy in both drug and placebo visits.

OVERALL SUMMARY

In summary, this thesis focusses on the use of experimental pain models in conjunction with fMRI to explore and characterise biomarkers for pain and analgesia. It begins with a systematic literature review of the previous research conducted in this area in the first experimental chapter, and goes on to present results produced using these techniques in a variety of applications. The work presented provides novel insights, firstly the second experimental chapter explores the onset of a centrally sensitised state using topical capsaicin, a feature of this experimental model that is not frequently observed in imaging studies as imaging is usually employed only once central sensitisation is established. The later chapters focussing on the results from the BioPain study add further and novel insights to the use of experimental pain models in conjunction with fMRI for the assessment of analgesic efficacy and target engagement. The results support the value of these types of study in the development of new analgesics, by demonstrating distinct modulation of neural pain processing in the 4 treatment arms of the study. This validates the use of such a study to explore the neural responses to a new pain drug prior to larger scale clinical trials, helping to bridge the gap between preclinical and clinical research and ultimately improve the success rate of trials.

REFERENCES

Allen, S. F., S. Gilbody, K. Atkin, and C. van der Feltz-Cornelis. 2020. 'The associations between loneliness, social exclusion and pain in the general population: A N=502,528 cross-sectional UK Biobank study', *Journal of Psychiatric Research*, 130: 68-74.

Amanzio, M., F. Benedetti, C. A. Porro, S. Palermo, and F. Cauda. 2013. 'Activation likelihood estimation meta-analysis of brain correlates of placebo analgesia in human experimental pain', *Human Brain Mapping*, 34: 738-52.

Andresen, T., D. Lunden, A. M. Drewes, and L. Arendt-Nielsen. 2011. 'Pain sensitivity and experimentally induced sensitisation in red haired females', *Scandinavian Journal of Pain*, 2: 3-6.

Arendt-Nielsen, L., B. Morlion, S. Perrot, A. Dahan, A. Dickenson, H. G. Kress, C. Wells, D. Bouhassira, and A. M. Drewes. 2018. 'Assessment and manifestation of central sensitisation across different chronic pain conditions', *European Journal of Pain*, 22: 216-41.

Asghar, M. S., M. P. Pereira, M. U. Werner, J. Mårtensson, H. B. Larsson, and J. B. Dahl. 2015. 'Secondary hyperalgesia phenotypes exhibit differences in brain activation during noxious stimulation', *PLOS ONE*, 10: e0114840.

Atlas, L. Y., and T. D. Wager. 2014. 'A meta-analysis of brain mechanisms of placebo analgesia: consistent findings and unanswered questions', *Handbook of Experimental Pharmacology*, 225: 37-69.

Atlas, L. Y., R. A. Whittington, M. A. Lindquist, J. Wielgosz, N. Sonty, and T. D. Wager. 2012. 'Dissociable influences of opiates and expectations on pain', *Journal of Neuroscience*, 32: 8053-64.

Atlas, Lauren Y., and Tor D. Wager. 2012. 'How expectations shape pain', *Neuroscience Letters*, 520: 140-48.

Bandettini, Peter A. 2012. 'Twenty years of functional MRI: The science and the stories', *Neuroimage*, 62: 575-88.

Baron, R., Y. Baron, E. Disbrow, and T. P. L. Roberts. 1999. 'Brain processing of capsaicin-induced secondary hyperalgesia - A functional MRI study', *Neurology*, 53: 548-57.

Benedetti, F., M. Amanzio, R. Rosato, and C. Blanchard. 2011. 'Nonopioid placebo analgesia is mediated by CB1 cannabinoid receptors', *Nature Medicine*, 17: 1228-30.

Benedetti, F., E. Carlino, and A. Piedimonte. 2016. 'Increasing uncertainty in CNS clinical trials: the role of placebo, nocebo, and Hawthorne effects', *The Lancet Neurology*, 15: 736-47.

Berna, C., S. Leknes, E. A. Holmes, R. R. Edwards, G. M. Goodwin, and I. Tracey. 2010. 'Induction of depressed mood disrupts emotion regulation neurocircuitry and enhances pain unpleasantness', *Biological Psychiatry*, 67: 1083-90.

Beyreuther, B. K., J. Freitag, C. Heers, N. Krebsfänger, U. Scharfenecker, and T. Stöhr. 2007. 'Lacosamide: A Review of Preclinical Properties', *CNS Drug Reviews*, 13: 21-42.

Bingel, U., J. Lorenz, E. Schoell, C. Weiller, and C. Büchel. 2006. 'Mechanisms of placebo analgesia: rACC recruitment of a subcortical antinociceptive network', *Pain*, 120: 8-15.

Bingel, U., and I. Tracey. 2008. 'Imaging CNS Modulation of Pain in Humans', *Physiology*, 23: 371-80.

Bingel, U., I. Tracey, and K. Wiech. 2012. 'Neuroimaging as a tool to investigate how cognitive factors influence analgesic drug outcomes', *Neuroscience Letters*, 520: 149-55.

Bingel, U., V. Wanigasekera, K. Wiech, R. Ni Mhuircheartaigh, M. C. Lee, M. Ploner, and I. Tracey. 2011. 'The effect of treatment expectation on drug efficacy: imaging the analgesic benefit of the opioid remifentanil', *Science Translational Medicine*, 3: 70ra14.

Biurrun Manresa, J., O. Kæseler Andersen, A. Mouraux, and E. N. van den Broeke. 2018. 'High frequency electrical stimulation induces a long-lasting enhancement of event-related potentials but does not change the perception elicited by intra-epidermal electrical stimuli delivered to the area of increased mechanical pinprick sensitivity', *PLOS ONE*, 13: e0203365.

Borsook, D., L. Becerra, and R. Hargreaves. 2011a. 'Biomarkers for chronic pain and analgesia. Part 1: the need, reality, challenges, and solutions', *Discovery Medicine*, 11: 197-207.

———. 2011b. 'Biomarkers for chronic pain and analgesia. Part 2: how, where, and what to look for using functional imaging', *Discovery Medicine*, 11: 209-19.

Boussageon, R., J. Howick, R. Baron, F. Naudet, B. Falissard, G. Harika-Germaneau, I. Wassouf, F. Gueyffier, N. Jaafari, and C. Blanchard. 2022. 'How do they add up? The interaction between the placebo and treatment effect: A systematic review', *Br J Clin Pharmacol*, 88: 3638-56.

Breivik, H., E. Eisenberg, and T. O'Brien. 2013. 'The individual and societal burden of chronic pain in Europe: the case for strategic prioritisation and action to improve knowledge and availability of appropriate care', *BMC Public Health*, 13: 1229.

Bushnell, M. C., M. Ceko, and L. A. Low. 2013. 'Cognitive and emotional control of pain and its disruption in chronic pain', *Nature Reviews Neuroscience*, 14: 502-11.

Carlson, J. D., J. J. Maire, M. E. Martenson, and M. M. Heinricher. 2007. 'Sensitization of pain-modulating neurons in the rostral ventromedial medulla after peripheral nerve injury', *Journal of Neuroscience*, 27: 13222-31.

Carmland, M. E., M. Kreutzfeldt, J. V. Holbech, N. T. Andersen, T. S. Jensen, F. W. Bach, S. H. Sindrup, and N. B. Finnerup. 2019. 'Effect of lacosamide in peripheral neuropathic pain: study protocol for a randomized, placebo-controlled, phenotype-stratified trial', *Trials*, 20: 588.

Carp, J. 2012. 'On the Plurality of (Methodological) Worlds: Estimating the Analytic Flexibility of fMRI Experiments', *Frontiers in Neuroscience*, 6.

Carville, S., M. Constanti, N. Kosky, C. Stannard, and C. Wilkinson. 2021. 'Chronic pain (primary and secondary) in over 16s: summary of NICE guidance', *British Medical Journal*, 373: n895.

Caterina, M. J., M. A. Schumacher, M. Tominaga, T. A. Rosen, J. D. Levine, and D. Julius. 1997. 'The capsaicin receptor: a heat-activated ion channel in the pain pathway', *Nature*, 389: 816-24.

Cayrol, T., J. Lebleu, A. Mouraux, N. Roussel, L. Pitance, and E. N. van den Broeke. 2020. 'Within- and between-session reliability of secondary hyperalgesia induced by electrical high-frequency stimulation', *European Journal of Pain*, 24: 1585-97.

Chen, Qiliang, and Mary M. Heinricher. 2022. 'Shifting the Balance: How Top-Down and Bottom-Up Input Modulate Pain via the Rostral Ventromedial Medulla', *Frontiers in Pain Research*, 3.

Cho, C., H. K. Deol, and L. J. Martin. 2021. 'Bridging the Translational Divide in Pain Research: Biological, Psychological and Social Considerations', *Frontiers in Pharmacology*, 12.

Cohen, S. P., and J. Mao. 2014. 'Neuropathic pain: mechanisms and their clinical implications', *British Medical Journal*, 348: f7656.

Cohen, S. P., L. Vase, and W. M. Hooten. 2021. 'Chronic pain: an update on burden, best practices, and new advances', *The Lancet*, 397: 2082-97.

Coleshill, M. J., L. Sharpe, L. Colloca, R. Zachariae, and B. Colagiuri. 2018. 'Placebo and Active Treatment Additivity in Placebo Analgesia: Research to Date and Future Directions', *Int Rev Neurobiol*, 139: 407-41.

Colloca, L., R. Klinger, H. Flor, and U. Bingel. 2013. 'Placebo analgesia: psychological and neurobiological mechanisms', *Pain*, 154: 511-14.

Corder, G., D. C. Castro, M. R. Bruchas, and G. Scherrer. 2018. 'Endogenous and Exogenous Opioids in Pain', *Annual Review of Neuroscience*, 41: 453-73.

Craig, A. D., K. Chen, D. Bandy, and E. M. Reiman. 2000. 'Thermosensory activation of insular cortex', *Nature Neuroscience*, 3: 184-90.

David, Sean P., Jennifer J. Ware, Isabella M. Chu, Pooja D. Loftus, Paolo Fusar-Poli, Joaquim Radua, Marcus R. Munafò, and John P. A. Ioannidis. 2013. 'Potential Reporting Bias in fMRI Studies of the Brain', *PLOS ONE*, 8: e70104.

Davis, K. D., N. Aghaeepour, A. H. Ahn, M. S. Angst, D. Borsook, A. Brenton, M. E. Burczynski, C. Crean, R. Edwards, B. Gaudilliere, G. W. Hergenroeder, M. J. Iadarola, S. Iyengar, Y. Jiang, J. T. Kong, S. Mackey, C. Y. Saab, C. N. Sang, J. Scholz, M. Segerdahl, I. Tracey, C. Veasley, J. Wang, T. D. Wager, A. D. Wasan, and M. A. Pelleymounter. 2020. 'Discovery and validation of biomarkers to aid the development of safe and effective pain therapeutics: challenges and opportunities', *Nature Reviews Neurology*, 16: 381-400.

de Greef, Bianca T. A., Janneke G. J. Hoeijmakers, Margot Geerts, Mike Oakes, Tim J. E. Church, Stephen G. Waxman, Sulayman D. Dib-Hajj, Catharina G. Faber, and Ingemar S. J. Merkies. 2019. 'Lacosamide in patients with Nav1.7 mutations-related small fibre neuropathy: a randomized controlled trial', *Brain*, 142: 263-75.

de Heer, E. W., M. Ten Have, H. W. J. van Marwijk, J. Dekker, R. de Graaf, A. T. F. Beekman, and C. M. van der Feltz-Cornelis. 2018. 'Pain as a risk factor for common mental disorders. Results from the Netherlands Mental Health Survey and Incidence Study-2: a longitudinal, population-based study', *Pain*, 159: 712-18.

de la Fuente-Fernández, R. 2009. 'The placebo-reward hypothesis: dopamine and the placebo effect', *Parkinsonism Related Disorders*, 15 Suppl 3: S72-4.

Denayer, Tinneke, Thomas Stöhr, and Maarten Van Roy. 2014. 'Animal models in translational medicine: Validation and prediction', *New Horizons in Translational Medicine*, 2: 5-11.

Denk, F., S. B. McMahon, and I. Tracey. 2014. 'Pain vulnerability: a neurobiological perspective', *Nature Neuroscience*, 17: 192-200.

Desikan, R. S., F. Ségonne, B. Fischl, B. T. Quinn, B. C. Dickerson, D. Blacker, R. L. Buckner, A. M. Dale, R. P. Maguire, B. T. Hyman, M. S. Albert, and R. J. Killiany. 2006. 'An automated labeling system for subdividing the human cerebral cortex on MRI scans into gyral based regions of interest', *NeuroImage*, 31: 968-80.

Drake, Robert Ar, Kenneth A. Steel, Richard Apps, Bridget M. Lumb, and Anthony E. Pickering. 2021. 'Loss of cortical control over the descending pain modulatory system determines the development of the neuropathic pain state in rats', *Elife*, 10: e65156.

Dubin, A. E., and A. Patapoutian. 2010. 'Nociceptors: the sensors of the pain pathway', *Journal of Clinical Investigation*, 120: 3760-72.

Dueñas, M., B. Ojeda, A. Salazar, J. A. Mico, and I. Failde. 2016. 'A review of chronic pain impact on patients, their social environment and the health care system', *Journal of Pain Research*, 9: 457-67.

Duff, E. P., W. Vennart, R. G. Wise, M. A. Howard, R. E. Harris, M. Lee, K. Wartolowska, V. Wanigasekera, F. J. Wilson, M. Whitlock, I. Tracey, M. W. Woolrich, and S. M. Smith. 2015. 'Learning to identify CNS drug action and efficacy using multistudy fMRI data', *Science Translational Medicine*, 7: 274ra16.

'Duvernoy's Atlas of the Human Brain Stem and Cerebellum'. 2009. *American Journal of Neuroradiology*, 30: e75-e75.

Dydyk, A. M., and T. Conermann. 2023. 'Chronic Pain.' in, *StatPearls* (StatPearls Publishing

Copyright © 2023, StatPearls Publishing LLC.: Treasure Island (FL)).

Eccleston, C., and G. Crombez. 2017. 'Advancing psychological therapies for chronic pain', *F1000Research*, 6: 461.

Eickhoff, S. B., K. Amunts, H. Mohlberg, and K. Zilles. 2006. 'The human parietal operculum. II. Stereotaxic maps and correlation with functional imaging results', *Cerebral Cortex*, 16: 268-79.

Eickhoff, S. B., D. Bzdok, A. R. Laird, F. Kurth, and P. T. Fox. 2012. 'Activation likelihood estimation meta-analysis revisited', *NeuroImage*, 59: 2349-61.

Eickhoff, S. B., A. R. Laird, C. Grefkes, L. E. Wang, K. Zilles, and P. T. Fox. 2009. 'Coordinate-based activation likelihood estimation meta-analysis of neuroimaging data: a random-effects approach based on empirical estimates of spatial uncertainty', *Human Brain Mapping*, 30: 2907-26.

Eickhoff, S. B., A. Schleicher, K. Zilles, and K. Amunts. 2006. 'The human parietal operculum. I. Cytoarchitectonic mapping of subdivisions', *Cerebral Cortex*, 16: 254-67.

Eippert, F., U. Bingel, E. D. Schoell, J. Yacubian, R. Klinger, J. Lorenz, and C. Büchel. 2009. 'Activation of the Opioidergic Descending Pain Control System Underlies Placebo Analgesia', *Neuron*, 63: 533-43.

Eisenblätter, A., R. Lewis, A. Dörfler, C. Forster, and K. Zimmermann. 2017. 'Brain mechanisms of abnormal temperature perception in cold allodynia induced by ciguatoxin', *Annals of Neurology*, 81: 104-16.

Enck, P., and S. Klosterhalfen. 2013. 'The placebo response in clinical trials—the current state of play', *Complementary Therapies in Medicine*, 21: 98-101.

———. 2019. 'Does Sex/Gender Play a Role in Placebo and Nocebo Effects? Conflicting Evidence From Clinical Trials and Experimental Studies', *Frontiers in Neuroscience*, 13: 160.

Evers, A. W. M., L. Colloca, C. Blease, M. Annoni, L. Y. Atlas, F. Benedetti, U. Bingel, C. Büchel, C. Carvalho, B. Colagiuri, A. J. Crum, P. Enck, J. Gaab, A. L. Geers, J. Howick, K. B. Jensen, I. Kirsch, K. Meissner, V. Napadow, K. J. Peerdeman, A. Raz, W. Rief, L. Vase, T. D. Wager, B. E. Wampold, K. Weimer, K. Wiech, T. J. Kaptchuk, R. Klinger, and J. M. Kelley. 2018. 'Implications of Placebo and Nocebo Effects for Clinical Practice: Expert Consensus', *Psychotherapy and Psychosomatics*, 87: 204-10.

Ezra, M., O. K. Faull, S. Jbabdi, and K. T. Pattinson. 2015. 'Connectivity-based segmentation of the periaqueductal gray matter in human with brainstem optimized diffusion MRI', *Human Brain Mapping*, 36: 3459-71.

Farrar, J. T., A. B. Troxel, K. Haynes, I. Gilron, R. D. Kerns, N. P. Katz, B. A. Rappaport, M. C. Rowbotham, A. M. Tierney, D. C. Turk, and R. H. Dworkin. 2014. 'Effect of variability in the 7-day baseline pain diary on the assay sensitivity of neuropathic pain randomized clinical trials: an ACTTION study', *Pain*, 155: 1622-31.

Faull, O. K., and K. T. Pattinson. 2017. 'The cortical connectivity of the periaqueductal gray and the conditioned response to the threat of breathlessness', *Elife*, 6.

Fayaz, A., P. Croft, R. M. Langford, L. J. Donaldson, and G. T. Jones. 2016. 'Prevalence of chronic pain in the UK: a systematic review and meta-analysis of population studies', *British Medical Journal Open*, 6: e010364.

FDA, Food and Drug Administration, and National Institutes of Health NIH. 2016. 'BEST (Biomarkers, Endpoints, and other tools) resource', *Silver Spring, MD: FDA-NIH Biomarker Working Group*.

Fingleton, C., K. Smart, N. Moloney, B. M. Fullen, and C. Doody. 2015. 'Pain sensitization in people with knee osteoarthritis: a systematic review and meta-analysis', *Osteoarthritis Cartilage*, 23: 1043-56.

Finnerup, N. B., N. Attal, S. Haroutounian, E. McNicol, R. Baron, R. H. Dworkin, I. Gilron, M. Haanpää, P. Hansson, T. S. Jensen, P. R. Kamerman, K. Lund, A. Moore, S. N. Raja, A. S. C. Rice, M. Rowbotham, E. Sena, P. Siddall, B. H. Smith, and M. Wallace. 2015. 'Pharmacotherapy for neuropathic pain in adults: a systematic review and meta-analysis', *The Lancet Neurology*, 14: 162-73.

Foerster, B. R., M. Petrou, R. A. Edden, P. C. Sundgren, T. Schmidt-Wilcke, S. E. Lowe, S. E. Harte, D. J. Clauw, and R. E. Harris. 2012. 'Reduced insular γ-aminobutyric acid in fibromyalgia', *Arthritis & Rheumatology*, 64: 579-83.

Forstenpointner, J., A. Binder, R. Maag, O. Granert, P. Hüllemann, M. Peller, G. Wasner, S. Wolff, O. Jansen, H. R. Siebner, and R. Baron. 2019. 'Neuroimaging Of Cold Allodynia Reveals A Central Disinhibition Mechanism Of Pain', *Journal of Pain Research*, 12: 3055-66.

Fox, M D., A Z. Snyder, J L. Vincent, M. Corbetta, D C. Van Essen, and M E. Raichle. 2005. 'The human brain is intrinsically organized into dynamic, anticorrelated functional networks', *Proceedings of the National Academy of Sciences*, 102: 9673-78.

Gazerani, P., O. K. Andersen, and L. Arendt-Nielsen. 2005. 'A human experimental capsaicin model for trigeminal sensitization. Gender-specific differences', *Pain*, 118: 155-63.

Goldberg, D. S., and S. J. McGee. 2011. 'Pain as a global public health priority', *BMC Public Health*, 11: 770.

Griffanti, L., G. Salimi-Khorshidi, C. F. Beckmann, E. J. Auerbach, G. Douaud, C. E. Sexton, E. Zsoldos, K. P. Ebmeier, N. Filippini, C. E. Mackay, S. Moeller, J. Xu, E. Yacoub, G. Baselli, K. Ugurbil, K. L. Miller, and S. M. Smith. 2014. 'ICA-based artefact removal and accelerated fMRI acquisition for improved resting state network imaging', *NeuroImage*, 95: 232-47.

Grönroos, M., and A. Pertovaara. 1993. 'Capsaicin-induced central facilitation of a nociceptive flexion reflex in humans', *Neuroscience Letters*, 159: 215-8.

Hans, G. H., E. Vandervliet, K. Deseure, and P. M. Parizel. 2013. 'Cerebral activation during von Frey filament stimulation in subjects with endothelin-1-induced mechanical hyperalgesia: a functional MRI study', *BioMed Research International*, 2013: 610727.

Hansen, M. S., M. S. Asghar, J. Wetterslev, C. B. Pipper, J. Mårtensson, L. Becerra, A. Christensen, J. D. Nybing, I. Havsteen, M. Boesen, and J. B. Dahl. 2018. 'The association between areas of secondary hyperalgesia and volumes of the caudate nuclei and other pain relevant brain structures-A 3-tesla MRI study of healthy men', *PLOS ONE*, 13: e0201642.

Hansen, M. S., L. Becerra, J. B. Dahl, D. Borsook, J. Mårtensson, A. Christensen, J. D. Nybing, I. Havsteen, M. Boesen, and M. S. Asghar. 2019. 'Brain resting-state connectivity in the development of secondary hyperalgesia in healthy men', *Brain Structure and Function* 224: 1119-39.

Harris, R. E., V. Napadow, J. P. Huggins, L. Pauer, J. Kim, J. Hampson, P. C. Sundgren, B. Foerster, M. Petrou, T. Schmidt-Wilcke, and D. J. Clauw. 2013. 'Pregabalin rectifies aberrant brain chemistry, connectivity, and functional response in chronic pain patients', *Anesthesiology*, 119: 1453-64.

Harris, R. E., D. A. Williams, S. A. McLean, A. Sen, M. Hufford, R. M. Gendreau, R. H. Gracely, and D. J. Clauw. 2005. 'Characterization and consequences of pain variability in individuals with fibromyalgia', *Arthritis & Rheumatology*, 52: 3670-4.

Heinricher, M. M., I. Tavares, J. L. Leith, and B. M. Lumb. 2009. 'Descending control of nociception: Specificity, recruitment and plasticity', *Brain Research Reviews*, 60: 214-25.

Henrich, Florian, Walter Magerl, Thomas Klein, Wolfgang Greffrath, and Rolf-Detlef Treede. 2015. 'Capsaicin-sensitive C- and A-fibre nociceptors control long-term potentiation-like pain amplification in humans', *Brain*, 138: 2505-20.

Higgins, J. P., D. G. Altman, P. C. Gøtzsche, P. Jüni, D. Moher, A. D. Oxman, J. Savovic, K. F. Schulz, L. Weeks, and J. A. Sterne. 2011. 'The Cochrane Collaboration's tool for assessing risk of bias in randomised trials', *British Medical Journal*, 343: d5928.

Howard, M. A., K. Krause, N. Khawaja, N. Massat, F. Zelaya, G. Schumann, J. P. Huggins, W. Vennart, S. C. Williams, and T. F. Renton. 2011. 'Beyond patient reported pain: perfusion magnetic resonance imaging demonstrates reproducible cerebral representation of ongoing post-surgical pain', *PLOS ONE*, 6: e17096.

Huang, J., V. M. Gadotti, L. Chen, I. A. Souza, S. Huang, D. Wang, C. Ramakrishnan, K. Deisseroth, Z. Zhang, and G. W. Zamponi. 2019. 'A neuronal circuit for activating descending modulation of neuropathic pain', *Nature Neuroscience*, 22: 1659-68.

Iannetti, G. D., L. Zambreanu, R. G. Wise, T. J. Buchanan, J. P. Huggins, T. S. Smart, W. Vennart, and I. Tracey. 2005. 'Pharmacological modulation of pain-related brain activity during normal and central sensitization states in humans', *Proceedings of the National Academy of Sciences*, 102: 18195-200.

IASP. 2011. 'IASP Terminology', International Association for the Study of Pain, Accessed 03 January 2022. https://www.iasp-pain.org/resources/terminology/.

Jancso, N. 1960. 'Role of the nerve terminals in the mechanism of inflammatory reactions.', *Bull. Millard Fillmore Hosp., Buffalo, N.Y.*, 7: 53-77.

Jenkinson, M., C. F. Beckmann, T. E. Behrens, M. W. Woolrich, and S. M. Smith. 2012. 'FSL', *NeuroImage*, 62: 782-90.

Jenkinson, M., and M. Chappell. 2018. *Introduction to Neuroimaging Analysis* (Oxford University Press: Oxford).

Jensen, K. B., T. B. Lonsdorf, M. Schalling, E. Kosek, and M. Ingvar. 2009. 'Increased sensitivity to thermal pain following a single opiate dose is influenced by the COMT val(158)met polymorphism', *PLOS ONE*, 4: e6016.

Jensen, T. S., and N. B. Finnerup. 2014. 'Allodynia and hyperalgesia in neuropathic pain: clinical manifestations and mechanisms', *The Lancet Neurology*, 13: 924-35.

JeYoung, Jung, A. Lambon Ralph Matthew, and L. Jackson Rebecca. 2022. 'Subregions of DLPFC Display Graded yet Distinct Structural and Functional Connectivity', *Journal of Neuroscience*, 42: 3241.

Julien, N., P. Goffaux, P. Arsenault, and S. Marchand. 2005. 'Widespread pain in fibromyalgia is related to a deficit of endogenous pain inhibition', *Pain*, 114: 295-302.

Kim, S. H., Y. Lee, S. Lee, and C. W. Mun. 2013. 'Evaluation of the effectiveness of pregabalin in alleviating pain associated with fibromyalgia: using functional magnetic resonance imaging study', *PLOS ONE*, 8: e74099.

Klein, T., W. Magerl, A. Hanschmann, M. Althaus, and R. D. Treede. 2008. 'Antihyperalgesic and analgesic properties of the N-methyl-D-aspartate (NMDA) receptor antagonist neramexane in a human surrogate model of neurogenic hyperalgesia', *European Journal of Pain*, 12: 17-29.

Klein, T., W. Magerl, H. C. Hopf, J. Sandkühler, and R. D. Treede. 2004. 'Perceptual correlates of nociceptive long-term potentiation and long-term depression in humans', *Journal of Neuroscience*, 24: 964-71.

Klein, T., W. Magerl, and R. D. Treede. 2006. 'Perceptual correlate of nociceptive long-term potentiation (LTP) in humans shares the time course of early-LTP', *Journal of Neurophysiology*, 96: 3551-5.

Klein, T., S. Stahn, W. Magerl, and R. D. Treede. 2008. 'The role of heterosynaptic facilitation in long-term potentiation (LTP) of human pain sensation', *Pain*, 139: 507-19.

Kong, J., R. L. Gollub, I. S. Rosman, J. M. Webb, M. G. Vangel, I. Kirsch, and T. J. Kaptchuk. 2006. 'Brain activity associated with expectancy-enhanced placebo analgesia as measured by functional magnetic resonance imaging', *Journal of Neuroscience*, 26: 381-8.

Kong, J., P. C. Tu, C. Zyloney, and T. P. Su. 2010. 'Intrinsic functional connectivity of the periaqueductal gray, a resting fMRI study', *Behav Brain Res*, 211: 215-9.

Koppert, W., S. K. Dern, R. Sittl, S. Albrecht, J. Schüttler, and M. Schmelz. 2001. 'A new model of electrically evoked pain and hyperalgesia in human skin: the effects of intravenous alfentanil, S(+)-ketamine, and lidocaine', *Anesthesiology*, 95: 395-402.

Koyama, Tetsuo, John G. McHaffie, Paul J. Laurienti, and Robert C. Coghill. 2005. 'The subjective experience of pain: Where expectations become reality', *Proceedings of the National Academy of Sciences*, 102: 12950-55.

Kraff, Oliver, Anja Fischer, Armin M. Nagel, Christoph Mönninghoff, and Mark E. Ladd. 2015. 'MRI at 7 tesla and above: Demonstrated and potential capabilities', *Journal of Magnetic Resonance Imaging*, 41: 13-33.

Kress, H. G. 2010. 'Tapentadol and its two mechanisms of action: is there a new pharmacological class of centrally-acting analgesics on the horizon?', *European Journal of Pain*, 14: 781-3.

Krummenacher, P., V. Candia, G. Folkers, M. Schedlowski, and G. Schönbächler. 2010. 'Prefrontal cortex modulates placebo analgesia', *Pain*, 148: 368-74.

Laird, A. R., P. M. Fox, C. J. Price, D. C. Glahn, A. M. Uecker, J. L. Lancaster, P. E. Turkeltaub, P. Kochunov, and P. T. Fox. 2005. 'ALE meta-analysis: controlling the false discovery rate and performing statistical contrasts', *Human Brain Mapping*, 25: 155-64.

LaMotte, R. H., C. N. Shain, D. A. Simone, and E. F. Tsai. 1991. 'Neurogenic hyperalgesia: psychophysical studies of underlying mechanisms', *Journal of Neurophysiology*, 66: 190-211.

Langford, R. M., R. Knaggs, P. Farquhar-Smith, and A. H. Dickenson. 2016. 'Is tapentadol different from classical opioids? A review of the evidence', *British Journal of Pain*, 10: 217-21.

Latremoliere, A., and C. J. Woolf. 2009. 'Central sensitization: a generator of pain hypersensitivity by central neural plasticity', *The Journal of Pain*, 10: 895-926.

Lee, M. C., M. Ploner, K. Wiech, U. Bingel, V. Wanigasekera, J. Brooks, D. K. Menon, and I. Tracey. 2013. 'Amygdala activity contributes to the dissociative effect of cannabis on pain perception', *Pain*, 154: 124-34.

Lee, M. C., and I. Tracey. 2013. 'Imaging pain: a potent means for investigating pain mechanisms in patients', *British Journal of Anaesthesia*, 111: 64-72.

Lee, M. C., L. Zambreanu, D. K. Menon, and I. Tracey. 2008. 'Identifying Brain Activity Specifically Related to the Maintenance and Perceptual Consequence of Central Sensitization in Humans', *Journal of Neuroscience*, 28: 11642-49.

Lee, M. H., C. D. Smyser, and J. S. Shimony. 2013. 'Resting-state fMRI: a review of methods and clinical applications', *AJNR: American Journal of Neuroradiology*, 34: 1866-72.

Leone, C., A. Di Lionardo, G. Di Pietro, G. Di Stefano, P. Falco, A. J. Blockeel, O. Caspani, L. Garcia-Larrea, A. Mouraux, K. G. Phillips, R. D. Treede, and A. Truini. 2021. 'How different experimental models of secondary hyperalgesia change the nociceptive flexion reflex', *Clinical Neurophysiology*, 132: 2989-95.

Leone, C., G. Di Stefano, G. Di Pietro, P. Bloms-Funke, I. Boesl, O. Caspani, S. C. Chapman, N. B. Finnerup, L. Garcia-Larrea, T. Li, M. Goetz, A. Mouraux, B. Pelz, E. Pogatzki-Zahn, A. Schilder, E. Schnetter, K. Schubart, I. Tracey, I. F. Troconiz, H Van Niel, J. Hernandez, K. Vincent, J. Vollert, V. Wanigasekera, M. Wittayer, K. G. Phillips, A. Truini, and R. D. Treede. 2022. 'IMI2-PainCare-BioPain-RCT2 protocol: a randomized, double-blind, placebo-controlled, crossover, multicenter trial in healthy subjects to investigate the effects of lacosamide, pregabalin, and tapentadol on biomarkers of pain processing observed by non-invasive neurophysiological measurements of human spinal cord and brainstem activity', *Trials*, 23: 739.

Liang, Z., J. King, and N. Zhang. 2012. 'Anticorrelated resting-state functional connectivity in awake rat brain', *NeuroImage*, 59: 1190-9.

Liberati, G., A. Klöcker, M. M. Safronova, S. Ferrão Santos, J. G. Ribeiro Vaz, C. Raftopoulos, and A. Mouraux. 2016. 'Nociceptive Local Field Potentials Recorded from the Human Insula Are Not Specific for Nociception', *PLOS Biology*, 14: e1002345.

Liljencrantz, J., M. Björnsdotter, I. Morrison, S. Bergstrand, M. Ceko, D. A. Seminowicz, J. Cole, C. M. Bushnell, and H. Olausson. 2013. 'Altered C-tactile processing in human dynamic tactile allodynia', *Pain*, 154: 227-34.

Lin, Richard L., Gwenaëlle Douaud, Nicola Filippini, Thomas W. Okell, Charlotte J. Stagg, and Irene Tracey. 2017. 'Structural Connectivity Variances Underlie Functional and Behavioral Changes During Pain Relief Induced by Neuromodulation', *Scientific Reports*, 7: 41603.

Liu, M., M. B. Max, E. Robinovitz, R. H. Gracely, and G. J. Bennett. 1998. 'The human capsaicin model of allodynia and hyperalgesia: sources of variability and methods for reduction', *The Journal of Pain and Symptom Management*, 16: 10-20.

Livrizzi, G., S. Lubejko, D. Johnson, C. Weiss, J. Patel, and M. Banghart. 2022. 'Prefrontal Input to the Periaqueductal Gray Controls Placebo Analgesia', *The Journal of Pain*, 23: 19-20.

Loggia, M. L., J. Kim, R. L. Gollub, M. G. Vangel, I. Kirsch, J. Kong, A. D. Wasan, and V. Napadow. 2013. 'Default mode network connectivity encodes clinical pain: an arterial spin labeling study', *Pain*, 154: 24-33.

Loggia, M. L., A. R. Segerdahl, M. A. Howard, and I. Tracey. 2019. 'Imaging Clinically Relevant Pain States Using Arterial Spin Labeling', *Pain Reports*, 4.

Löken, L. S., E. P. Duff, and I. Tracey. 2017. 'Low-threshold mechanoreceptors play a frequency-dependent dual role in subjective ratings of mechanical allodynia', *Journal of Neurophysiology*, 118: 3360-69.

Lund, K., L. Vase, G. L. Petersen, T. S. Jensen, and N. B. Finnerup. 2014. 'Randomised controlled trials may underestimate drug effects: balanced placebo trial design', *PLOS ONE*, 9: e84104.

Maher, D. P., C. H. Wong, K. W. Siah, and A. W. Lo. 2022. 'Estimates of Probabilities of Successful Development of Pain Medications: An Analysis of Pharmaceutical Clinical Development Programs from 2000 to 2020', *Anesthesiology*, 137: 243-51.

Maihöfner, C., and H. O. Handwerker. 2005. 'Differential coding of hyperalgesia in the human brain: a functional MRI study', *NeuroImage*, 28: 996-1006.

Maihofner, C., R. Ringler, F. Hermdobler, and W. Koppert. 2007. 'Brain imaging of analgesic and antihyperalgesic effects of cyclooxygenase inhibition in an experimental human pain model: a functional MRI study', *European Journal of Neuroscience*, 26: 1344-56.

Maihöfner, C., R. Ringler, F. Herrndobler, and W. Koppert. 2007. 'Brain imaging of analgesic and antihyperalgesic effects of cyclooxygenase inhibition in an experimental human pain model: a functional MRI study', *European Journal of Neuroscience*, 26: 1344-56.

Maihöfner, C., M. Schmelz, C. Forster, B. Neundörfer, and H. O. Handwerker. 2004. 'Neural activation during experimental allodynia: a functional magnetic resonance imaging study', *European Journal of Neuroscience*, 19: 3211-8.

Mainero, C., W. T. Zhang, A. Kumar, B. R. Rosen, and A. G. Sorensen. 2007. 'Mapping the spinal and supraspinal pathways of dynamic mechanical allodynia in the human trigeminal system using cardiac-gated fMRI', *NeuroImage*, 35: 1201-10.

Martinez-Gutierrez, E., A. Jimenez-Marin, S. Stramaglia, and J M. Cortes. 2022. 'The structure of anticorrelated networks in the human brain', *Frontiers in Network Physiology*, 2.

Meeker, T. J., M. L. Keaser, S. A. Khan, R. P. Gullapalli, D. A. Seminowicz, and J. D. Greenspan. 2019. 'Non-invasive motor cortex neuromodulation reduces secondary hyperalgesia and enhances activation of the descending pain modulatory network', *Frontiers in Neuroscience*, 13.

Meeker, Timothy J., Anne-Christine Schmid, Michael L. Keaser, Shariq A. Khan, Rao P. Gullapalli, Susan G. Dorsey, Joel D. Greenspan, and David A. Seminowicz. 2022. 'Tonic pain alters functional connectivity of the descending pain modulatory network involving amygdala, periaqueductal gray, parabrachial nucleus and anterior cingulate cortex', *NeuroImage*, 256: 1-13.

Millan, Mark J. 1999. 'The induction of pain: an integrative review', *Progress in Neurobiology*, 57: 1-164.

Mohr, C., S. Leyendecker, and C. Helmchen. 2008. 'Dissociable neural activity to self- vs. externally administered thermal hyperalgesia: a parametric fMRI study', *European Journal of Neuroscience*, 27: 739-49.

Mohr, C., S. Leyendecker, I. Mangels, B. Machner, T. Sander, and C. Helmchen. 2008. 'Central representation of cold-evoked pain relief in capsaicin induced pain: an event-related fMRI study', *Pain*, 139: 416-30.

Morris, V. H., S. C. Cruwys, and B. L. Kidd. 1997. 'Characterisation of capsaicin-induced mechanical hyperalgesia as a marker for altered nociceptive processing in patients with rheumatoid arthritis', *Pain*, 71: 179-86.

Morton, D. L., J. S. Sandhu, and A. K. Jones. 2016. 'Brain imaging of pain: state of the art', *Journal of Pain Research*, 9: 613-24.

Moulton, E. A., G. Pendse, S. Morris, A. Strassman, M. Aiello-Lammens, L. Becerra, and D. Borsook. 2007. 'Capsaicin-induced thermal hyperalgesia and sensitization in the human trigeminal nociceptive pathway: an fMRI study', *NeuroImage*, 35: 1586-600.

Mouraux, A., P. Bloms-Funke, I. Boesl, O. Caspani, S. C. Chapman, G. Di Stefano, N. B. Finnerup, L. Garcia-Larrea, M. Goetz, A. Kostenko, B. Pelz, E. Pogatzki-Zahn, K. Schubart, A. Stouffs, A. Truini, I. Tracey, I. F. Troconiz, J. Van Niel, J. M. Vela, K. Vincent, J. Vollert, V. Wanigasekera, M. Wittayer, K. G. Phillips, and R. D. Treede. 2021. 'IMI2-PainCare-BioPain-RCT3: a randomized, double-blind, placebo-controlled, crossover, multi-center trial in healthy subjects to investigate the effects of lacosamide, pregabalin, and tapentadol on biomarkers of pain processing observed by electroencephalography (EEG)', *Trials*, 22: 404.

Mouraux, A., and G. D. Iannetti. 2018. 'The search for pain biomarkers in the human brain', *Brain*, 141: 3290-307.

Müller, V. I., E. C. Cieslik, A. R. Laird, P. T. Fox, J. Radua, D. Mataix-Cols, C. R. Tench, T. Yarkoni, T. E. Nichols, P. E. Turkeltaub, T. D. Wager, and S. B. Eickhoff. 2018. 'Ten simple rules for neuroimaging meta-analysis', *Neuroscience & Biobehavioral Reviews*, 84: 151-61.

Napadow, V., R. Sclocco, and L. A. Henderson. 2019. 'Brainstem neuroimaging of nociception and pain circuitries', *Pain Reports*, 4: e745.

Nelson, E. K. 1919. 'THE CONSTITUTION OF CAPSAICIN, THE PUNGENT PRINCIPLE OF CAPSICUM', *Journal of the American Chemical Society*, 41: 1115-21.

Nichols, T. E., S. Das, S. B. Eickhoff, A. C. Evans, T. Glatard, M. Hanke, N. Kriegeskorte, M. P. Milham, R. A. Poldrack, J. B. Poline, E. Proal, B. Thirion, D. C. Van Essen, T. White, and B. T. Yeo. 2017. 'Best practices in data analysis and sharing in neuroimaging using MRI', *Nature Neuroscience*, 20: 299-303.

Niesters, M., P. L. Proto, L. Aarts, E. Y. Sarton, A. M. Drewes, and A. Dahan. 2014. 'Tapentadol potentiates descending pain inhibition in chronic pain patients with diabetic polyneuropathy', *Br J Anaesth*, 113: 148-56.

Nochi, Z., H. Pia, P. Bloms-Funke, I. Boesl, O. Caspani, S. C. Chapman, F. Fardo, B. Genser, M. Goetz, A. V. Kostenko, C. Leone, T. Li, A. Mouraux, B. Pelz, E. Pogatzki-Zahn, A. Schilder, E. Schnetter, K. Schubart, A. Stouffs, I. Tracey, I. F. Troconiz, A. Truini, J. Van Niel, J. M. Vela, K. Vincent, J. Vollert, V. Wanigasekera, M. Wittayer, H. Tankisi, N. B. Finnerup, K. G. Phillips, and R. D. Treede. 2022. 'IMI2-PainCare-BioPain-RCT1: study protocol for a randomized, double-blind, placebo-controlled, crossover, multi-center trial in healthy subjects to investigate the effects of lacosamide, pregabalin, and tapentadol on biomarkers of pain processing observed by peripheral nerve excitability testing (NET)', *Trials*, 23: 163.

O'Neill, Jessica, Christina Brock, Anne Estrup Olesen, Trine Andresen, Matias Nilsson, and Anthony H. Dickenson. 2012. 'Unravelling the mystery of capsaicin: a tool to understand and treat pain', *Pharmacological Reviews*, 64: 939-71.

Olesen, A. E., T. Andresen, C. Staahl, and A. M. Drewes. 2012. 'Human Experimental Pain Models for Assessing the Therapeutic Efficacy of Analgesic Drugs', *Pharmacological Reviews*, 64: 722-79.

Ossipov, Michael H., Kozo Morimura, and Frank Porreca. 2014. 'Descending pain modulation and chronification of pain', *Current opinion in supportive and palliative care*, 8: 143-51.

Page, M. J., J. E. McKenzie, P. M. Bossuyt, I. Boutron, T. C. Hoffmann, C. D. Mulrow, L. Shamseer, J. M. Tetzlaff, E. A. Akl, S. E. Brennan, R. Chou, J. Glanville, J. M. Grimshaw, A. Hróbjartsson, M. M. Lalu, T. Li, E. W. Loder, E. Mayo-Wilson, S. McDonald, L. A. McGuinness, L. A. Stewart, J. Thomas, A. C. Tricco, V. A. Welch, P. Whiting, and David Moher. 2021. 'The PRISMA 2020 statement: an updated guideline for reporting systematic reviews', *British Medical Journal*, 372: n71.

Petersen, K. L., and M. C. Rowbotham. 1999. 'A new human experimental pain model: the heat/capsaicin sensitization model', *Neuroreport*, 10: 1511-6.

Petrovic, P., E. Kalso, K. M. Petersson, J. Andersson, P. Fransson, and M. Ingvar. 2010. 'A prefrontal non-opioid mechanism in placebo analgesia', *Pain*, 150: 59-65.

Petrovic, P., E. Kalso, K. M. Petersson, and M. Ingvar. 2002. 'Placebo and opioid analgesia-- imaging a shared neuronal network', *Science*, 295: 1737-40.

Pfau, D. B., T. Klein, D. Putzer, E. M. Pogatzki-Zahn, R. D. Treede, and W. Magerl. 2011. 'Analysis of hyperalgesia time courses in humans after painful electrical high-frequency stimulation identifies a possible transition from early to late LTP-like pain plasticity', *Pain*, 152: 1532-39.

Phillips, C. J. 2009. 'The Cost and Burden of Chronic Pain', *Reviews in Pain*, 3: 2-5.

Ploghaus, A., C. Narain, C. F. Beckmann, S. Clare, S. Bantick, R. Wise, P. M. Matthews, J. N. Rawlins, and I. Tracey. 2001. 'Exacerbation of pain by anxiety is associated with activity in a hippocampal network', *Journal of Neuroscience*, 21: 9896-903.

Ploghaus, A., I. Tracey, J. S. Gati, S. Clare, R. S. Menon, P. M. Matthews, and J. N. Rawlins. 1999. 'Dissociating pain from its anticipation in the human brain', *Science*, 284: 1979-81.

Price, D. D., J. Craggs, Nicholas V. G., W. M. Perlstein, and M. E. Robinson. 2007. 'Placebo analgesia is accompanied by large reductions in pain-related brain activity in irritable bowel syndrome patients', *Pain*, 127: 63-72.

Price, P., R. Jhangiani, I. Chiang, D. Leighton, and C. Cuttler. 2017. '5.2 Experimental Design.' in, *Research Methods in Psychology*.

Quesada, C., A. Kostenko, I. Ho, C. Leone, Z. Nochi, A. Stouffs, M. Wittayer, O. Caspani, N. Brix Finnerup, A. Mouraux, G. Pickering, I. Tracey, A. Truini, R. D. Treede, and L. Garcia-Larrea. 2021. 'Human surrogate models of central sensitization: A critical review and practical guide', *European Journal of Pain*, 25: 1389-428.

Rempe, T., S. Wolff, C. Riedel, R. Baron, P. W. Stroman, O. Jansen, and J. Gierthmühlen. 2014. 'Spinal fMRI reveals decreased descending inhibition during secondary mechanical hyperalgesia', *PLOS ONE*, 9: e112325.

———. 2015. 'Spinal and supraspinal processing of thermal stimuli: an fMRI study', *Journal of Magnetic Resonance Imaging*, 41: 1046-55.

Rief, W., U. Bingel, M. Schedlowski, and P. Enck. 2011. 'Mechanisms involved in placebo and nocebo responses and implications for drug trials', *Clinical Pharmacology & Therapeutics*, 90: 722-26.

Ringkamp, M., P. M. Dougherty, and S. N. Raja. 2018. 'Chapter 1 - Anatomy and Physiology of the Pain Signaling Process.' in Honorio T. Benzon, Srinivasa N. Raja, Spencer S. Liu, Scott M. Fishman and Steven P. Cohen (eds.), *Essentials of Pain Medicine (Fourth Edition)* (Elsevier).

Rogers, R., R. G. Wise, D. J. Painter, S. E. Longe, and I. Tracey. 2004. 'An investigation to dissociate the analgesic and anesthetic properties of ketamine using functional magnetic resonance imaging', *Anesthesiology*, 100: 292-301.

Romualdi, P., M. Grilli, P. L. Canonico, M. Collino, and A. H. Dickenson. 2019. 'Pharmacological rationale for tapentadol therapy: a review of new evidence', *Journal of Pain Research*, 12: 1513-20.

Salimi-Khorshidi, G., G. Douaud, C. F. Beckmann, M. F. Glasser, L. Griffanti, and S. M. Smith. 2014. 'Automatic denoising of functional MRI data: combining independent component analysis and hierarchical fusion of classifiers', *NeuroImage*, 90: 449-68.

Samartsidis, P., S. Montagna, T. D. Johnson, and T. E. Nichols. 2017. 'The Coordinate-Based Meta-Analysis of Neuroimaging Data', *Statistical Science*, 32: 580-99, 20.

Schmelz, M., R. Schmid, H. O. Handwerker, and H. E. Torebjörk. 2000. 'Encoding of burning pain from capsaicin-treated human skin in two categories of unmyelinated nerve fibres', *Brain*, 123 Pt 3: 560-71.

Schmidt-Wilcke, T., E. Ichesco, J. P. Hampson, A. Kairys, S. Peltier, S. Harte, D. J. Clauw, and R. E. Harris. 2014. 'Resting state connectivity correlates with drug and placebo response in fibromyalgia patients', *NeuroImage: Clinical*, 6: 252-61.

Segerdahl, A. R., M. Mezue, T. W. Okell, J. T. Farrar, and I. Tracey. 2015. 'The dorsal posterior insula subserves a fundamental role in human pain', *Nature Neuroscience*, 18: 499-500.

Seifert, F., K. Bschorer, R. De Col, J. Filitz, E. Peltz, W. Koppert, and C. Maihöfner. 2009. 'Medial prefrontal cortex activity is predictive for hyperalgesia and pharmacological antihyperalgesia', *Journal of Neuroscience*, 29: 6167-75.

Seifert, F., O. Fuchs, F. T. Nickel, M. Garcia, A. Dörfler, G. Schaller, J. Kornhuber, W. Sperling, and C. Maihöfner. 2010. 'A functional magnetic resonance imaging navigated repetitive transcranial magnetic stimulation study of the posterior parietal cortex in normal pain and hyperalgesia', *Neuroscience*, 170: 670-7.

Seifert, F., I. Jungfer, M. Schmelz, and C. Maihöfner. 2008. 'Representation of UV-B-induced thermal and mechanical hyperalgesia in the human brain: a functional MRI study', *Human Brain Mapping*, 29: 1327-42.

Seifert, F., and C. Maihofher. 2007. 'Representation of cold allodynia in the human brain - A functional MRI study', *NeuroImage*, 35: 1168-80.

Sevel, L. S., J. G. Craggs, D. D. Price, R. Staud, and M. E. Robinson. 2015. 'Placebo analgesia enhances descending pain-related effective connectivity: a dynamic causal modeling study of endogenous pain modulation', *The Journal of Pain*, 16: 760-8.

Shafir, R., E. Olson, and L. Colloca. 2022. 'The neglect of sex: A call to action for including sex as a biological variable in placebo and nocebo research', *Contemporary Clinical Trials*, 116: 106734.

Shenoy, R., K. Roberts, A. Papadaki, D. McRobbie, M. Timmers, T. Meert, and P. Anand. 2011. 'Functional MRI brain imaging studies using the Contact Heat Evoked Potential Stimulator (CHEPS) in a human volunteer topical capsaicin pain model', *Journal of Pain Research*, 4: 365-71.

Simone, D. A., T. K. Baumann, and R. H. LaMotte. 1989. 'Dose-dependent pain and mechanical hyperalgesia in humans after intradermal injection of capsaicin', *Pain*, 38: 99-107.

Sirucek, L., R. C. Price, W. Gandhi, M. E. Hoeppli, E. Fahey, A. Qu, S. Becker, and P. Schweinhardt. 2021. 'Endogenous opioids contribute to the feeling of pain relief in humans', *Pain*, 162: 2821-31.

Smith, S. M. 2002. 'Fast robust automated brain extraction', *Human Brain Mapping*, 17: 143-55.

Smith, S. M., D. Amtmann, R. L. Askew, J. S. Gewandter, M. Hunsinger, M. P. Jensen, M. P. McDermott, K. V. Patel, M. Williams, E. D. Bacci, L. B. Burke, C. T. Chambers, S. A. Cooper, P. Cowan, P. Desjardins, M. Etropolski, J. T. Farrar, I. Gilron, I. Z. Huang, M. Katz, R. D. Kerns, E. A. Kopecky, B. A. Rappaport, M. Resnick, V. Strand, G. F. Vanhove, C. Veasley, M. Versavel, A. D. Wasan, D. C. Turk, and R. H. Dworkin. 2016. 'Pain intensity rating training: results from an exploratory study of the ACTTION PROTECCT system', *Pain*, 157: 1056-64.

Smith, S. M., R. H. Dworkin, D. C. Turk, R. Baron, M. Polydefkis, I. Tracey, D. Borsook, R. R. Edwards, R. E. Harris, T. D. Wager, L. Arendt-Nielsen, L. B. Burke, D. B. Carr, A. Chappell, J. T. Farrar, R. Freeman, I. Gilron, V. Goli, J. Haeussler, T. Jensen, N. P. Katz, J. Kent, E. A. Kopecky, D. A. Lee, W. Maixner, J. D. Markman, J. C. McArthur, M. P. McDermott, L. Parvathenani, S. N. Raja, B. A. Rappaport, A. S. C. Rice, M. C. Rowbotham, J. K. Tobias, A. D. Wasan, and J. Witter. 2017. 'The Potential Role of Sensory Testing, Skin Biopsy, and Functional Brain Imaging as Biomarkers in Chronic Pain Clinical Trials: IMMPACT Considerations', *The Journal of Pain*, 18: 757-77.

Smith, S. M., M. Jenkinson, M. W. Woolrich, C. F. Beckmann, T. E. Behrens, H. Johansen-Berg, P. R. Bannister, M. De Luca, I. Drobnjak, D. E. Flitney, R. K. Niazy, J. Saunders, J. Vickers, Y. Zhang, N. De Stefano, J. M. Brady, and P. M. Matthews. 2004. 'Advances in functional and structural MR image analysis and implementation as FSL', *NeuroImage*, 23 Suppl 1: S208-19.

Stammler, T., R. De Col, F. Seifert, and C. Maihöfner. 2008. 'Functional imaging of sensory decline and gain induced by differential noxious stimulation', *NeuroImage*, 42: 1151-63.

Stein, C. 2016. 'Opioid Receptors', *Annual Review of Medicine*, 67: 433-51.

Tanasescu, R., W. J. Cottam, L. Condon, C. R. Tench, and D. P. Auer. 2016. 'Functional reorganisation in chronic pain and neural correlates of pain sensitisation: A coordinate based meta-analysis of 266 cutaneous pain fMRI studies', *Neuroscience & Biobehavioral Reviews*, 68: 120-33.

Tétreault, P., A. Mansour, E. Vachon-Presseau, T. J. Schnitzer, A. V. Apkarian, and M. N. Baliki. 2016. 'Brain Connectivity Predicts Placebo Response across Chronic Pain Clinical Trials', *PLOS Biology*, 14: e1002570.

Tognarelli, J. M., M. Dawood, M. I. Shariff, V. P. Grover, M. M. Crossey, I. J. Cox, S. D. Taylor-Robinson, and M. J. McPhail. 2015. 'Magnetic Resonance Spectroscopy: Principles and Techniques: Lessons for Clinicians', *Journal of Clinical and Experimental Hepatology*, 5: 320-8.

Tracey, I. 2008. 'Imaging pain', *British Journal of Anaesthesia*, 101: 32-9.

———. 2010. 'Getting the pain you expect: mechanisms of placebo, nocebo and reappraisal effects in humans', *Nature Medicine*, 16: 1277-83.

Tracey, I., and E. Johns. 2010. 'The pain matrix: reloaded or reborn as we image tonic pain using arterial spin labelling', *Pain*, 148: 359-60.

Tracey, I., and P. Mantyh. 2007. 'The Cerebral Signature for Pain Perception and Its Modulation', *Neuron*, 55: 377-91.

Tracey, I., C. J. Woolf, and N. A. Andrews. 2019. 'Composite Pain Biomarker Signatures for Objective Assessment and Effective Treatment', *Neuron*, 101: 783-800.

Treede, R. D., R. A. Meyer, S. N. Raja, and J. N. Campbell. 1992. 'Peripheral and central mechanisms of cutaneous hyperalgesia', *Progress in Neurobiology*, 38: 397-421.

Treede, R. D., W. Rief, A. Barke, Q. Aziz, M. I. Bennett, R. Benoliel, M. Cohen, S. Evers, N. B. Finnerup, M. B. First, M. A. Giamberardino, S. Kaasa, B. Korwisi, E. Kosek, P. Lavand'homme, M. Nicholas, S. Perrot, J. Scholz, S. Schug, B. H. Smith, P. Svensson, J. W. S. Vlaeyen, and S. J. Wang. 2019. 'Chronic pain as a symptom or a disease: the IASP Classification of Chronic Pain for the International Classification of Diseases (ICD-11)', *Pain*, 160: 19-27.

Treede, R. D., W. Rief, A. Barke, Q. Aziz, M. I. Bennett, R. Benoliel, M. Cohen, S. Evers, N. B. Finnerup, M. B. First, M. A. Giamberardino, S. Kaasa, E. Kosek, P. Lavand'homme, M. Nicholas, S. Perrot, J. Scholz, S. Schug, B. H. Smith, P. Svensson, J. W. Vlaeyen, and S. J. Wang. 2015. 'A classification of chronic pain for ICD-11', *Pain*, 156: 1003-7.

Turk, D. C., H. D. Wilson, and A. Cahana. 2011. 'Treatment of chronic non-cancer pain', *The Lancet*, 377: 2226-35.

Turkeltaub, P. E., S. B. Eickhoff, A. R. Laird, M. Fox, M. Wiener, and P. Fox. 2012. 'Minimizing within-experiment and within-group effects in Activation Likelihood Estimation meta-analyses', *Human Brain Mapping*, 33: 1-13.

Tuttle, A. H., S. Tohyama, T. Ramsay, J. Kimmelman, P. Schweinhardt, G. J. Bennett, and J. S. Mogil. 2015. 'Increasing placebo responses over time in US clinical trials of neuropathic pain', *Pain*, 156: 2616-26.

Upadhyay, J., J. Anderson, A. J. Schwarz, A. Coimbra, R. Baumgartner, G. Pendse, E. George, L. Nutile, D. Wallin, J. Bishop, S. Neni, G. Maier, S. Iyengar, J. L. Evelhoch, D. Bleakman, R. Hargreaves, L. Becerra, and D. Borsook. 2011. 'Imaging Drugs with and without Clinical Analgesic Efficacy', *Neuropsychopharmacology*, 36: 2659-73.

Urban, M. O., and G. F. Gebhart. 1999. 'Supraspinal contributions to hyperalgesia', *Proceedings of the National Academy of Sciences*, 96: 7687-92.

van den Broeke, E. N., B. de Vries, J. Lambert, D. M. Torta, and A. Mouraux. 2017. 'Phase-locked and non-phase-locked EEG responses to pinprick stimulation before and after experimentally-induced secondary hyperalgesia', *Clinical Neurophysiology*, 128: 1445-56.

van den Broeke, E. N., S. Gousset, J. Bouvy, A. Stouffs, L. Lebrun, S. G. A. van Neerven, and A. Mouraux. 2019. 'Heterosynaptic facilitation of mechanical nociceptive input is dependent on the frequency of conditioning stimulation', *Journal of Neurophysiology*, 122: 994-1001.

van den Broeke, E. N., and A. Mouraux. 2014. 'High-frequency electrical stimulation of the human skin induces heterotopical mechanical hyperalgesia, heat hyperalgesia, and enhanced responses to nonnociceptive vibrotactile input', *Journal of Neurophysiology*, 111: 1564-73.

van der Miesen, M. M., M. A. Lindquist, and T. D. Wager. 2019. 'Neuroimaging-based biomarkers for pain: state of the field and current directions', *Pain Reports*, 4: e751.

van Niel, J., P. Bloms-Funke, O. Caspani, J. M. Cendros, L. Garcia-Larrea, A. Truini, I. Tracey, S. C. Chapman, N. Marco-Ariño, I. F. Troconiz, K. Phillips, N. B. Finnerup, A. Mouraux, and R. D. Treede. 2022. "Pharmacological Probes to Validate Biomarkers for Analgesic Drug Development." In *International Journal of Molecular Sciences*.

Vase, Lene, and Karolina Wartolowska. 2019. 'Pain, placebo, and test of treatment efficacy: a narrative review', *British Journal of Anaesthesia*, 123: e254-e62.

Vera-Portocarrero, L. P., E. T. Zhang, M. H. Ossipov, J. Y. Xie, T. King, J. Lai, and F. Porreca. 2006. 'Descending facilitation from the rostral ventromedial medulla maintains nerve injury-induced central sensitization', *Neuroscience*, 140: 1311-20.

Verma, V., N. Singh, and A. Singh Jaggi. 2014. 'Pregabalin in neuropathic pain: evidences and possible mechanisms', *Current Neuropharmacology*, 12: 44-56.

von Hehn, C. A., R. Baron, and C. J. Woolf. 2012. 'Deconstructing the neuropathic pain phenotype to reveal neural mechanisms', *Neuron*, 73: 638-52.

Wager, T. D., L. Y. Atlas, M. A. Lindquist, M. Roy, C. W. Woo, and E. Kross. 2013. 'An fMRI-based neurologic signature of physical pain', *New England Journal of Medicine*, 368: 1388-97.

Wager, T. D., M. A. Lindquist, T. E. Nichols, H. Kober, and J. X. Van Snellenberg. 2009. 'Evaluating the consistency and specificity of neuroimaging data using meta-analysis', *NeuroImage*, 45: S210-21.

Wager, T. D., J. K. Rilling, E. E. Smith, A. Sokolik, K. L. Casey, R. J. Davidson, S. M. Kosslyn, R. M. Rose, and J. D. Cohen. 2004. 'Placebo-induced changes in FMRI in the anticipation and experience of pain', *Science*, 303: 1162-7.

Wager, T. D., and M. Roy. 2010. 'Separate mechanisms for placebo and opiate analgesia?', *Pain*, 150: 8-9.

Wager, Tor D., David J. Scott, and Jon-Kar Zubieta. 2007. 'Placebo effects on human μ-opioid activity during pain', *Proceedings of the National Academy of Sciences*, 104: 11056-61.

Wagner, I. C., M. Rütgen, A. Hummer, C. Windischberger, and C. Lamm. 2020. 'Placebo-induced pain reduction is associated with negative coupling between brain networks at rest', *NeuroImage*, 219: 117024.

Wanigasekera, V., M. C. H. Lee, R. Rogers, P. Hu, and I. Tracey. 2011. 'Neural Correlates of an Injury-Free Model of Central Sensitization Induced by Opioid Withdrawal in Humans', *Journal of Neuroscience*, 31: 2835-42.

Wanigasekera, V., M. Mezue, J. Andersson, Y. Kong, and I. Tracey. 2016. 'Disambiguating Pharmacodynamic Efficacy from Behavior with Neuroimaging: Implications for Analgesic Drug Development', *Anesthesiology*, 124: 159-68.

Wanigasekera, V., K. Wartolowska, J. P. Huggins, E. P. Duff, W. Vennart, M. Whitlock, N. Massat, L. Pauer, P. Rogers, B. Hoggart, and I. Tracey. 2018. 'Disambiguating pharmacological mechanisms from placebo in neuropathic pain using functional neuroimaging', *British Journal of Anaesthesia*, 120: 299-307.

Wiech, K., M. Ploner, and I. Tracey. 2008. 'Neurocognitive aspects of pain perception', *Trends in Cognitive Sciences*, 12: 306-13.

Wiech, K., and I. Tracey. 2009. 'The influence of negative emotions on pain: behavioral effects and neural mechanisms', *NeuroImage*, 47: 987-94.

Winkler, A. M., G. R. Ridgway, M. A. Webster, S. M. Smith, and T. E. Nichols. 2014. 'Permutation inference for the general linear model', *NeuroImage*, 92: 381-97.

Wise, R. G., R. Rogers, D. Painter, S. Bantick, A. Ploghaus, P. Williams, G. Rapeport, and I. Tracey. 2002. 'Combining fMRI with a pharmacokinetic model to determine which brain areas activated by painful stimulation are specifically modulated by remifentanil', *NeuroImage*, 16: 999-1014.

Wise, Richard G., Pauline Williams, and Irene Tracey. 2004. 'Using fMRI to Quantify the Time Dependence of Remifentanil Analgesia in the Human Brain', *Neuropsychopharmacology*, 29: 626-35.

Woolf, C. J. 2011. 'Central sensitization: implications for the diagnosis and treatment of pain', *Pain*, 152: S2-s15.

Woolf, Clifford J. 1983. 'Evidence for a central component of post-injury pain hypersensitivity', *Nature*, 306: 686-88.

Woolrich, M. W., T. E. Behrens, C. F. Beckmann, M. Jenkinson, and S. M. Smith. 2004. 'Multilevel linear modelling for FMRI group analysis using Bayesian inference', *NeuroImage*, 21: 1732-47.

Woolrich, M. W., S. Jbabdi, B. Patenaude, M. Chappell, S. Makni, T. Behrens, C. Beckmann, M. Jenkinson, and S. M. Smith. 2009. 'Bayesian analysis of neuroimaging data in FSL', *NeuroImage*, 45: S173-86.

Woolrich, M. W., B. D. Ripley, M. Brady, and S. M. Smith. 2001. 'Temporal autocorrelation in univariate linear modeling of FMRI data', *NeuroImage*, 14: 1370-86.

Xia, W., C. D. Mørch, and O. K. Andersen. 2016. 'Exploration of the conditioning electrical stimulation frequencies for induction of long-term potentiation-like pain amplification in humans', *Experimental Brain Research*, 234: 2479-89.

Zambreanu, L., R. G. Wise, J. C. W. Brooks, G. D. Iannetti, and I. Tracey. 2005. 'A role for the brainstem in central sensitisation in humans. Evidence from functional magnetic resonance imaging', *Pain*, 114: 397-407.

Zhang, X., Y. Dou, L. Yuan, Q. Li, Y. Zhu, M. Wang, and Y. Sun. 2020. 'Different neuronal populations mediate inflammatory pain analgesia by exogenous and endogenous opioids', *Elife*, 9: e55289.

Zunhammer, M., T. Spisák, T. D. Wager, U. Bingel, L. Atlas, F. Benedetti, C. Büchel, J. Choi, L. Colloca, D. Duzzi, F. Eippert, D. Ellingsen, S. Elsenbruch, S. Geuter, T. Kaptchuk, S. Kessner, I. Kirsch, J. Kong, C. Lamm, S. Leknes, F. Lui, A. Müllner-Huber, C. Porro, M. Rütgen, L. Schenk, J. Schmid, N. Theysohn, I. Tracey, N. Wrobel, and F. Zeidan. 2021. 'Meta-analysis of neural systems underlying placebo analgesia from individual participant fMRI data', *Nature Communications*, 12: 1391.